JOURNAL OF POLYMER SCIENCE: PART A-1 VOL. 4, 257–274 (1966)

NMR Study of Model Compounds of Vinyl Polymers

YUZURU FUJIWARA and SHIZUO FUJIWARA, *Department of Chemistry, Faculty of Science, The University of Tokyo, Tokyo, Japan,* and KIYOSHI FUJII, *The Kurashiki Rayon Company, Kurashiki, Okayama, Japan*

Synopsis

Complicated NMR spectra of vinyl polymers provide conformational and configurational knowledge of the polymers in solution. Explicit expressions for the spectral frequencies and intensities are obtained by the analysis of vinyl polymers and their model compounds as weakly coupled systems. The classified spectra expected for common vinyl polymers are presented by using the results of the analysis. The analysis is applied to model compounds of poly(vinyl alcohol) and poly(vinyl acetate) in solution. The results show that conformations of poly(vinyl alcohol) are determined by the intramolecular hydrogen bonding so that the syndiotactic isomer forms a helical structure, the isotactic one a planar zigzag structure. The poly(vinyl acetate) produces a helical structure for isotactic isomer by the repulsion of side chains and a planar zigzag for the syndiotactic isomer.

INTRODUCTION

Stereoregularity has a close relationship to the properties of polymers, and various stereoregular polymers have actually been prepared. It has been shown in many instances that stereoregularity can be predicted from a knowledge of the physical and chemical properties of polymers or from conditions used in preparing polymers.

The principles of high resolution nuclear magnetic resonance suggest their usefulness for determinations of stereochemical configurations and conformations of polymers in solutions, and NMR techniques have been used for the quantitative analysis of tacticities.[1,2] With polymers such as poly(methyl methacrylate) and poly-α-methylstyrene, no appreciable spin-spin coupling occurs between the methylene and the methyl protons, but there are considerable changes depending on the stereoregularity. Therefore, the spectra are not complicated, and the NMR method is effective. With vinyl polymers, many protons interact with each other and the shift due to tacticity is small. Hence complicated spectra are obtained. The spin decoupling by double resonance[3] and deuterium substitution of some protons[4] have proved to be useful for the analysis of poly(vinyl halides) and polypropylene. However those methods are not always

effective[3] and often require elaborate processes. Signals of side chains are useful for the study of tacticity in poly(vinyl acetate)[3] and poly(methyl vinyl ether)[5] but not directly useful for the study of conformations. On the other hand, complete analysis of vinyl polymers may provide sufficient information concerning configurations and conformations. In this paper, analysis of spin systems in vinyl polymers are presented with points to be noticed in the interpretation of NMR spectra, and calculated reference patterns are presented which will be encountered in the spectral analysis of vinyl polymers. Application of the reference patterns is also made for 2,4-pentanediol, 2,4,6-heptanetriol, and their acetates for configuration and conformation determinations. These compounds were chosen as model compounds for poly(vinyl alcohol) and poly(vinyl acetate), respectively, so as to avoid difficulties in spectral analysis due to the broad line width encountered in common polymers. The stereoisomers were measured separately.

ANALYSIS OF SPECTRA

Vinyl polymers are schematically represented and the protons designated A, B, K, L, M, N as shown in I.

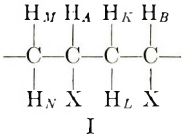

I

For simplicity, it is assumed that spin-spin coupling with protons at a distance of four or more bond lengths is negligible. This is the case for vinyl polymers such as poly(vinyl chloride), poly(vinyl alcohol) and its esters, and poly(vinyl ethers). On the other hand, this is not valid for strongly coupled systems such as polypropylene and polystyrene, whose spectra show another type of complexity and asymmetry which is manifest through higher order calculations than the one mentioned in the present paper. With the above assumptions, systems with infinite numbers of spins can be reduced to the KL part in the $ABKL$ system, and the A part in the $AKLMN$ system which is replaced by $AKLX_2$ at the end of the molecules of model compounds. The calculations for these systems are straightforward, and A in $AKLX_3$ and KL in $ABKL$ have already been reported by the authors.[6]

CALCULATED SPECTRA

The spectra of vinyl polymers can be predicted, provided a set of parameters is decided upon. Figures 1–16 show the spectra of α and β protons with parameters which are chosen to be close to actual ones and which cover all typical cases. Chemical shifts ν as well as coupling constants J are expressed in cycles per second.

α Proton

The α proton spectrum consists of a maximum of 36 lines, 16 lines having large intensities and the other 20 lines being hardly observable. The 16 strong lines whose spectra are always symmetric are shown in Figures 1–6. The spectra of real polymers may naturally have asymmetric forms because of the superposition of two or more kinds of spectra. The commonest quintet pattern with intensity ratio 1:4:6:4:1 appears when all β hydrogens are equivalent (i.e., all methylene protons have the same interaction with methine protons and have the same chemical shift). It should be noticed that the quintet is also observed if all spin couplings between α and β protons are the same (cf. Fig. 1*a*), or if the sum of the coupling constants over β protons is the same for both neighbors of the α protons (i.e., $J_{AK} + J_{AL} = J_{AM} + J_{AN}$), and all β protons have the same chemical shifts (cf. Figs. 2*a* and 3*a*). Since the former situation is indifferent to the chemical shifts, the quintet always holds, being independent of the chemical shifts. On the other hand, each coupling constant may have a different value for the latter, where spin decoupling of α protons from β protons reduces the quintet to a singlet. The quintet which appears for different coupling constants changes with the chemical shifts, as shown in Figures 2 and 3. The quintet which appears for different chemical shifts of β protons changes its shape if J_{AK} is different from J_{AM}, even if $J_{AK} = J_{AL}$, and $J_{AM} = J_{AN}$ (cf. Fig. 4). As long as $J_{AK} = J_{AL}$, and $J_{AM} = J_{AN}$, the spectrum is independent of the chemical shifts of β protons (cf. Fig. 4*a*). If $J_{AK} = J_{AL} \gg J_{AM} = J_{AN}$, the spectrum exhibits a triple triplet (Fig. 4*d*). A heptet with an intensity ratio or 1:2:3:4:3:2:1 is observed regardless of the chemical shifts, if $J_{AK} = J_{AL} = {}^1/_2 J_{AM} = {}^1/_2 J_{AN}$, or if all chemical shifts of β protons are the same and $J_{AK} + J_{AL} = {}^1/_2(J_{AM} +$

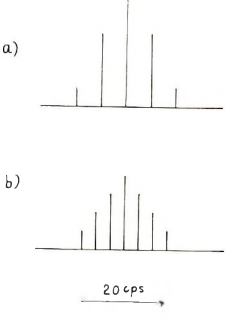

	J_{AK}	J_{AL}	J_{KL}	V_{LK}	J_{AM}	J_{AN}	J_{MN}	V_{NM}
a)	7	7	12	0	7	7	12	0
	7	7	12	12	7	7	12	12
	7	7	12	24	7	7	12	12
b)	4	4	12	0	8	8	12	0
	4	4	12	12	8	8	12	12
	4	4	12	24	8	8	12	12

Fig. 1. Spectra of A in $AKLMN$.

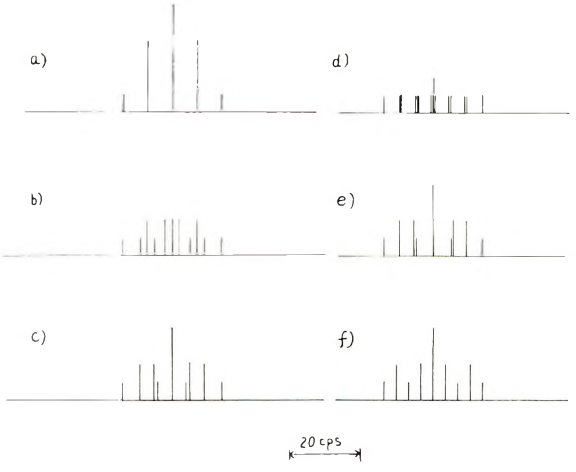

	J_{AK}	J_{AL}	J_{KL}	V_{LK}	J_{AM}	J_{AN}	J_{MN}	V_{NM}
a	2	12	12	0	2	12	12	0
b	2	12	12	6	2	12	12	0
c	2	12	12	6	2	12	12	6
d	2	12	12	12	2	12	12	6
e	2	12	12	12	2	12	12	12
f	2	12	12	24	2	12	12	24

Fig. 2. Spectra of A in $AKLMN$.

J_{AN}), regardless of the magnitude of individual spin coupling constant (cf. Figs. 1*b* and 5*a*). The relationship between chemical shifts and coupling constants are similar to the case of the quintet, and any diversion from the above conditions changes the heptet as shown in Figure 5. Figure 6 shows the effect of β proton chemical shifts on the spectrum, where all coupling constants between α and β protons have different values and no special relationship exists between them.

β Protons

The β proton spectrum has a maximum of 16 lines whose intensities vary over a wide range. Strictly speaking, the well known triplet of 1:2:1 appears only if all α protons are equivalent and all β protons are equivalent (cf. Fig. 7*a*). However, apparent triplets are observed if β protons have the same chemical shifts and $J_{AK} + J_{AL} = J_{BL} + J_{BK}$, where the individual coupling constants may, and are usually expected to, be different (cf. Figs. 8*a*, 9*a*, 10*a*, 11*a*, 12*a*, and 13*a*). Apparent triplets may be distinguished from real triplets by the presence of faint satellites. The difference in the chemical shifts of β protons causes spectral change even if all coupling constants are the same (cf. Fig. 7). This is in marked contrast to the spectrum

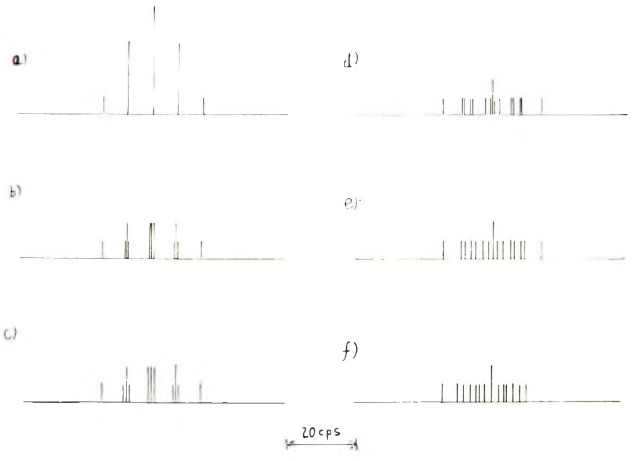

	J_{AK}	J_{AL}	J_{KL}	V_{LK}	J_{AM}	J_{AN}	J_{MN}	V_{NM}
(a)	6	8	12	0	4	10	12	0
(b)	6	8	12	6	4	10	12	0
(c)	6	8	12	12	4	10	12	0
(d)	6	8	12	12	4	10	12	6
(e)	6	8	12	12	4	10	12	12
(f)	6	8	12	24	4	10	12	24

Fig. 3. Spectra of A in $AKLMN$.

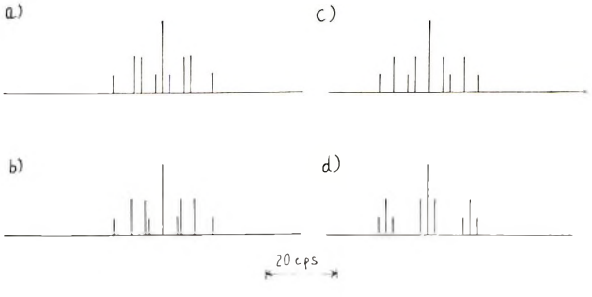

	J_{AK}	J_{AL}	J_{KL}	V_{LK}	J_{AM}	J_{AN}	J_{MN}	V_{NM}
(a)	6	6	12	0	8	8	12	0
	6	6	12	12	8	8	12	0
	6	6	12	12	8	8	12	24
(b)	5	5	12	0	9	9	12	0
(c)	4	4	12	0	10	10	12	0
(d)	2	2	12	0	12	12	12	0

Fig. 4. Spectra of A in $AKLMN$.

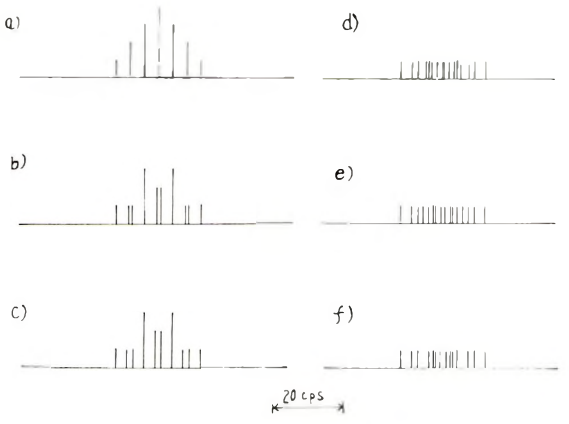

	J_{AK}	J_{AL}	J_{KL}	V_{LK}	J_{AM}	J_{AN}	J_{MN}	V_{NN}
(a)	3	5	12	0	6	10	12	0
(b)	3	5	12	6	6	10	12	0
(c)	3	5	12	12	6	10	12	0
(d)	3	5	12	12	6	10	12	6
(e)	3	5	12	12	6	10	12	12
(f)	3	5	12	24	6	10	12	24

Fig. 5. Spectra of A in $AKLMN$.

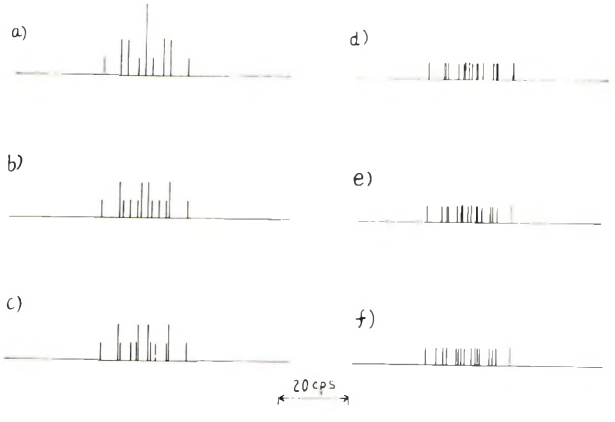

	J_{AK}	J_{AL}	J_{KL}	V_{LK}	J_{AM}	J_{AN}	J_{MN}	V_{NN}
(a)	5	9	12	0	4	6	12	0
(b)	5	9	12	6	4	6	12	0
(c)	5	9	12	12	4	6	12	0
(d)	5	9	12	12	4	6	12	6
(e)	5	9	12	12	4	6	12	12
(f)	5	9	12	24	4	6	12	24

Fig. 6. Spectra of A in $AKLMN$.

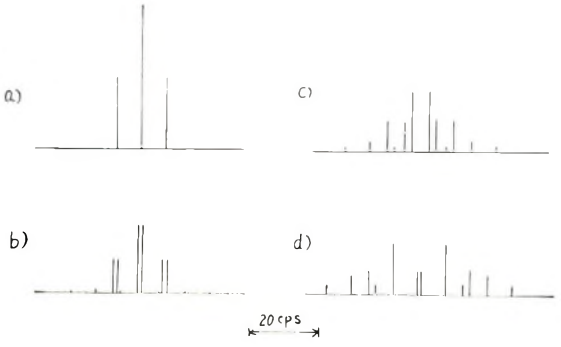

	J_{AK}	J_{AL}	J_{BK}	J_{BL}	J_{LK}	ν_{LK}
(a)	7	7	7	7	12	0
(b)	7	7	7	7	12	6
(c)	7	7	7	7	12	12
(d)	7	7	7	7	12	24

Fig. 7. Spectra of KL in $ABKL$.

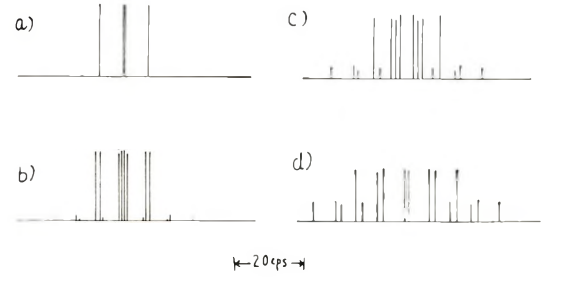

	J_{AK}	J_{AL}	J_{BK}	J_{BL}	J_{LK}	ν_{LK}
(a)	6	8	8	6	12	0
(b)	6	8	8	6	12	6
(c)	6	8	8	6	12	12
(d)	6	8	8	6	12	24

Fig. 8. Spectra of KL in $ABKL$.

of α protons. Apparent triplets with different coupling constants change the shape of the spectrum as their chemical shifts change (cf. Figs. 8–13). It is noticed that if the α protons located on either side of the β protons interact with the β protons in a similar manner (i.e., $J_{AK} = J_{BK}$, and $J_{AL} = J_{BL}$), the spectrum is asymmetric. Conversely if $J_{AK} = J_{BL}$, and $J_{AL} = J_{BK}$, the spectrum is symmetric (compare Fig. 8 with Fig. 9 and Fig. 10 with Fig. 11). These differences in symmetry can be useful for determining

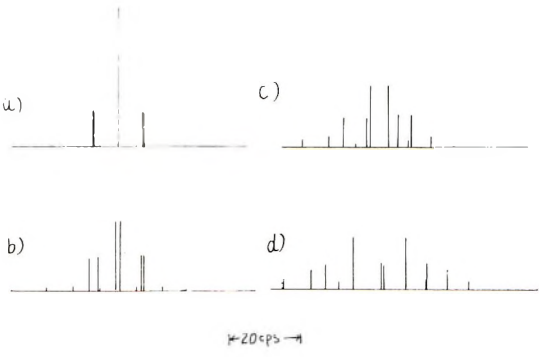

	J_{AK}	J_{AL}	J_{BK}	J_{BL}	J_{LK}	ν_{LK}
a)	6	8	6	8	12	0
b)	6	8	6	8	12	6
c)	6	8	6	8	12	12
d)	6	8	6	8	12	24

Fig. 9. Spectra of KL in $ABKL$.

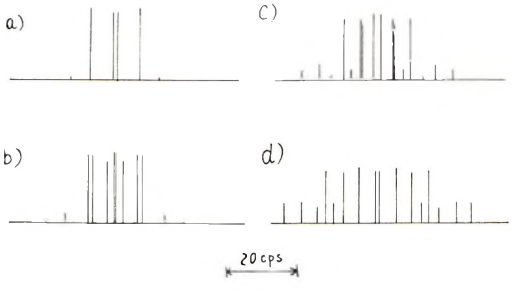

	J_{AK}	J_{AL}	J_{BK}	J_{BL}	J_{LK}	ν_{LK}
(a)	2	12	12	2	12	0
(b)	2	12	12	2	12	6
(c)	2	12	12	2	12	12
(d)	2	12	12	2	12	24

Fig. 10. Spectra of KL in $ABKL$.

the structure and conformational relationship between α and β protons if the chemical shift ν_{LK} is known. In a like manner, the chemical shift can be determined if the conformational relationship of α and β protons, through the magnitude of their coupling constants, is known. Figures 12 and 13 also show the spectral change with the reversion of β proton coupling on one side i.e., $J_{BK} \rightarrow J_{BL}$ and $J_{BL} \rightarrow J_{BK}$. Figure 14

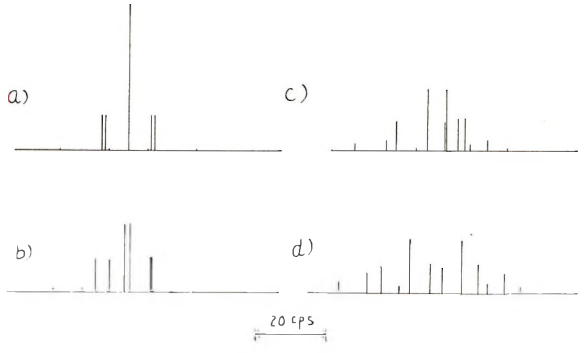

	J_{AK}	J_{AL}	J_{BK}	J_{BL}	J_{LK}	ν_{LK}
a)	2	12	2	12	12	0
b)	2	12	2	12	12	6
c)	2	12	2	12	12	12
d)	2	12	2	12	12	24

Fig. 11. Spectra of KL in $ABKL$.

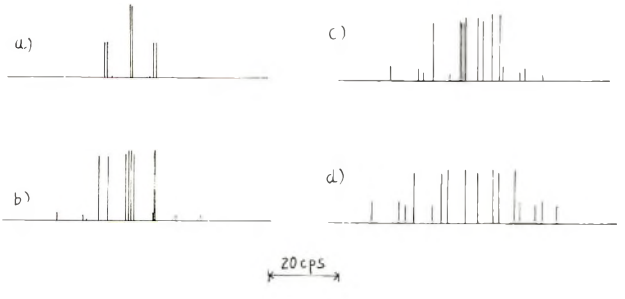

	J_{AK}	J_{AL}	J_{BK}	J_{BL}	J_{LK}	ν_{LK}
a)	4	10	6	8	12	0
b)	4	10	6	8	12	6
c)	4	10	6	8	12	12
d)	4	10	6	8	12	24

Fig. 12. Spectra of KL in $ABKL$.

applies where $J_{AK} = J_{AL} \neq J_{BK} = J_{BL}$, and if the chemical shift is the same, the spectrum consists of a double doublet. Figure 15 is expected for a certain syndiotactic case. When each coupling constant has a different value, and no special relationship exists among them, the spectra are as shown in Figure 16. If the chemical shift is the same for both β protons, the spectrum appears as a double doublet (cf. Figs. 15*a* and 16*a*). β proton

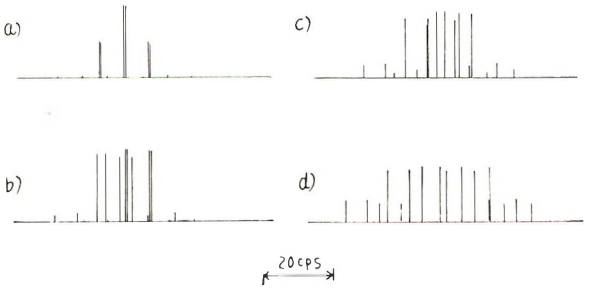

	J_{AK}	J_{AL}	J_{BK}	J_{BL}	J_{LK}	ν_{LK}
a)	4	10	8	6	12	0
b)	4	10	8	6	12	6
c)	4	10	8	6	12	12
d)	4	10	8	6	12	24

Fig. 13. Spectra of KL in $ABKL$.

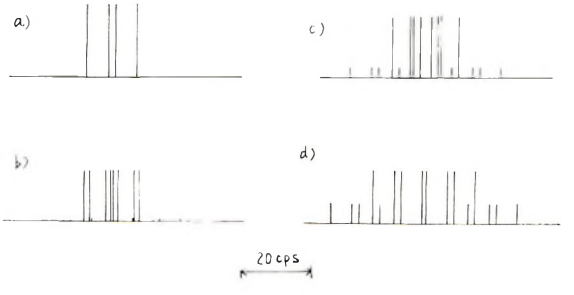

	J_{AK}	J_{AL}	J_{BK}	J_{BL}	J_{LK}	ν_{LK}
a)	6	6	8	8	12	0
b)	6	6	8	8	12	6
c)	6	6	8	8	12	12
d)	6	6	8	8	12	24

Fig. 14. Spectra of KL in $ABKL$.

spectra of real polymers may be the superposition of some of the above spectra as previously mentioned for α protons. Furthermore, it may be considered that the spectrum of β protons is the KL part of the $ABKL$ system and that K and L have different chemical shifts which may be different from those of MN. This means that spin decoupling of β protons from α protons may leave two or more residual lines for polymer solutions. In all of the above figures, the change of the geminal coupling constant of methyl-

ene protons is not illustrated because it seems to remain the same, regardless of the configurational and conformational change of the polymers in solution. The chemical shift of α protons was not considered because it results only in the shift of the whole α proton spectrum and does not result in a

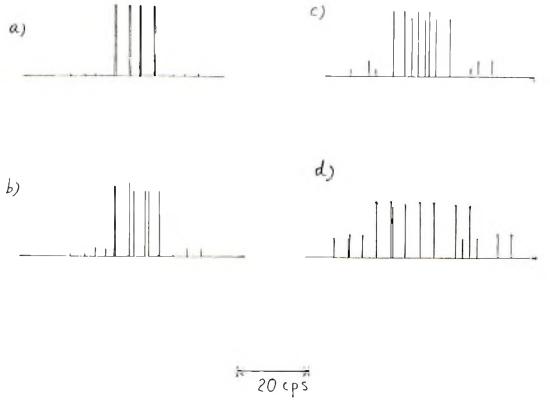

	J_{AK}	J_{AL}	J_{BK}	J_{BL}	J_{KL}	ν_{LK}
a	10	4	4	4	12	0
b	10	4	4	4	12	6
c	10	4	4	4	12	12
d	10	4	4	4	12	24

Fig. 15. Spectra of KL in $ABKL$.

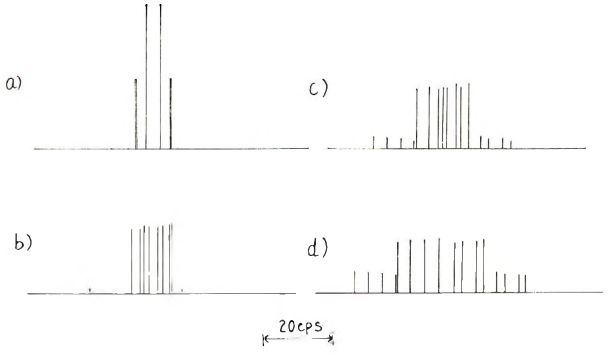

	J_{AK}	J_{AL}	J_{BK}	J_{BL}	J_{LK}	ν_{LK}
a)	2	4	6	8	12	0
b)	2	4	6	8	12	6
c)	2	4	6	8	12	12
d)	2	4	6	8	12	24

Fig. 16. Spectra of KL in $ABKL$.

change of shape. The effect of the sign of ν_{LK} and coupling constants were discussed in the previous paper.[6]

CONFIGURATION AND CONFORMATION

Experimental

NMR spectra were obtained at 60 Mc./sec. and line positions were determined by the sideband method. 2,4-Pentanediol and its diacetate and 2,4,6-heptanetriol and its triacetate were prepared and separated into individual isomers corresponding to isotactic (meso), syndiotactic (racemic), and heterotactic structures.[7] 2,4-Pentanediol diacetate (model compounds of PVAc dimer), and 2,4,6-heptanetriol triacetate (PVAc trimer) are viscous in bulk at room temperature, and resolution of the spectra is not sufficient to allow analysis. However they gave well resolved spectra in solution, and acetates were measured in 10 mole-% benzene solution and alcohols in pyridine solution of the same concentration.

PVAc Model Compounds

PVAc dimers gave the spectra shown in Figures 17 and 18; the methylene regions of these compounds belong to the types shown in Figures 9*c* and 10*a*, respectively. The assignment is also shown. The methylene signals show great differences in shape and symmetry according to the configuration, while signals of methine protons are nearly the same for both isomers. The enlarged methylene spectra in Figure 19 are compared with spectra calculated on the basis of the above mentioned procedure. The coupling constants and chemical shifts obtained by using only line positions were satisfactory. Trimers have similar spectra and are also analyzed. The results are shown in Table I. It is natural that parameters of dimers

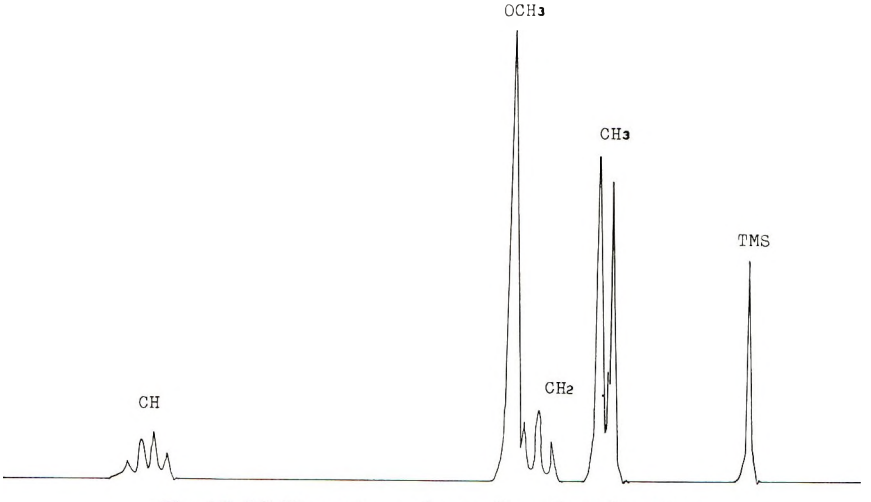

Fig. 17. NMR spectrum of a syndiotactic PVAc dimer.

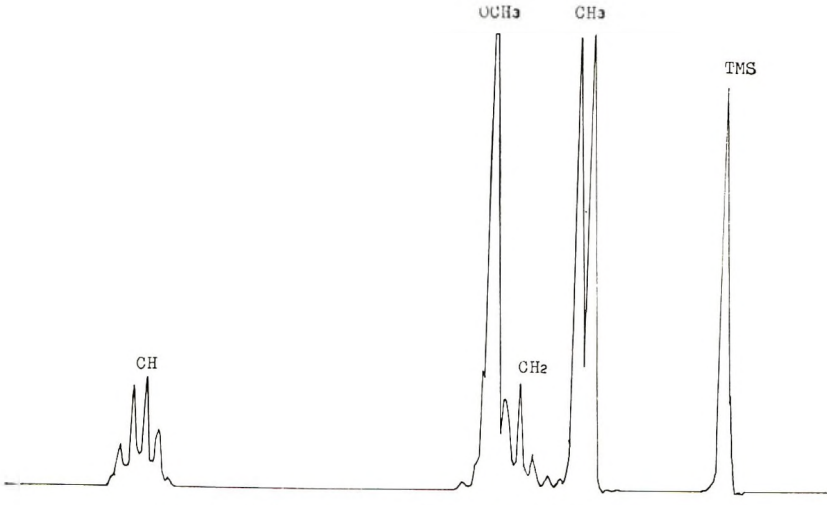

Fig. 18. NMR spectrum of an isotactic PVAc dimer.

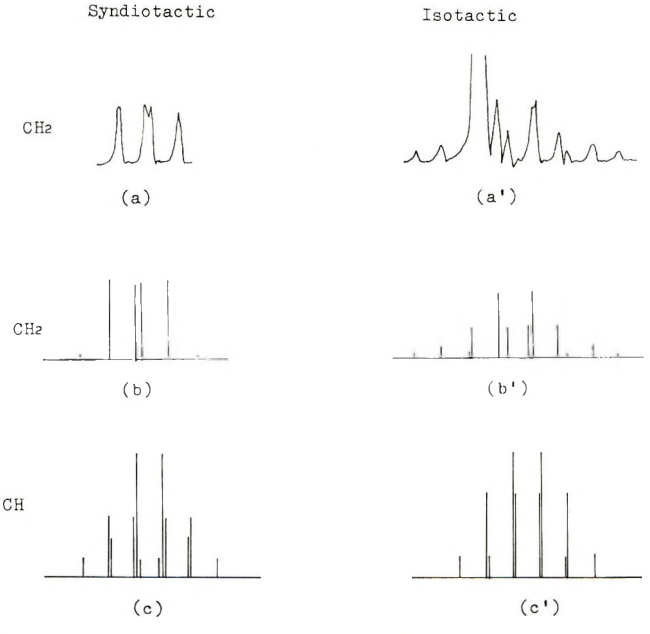

Fig. 19. NMR spectra of PVAc model compounds (dimer): (a, a') observed methylene spectra; (b, b') calculated methylene spectra; (c, c') calculated methine spectra.

are similar to those corresponding to trimers. There appear several features. First, methylene protons in syndiotactic dimer have the same chemical shifts, and those in isotactic dimer have different chemical shifts. This shows that the former has symmetry about the plane including carbons 2, 3, and 4 but the latter does not. Second, in syndiotactic dimer, $J_{AK} \neq J_{AL}$, and the difference is considerable, but is isotactic dimer $J_{AK} = J_{AL}$.

TABLE I
Coupling Constants and Chemical Shifts in PVAc Model Compounds

		J_{AK}	J_{AL}	J_{BK}	J_{BL}	J_{KL}	ν_{LK}	J_{AX}
Isotactic	Dimer	6.8	6.0	6.8	6.0	14.1	−16.3	6.5
	Trimer	6.8	5.7	6.8	5.7	14.1	−18.8	6.1
Syndiotactic	Dimer	10.1	3.6	3.6	10.1	14.1	0	6.4
	Trimer	10.1	3.3	3.3	10.1	14.1	14.1	6.6

This suggests that the conformation of the former is of a fixed form but that of the latter is due to rotation or vibration between two or more forms. This inference is in accord with the fact that for these compounds the same spin couplings between α and β protons must be small (say, 3 cycle/sec.) provided the conformation is fixed in single form where all vicinal protons are in gauche positions. Third, in syndiotactic dimer $J_{AK} = J_{BL}$ and $J_{AL} = J_{BK}$ and hence the spectrum is symmetric, while in isotactic dimer $J_{AK} = J_{BK}$ and $J_{AL} = J_{BL}$, and the spectrum is asymmetric. This indicates that the syndiotactic dimer has a point symmetry with respect to the methylene carbon and the latter has a reflective symmetry about the plane including methylene. Nine conformations are possible for these dimers, but the above three facts exclude most of those. Syndiotactic dimers should have one of the conformations shown in Figure 20, where one conformation corresponds to a planar zigzag chain, and the other to a helical chain of four units per turn. Considering that the spectra of syndiotactic trimers of the type shown in Figure 10*b* are close to those of dimers and that the helical conformation should have a chain in the sequence of *gauche-gauche-trans-trans* or *t-t-g-g*, a planar zigzag may be the only

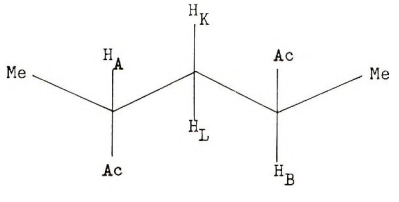

(I)

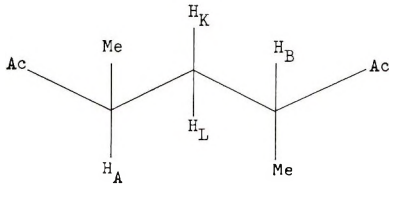

(II)

Fig. 20. Conformations of a syndiotactic PVAc model compound.

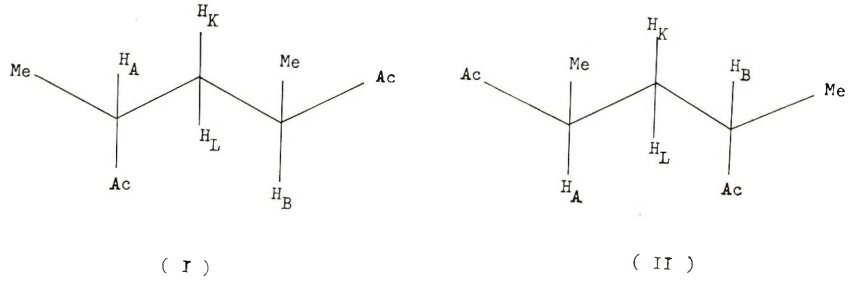

Fig. 21. Conformations of an isotactic PVAc model compound.

possible conformation for syndiotactic PVAc. The chemical shift which appeared in trimers is due to the asymmetry of the structure with respect to methylene protons and may disappear in polymers as in dimer. Isotactic dimers may have both the conformations shown in Figure 21, which correspond to right, and left-handed helices, with the same residence time in each. The molecule undergoes rapid exchange between the two conformations. The rate of exchange should be much faster than 10^{-2} sec., since the spectra are spread over approximately a 50 cycle/sec. range, and lines are as sharp as in other parts of the spectrum. Isotactic trimers may have combination of half right-handed, and half left-handed helices as well as pure right- and left-handed helices. This results in increasing magnitude of the difference between the two couplings between α and β protons. Conformations determined thus are reasonable, since repulsive forces exist between side chain groups in these molecules. Configurations are easily determined by the difference in chemical shifts of methylene protons. The spectrum of heterotactic trimers can be interpreted as a combination of isotactic and syndiotactic parts.

PVA Model Compounds

PVA dimers gave different spectra in the α and the β proton region, as shown in Figure 22, where calculated spectra are also included. The methylene spectra belong to the type of Figures 8*a* and 10*c*. Again, agreement between observed and calculated spectra was found to be satisfactory. The results of analysis are in Table II. Considerations of symmetry and

TABLE II
Coupling Constants and Chemical Shifts in PVA Model Compounds

		J_{AK}	J_{AL}	J_{BK}	J_{BL}	J_{AX}	J_{KL}	ν_{LK}
Syndiotactic	Dimer	7.0[a]	5.1[a]	5.1[a]	7.0[a]	6.2	(14.3)	0
	Trimer	7.0	4.6	4.6	7.0	6.1	14.1	± 3.6
Isotactic	Dimer	9.4	3.7	9.4	3.7	6.2	14.3	15.5
	Trimer	8.6	3.8	8.6	3.8	6.2	14.1	11.4

[a] Values with of error ±1.0 c./sec.; other data carry experimental error of ±0.5 c./sec.

motion lead to the conclusion that isotactic dimers and trimers have a planar zigzag conformation, and syndiotactic dimers take the forms of both right- and left-handed helices of *t-g-t-g'* type. Syndiotactic trimers may have a mixture of both types of helices, as well as either type of pure helices. The methylene spectrum of isotactic trimers belongs to the type of Figure 8*b*, where the chemical shift of β protons may be attributed to the

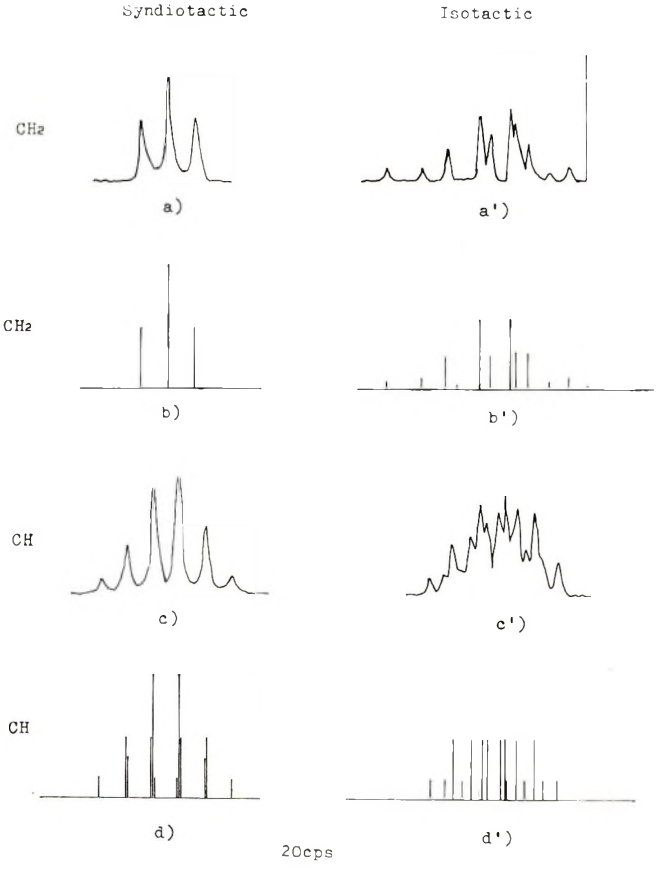

Fig. 22. NMR spectra of PVA model compounds (dimer): (a, a') observed methylene spectra; (b, b') calculated methylene spectra; (c, c') observed methine spectra; (d, d') calculated methine spectra.

asymmetry of the molecule with respect to the methylene. The spectrum of isotactic polymer seems to be more similar to that of dimers than trimers because of the symmetry. Heterotactic trimers may be interpreted as a superposition of isotactic and syndiotactic parts. These conformations are reasonable because of attraction between the side chain groups. Configurations can be distinguished through chemical shifts of methylene protons.

CONCLUSION

The analysis of the NMR spectra of vinyl polymers is discussed. Normal triplets for β protons and quintets for α hydrogens do not necessarily mean that α protons and β protons are equivalent. α protons have a symmetric form, consisting of 36 lines, and β protons an asymmetric or symmetric form of 16 lines, without superposition of different sets. Expected spectra for common vinyl polymers are shown. Conformations and configurations can be determined by the complete analysis of the spectra of vinyl polymers. Examples are shown for poly(vinyl alcohol) and poly(vinyl acetate) by using model compounds; this avoids the poor resolution of spectra obtained for polymer solutions.

The authors wish to thank Dr. Osame Yamamoto of the Government Chemical Industrial Research Institute, and Dr. Ichiro Yamaguchi and Mr. Naohiro Hayakawa of the Japan Atomic Energy Institute for their aid in obtaining NMR spectra. Thanks are also due to Dr. Shoichi Matsumoto for his encouragement of this work.

References

1. Bovey, F. A., and G. V. D. Tiers, *J. Polymer Sci.*, **44**, 173 (1960).
2. Nishioka, A., H. Watanabe, I. Yamaguchi, and H. Shimizu, *J. Polymer Sci.*, **45**, 232 (1960).
3. Bovey, F. A., E. W. Anderson, and D. C. Douglass, *J. Chem. Phys.*, **39**, 1199 (1963).
4. Stehling, F. C., *J. Polymer Sci. A*, **2**, 1815 (1964).
5. Brownstein, S., and D. M. Wiles, *J. Polymer Sci. A*, **2**, 1901 (1964).
6. Fujiwara, Y., and S. Fujiwara, *Bull. Chem. Soc. Japan*, **37**, 1005 (1964).
7. Fujii, K., *J. Polymer Sci. B*, **3**, 375 (1965).

Résumé

Les spectres complexes de RMN de polymères vinyliques fournissent des informations concernant la conformation et la configuration des polymères en solution. On a obtenu l'expression explicite des fréquences et intensités spectrales par l'analyse des polymères vinyliques et leurs composés modèles en tant que systèmes faiblement couplés. On présente les spectres classifiés prévus pour les polymères vinyliques communs en utilisant les résultats de l'analyse. On applique l'analyse des composés modèles de l'alcool polyvinylique et de l'acétate de polyvinyle en solution. Les résultats montrent que les conformations de l'alcool polyvinylique sont déterminées par les liaisons hydrogènes intramoléculaires de sorte que l'isomère syndiotactique forme une hélice alpha et l'isotactique des structures planaires en zigzag et que, dans l'acétate de polyvinyle, la répulsion des chaînes latérales conduit à une structure hélicoïdale pour le polymère isotactique et un zigzag planaire pour le syndiotactique.

Zusammenfassung

Komplizierte NMR-Spektren von Vinylpolymeren liefern Angaben über die Konformation und Konfiguration der Polymeren in Lösung. Explizite Ausdrücke für die Frequenzen und Intensitäten der Spektren werden durch die Analyse von Vinylpolymeren und ihren Modellverbindungen als schwach gekoppelte Systeme erhalten. Eine Liste der unter Verwendung der Ergebnisse der Analyse erwarteten Spektren der üblichen Vinylpolymeren wird vorgelegt. Die Analyse wird auf Modellverbindungen für Polyvinylalkohol und Polyvinylacetat in Lösung angewandt. Die Ergebnisse zeigen, dass die Konformation von Polyvinylalkohol durch intramolekulare Wasserstoffbindungen

bestimmt ist; so bildet das sydiotaktische Isomere eine Helix- und das isotaktische eine ebene Zickzackstruktur. Bei Polyvinylacetat führt die Abstossung der Seitenketten zu einer Helixstruktur für das isotaktische Isomere und zu einer ebenen Zickzackstruktur für das syndiotaktische.

Received July 15, 1964
Revised February 9, 1965
Prod. No. 4648A

JOURNAL OF POLYMER SCIENCE: PART A-1 VOL. 4, 275-282 (1966)

Polymerization with Organoboron Compounds

F. S. ARIMOTO, *Jackson Laboratory, Organic Chemicals Department, E. I. du Pont de Nemours and Company, Inc., Wilmington, Delaware*

Synopsis

In the presence of organoboron compounds, free-radical polymerization of vinyl monomers can proceed in spite of the presence of excess of typical radical inhibitors. The concept of free radical–organoboron complex formation is introduced to explain the unique role of organoboron compounds in such a polymerization system.

Polymerization of vinyl monomers with trialkylboron compounds was first reported by Kolesnikov[1] and Furukawa.[2] It was originally suggested that trialkylboron brought about polymerization by an anionic mechanism.[2] Fordham and Sturm,[3] however, have definitely established on the basis of copolymerization studies and on the types of vinyl monomers polymerized that the polymerization of vinyl monomers by trialkylboron compounds was a free-radical process. Most of the experiments reported indicate the necessity of peroxidation of trialkylborons for the polymerization to take place.[4–6] The polymerization-initiating radicals can then arise from homolysis of peroxyborons[7,8] or by the redox reaction of the peroxyboron with unoxidized trialkylborons.[9–11]

This paper describes the free-radical polymerization of vinyl monomers in the presence of substantial amounts of typical free radical inhibitors when organoboron compounds are present. Free radical–organoboron complex formation is postulated in the propagation step.

Experimental

Polymerizations in limited access to air were carried out in 20 × 70 mm. screw-cap vials. A 10-ml. portion of monomer containing 1.5 wt.-% of inhibitor was used for each run. A measured amount (0.2 ml.) of tri-*n*-butyl boron (0.8 mmole) or tri-*n*-hexylboron (0.5 mmole) was added by means of a hypodermic syringe. From the consideration of the volume of air present in the vial, the molar ratio of oxygen to trialkylboron is 0.12 for tri-*n*-butyl boron and 0.18 for tri-*n*-hexyl-boron. The amount of oxygen present is thus sufficient to initiate the polymerization by interaction with trialkylboron, but the ratio is such that enough unoxidized trialkylboron will remain in the system. After addition of organoboron compound, the vial was shaken and allowed to stand. The progress of the polymerization was followed by noting the increase in the viscosity of the system.

TABLE I
Polymerizations with Trialkylborons in Presence of Inhibitors
(Limited Access to Air)

No.	Monomers polymerized	Inhibitor	Inhibitor concn., wt.-% and mole/l.	R_3B	R_3B concn., wt.-% and mole/l.	Inhibitor R_3B
1	Methyl methacrylate (MMA) Styrene (St) Vinyl acetate (VA) Acrylonitrile (AN)	*p*-Phenylenediamine	1.5; 0.16	R = *n*-hexyl	1.5; 0.05	3.2
2	MMA	Di-*p*-aminodiphenylamine	1.5; 0.08	R = *n*-hexyl	1.5; 0.05	1.6
3	MMA, St, AN	*N*-Phenyl-1-naphthylamine	1.5; 0.07	R = *n*-butyl	1.5; 0.08	0.9
				R = *n*-hexyl	1.5; 0.05	1.4
4	St, VA, AN	*N*-Phenyl-2-naphthylamine	1.5; 0.07	R = *n*-butyl	1.5; 0.08	0.9
				R = *n*-hexyl	1.5; 0.05	1.4
4a	MMA	*N*-Phenyl-2-naphthylamine	10.0; 0.46	R = *n*-hexyl	0.75; 0.03	15.3
5	MMA, St, AN	Hydroquinone	1.5; 0.14	R = *n*-butyl	1.5; 0.08	1.7
				R = *n*-hexyl	1.5; 0.05	2.8
6	MMA, St, AN	*p*-Benzoquinone	1.5; 0.14	R = *n*-butyl	1.5; 0.08	1.7
				R = *n*-hexyl	1.5; 0.05	2.8
7	MMA, St, AN	Catechol	1.5; 0.14	R = *n*-hexyl	1.5; 0.05	2.8
8	MMA, St, AN	4-*tert*-Butylcatechol	1.5; 0.09	R = *n*-butyl	1.5; 0.08	1.1
				R = *n*-hexyl	1.5; 0.05	1.8
9	MMA, VA, AN	2,6-Di-*tert*-butyl-*p*-cresol	1.5; 0.07	R = *n*-butyl	1.5; 0.08	0.9
				R = *n*-hexyl	1.5; 0.05	1.4
9a	MMA	2,6-Di-*tert*-butyl-*p*-cresol	10.0; 0.48	R = *n*-hexyl	1.5; 0.05	9.6
10	St, AN	Phenothiazine	1.5; 0.08	R = *n*-butyl	1.5; 0.08	1.0
				R = *n*-hexyl	1.5; 0.05	1.6
10a	MMA	Phenothiazine	10.0; 0.50	R = *n*-hexyl	0.75; 0.03	16.7

Polymerizations in the absence of oxygen were carried out in sealed tubes; 20 ml. of monomer with dissolved inhibitor was placed in a constricted polymer tube (20 mm. O.D.) and degassed by alternate freezing and thawing (3×). Helium was used as the replacement atmosphere. With triarylborons, the compounds were dissolved in the monomer before placing in the tube. With trialkylborons, addition was made to the degassed monomer through a rubber serum vial stopper by means of a hypodermic syringe and needle. The polymer tubes were sealed while under vacuum. Polymers were precipitated by pouring into methanol, washed, dried, and weighed.

Peroxyboron compounds were prepared by allowing trialkylborons to react with oxygen at 0°C. until absorption of oxygen ceased. The peroxyboron compounds were used without further purification.

Results and Discussion

One of the generally accepted criteria used to characterize a free-radical chain process is the susceptibility of the reaction system to small amounts of inhibitors which are either stable free radicals or acceptors of free radicals.[12] Experiments summarized in Table I show that polymerization of methyl methacrylate, styrene, vinyl acetate, and acrylonitrile by trialkylborons in limited access to air proceed in the presence of substantial amounts of a variety of free radical polymerization inhibitors. Since the primary interest in this work was in the demonstration of the phenomenon of polymerization in the presence of inhibitors, very little work was done on the quantitative aspects of the polymerization reaction or in the characterization of the polymers obtained. However, in one case in which the resultant polymer was analyzed, that of poly(methyl methacrylate) obtained in the presence of hydroquinone with tri-*n*-hexyl boron, the analysis indicated formation of high molecular weight polymer. The poly(methyl methacrylate) thus obtained had intrinsic viscosity of 2.55 (0.5% in $CHCl_3$), indicating a weight-average molecular weight of 1.4×10^6 and a number-average molecular weight of 0.6×10^6. The amount of inhibitors used in the experiments summarized in Table I was arbitrarily chosen at 1.5 wt.-%. However, with several selected inhibitors, *N*-phenyl-2-naphthylamine (4a), 2,6-di-*tert*-butyl-*p*-cresol (9a), and phenothiazine (10a), 10 wt.-% of the inhibitors was employed to demonstrate the inertness of these inhibitors, even when present in considerable excess, to the polymerization of methyl methacrylate in the presence of trialkylborons. It should be noted that the molar ratio of inhibitor to trialkylboron in these cases is 15.3, 9.6, and 16.7, respectively. Characteristically, polymerization of these monomers in the presence of inhibitors initiated by the trialkylboron–oxygen system proceeds with no induction period, as indicated by the immediate increase in the viscosity of the system. The absence of induction periods and the excess of inhibitors present in comparison to the trialkylborons used indicate that the depletion of inhibitors by the radicals is not the reason that the polymerization can proceed in these systems.

TABLE II
Polymerization of Methyl Methacrylate with Peroxyboron Compound
(25°C., 15 hr.)

Initiating system[a]	Initiator concn., mole/l.	Inhibitor	Inhibitor concn., mole/l.	Polymer formation
R_2BOOR	0.11	None	—	Solid polymer
R_2BOOR	0.11	Hydroquinone	0.05	None
R_2BOOR	0.11	Phenothiazine	0.03	None
$R_2BOOR + R_3B$	0.05 0.05	Hydroquinone	0.05	Solid polymer
$R_2BOOR + R_3B$	0.05 0.05	Phenothiazine	0.03	Solid polymer

[a] R = *n*-hexyl.

TABLE III
Polymerization of Inhibited Methyl acrylate with AIBN in Presence of Trialkylboron
(Absence of Oxygen) (70°C., 3 hr.)

Initiating system[a]	Initiator concn., wt.-% and mole/l.	Inhibitor	Inhibitor concn., wt.-% and mole/l.	Inhibitor/ initiator	Conversion
AIBN	1.0; 0.06	Phenothiazine + hydroquinone	1.0; 0.05 1.0; 0.09	2.3	0
R_3B	1.0; 0.04	Phenothiazine + hydroquinone	1.0; 0.05 1.0; 0.09	3.8	0
AIBN + R_3B	1.0; 0.06 1.0; 0.04	Phenothiazine + hydroquinone	1.0; 0.05 1.0; 0.09	1.4	~100

[a] R = *n*-hexyl.

As has been mentioned earlier and reported by various investigators,[6,13] oxidation of trialkylborons with oxygen leads to peroxyborons of the type R_2BOOR. Some polymerization experiments with peroxidized tri-*n*-hexylboron are summarized in Table II. The results show that polymerization of methyl methacrylate is brought about by homolysis of peroxyboron and that such polymerization is susceptible to the effects of inhibitors. However, addition of unoxidized tri-*n*-hexylboron to the peroxyboron–monomer system allows the polymerization to proceed in the presence of inhibitors. These results indicate a unique role of unoxidized trialkylboron in a free-radical polymerization system.

If unoxidized trialkylboron, by its presence, permits the polymerization to proceed in the presence of inhibitors, then its function appears to be independent of its possible role as a part of the initiating system. Radicals independently generated in the presence of unoxidized trialkylboron should then be capable of polymerizing monomers in the presence of inhibitors.

TABLE IV
Polymerization of Inhibited Methyl Methacrylate in Presence of Triarylborons (70°C., 3 hr.)

Initiating system[a]	Initiator concn., wt.-% and mole/l.	Inhibitor	Inhibitor concn., wt.-% and mole/l.	Conversion, %
Triphenylboron (TPB)				
AIBN	1.0; 0.06	Phenothiazine	1.0; 0.05	0
TPB	1.0; 0.04	Phenothiazine	1.0; 0.05	0
AIBN + TPB	0.5; 0.03 / 1.0; 0.04	Phenothiazine	1.0; 0.05	36
Tri-α-naphthylboron (TNB)				
TNB	3.0; 0.08	Phenothiazine	1.0; 0.05	0
AIBN	1.0; 0.06	+ hydroquinone	1.0; 0.14	
TNB	3.0; 0.08	Phenothiazine + hydroquinone	1.0; 0.05 / 1.0; 0.14	64
Bz_2O_2	0.5; 0.02	2,6-Di-*tert*-butyl-*p*-cresol	1.0; 0.05	0
TNB	1.0; 0.03	2,6-Di-*tert*-butyl-*p*-cresol	1.0; 0.05	0
Bz_2O_2 + TNB	0.5; 0.02 / 1.0; 0.03	2,6-Di-*tert*-butyl-*p*-cresol	1.0; 0.05	12
Trimesitylboron (TMB)				
AIBN + TMB	1.0; 0.06 / 3.0; 0.08	Phenothiazine	1.0; 0.05	0

[a] AIBN = azobisisobutyronitrile; Bz_2O_2 = benzoyl peroxide.

Experimental results summarized in Table III show that such is the case. In the presence of phenothiazine and hydroquinone as inhibitors, neither azobisisobutyronitrile (AIBN) nor tri-*n*-hexylboron in the absence of oxygen did polymerize methyl acrylate. Radicals generated by thermolysis of AIBN cannot polymerize methyl acrylate in the presence of inhibitors. Presumably, with tri-*n*-hexylboron in the absence of oxygen, no generation of radicals takes place. It should be noted that introduction of small amount of air to the methyl acrylate–inhibitor–tri-*n*-hexylboron system causes immediate and vigorous polymerization to take place. When radicals were generated from AIBN in the presence of tri-*n*-hexylboron in the absence of oxygen, vigorous polymerization took place even in the presence of inhibitors.

The part played by trialkylboron compounds in the free-radical polymerization in the presence of inhibitors is also shown by certain triarylborons as indicated in Table IV. Generally, very little or no polymerization of methyl methacrylate takes place with triarylborons, with or without oxygen. In the presence of small amount of inhibitor, no polymerization has been observed. As Table IV indicates, polymerization of methyl methacrylate occurs in the presence of inhibitors when radicals are generated by thermal decomposition of AIBN or benzoyl peroxide if triphenylboron or tri-α-naphthylboron is present. However, no such polymerization occurs in the presence of trimesitylboron.

Mechanism

Polymerization of vinyl monomers by the trialkylboron–oxygen initiating system is a free-radical process. Copolymerization of an equimolar mixture of methyl methacrylate and styrene with tri-*n*-butylboron–oxygen gave a copolymer with methyl methacrylate content of 49 mole-%, in agreement with results of Fordham and Sturm.[3] The possibility that polymerization by trialkylborons proceeds in the presence of inhibitors because of depletion or removal of inhibitors by trialkylborons may be eliminated because of the absence of induction periods and the stoichiometry of the reagents involved, a large excess of inhibitors to trialkylborons being used.

The possibility that peroxyboron offers a unique initiating system may also be eliminated, since polymerization initiated solely by peroxyboron is readily susceptible to the action of inhibitors. Regardless of the nature of initiating radical, once the polymerization is started, the nature of propagating chain should be identical and should behave similarly for a given monomer.

The only consistent and reasonable explanation to account for the polymerization of vinyl monomers in the presence of inhibitors when organoboron compounds are present is that the propagating free radical is complexed with the electronically deficient boron atom of the organoboron molecule. The presence of unoxidized organoboron compounds is necessary for the polymerization to proceed in the presence of inhibitors.

Peroxyboron presumably does not form a radical complex of sufficient stability because of back-coordination of the boron atom with the electrons of the adjacent oxygen atom.

In the cases of polymerizations in the presence of excess amine inhibitors, a question may be raised regarding the availability of trialkylborons for complexing with the growing free radicals in view of possible prior complexing of the trialkylborons with the amine inhibitors present in excess. However, such possibility may be eliminated, since not only are the amine inhibitors employed (e.g., *N*-phenyl-2-naphthylamine, phenothiazine) very weak bases but, more significantly, steric considerations with respect to the amines and the trialkylborons used preclude the formation of such amine–trialkylboron complexes to any extent. The possibility of amine inhibitor–organoboron complex formation is even more remote in the cases of triarylborons.

In those experiments where radicals were generated by thermal decomposition of AIBN or by benzoyl peroxide, the polymerization reaction was completely stopped by the inhibitors present. However, when the same radicals were generated in the presence of unoxidized organoboron compounds, polymerization proceeded in the presence of inhibitors because the propagating radicals were complexed with the organoboron compound. The failure of trimesitylboron, in contrast to triphenyl- and tri-α-naphthylborons, to allow polymerization to proceed in the presence of inhibitors is significant. Brown and Dodson[14] have shown that, while triphenylboron and tri-α-naphthylboron will form addition compounds with ammonia and with methoxide ion and will undergo oxidation with oxygen, trimesitylboron is completely inert to these reagents. The difference in reactivity is explained on the basis of steric hindrance around the boron atom, which in the case of trimesitylboron is completely enclosed within a cage of three phenyl rings and the six *o*-methyl groups such that no reaction is possible without disruption of this protecting cage.

The steps involved in the propagation may be written as in eqs. (1)–(3).

$$—C—C—\cdot + BR_3 \rightarrow \underset{\text{I}}{[—C—C\cdot BR_3]} \tag{1}$$

$$[—C—C\cdot BR_3] + C{=}C \rightarrow \underset{\text{II}}{\left[\begin{array}{l} —C—C\cdot\ \ \cdot BR_3 \\ \qquad\ \ \cdot\ \ \cdot \\ \qquad\ \ \cdot\ \ \cdot \\ \qquad C——C \end{array}\right]} \tag{2}$$

$$\underset{\text{II}}{\left[\begin{array}{l} —C—C\cdot\ \ \cdot BR_3 \\ \qquad\ \ \cdot\ \ \cdot \\ \qquad\ \ \cdot\ \ \cdot \\ \qquad C——C \end{array}\right]} \rightarrow \underset{\text{III}}{[—C—C—C—C\cdot BR_3]} \tag{3}$$

The formation of organoboron radical complex (I) should be essentially irreversible; otherwise, the polymerization will be susceptible to inhibition.

The formation of a four-centered intermediate (II), which collapses to a new organoboron radical complex (III), accounts for the chain propagation. In the propagation step outlined above, the reaction of the propagating radical chain, because of complex formation with organoboron compound, is altered from that of a usual radical to that of a radical complex. (A study of reactions of simple free radical–organoboron complex will be published elsewhere.) The four-centered intermediate (II), should lead to polymers which are more stereoregular than the randomly oriented polymers formed in the usual free radical process. Furukawa[15] and Welch[16] have shown that poly(vinyl chloride) and poly(vinyl fluoride) formed by polymerization with trialkylborons have a considerably higher degree of stereoregularity than the corresponding polymers produced by the conventional free-radical processes.

References

1. Kolesnikov, G. S., and N. V. Klimentova, *Izv. Akad. Nauk SSSR*, **1957**, 652.
2. Furukawa, J., T. Tsuruta, and S. Inoue, *J. Polymer Sci.*, **26**, 234 (1957).
3. Fordham, J. W. L., and C. L. Sturm, *J. Polymer Sci.*, **33**, 503 (1958).
4. Ashikari, N., and N. Nishimura, *J. Polymer Sci.*, **31**, 249 (1958).
5. Furukawa, J., and T. Tsuruta, *J. Polymer Sci.*, **28**, 227 (1958).
6. Zutty, N. L., and F. J. Welch, *J. Polymer Sci.*, **43**, 445 (1960).
7. Inoue, S., T. Tsuruta, and J. Furukawa, *Makromol. Chem.*, **40**, 13 (1961).
8. Mirviss, S. B., *J. Am. Chem. Soc.*, **83**, 3051 (1961).
9. Bawn, C. E., H. D. Margerison, and N. M. Richardson, *Proc. Chem. Soc.*, **1959**, 397.
10. Welch, F. J., *J. Polymer Sci.*, **61**, 243 (1962).
11. Hansen, R. L., and R. R. Hamann, *J. Phys. Chem.*, **67**, 2868 (1963).
12. Walling, C., *Free Radicals in Solution*, Wiley, New York, 1957, p. 36.
13. Davies, A. G., and D. G. Hare, *J. Chem. Soc.*, **1959**, 438.
14. Brown, H. C., and V. H. Dodson, *J. Am. Chem. Soc.*, **79**, 2302 (1957).
15. Furukawa, J., and T. Tsuruta, *Kogyo Kagaku Zasshi*, **61**, 1362 (1958).
16. Welch, F. J., U. S. Pat. 3,112,298 (1963).

Résumé

En présence de composés organoboriques, la polymérisation radicalaire de monomères vinyliques peut avoir lieu même si on introduit des inhibiteurs typiques de réaction radicalaire. Afin d'expliquer le rôle unique joué par les composés organoboriques dans cette polymérisation, on suggère la formation d'un complexe entre le radical libre et le dérivé organoborique.

Zusammenfassung

In Gegenwart von Organoborverbindungen kann die radikalische Polymerisation von Vinylmonomeren auch in Anwesenheit eines Überschusses typischer Radikalinhibitoren stattfinden. Zur Erklärung der eigenartigen Rolle der Organoborverbindungen in einem solchen Polymerisationssystem wird die Annahme einer Komplexbildung zwischen freien Radikalen und der Organoborverbindung eingeführt.

Received September 25, 1964
Revised April 16, 1965
Prod. No. 4739A

JOURNAL OF POLYMER SCIENCE: PART A-1 VOL. 4, 283–291 (1966)

Short-Chain Branching in γ-Radiation-Induced Polymerization of Ethylene

SUEO MACHI, TAKASHI TAMURA, MIYUKI HAGIWARA, MASAO GOTODA, and TSUTOMU KAGIYA, *Japan Atomic Energy Research Institute, Takasaki Radiation Chemistry Establishment, Gunnanmura, Gunma, Japan*

Synopsis

In an attempt to elucidate the mechanism of chain-branch formation in the polymerization of ethylene, the effect of reaction conditions on short-chain branching in γ-radiation-induced polymerization of ethylene was investigated by using infrared spectroscopy. The concentration of methyl groups, i.e., the frequency of short-chain branching, increases with temperature and pressure and is independent of ethylene conversion to polymer and radiation intensity. The number of methyl groups per polymer molecule increases almost proportionally with the degree of polymerization. These facts indicate that short-chain branching occurs mainly by the mechanism of intramolecular hydrogen transfer. The effect of pressure on the rate of chain branching can be postulated by considering the transition state to be six-membered rings in hydrogen transfer reactions. The activation energy of chain branching is found to exceed that of propagation by 6 kcal./mole.

Introduction

Several papers have been published on the branched structure of conventional high-pressure polyethylene.

Roedel[1] pointed out that two types of branching could arise in the free-radical polymerization of ethylene: one is the branching which occurs as a result of intermolecular chain transfer and leads to long-chain branching; the other arises by intramolecular hydrogen transfer through formation of a transient ring structure. Morrel[2] reported that the degree of chain branching increases with reaction temperature and with ethylene conversion in high-pressure polymerization. Willborn[3] showed a method of measuring the number and length of branches; the branches were almost ethyls and butyls. More recently, Boyle et al.[4] obtained similar results which supported the theory of multiple intramolecular hydrogen transfer.

It was reported by Steinberg et al.[5] that the polyethylene produced by γ-radiation-induced polymerization has several types of chain branching. Few papers, however, have been published on the structure of polyethylene produced by γ-radiation.

The present paper is concerned with the effect of reaction conditions on the chain branching in the γ-ray radiation polymerization of ethylene in

bulk under intermediate pressure at a radiation intensity of 10^4–10^5 rad/hr.; the main purpose is to elucidate the mechanism of chain branching.

Experimental

The polymers were prepared under various conditions, in the pressure range of 70–400 kg./cm.^{2}, at temperatures of 20–200°C., dose rates of 10^4–4×10^5 rad/hr. and irradiation times of 0.5–5.0 hr. Polymerization was carried out in bulk.

The solution viscosity of the polymers in tetralin at 130°C. was measured, and the number-average molecular weight of the polymers was estimated by Tung's equation:[6]

$$[\eta] = 5.10 \times 10^4 \bar{M}_n^{0.725}$$

The methyl content of the polymers was determined from the absorption spectrum at 1378 cm.$^{-1}$ according to the directions of Bryant and Voter.[7] For infrared analysis and density measurement, the samples were hot-pressed into films of ca. 0.2 mm. thickness, quenched to room temperature for 15 min. and subsequently kept at room temperature in a desiccator for more than 24 hr. The infrared absorption spectra were measured with a Nippon-Bunko Model DS301 infrared spectrophotometer using NaCl optics. The polymer density was determined by the gradient-tube method at 23°C. with the use of a water–methanol mixed solution. In this paper the degree of short chain branching is considered to correspond to the concentration of methyl groups in polymer side chains.

Results

All experimental results are summarized in Table I.

The number of methyl groups per 1000 carbon atoms is plotted against the ethylene conversion to polymer in Figure 1. It is clear that the degree of short-chain branching is not influenced by the conversion up to 5% conversion. The degree of branching is also found to increase with ethylene pressure. Figure 2 indicates that the methyl content increases rapidly with polymerization temperature at a pressure of 390 kg./cm.^{2}. It is characteristic that the degree of chain branching is almost independent of the radiation dose rate over the range of 1.3×10^4–4.3×10^5 rad/hr., as shown in Figure 3.

Discussion

The schemes shown in eqs. (1) and (2) have been proposed as probable mechanisms of chain branching.

Intermolecular hydrogen transfer:

$$R_1CH_2CH_2\cdot + R_2CH_2CH_2R_3 \rightarrow R_1CH_2CH_3 + R_2\dot{C}HCH_2R_3 \qquad (1)$$

TABLE I
Summary of Experimental Results

Run no.	Initial pressure, kg./cm.²	Initial temperature, °C.[a]	Dose rate, rad/hr. × 10^{-4}	Irradiation time, hr.	Conversion, %	$\bar{M}_n$ × 10^{-4}	Methyl groups per 1000 carbon atoms	Methyl groups per molecule[b]
PG-14	70	28	2.5	20.7	2.6	1.6	6.5	5.4
PG-3	70	26	2.5	44.6	12.5	4.3	7.4	20.7
PG-47	152	23	2.5	1.7	0.5	6.3	2.8	10.6
PG-24	155	24	2.5	2.5	0.8	8.8	3.0	16.9
PG-16	152	28	2.5	4.0	1.9	16.4	3.0	33.2
PG-15	154	28	2.5	8.0	5.3	19.4	3.4	45.2
PG-46	295	19	2.5	0.7	0.4	13.3	1.9	16.0
PG-34	294	23	2.5	1.0	0.6	17.4	1.8	20.4
PG-48	300	22	2.5	1.7	1.6	26.5	1.5	26.4
PG-31	300	24	2.5	4.0	5.9	32.0	2.0	43.7
PG-9	404	27	2.5	0.53	0.3	14.4	1.2	10.3
PG-8	408	28	2.5	1.0	1.4	26.6	1.3	22.7
PG-59	390	30	2.5	1.0	1.6	27.5	1.0	17.6
PG-57	390	40	2.5	1.5	3.2	29.0	2.1	41.5
PG-56	390	60	2.5	2.5	2.2	14.3	4.6	45.0
PG-58	390	86	2.5	3.1	1.7	3.9	11.1	28.9
PG-55	390	100	2.5	3.0	1.2	3.1	11.2	22.8
PG-68	390	150	2.5	5.0	6.0	1.5	29.5	29.6
PT-9	390	160	2.5	2.0	1.4	0.99	39.2	25.7
PT-10	390	180	2.5	2.0	1.8	0.83	47.6	26.2
PG-69	390	200	2.5	8.0	14.5	0.67	62.0	27.7
PG-44	205	30	43.0	1.0	2.3	4.4	2.4	5.5
PG-43	204	30	21.0	1.0	1.4	5.5	2.3	7.0
PG-66	200	30	12.0	1.0	0.9	5.8	1.9	5.9
PG-67	200	30	5.6	1.0	0.6	6.6	2.2	8.4
PG-26	202	23	2.5	1.2	0.3	6.6	2.4	9.3
PG-50	200	30	1.3	5.0	2.7	24.5	2.6	42.0

[a] In experiments of PG-44, PG-43, and PG-66, the increase in temperature due to the heat of reaction in the course of polymerization was less than 10°C.; in other experiments, it was less than 3°C.

[b] Terminal methyl groups were subtracted.

Intramolecular hydrogen transfer:

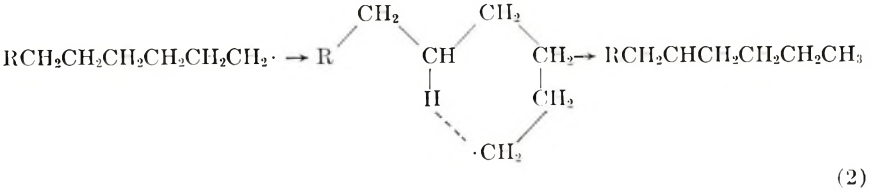

(2)

The first scheme was proposed by Flory[8,9] for chain branching in vinyl polymers. According to this mechanism, chain branching may occur be-

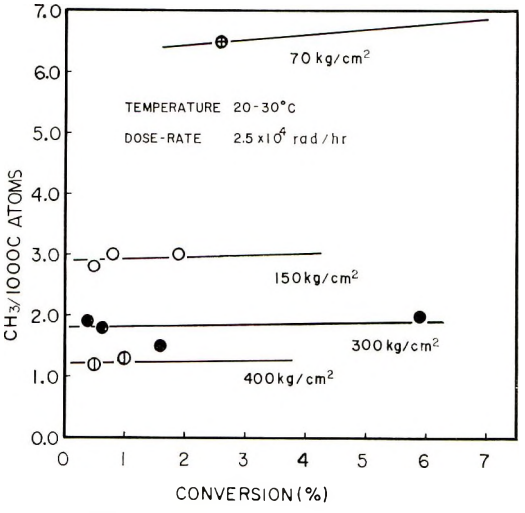

Fig. 1. CH_3/1000 C atoms vs. ethylene conversion.

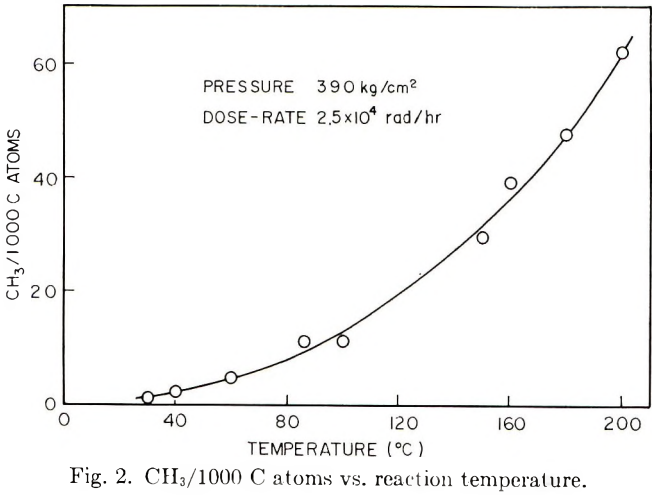

Fig. 2. CH_3/1000 C atoms vs. reaction temperature.

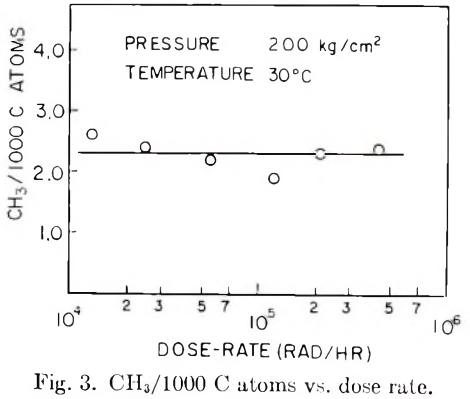

Fig. 3. CH_3/1000 C atoms vs. dose rate.

cause of the kinetic possibility of transfer of activity from an active growing chain to dead polymer by hydrogen abstraction. This mechanism leads to long-chain branching.

Another mechanism, one by which short-chain branching in polyethylene may arise, was suggested by Roedel[1] and is widely accepted. As shown in eq. (2), an active growing chain abstracts a hydrogen from the fifth-from-the-last carbon atom, because of the steric probability of formation of six-membered ring as transition state.

In addition to the above mechanisms, in the radiation-induced polymerization a third scheme may be possible. This scheme, eq. (3) indicates the polymer radical may be produced because of cleavage of a C–H bond by the interaction between polymer and a high energy photon, and the growth of chain takes place from this radical to form a branched structure.

$$R_1CH_2CH_2R_2 \xrightarrow[\text{Radiation}]{} R_1\dot{C}HCH_2R_2 + H\cdot \xrightarrow{C_2H_4} R_1\text{—}\underset{\displaystyle R_3}{\underset{|}{C}}HCH_2R_2 \qquad (3)$$

The fact that the degree of short-chain branching is almost independent of the conversion in our radiation-induced polymerization is evidence against the scheme involving intermolecular hydrogen transfer. The observation that the degree of chain branching is not influenced by the dose rate would appear to exclude the reaction shown in eq. (3).

In conclusion, it seems to be the most reasonable assumption that chain branching occurs owing to intramolecular hydrogen transfer via transient six-membered ring formation, often called the "backbiting mechanism." According to this mechanism, propagation and chain branching proceed in parallel with the number of polymer chains. The degree of polymerization increases with the reaction time in this polymerization at normal temperature as reported previously.[10]

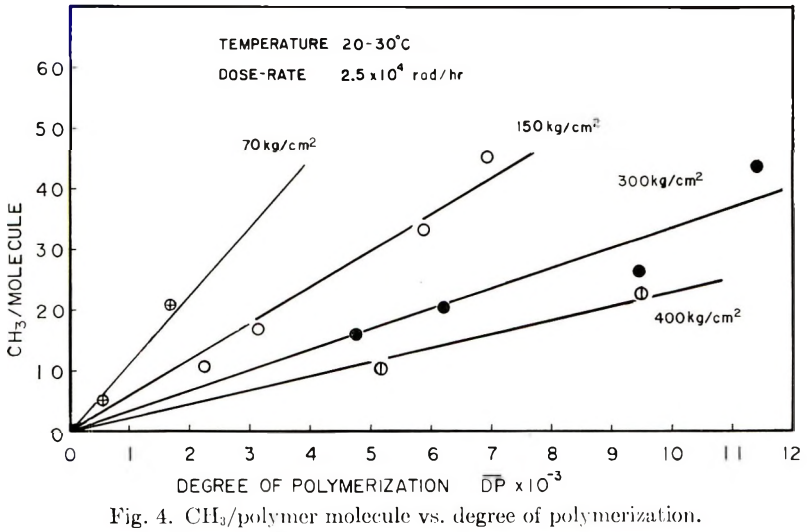

Fig. 4. CH_3/polymer molecule vs. degree of polymerization.

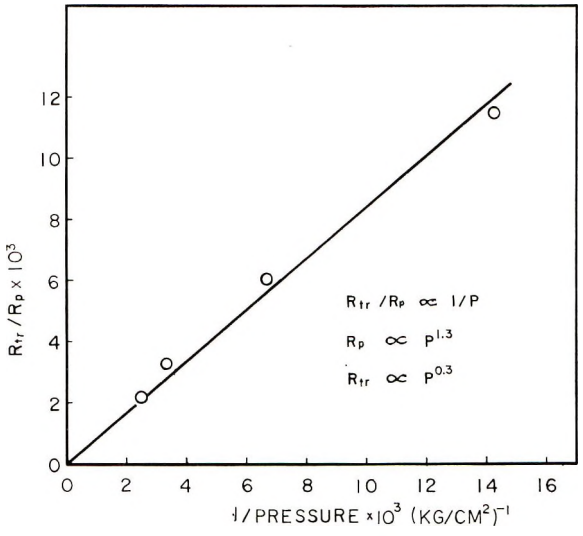

Fig. 5. R_{tr}/R_p vs. reciprocal pressure.

The number of branches in a polymer molecule are plotted against the degree of polymerization at each pressure in Figure 4. An almost linear relation exists between them. This fact indicates that the chain growth and chain branching formation occur in parallel. The ratio of the rate of branch formation (R_{tr}) to that of propagation (R_p) is found to be independent of the length of the polymer chain. The ratio is given by the slope of the line in Figure 4.

Figure 5 illustrates that R_{tr}/R_p is proportional to the reciprocal pressure of ethylene, while the rate of propagation is proportional to the 1.3 power of ethylene pressure (second power of fugacity) according to our earlier investigation.[11] Consequently, the pressure exponent for the chain branching rate is 0.3. Since the chain formation involves a monomolecular reaction of the growing chain, the effect of pressure on the rate is probably due to the change in rate constant with pressure. The effect of pressure on the rate constant with pressure. The effect of pressure on the rate constant for a reaction is written

$$d \ln k/dP = -\Delta V^{\ddagger}/RT$$

where k represents the rate constant and $\Delta V^{\ddagger}$ is the volume of activation, i.e., the difference between the molar volume of the initial state and that of the activated state. If the volume of the activated state is smaller than that of initial state, the rate constant will increase with pressure.

In Table II, the values of R_{tr}/R_p, R_p, R_{tr}, and $(R_{tr})_p/(R_{tr})_{70}$ at various pressure are listed.

The values of R_{tr}/R_p were obtained from the slope of the line in Figure 4 and values of R_p were taken from our earlier investigation.[11] Since R_{tr} is proportional to k_{tr} (rate constant of chain transfer) in this monomolecular reaction, the ratio $(R_{tr})_p/(R_{tr})_{70}$ is equal to $(k_{tr})_p/(k_{tr})_{70}$.

TABLE II
Effect of Pressure on Chain Branching

Pressure, kg./cm².	R_{tr}/R_p, times/ C_2H_4 molecule $\times 10^3$	R_p, C_2H_4 molecule/ sec.	R_{tr}, times/sec. $\times 10^3$	$(R_{tr})_p/(R_{tr})_{70} = (k_{tr})_p/(k_{tr})_{70}$	$\log[(k_{tr})_p/(k_{tr})_{70}]$
70	11.5	0.223	2.565	1.00	0
150	6.0	0.446	2.676	1.043	0.018
300	3.3	1.014	3.346	1.305	0.115
400	2.2	1.673	3.681	1.435	0.157

The plot of log $[(k_{tr})_p/(k_{tr})_{70}]$ against pressure p is shown in Figure 6; this leads to a volume of activation of -26.4 cc./mole. According to the backbiting mechanism, the transition state of the chain-branching reaction is a six-membered ring. There is apparently a volume contraction on going from a normal chain in the initial state to the cyclic form of the transition state. As an approximation if we calculate the volume contraction between *n*-hexane and cyclohexane, we obtain 22.7 cc./mole. which is approximately equal to $\Delta V^{\ddagger}$ mentioned above. The numerical value of experimental $\Delta V^{\ddagger}$ should not be emphasized; however, the effect of pressure on the chain branching is consistent with the hypothesis of the backbiting mechanism.

Since the concentration of methyl groups increases with temperature, the rate ratio of chain branching to propagation increases with temperature. For instance, the methyl content reaches a value of 6 per 100 carbon atoms at 200°C., which means that the chain branching occurs once in the addition of nine ethylene units. This frequency of chain branching is comparable to that of conventional high-pressure polymerization. An Arrhenius plot is shown in Figure 7, from which we find the activation energy of chain branching exceeds that of propagation by 6.0 kcal./mole. For the high-pressure polymerization with acetoxime and by thermal means, a value of

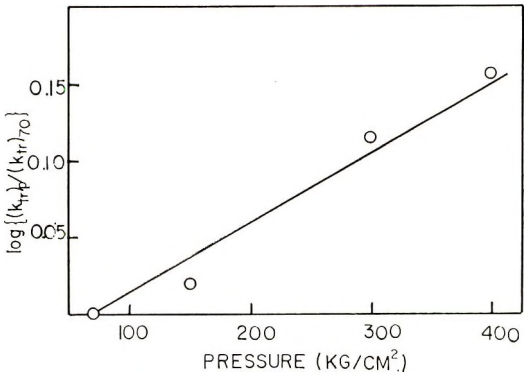

Fig. 6. Log $[(k_{tr})_p/(k_{tr})]_{70}$ vs. pressure.

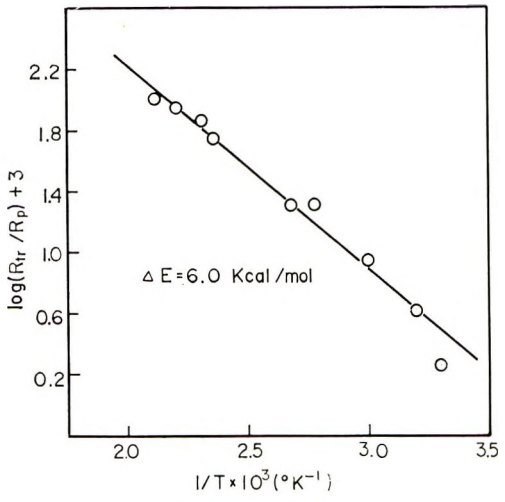

Fig. 7. Log (R_{tr}/R_p) vs. reciprocal temperature.

5.0 kcal./mole was reported.[2] This good agreement probably indicates that the mechanism of chain-branch formation in radiation polymerization is similar to that of free-radical polymerization at high pressure.

References

1. Roedel, M. J., *J. Am. Chem. Soc.*, **75**, 6110 (1953).
2. Morrel, A. G., *Discussions Faraday Soc.*, **22**, 153 (1956).
3. Willborn, A. H., *J. Polymer Sci.*, **34**, 569 (1959).
4. Boyle, D. A., W. Sympson, and J. D. Waldron, *Polymer*, **2**, 335 (1961).
5. Steinberg, M., P. Colombo, L. Kukacka, R. N. Chapman, and G. Adler, *Proc. Intern. Symp. Radiation Induced Polymerization Copolymerization, Battelle Memorial Inst. (Nov. 29–30, 1962)*, p. 70.
6. Tung, L. H., *J. Polymer Sci.*, **24**, 333 (1957).
7. Bryant, W. M., and R. C. Voter, *J. Am. Chem. Soc.*, **75**, 6112 (1953).
8. Flory, P. J., *J. Am. Chem. Soc.*, **59**, 241 (1957).
9. Flory, P. J., *J. Am. Chem. Soc.*, **69**, 2839 (1947).
10. Machi, S., M. Hagiwara, M. Gotoda, and T. Kagiya, *J. Polymer Sci. B*, **2**, 765 (1964).
11. Machi, S., M. Hagiwara, M. Gotoda, and T. Kagiya, *Bull. Chem. Soc. Japan*, to be published; *J. Polymer Sci. A*, **3**, 2931 (1965).

Résumé

Comme contribution à l'interprétation du mécanisme de formation de ramification dans la polymérisation de l'éthylène, on examine au moyen de la spectroscopie infrarouge, l'effet des conditions de réactions sur la ramification à chaîne courte dans la polymérisation de l'éthylène sous l'influence de rayons-γ. La concentrations des groupes méthyles c.à.d. la fréquence de ramifications courtes, croît en fonction de la température et de la pression, et est indépendante de la conversion de l'éthylène en polymère et de l'intensité de radiation. Le nombre des groupes méthyles par molécule du polymère augmente généralement proportionnellement en fonction du degré de polymérisation. Tenant compte de ces faits, on admet que les ramifications courtes résultent principalement d'un mécanisme du transfert d'hydrogène intramoléculaire. L'effet de la pression sur la

vitesse de ramification peut être attribué, en considérant un état de transition constitué de noyaux hexaatomiques dans la réaction de transfert d'hydrogène. L'énergie d'activation de ramification de chaîne dépasse celle de la propagation de 6 kcal/mole.

Zusammenfassung

In einem Versuch, einen Beitrag zur Aufstellung des Bildungsmechanismus für die Kettenverzweigung bei der Äthylenpolymerisation zu lifern, wird der Einfluss der Reaktionsbedingungen auf die Kurzkettenverzweigung bei der γ-Strahlungsinduzierten Äthylenpolymerisation mittels infrarotspetroskopie untersucht. Die Methylgruppenkonzentration, d.h. die Häufigkeit der Kurzkettenverzweigung nimmt mit Temperatur und Druck zu und ist vom Äthylenumsatz und der Strahlungsintensität unabhängig. Die Zahl der Methylgruppen pro Polymermolekül nimmt fast proportional mit dem Polymerisationgrad zu. Diese Tatsachen zeigen, dass die Kurzkettenverzweigung hauptsächlich durch einen intramolekularen Wasserstoffübertragungsmechanismus bedingt ist. Der Druckeinfluss auf die Geschwindigkeit der Kettenverzweigung kann durch Annahme eines sechgliedrigen Ringes als Übergangszustand bei der Wasserstoffübertragungsreaktion erklärt werden. Die Aktivierungsnergie der Kettenverzweigung ist um 6 kcal/mol grösser als diejenige des Kettenwachstums.

Received August 10, 1964
Revised July 1, 1965
Prod. No. 4784A

JOURNAL OF POLYMER SCIENCE: PART A-1 VOL. 4, 293–299 (1966)

Alternative Copolymerization of Aziridines and Carbon Monoxide by γ-Ray Irradiation

TSUTOMU KAGIYA, SHIZUO NARISAWA, TAIZO ICHIDA, and KENICHI FUKUI, *Faculty of Engineering, Kyoto University, Kyoto, Japan*, and HISAO YOKOTA and MASATSUNE KONDO, *Sumitomo Atomic Energy Industries, Ltd., Osaka, Japan*

Synopsis

The copolymerization of carbon monoxide and aziridines such as ethylenimine and propylenimine was carried out by γ-ray irradiation. Aziridines and carbon monoxide were allowed to copolymerize under γ-ray irradiation from a Co^{60} source and gave a crystalline solid copolymer. The yield of the copolymer increased with reaction temperature. The composition of copolymers obtained did not depend on the feed ratio of monomers and was found to be almost equimolar. The copolymer of ethylenimine and carbon monoxide melted at about 322–335°C. with decomposition and has an infrared spectrum identical with that of poly-β-alanine obtained by the hydrogen-migration polymerization of acrylamide. The hydrolyzed product of the ethylenimine–carbon monoxide copolymer was confirmed to be β-alanine by paper chromatography. These results lead to the conclusion that the copolymerization of aziridines and carbon monoxide took place alternatively by γ-ray irradiation, and produced crystalline poly-β-alanines.

Introduction

It is well documented in the literature that aziridines polymerize with various kinds of cationic catalysts to polyimines[1] and easily react with many kinds of compounds containing a carbonyl group, such as ketenes, aldehydes, and ketones.[2,3]

In recent years, the γ-radiation-induced copolymerization of ethylene and carbon monoxide has been studied by several groups of workers.[4–6] Poly-β-alanines can be obtained by the ring-scission polymerization of β-lactams[7–9] and the hydrogen-migration polymerization of acrylamides.[10–12]

The present paper concerns a continuation of our study on the copolymerization of aziridines and various kinds of cyclic compounds.[13,14] It has been found that aziridines and carbon monoxide can be copolymerized to poly-β-alanines with γ-ray irradiation. We report here the experimental results of the novel radiation-induced copolymerization of aziridines and carbon monoxide.

Experimental

Ethylenimine and carbon monoxide (99.2% purity) were obtained commercially. Propylenimine was prepared according to the literature.[15]

The aziridines were dried over potassium hydroxide pellets and sodium hydride and then fractionated before use (ethylenimine, 55.5–56°C., propylenimine 65.7–66°C.).

The radiation copolymerizations were carried out as follows. A glass tube containing a measured amount of liquid aziridine was placed into a stainless steel high-pressure reaction vessel of 30 or 40 ml. capacity. The vessel was degassed twice *in vacuo* under cooling with liquid nitrogen. Then, a measured amount of carbon monoxide gas was fed into the vessel from a reservoir. The vessel was exposed to γ-radiation from a Co^{60} (5000 C.) source without agitation. After the irradiation, the vessel was opened and the unreacted carbon monoxide was purged. The copolymer formed was washed thoroughly with large amount of ethyl ether to remove the unreacted aziridine, then dried *in vacuo* and weighed.

The composition of the copolymer was determined by elementary analysis. The reduced viscosity was measured, whenever possible, as 0.1% solution in formic acid at 35°C. in an Ostwald viscometer. The melting point of the copolymer was visually determined in a nitrogen atmosphere in an electric heater. The infrared spectrum was obtained by using the potassium bromide pellet technique on a Hitachi double-beam infrared spectrophotometer, Model EPI-2, with sodium chloride prism. The x-ray diffraction diagram was recorded with a powder camera on a Rigaku Denki x-ray diffractometer, Model D-3F, employing Ni-filtered CuKα radiation by the use of standard techniques. The differential thermograms were obtained by using sandwiches with α-alumina powder as a diluent on a Shimadzu differential thermal apparatus, Model DT-10, with platinum cell.

The hydrolysis product from the ethylenimine–carbon monoxide copolymer was analyzed for identification of poly-β-alanine structure by means of paper chromatography as follows. The copolymer was hydrolyzed in a sealed tube with 20% constant boiling hydrochloric acid.[14] The hydrolyzed product was filtered and the filtrate was dried *in vacuo*. The colored crystalline material obtained was compared with a commercial β-alanine by the usual one-dimensional ascending techniques of chromatography for amino acid.[17] Both samples were developed on Toyo Roshi No. 50 paper for chromatography with *n*-butanol–glacial acetic acid–water (4:1:5) and also with phenol–water (7:3) as solvents. Both spots were detected by using a *n*-butanol solution of ninhydrin.

Results and Discussion

The results of the γ-ray irradiation copolymerization of aziridines and carbon monoxide are shown in Table I. Aziridines, which did not readily homopolymerize in a radiation field, were allowed to copolymerize with carbon monoxide under irradiation with γ-rays from a Co^{60} source. No copolymer could be obtained without irradiation. The yield of the copolymer produced increased with rising reaction temperature. In the reaction of dimethylamine and carbon monoxide, sodium methylate

TABLE I

γ-Ray Irradiation Copolymerization of Aziridines and Carbon Monoxide[a]

Expt. no.	Aziridines, g.[b]	Carbon monoxide, g.	Additive ($NaOCH_3$), g.	Polymerization conditions: Temp., °C.	Time, hr.	Dose rate, rad/hr. × 10^{-5}	Total dose, rad × 10^{-7}	Polymer yield, g.	η_{sp}/c dl./g.	Melting point, °C.	Elementary analysis found[c]: C, %	H, %	N, %
1	4.1	3.0	—	17	47	—	—	—	—	—	—	—	—
2	1.1	—	—	17	47	4.5	2.11	—	—	—	—	—	—
3	4.1	3.0	—	0	132	2.0	2.64	0.149	0.25	330–335	—	—	—
4	4.3	2.9	—	17	47	4.5	2.11	0.123	—	330–335	48.78	8.30	18.93
5	1.69	5.4	—	17	47	4.5	2.11	0.439	—	324–327	49.14	8.28	19.87
6	4.69	4.0	—	100	20	2.0	0.4	0.154	—	322–325	49.40	8.22	19.66
7	4.55	4.1	0.136	17	20	2.0	0.4	0.036	—	—	—	—	—
8	4.2	4.15	0.126	50	20	2.0	0.4	0.139	—	330–335	49.68	7.86	19.16
9	3.9	4.2	—	17	69	4.5	3.1	0.269	0.16	287–288	55.09	8.50	16.26

[a] Autoclave of 40 ml. capacity was used except in expt. 4, in which autoclave of 30 ml. capacity was used.

[b] Ethylenimine was used as aziridine, except in expt. 9, in which propylenimine was used.

[c] Calcd. for mole ratio of aziridine: carbon monoxide in the copolymer of 1.0: for copolymer of ethylenimine and carbon monoxide: C, 50.69%; H, 7.09%; N, 19.71%; for copolymer of propylenimine and carbon monoxide: C, 56.45%; H, 8.29%; N, 16.46%.

is known to be an effective catalyst for formation of dimethylformamide.[18] In the present copolymerization, however, sodium methylate did not exhibit any appreciable catalytic action.

Figure 1 shows the infrared spectra of the copolymers obtained by radiation-induced copolymerization of aziridines and carbon monoxide.

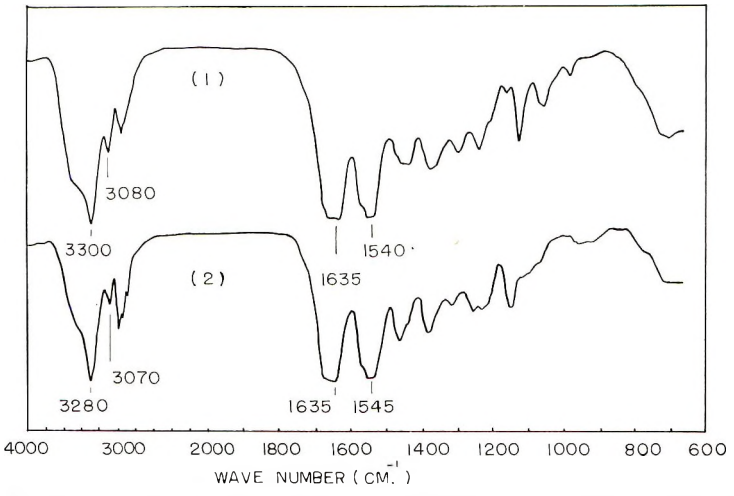

Fig. 1. Infrared spectra of: (*1*) copolymer of ethylenimine and carbon monoxide; (*2*) copolymer of propylenimine and carbon monoxide.

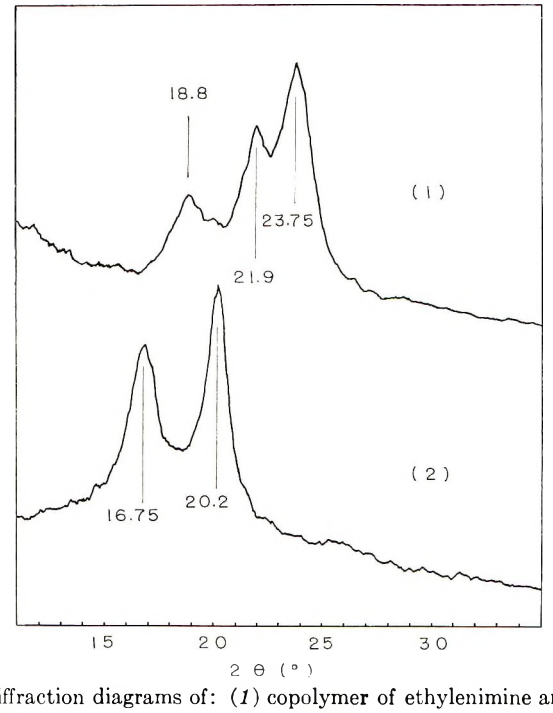

Fig. 2. X-ray diffraction diagrams of: (*1*) copolymer of ethylenimine and carbon monoxide; (*2*) copolymer of propylenimine and carbon monoxide.

The spectrum of the copolymer of ethylenimine and carbon monoxide exhibited characteristic absorption peaks at 3300, 3080, 1660–1635, and 1540 cm.$^{-1}$, and was identical with that of poly-β-alanine obtained by the hydrogen migration polymerization of acrylamide.[11,12]

As shown in Figure 2, the copolymer of aziridines and carbon monoxide was confirmed to be crystalline from the x-ray diffraction diagrams. The lattice spacings of 4.72, 4.60, and 3.75 A. for the ethylenimine–carbon monoxide copolymer are different from those of 4.6, 3.9, and 3.55 A., having relative intensities of 60, 10, and 100, respectively, for the polymer

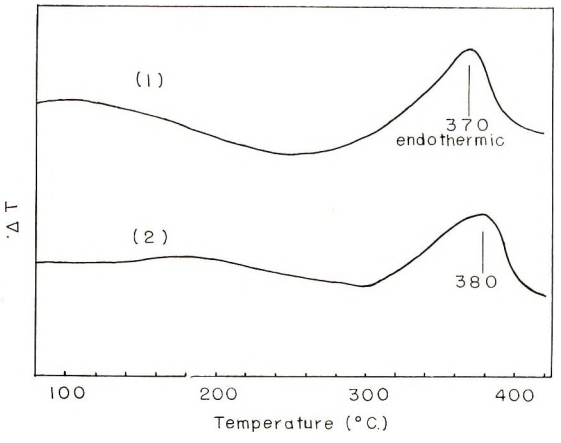

Fig. 3. Differential thermograms of: (*1*) copolymer of ethylenimine and carbon monoxide; (*2*) copolymer of propylenimine and carbon monoxide.

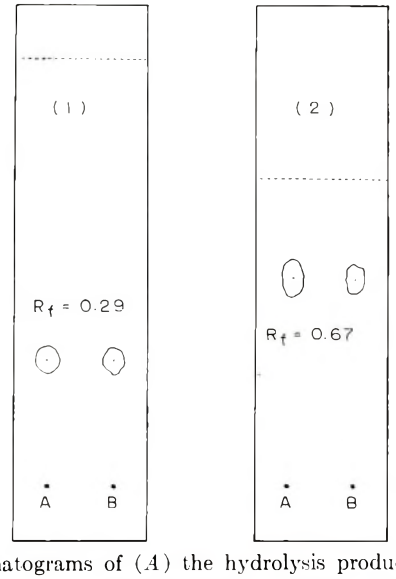

Fig. 4. Paper chromatograms of (*A*) the hydrolysis product of the ethylenimine-carbon monoxide copolymer and (*B*) commercial β-alanine: (*1*) *n*-butanol–glacial acetic acid–water (4:1:5); (*2*) phenol–water (7:3).

obtained by the hydrogen-migration polymerization of acrylamide[10] and those of 4.78 (weak), 3.40 (weak), 3.14 (strong), and 2.82 A. (very weak) for the poly-β-alanine obtained by the ring-scission polymerization of β-propiolactam.[9]

The differential thermograms of the aziridine–carbon monoxide copolymers are shown in Figure 3. Maximum endothermic peaks of the thermograms of the copolymers of ethylenimine, and propylenimine with carbon monoxide were shown at 370 and 380°C., respectively. Poly-β-alanine obtained by the ring-scission polymerization of β-propiolactam[9] and the polymer obtained by the hydrogen-migration polymerization of acrylamide[10–12] have melting points of over 300°C. and 320–340°C., respectively. The melting point of the copolymer obtained by the radiation copolymerization of ethylenimine and carbon monoxide was visually observed at about 322–335°C. (dec.).

Figure 4 shows the paper chromatograms of the hydrolysis product of the ethylenimine–carbon monoxide copolymer and a commercial β-alanine. Since the R_f values of the hydrolysis product of the copolymer were in good agreement with those of a commercial β-alanine, it may be concluded that the copolymer has the poly-β-alanine structure.

Elementary analysis of the aziridines–carbon monoxide copolymer showed that the composition did not depend on the mole ratio of feed monomers and was constant at a molar ratio of ca. 1.0.

These elementary analysis, infrared spectra, x-ray diffraction, and chemical analysis results confirmed that the copolymers obtained were poly-β-alanines. Accordingly, it was concluded that the copolymerization of aziridines and carbon monoxide took place alternatively by γ-ray irradiation.

Further work on this alternative copolymerization is now in progress. Detailed results and discussion will be reported in the near future.

References

1. Jones, G. D., in *The Chemistry of Cationic Polymerization*, P. H. Plesch, Ed., Pergamon, Oxford, 1963, Chap. 14.

2. Bestian, H., *Ann.*, **566**, 210 (1949).

3. Dornow, A., and W. Schacht, *Ber.*, **82**, 464 (1949).

4. Roberts, R., and S. J. Skinner, Brit. Pat. 778,225, July 3, 1957.

5. Chatani, Y., T. Takizawa, S. Murahashi, Y. Sakata, and Y. Nishimura, *J. Polymer Sci.*, **55**, 811 (1961).

6. Colombo, P., M. Steinberg, and J. Fontana, *J. Polymer Sci. B*, **1**, 447 (1963).

7. Graf, R., G. Lohaus, K. Körner, E. Schmidt, and R. Bestian, *Angew. Chem.*, **74**, 523 (1962).

8. Kagiya, T., H. Kishimoto, S. Narisawa, and K. Fukui, *J. Polymer Sci. A*, **3**, 145 (1965).

9. Kodaira, T., H. Miyake, K. Hayashi, and S. Okamura, *Bull. Chem. Soc. Japan*, **38**, 1788 (1965).

10. Breslow, D. S., G. E. Hulse, and A. S. Matlack, *J. Am. Chem. Soc.*, **99**, 3760 (1957).

11. Ogata, N., *Bull. Chem. Soc. Japan*, **33**, 906 (1960).

12. Ogata, N., *Makromol. Chem.*, **40**, 55 (1960).
13. Kagiya, T., S. Narisawa, and K. Fukui, paper presented at 13th Symposium on High Polymer Chemistry, Tokyo, November 1964.
14. Kagiya, T., S. Narisawa, K. Manabe, and K. Fukui, *J. Polymer Sci. B*, **3**, 617 (1965).
15. Minoura, Y., M. Takebayashi and C. C. Price, *J. Am. Chem. Soc.*, **81**, 4689 (1957).
16. Ishii, S., *Biochemistry I, Series of Chemical Experiments XXIII (Seibutsu Kagaku I, Jikken Kagako Kōza XXIII)*, Maruzen, Tokyo, 1957, p. 104.
17. Shibata, M., *Experimental Methods of Paper Chromatography (Paper Chromatography-Hō no Jissai)*, Kyoritsu, Tokyo, 1960.
18. Winter, H., *Helv. Chim. Acta*, **37**, 2370 (1954).

Résumé

On a copolymérisé par irradiation aux rayons-γ l'oxyde de carbone et des aziridines tels que l'éthylèneimine et propylèneimine. Les aziridines et l'oxyde de carbone sont susceptibles de copolymériser sous l'effet de l'irradiation aux rayons-γ du cobalt-60 et de donner un copolymère cristallin solide. Le rendement du copolymère croît avec la température de la réaction. La composition des copolymères obtenus ne dépend pas du rapport de départ des monomères, et est le plus souvent équimoléculaire. Le copolymère d'éthylèneimine de d'oxyde de carbone fond à environ 322–335°C. avec décomposition, et il a le même spectre infrarouge que celui de la poly-β-alanine obtenu par polymèrisation isomérisante de l'acrylamide. On confirme par chromatographie que le produit obtenu par hydrolyse du copolymère éthylèneimine-oxyde de carbone est une alanine-β. Ces résultats permettent de conclure que la copolymérisation des aziridines et de l'oxyde de carbone se produit alternativement sous l'influence des rayons-γ et donne des poly-β-alanines cristallines.

Zusammenfassung

Die Copolymerisation von Kohlenmonoxyd und Aziridin en wie Äthylenimin und Propylenimin wurde durch γ-Bestrahlung ausgeführt. Aziridine und Kohlenmonoxyd wurden durch γ-Strahlung von Cobalt^{60} zur copolymerisation gebracht und lieferten ein kristallines festes Copolymeres. Die Ausbeute an Copolymerem nahm mit der Reaktionstemperatur zu. Die Zusammensetzung der erhaltenenen Copolymeren hing nicht von der Zusammensetzung der Monomerenmischung ab und erwies sich als fast äquimolar. Das Copolymere aus Äthylenimin und Kohlenmonoxyd schmilzt bei etwa 322–335°C unter Zersetzung und besitzt ein mit demjenigen durch Polymerisation unter Wasserstoffwanderung von Acrylamid erhaltenen Poly-β-alanin identisches Infrarotspektrum. Durch Papierchromatographie wurde das Hydrolysenprodukt aus Äthylenimin-Kohlenmonoxydcopolymeren als β-Alanin bestätigt. Die Ergebnisse führen zu dem Schluss, dass die Copolymerisation von Aziridin und Kohlenmonoxyd durch γ-Bestrahlung alternierend verläuft und zu kristallinen Poly-β-alaninen führt.

Received April 9, 1965
Revised June 10, 1965
Prod. No. 4788A

JOURNAL OF POLYMER SCIENCE: PART A-1 VOL. 4, 301–318 (1966)

Polymerization of Five-, Six-, and Seven-Membered Ring Lactams by Using Metallic Potassium or Metallic Aluminum Alkylate as Catalyst and Certain *N*-Acyl Lactams or Diphenyl Ketene as Initiator*

HISAYA TANI and TUYOSHI KONOMI,† *Department of Polymer Science, Faculty of Science, Osaka University, Kitatoneyama, Toyonaka, Osaka, Japan*

Synopsis

Polymerization of five-, six-, and seven-membered lactams by metallic potassium or $MAlEt_4$ (where M is Li, Na, or K) as a catalyst and *N*-acyl lactam or diphenylketene as an initiator was carried out at temperatures below 80°C. By using $MAlEt_4$ instead of a metallic potassium catalyst in the polymerization of α-piperidone the propagation was continued until the reduced viscosity of polymer reached a value of 0.9. The polymer obtained has a film-forming ability. The experimental results obtained in the gasometry suggest that $MAlEt_4$ reacts with lactam to form such a complex of the type

$$M\cdot N\!\!\left(\begin{array}{l}\text{———C=O}\cdot AlX_3\\ \text{└(CH}_2\text{)}_n\text{┘}\end{array}\right.$$

(where M is Li, Na, or K and X is an ethyl or 2-oxo-alkylene-imine group). The resulting complexes are considered to increase the solubility of catalyst and also to protect the polymer endgroups from side reactions by stabilizing the alkali metal as the complex. In addition, the mode of action of diphenylketene as an initiator was revealed by the facts that the corresponding *N*-diphenylacetyl lactam was obtained from the reaction of diphenyl ketene with lactam and *N*-diphenylacetyl lactam itself was useful for the polymerization of α-piperidone.

INTRODUCTION

The alkali-catalyzed polymerization of ε-caprolactam was first studied by Hanford and Joyce,[1] and in greater detail by Griehl,[2] Wichterle,[3–6] and others.[7–9] Numerous compounds have been reported to be able to act as catalyst. For example, alkali metals or their hydroxides, carbonates, and hydrides, Grignard reagent, or aluminum alkyls have catalytic activity.

Five- and six-membered ring lactams, α-pyrrolidone and α-piperidone, which had been considered to be unable to polymerize due to monomer

* Presented at the 12th Annual Meeting of the Society of Polymer Science, Japan, Tokyo, May 1963 and at the 13th Meeting of the Society of Polymer Science, Japan, Kyoto, June 1964.

† Present address: Textile Research Institute, Toyo Spinning Co., Ltd., Katata, Shiga, Japan.

stability, have been polymerized in the presence of the alkali metal–acyl compound catalyst system by Ney et al.,[10] and several investigations of these lactams have been reported.[11–15]

Several compounds such as acyl compounds or acyl lactams, isocyanates, or organo nitrous acid esters were known to be effective as initiators.

Recently, particular attention has been given to the six-membered ring lactam, α-piperidone, which can be derived from tetrachloroalkanes obtained by the telomerization of ethylene with carbon tetrachloride; detailed experiments on the polymerization of α-piperidone were reported by Yoda et al.[15] The degree of polymerization of the polymers obtained was low, however; that is, the intrinsic viscosity in *m*-cresol at 25°C. was about 0.3.

The mechanism of polymerization of these lactams with the alkali–acyl compound catalyst system has been interpreted[1–3,5–7,9,11,15] as the attack of an amide anion of the metal salt of the lactam on an electrophilic *N*,*N*-diacylimide group of the initiator or of the propagating polymer.

We carried out the polymerization of five-, six-, and seven-membered ring lactams with the alkali metal–acyl compound catalyst system in the usual method. The polymerization of five- and seven-membered ring lactams gave satisfactory results, but polymerization of a six-membered ring lactam yielded only polymers of very low molecular weight.

By using $MAlEt_4$ (where M = Li, Na, or K) as a catalyst and *N*-acyl lactams or diphenyl ketene as an initiator, we succeeded in obtaining an α-piperidone polymer having the highest degree of polymerization so far reported in the literature.

The alkaline polymerization of ε-caprolactam has been studied in most cases at a relatively low temperature.[16,17]

We tried, therefore, to polymerize ε-caprolactam at a temperature as high as 75°C. in order to obtain some new information. The present paper deals with the low temperature polymerization of five-, six-, and seven-membered ring lactams by use of metallic potassium–*N*-acyl lactam, $MAlEt_4$–*N*-acyl lactam, metallic potassium–diphenyl ketene, or $MAlEt_4$–diphenyl ketene as catalyst systems at temperatures below 80°C.

EXPERIMENTAL

Materials

Preparation of Monomers. α-Pyrrolidone was commercial product purified first by recrystallization from ethyl acetate, and then by fractional distillation *in vacuo* in the presence of a small amount of sodium hydroxide.

α-Piperidone was synthesized from cyclopentanone oxime by the Beckmann rearrangement and purified in the same way as α-pyrrolidone.

ε-Caprolactam was a commercial product purified by fractional distillation *in vacuo*.

Preparation of Initiators. *N*-Acetyl-α-pyrrolidone, *N*-acetyl-α-piperidone, and *N*-acetyl-ε-caprolactam were prepared by refluxing the corresponding lactams with acetic anhydride.

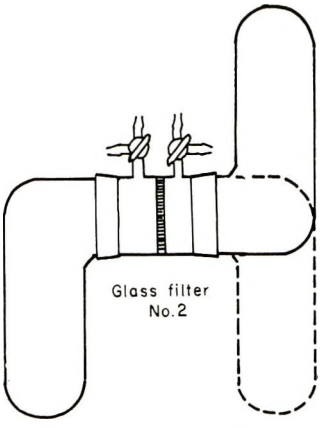

Fig. 1. Recrystallization apparatus used for $MAlEt_4$.

N-Benzoyl-α-pyrrolidone, *N*-benzoyl-α-piperidone, and *N*-ε-caprolactam were prepared by benzoylation of the corresponding lactam with benzoyl chloride in the presence of triethylamine in benzene, and were purified by recrystallization from benzene–hexane. Melting points of the products were: *N*-benzoyl-α-pyrrolidone, 92°C.; *N*-benzoyl-α-piperidone, 114–115°C.; *N*-benzoyl-ε-caprolactam, 72°C.

Diphenylacetyl-α-pyrrolidone, diphenylacetyl-α-piperidone, and diphenylacetyl-ε-caprolactam were prepared by the reaction of diphenyl ketene with the corresponding lactam in benzene at room temperature and purified by recrystallization from hexane or hexane–benzene. Melting points of the products were: *N*-diphenylacetyl-α-pyrrolidone, 133–133.5°C.; *N*-diphenylacetyl-α-piperidone, 116.5–117°C.; *N*-diphenylacetyl-ε-caprolactam, 84–85°C.

Preparation of Catalyst. $LiAlEt_4$, $NaAlEt_4$, and $KAlEt_4$ were prepared by stirring vigorously a mixture of alkali metal and triethyl aluminum in the presence of a small amount of toluene under reflux in dry nitrogen. Two of the resulting complexes, $LiAlEt_4$ and $NaAlEt_4$ were purified by recrystallization under a dry nitrogen atmosphere in the apparatus shown in Figure 1, because of the poor solubilities of these complexes in toluene, particularly at room temperature. Since $KAlEt_4$ was a highly viscous liquid and separated into two phases in concentrated solution in hexane, it was purified by washing several times with a small amount of hexane. The concentration of $MAlEt_4$ complex in tetrahydrofuran solution was determined by back-titration and gas analysis.

Polymerization

The lactams were further purified just before use by repeated distillation under dry nitrogen in order to remove traces of water as completely as possible. The content of water was measured by the Karl Fischer method and the purity was checked by infrared spectral and gas chromatographic

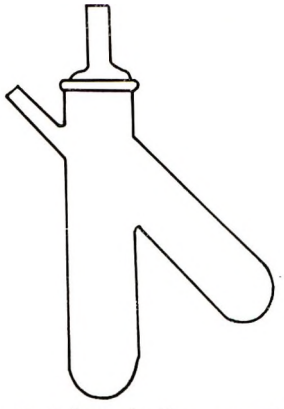

Fig. 2. Polymerization apparatus.

analysis. The water contents found were: α-pyrrolidone, 0.012 wt.-%; α-piperidone, 0.007 wt.-%; ε-caprolactam, 0.011 wt.-%; *N*-acetyl-α-pyrrolidone, 0.018 wt.-%; *N*-acetyl-α-piperidone, 0.025 wt.-%; *N*-acetyl-ε-caprolactam, 0.010 wt.-%.

Polymerization was carried out in an apparatus equipped with two reservoirs and two inlet-outlet tubes as shown in Figure 2.

This apparatus connected to the vacuum-nitrogen line was flushed thoroughly with dry nitrogen. The calculated amount of metallic potassium and initiator were introduced separately into each reservoir under a stream of dry nitrogen.

The desired amount of alkali metal was easily obtained by molding the metallic potassium in a hole of a definite size cut in a plate, and by cutting the metal in dry toluene. Toluene adhering to the metallic potassium was removed under reduced pressure, and then a calculated amount of monomer was introduced.

After the completion of the reaction of alkali metal with monomer in one of the reservoirs, the polymerization apparatus was placed in a constant temperature bath, and then the polymerization was initiated by mixing a monomer solution of catalyst with initiator. Polymerization temperatures were 45°C. for α-pyrrolidone (m.p. 27°C.) and α-piperidone (m.p. 40°C.) and 75°C. for ε-caprolactam (m.p. 68°C.).

After a sepecified time, polymerization was terminated by adding methanol and the yield of polymer was calculated after extraction of the resulting precipitate with methanol and water. The reduced viscosity (0.5 g. of polymer in 100 ml. of *m*-cresol solution, 30°C.) was used as a measure of the degree of polymerization of polymer.

RESULTS

Polymerization of Lactams with Alkali Metal as Catalyst

Effects of the molar ratio of catalyst (metallic potassium) to initiator (*N*-acetyl-α-piperidone) on the yield and on the degree of polymerization of

polymer in the polymerization of piperidone and of α-pyrrolidone are shown in Figures 3 and 4. It is evident that α-pyrrolidone gave high polymers in good yields, whereas α-piperidone gave only low molecular weight polymers in unsatisfactory yield.

In the case of α-piperidone, two conclusions may be drawn from the results shown in Figure 3. First, in order to obtain a polymer having a reduced viscosity of 0.28, the molar ratio of catalyst to initiator must be

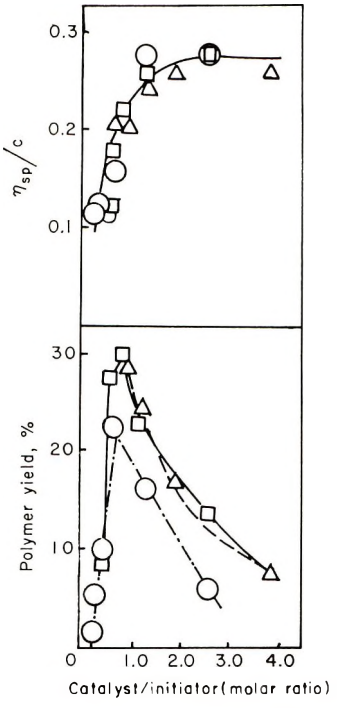

Fig. 3. Effect of the molar ratio of catalyst (metallic potassium) to initiator (*N*-acetyl-α-piperidone) on the yield and on the degree of polymerization of polymer in the polymerization of α-piperidone. Concentration of metallic potassium: (○) 2.58 mole-%, (□) 5.16 mole-%, (△) 7.74 mole-%. Polymerization temperature, 40°C.; polymerization time, 48 hr.

1.0, and the optimum ratio lies between 1.0 and 1.3. Secondly, it is impossible to obtain polymer having a reduced viscosity higher than 0.3 by using alkali metal catalyst.

It may be considered from the results shown above, particularly in the case of α-piperidone, that the initiator or the endgroup of the propagating polymer, that is, the *N*,*N*-diacylimide group, might be consumed by some side reactions.

The formation of piperidine as a by-product in the reaction of α-piperidone with alkali metal was considered. Indeed, a trace of amount of piperidine was detected in the distillate from the reaction mixture and was identified by the infrared spectrum.

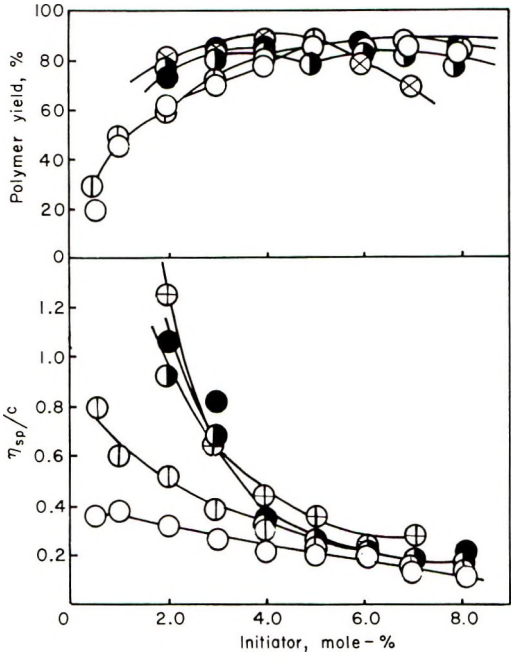

Fig. 4. Effect of the amount of initiator (*N*-benzoyl-α-pyrrolidone) on the yield and on the degree of polymerization of polymer in the polymerization of α-pyrrolidone by using a specified amount of catalyst (metallic potassium). Concentration of metallic potassium: (○) 0.61 mole-%, (◔) 1.08 mole-%, (◑) 2.16 mole-%, (●) 3.24 mole-%, (⊕) 4.32 mole-%; *N*-benzoyl-α-pyrrolidone, 2.0 mole-%. Polymerization temperature, 40°C.; polymerization time, 24 hr.; α-pyrrolidone, 0.0262 mole.

It has been reported that *N*-acetyl and *N*-benzoyl lactam are good acylating agents and acylate several amines to form the corresponding amides.[17] From the result, the consumption of the *N*,*N*-diacylimide group by a trace of piperidine might be considered.

TABLE I

Polymerization of α-Piperidone by Using Isolated Potassium Salt of α-Piperidone as Catalyst and *N*-Benzoyl-α-piperidone as Initiator[a]

Catalyst, mole-%	Initiator, mole-%	Polymer yield, %	η_{sp}/c
1.25	0.5	1.4	0.23
1.25	1.0	7.3	0.19
1.25	2.0	14.1	0.13
1.25	4.0	10.8	0.09
5.0	0.5	0	—
5.0	2.0	2.6	0.24
5.0	4.0	18.4	0.20
5.0	8.0	30.0	0.12

[a] Polymerization temperature, 45°C.; polymerization time, 20 hr.

The results of polymerization of α-piperidone in the presence of piperidine, triethylamine, benzene, or anisole are shown in Figure 5. The degree of polymerization of polymer is almost the same, but a marked decrease in the yield of polymer is observed only in the case of piperidine. These results show indirectly the consumption of the initiator or the endgroup of the oligomer, that is, the decrease in the number of propagating polymer

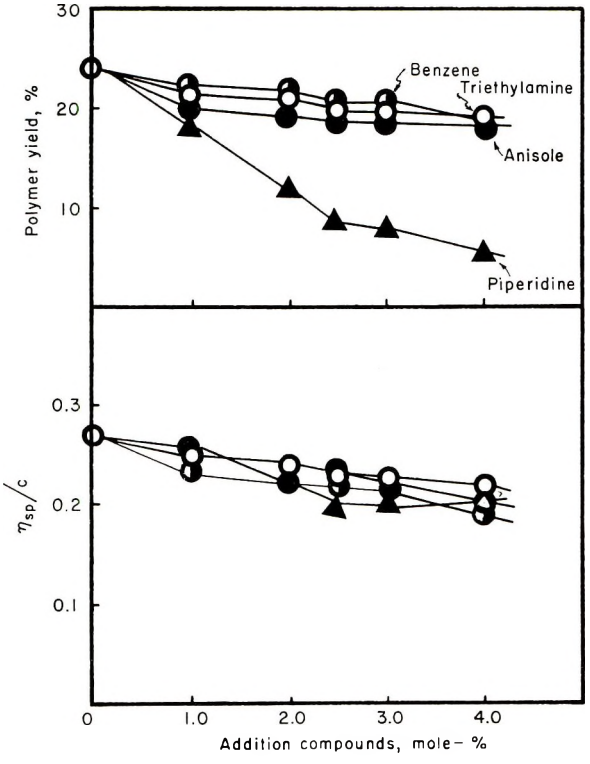

Fig. 5. Polymerization of α-piperidone in the presence of several added substances: (○) triethylamine; (◑) benzene; (●) anisole; (▲) piperidine. Polymerization temperature, 40°C.; polymerization time, 48 hr.; α-piperidone, 0.022 moles; metallic potassium, 2.58 mole-%; *N*-benzoyl-α-piperidone 2.0 mole-%.

chains. Piperidine not only decreases the polymerizability of α-piperidone by a dilution effect but also acts as an inhibitor.

In the experiments mentioned above, the potassium salt of α-piperidone was formed *in situ*. Even when the isolated salt was used as a catalyst, only a low molecular weight polymer was obtained (see Table I). These results indicate that piperidine added or formed *in situ* in the polymerization system attacks the *N*,*N*-diacylimide group at a rapid rate, and hence hardly affects the propagation after some polymerization has occurred.

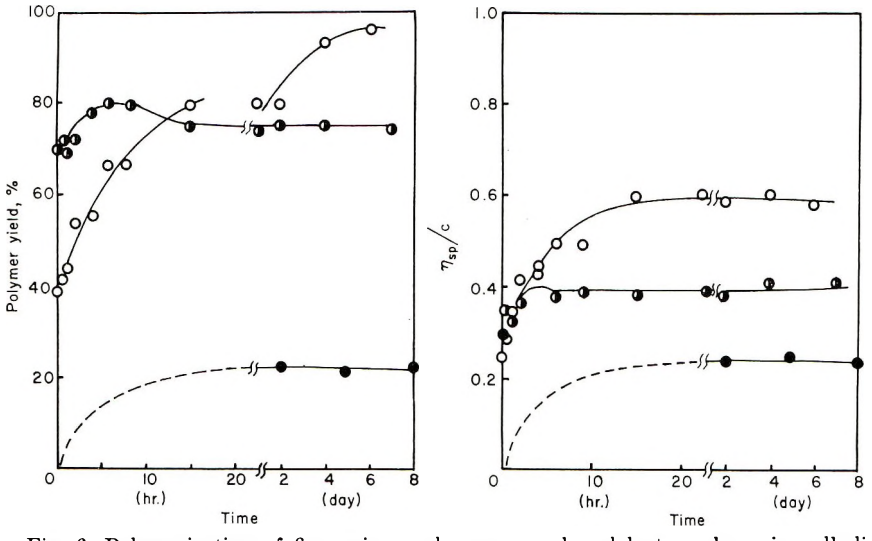

Fig. 6. Polymerization of five-, six-, and seven-membered lactams by using alkali metal as catalyst and *N*-acetyl derivative of monomer as initiator: (○) α-pyrrolidone, (●) α-piperidone; (◑) ε-caprolactam. Polymerization temperature: 45°C. for α-pyrrolidone and α-piperidone, 75°C. for ε-caprolactam; *N*-acetyl derivative of monomer, 2.58 mole-%; metallic potassium, 2.22 mole-% for α-pyrrolidone, 2.58 mole-% for α-piperidone and 2.95 mole-% for ε-caprolactam.

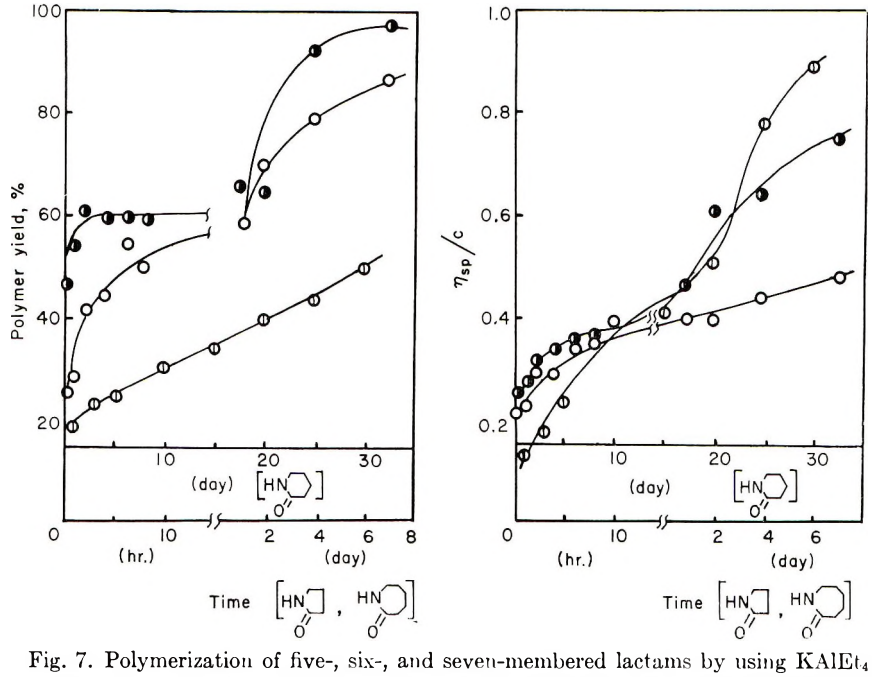

Fig. 7. Polymerization of five-, six-, and seven-membered lactams by using $KAlEt_4$ as catalyst and *N*-acetyl derivative of monomer as initiator: (○) α-pyrrolidone; (◐) α-piperidone; (◑) ε-caprolactam. Polymerization temperature, 45°C. for α-pyrrolidone and α-piperidone, 75°C. for ε-caprolactam; $KAlEt_4$, 2.58 mole-%; *N*-acetyl derivative of monomer, 2.58 mole-%.

Polymerization of Lactams with $MAlEt_4$ Complex as Catalyst

When $MAlEt_4$ (where M = Li, Na, or K) was used as a catalyst in place of an alkali metal, some interesting results were obtained, as shown in Figures 6 and 7.

In the polymerization of ϵ-caprolactam with an alkali metal as a catalyst, polymerization equilibrium was attained after 3–5 hr. at 75°C., but in the case of α-piperidone no propagation was detected, even after 20 hr., and both the yield and the degree of polymerization of polymer were unsatisfactory.

TABLE II
Polymerization of Five-, Six-, and Seven-Membered Lactams by Using $LiAlEt_4$ or $NaAlEt_4$ as Catalyst[a]

Monomer	Catalyst	Initiator[b]	Time, days	Polymer yield, %	η_{sp}/c
α-Pyrrolidone	$LiAlEt_4$	Ac-Pyr	2	42.2	0.29
	$LiAlEt_4$	Ac-Pyr	4	54.1	0.29
	$NaAlEt_4$	Ac-Pyr	2	50.4	0.39
	$NaAlEt_4$	Ac-Pyr	4	63.4	0.50
α-Piperidone	$LiAlEt_4$	Ac-Pip	5	17.8	0.14
	$LiAlEt_4$	Ac-Pip	10	17.3	0.16
	$LiAlEt_4$	Ac-Pip	15	18.6	0.16
	$LiAlEt_4$	Ac-Pip	20	20.9	0.19
	$NaAlEt_4$	Ac-Pip	5	25.6	0.26
	$NaAlEt_4$	Ac-Pip	10	31.3	0.44
	$NaAlEt_4$	Ac-Pip	15	32.2	0.51
	$NaAlEt_4$	Ac-Pip	20	36.4	0.50
ϵ-Caprolactam	$LiAlEt_4$	Ac-Cap	2	60.0	0.52
	$LiAlEt_4$	Ac-Cap	4	61.2	0.54
	$NaAlEt_4$	Ac-Cap	2	63.7	0.48
	$NaAlEt_4$	Ac-Cap	4	64.0	0.61

[a] Polymerization temperature, 40°C. for α-pyrrolidone and α-piperidone; 75°C. for ϵ-caprolactam; catalyst, 2.58 mole-%.

[b] Ac-Pyr, *N*-Acetyl-α-pyrrolidone; Ac-Pip, *N*-acetyl-α-piperidone; Ac-Cap, *N*-acetyl-ϵ-caprolactam.

$KAlEt_4$ was found to be a useful catalyst for the preparation of high polymer from five-, six-, or seven-membered ring lactams.

The case of α-piperidone is of considerable interest. In the polymerization of α-piperidone with $KAlEt_4$ as a catalyst, although the rate of polymerization was almost the same as that in the case of alkali metal, propagation was observed even after 30 days, and a high polymer having a reduced viscosity of 0.9 was obtained.

The results of polymerization with $NaAlEt_4$ or $LiAlEt_4$ as catalyst are listed in Table II. These results and those of Figure 7 indicate the catalytic activity of $MAlEt_4$ decreases in the order: $KAlEt_4 > NaAlEt_4 > LiAlEt_4$.

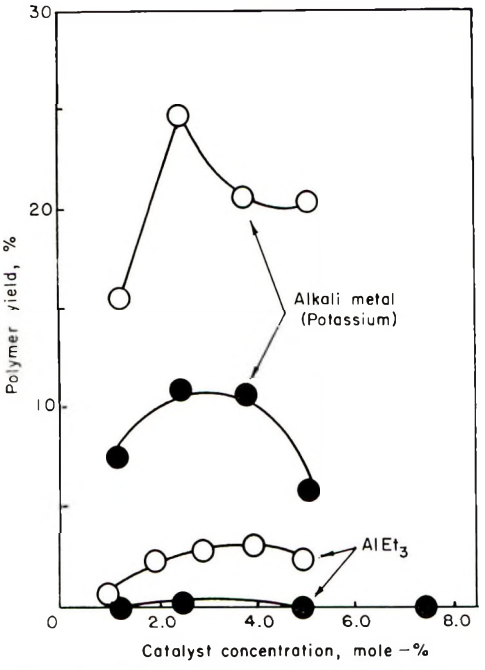

Fig. 8. Polymerization of α-piperidone in bulk or in solution by using metallic potassium or $AlEt_3$ as catalyst: (○) in bulk, (●) in solution, volume ratio of monomer to benzene, 4.0. Polymerization temperature, 40°C.; polymerization time, 240 hr.; *N*-benzoyl-α-piperidone (initiator), 2.0 mole-%.

The catalytic efficiency increases with the increase in the electropositivity of the alkali metal in the complex.

The same tendency has been detected in alkali metal catalyst.

It may be argued that the alkali metal and aluminum salt of α-piperidone formed by the reaction between the $MAlEt_4$ complex and α-piperidone might be the cause of the rather peculiar behavior of the $MAlEt_4$ complex. The aluminum salt has been known to be an active catalyst for the polymerization of lactams, so the possible additional effect of these two salts may be the cause of this behavior. The following experiments were carried out in order to clarify this possibility.

In the polymerization of α-piperidone, $AlEt_3$ was used as a catalyst in place of metallic potassium (see Fig. 8).

$AlEt_3$ was inferior to metallic potassium as a catalyst, and the reduced viscosity of the resulting polymer was as low as 0.11.

Experimental results in the gasometry indicated that $AlEt_3$ in α-piperidone was supposed to exist in the form $AlEt\left(\overset{\frown}{N{-}C}\underset{O}{\overset{\|}{}}\right)_2$ at room temperature. $AlEt_3$ reacted vigorously with α-piperidone at room temperature, and 1 mole of ethane/mole of $AlEt_3$ being evolved immediately and another mole of ethane evolved over a period of 40 min.

TABLE III
Determination of the Amount of Ethane Evolved in the Reaction of $MAlEt_4$ and Lactam[a]

Lactam	Ethane evolved, moles/mole $MAlEt_4$		
	$LiAlEt_4$	$NaAlEt_4$	$KAlEt_4$
α-Pyrrolidone	1.95	1.66	1.02
α-Piperidone	2.83	1.95	0.65
ε-Caprolactam	3.10	1.85	0.84

[a] 0.50 ml. of a solution of $MAlEt_4$ in tetrahydrofuran and 1.0 ml. of lactam were reacted in toluene at room temperature. Concentration $MAlEt_4$ solutions in tetrahydrofuran: $LiAlEt_4$, 0.50 mole/l.; $NaAlEt_4$, 0.74 mole/l.; $KAlEt_4$, 1.13 mole/l.

The amount of ethane evolved in the reaction of the $MAlEt_4$ complex with lactams is also listed in Table III.

These results, together with the data listed in Table I, indicate that the reaction between $MAlEt_4$ complex and lactam does not yield the alkali metal salt and the aluminum salt, but forms complexes of the type $MAlX_3Et$ (where X is an ethyl group or 2-oxo-alkylene-imine group).

All of the alkali metal salts of lactams are very slightly soluble in lactam and the order of solubility is as follows: K salt > Na salt > Li salt.

The reaction product of metallic potassium with α-piperidone (molar ratio 1:3) solidified at a temperature slightly higher than the melting point of α-piperidone.

In contrast to the alkali metal salts of lactams, the aluminum salt was a waxlike material and easily soluble in lactam.

TABLE IV
Polymerization of Five-, Six-, and Seven-Membered Lactams by Using Metallic Potassium as Catalyst and Diphenyl Ketene as Initiator[a]

Monomer	Catalyst K, mole-%	Initiator[b]	Amt. initiator mole-%	Time, days	Polymer yield, %	η_{sp}/c
α-Pyrrolidone	2.22	DPK	2.22	1	82.0	0.66
	2.22	DPK	2.22	2	95.1	0.67
	3.33	DPK	2.22	1	88.2	0.67
	2.22	Ac-Pyr	2.58	1	70.3	0.40
α-Piperidone	2.58	DPK	2.58	1	3.8	0.15
	2.58	DPK	2.58	24	24.1	0.22
	3.57	DPK	2.58	1	5.0	0.19
	2.58	Ac-Pip	2.58	1	24.0	0.22
ε-Caprolactam	2.94	DPK	2.94	1	91.1	0.55
	2.94	DPK	2.94	2	95.0	0.61
	4.41	DPK	2.94	1	99.2	0.61
	2.94	Ac-Cap	2.58	1	76.0	0.45

[a] Polymerization temperature, 40°C. for α-pyrrolidone and α-piperidone; 75°C. for ε-caprolactam.

[b] DPK, Diphenyl ketene; Ac-Pyr, *N*-acetyl-α-pyrrolidone; Ac-Pip, *N*-acetyl-α-piperidone; Ac-Cap, *N*-acetyl-ε-caprolactam.

Polymerization of Lactams with Diphenyl Ketene as Initiator

It has been found that diphenyl ketene could be used as an initiator for the polymerization of lactams, as shown in Tables IV and V. Diphenyl ketene gave the better results than *N*-acetyl or *N*-benzoyl lactams.

TABLE V

Polymerization of Five-, Six-, and Seven-Membered Lactam by Using $MAlEt_4$ as Catalyst and Diphenyl Ketene as Initiator[a]

Monomer	$MAlEt_4$	Time, days	Polymer yield, %	η_{sp}/c
α-Pyrrolidone	$LiAlEt_4$	1	40.6	0.41
	$LiAlEt_4$	2	40.9	0.34
	$NaAlEt_4$	1	45.5	0.45
	$NaAlEt_4$	2	53.3	0.44
	$KAlEt_4$	1	62.8	0.75
	$KAlEt_4$	2	72.4	0.68
	$AlEt_3$	1	38.6	0.21
	$AlEt_3$	2	42.9	0.23
α-Piperidone	$LiAlEt_4$	5	4.5	0.14
	$NaAlEt_4$	5	14.0	0.21
	$NaAlEt_4$	10	32.0	0.32
	$KAlEt_4$	5	15.0	0.26
	$KAlEt_3$	10	30.5	0.50
	$AlEt_3$	5	0	—
	$AlEt_3$	10	0	—
ε-Caprolactam	$LiAlEt_4$	1	47.2	0.45
	$LiAlEt_4$	2	91.7	0.47
	$NaAlEt_4$	1	89.6	0.51
	$NaAlEt_4$	2	92.5	0.54
	$KAlEt_4$	1	88.5	0.52
	$KAlEt_4$	2	92.5	0.73
	$AlEt_3$	1	41.0	0.18
	$AlEt_3$	2	53.1	0.22

[a] Polymerization temperature, 40°C. for α-pyrrolidone and α-piperidone; 75°C. for ε-caprolactam; $MAlEt_4$, 2.58 mole-%; diphenyl ketene, 2.58 mole-%.

TABLE VI

Polymerization of α-Pyrrolidone by Alkali Metal and Corresponding *N*-Diphenylacetyl-Lactam[a]

Initiator	Amt. initiator, mole-%	Polymer yield, %	η_{sp}/c
N-Diphenylacetyl pyrrolidone	1.0	42.7	0.93
	2.0	62.3	0.71
N-Diphenylacetyl piperidone	1.0	41.4	0.98
	2.0	58.3	0.70
N-Diphenylacetylcaprolactam	1.0	32.7	0.80
	2.0	56.4	0.73

[a] Polymerization temperature, 45°C.; polymerization time, 24 hr.; catalyst, metallic potassium, 2.62 mole-%.

In order to clarify the mechanism of polymerization initiated by diphenyl ketene, the reaction of diphenyl ketene with lactams was investigated as a model reaction. When these two compounds were reacted in benzene at room temperature, the corresponding *N*-diphenylacetyl lactam was obtained in good yield. Indeed, *N*-diphenylacetyl lactam itself was found to be a very good initiator for the polymerization of lactam, as shown in Table VI.

From these results, *N*-acyl lactam formed by the reaction between diphenyl ketene and alkali metal salt of lactam may be considered to act as an initiator.

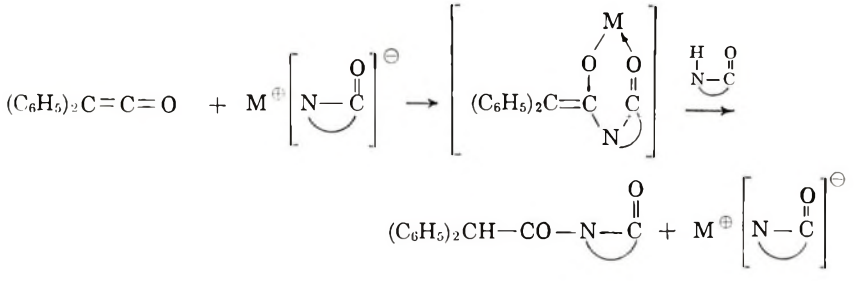

DISCUSSION

The alkaline polymerization of lactams in the presence of an initiator has been considered by many investigators to proceed by way of nucleophilic attack of an amide anion of the alkali metal salt of lactam on an acyl imide group of an initiator or of a propagating polymer.

In this polymerization it may be considered also that some side reactions would occur which cause the consumption of the catalyst system. For instance, it has been suggested that some acidic substances produced by the condensation of two acyl imide groups would consume the alkaline catalyst.[17,18]

In the polymerization of α-piperidone, the effects of heat treatment at 80°C. in the initiation stage on the yield and the degree of polymerization of polymer were studied (see Table VII). The heat treatment decreased the polymer yield, but the reduced viscosity of the resulting polymer remained at almost the same value in all cases. The polymer yield decreased gradually with increasing time of heat treatment, and after 120 hr. treatment no polymer was obtained. Even in this heat-treated polymerization system, the polymerization could be started again by adding *N*-acyl lactam, but not by the addition of alkali metal. From these results, it may be possible to conclude that *N*,*N*-diacyl imide was consumed by some side reaction during the heat treatment. Although the temperature of heat treatment is different from that of polymerization, these experiments give some insight into the nature of the side reaction occurring during the polymerization.

The effects of the addition of $AlEt_3$ to the polymerization system with the alkali metal–*N*-acyl lactam catalyst system were examined (Figs. 9 and 10).

TABLE VII
Effect of Heat Treatment at Initiation Stage on the Yield and the Degree of Polymerization of Poly-α-piperidone[a]

Heat treatment, time at 80°C., hr.	Polymerization conditions	Polymer yield, %	η_{sp}/c
200		0	—
24	40°C., 120 hr.	8.4	0.36
48	40°C., 120 hr.	5.4	0.33
96	40°C., 120 hr.	2.5	—
120	40°C., 24 hr.	0	—
120	Addition of potassium (2.0 mole-%) and 40°C., 120 hr.	0	—
120	Addition of *N*-benzoyl-α-piperidone (1.5 mole-%) and 40°C., 120 hrs.	25.4	0.33

[a] Catalyst, metallic potassium, 2.58 mole-%; $AlEt_3$, 1.5 mole-%; initiator, *N*-benzoyl-α-piperidone, 2.58 mole-%.

As shown in Figure 9, when the amount of the initiator was much lower than that of the catalyst, there was no difference in the viscosities of the two polymers prepared with alkali metal (3.0 mole-%) and with alkali metal–$AlEt_3$ (3.0 and 3.0 mole-%), but there was a remarkable difference in the polymer yield. On the other hand, when the molar ratios of catalyst to initiator were from 2.58 to 2.0 (Fig. 10), high viscosity polymers were obtained by the addition of a limited amount of $AlEt_3$, although the rate of polymerization was very low and much more time was required. These

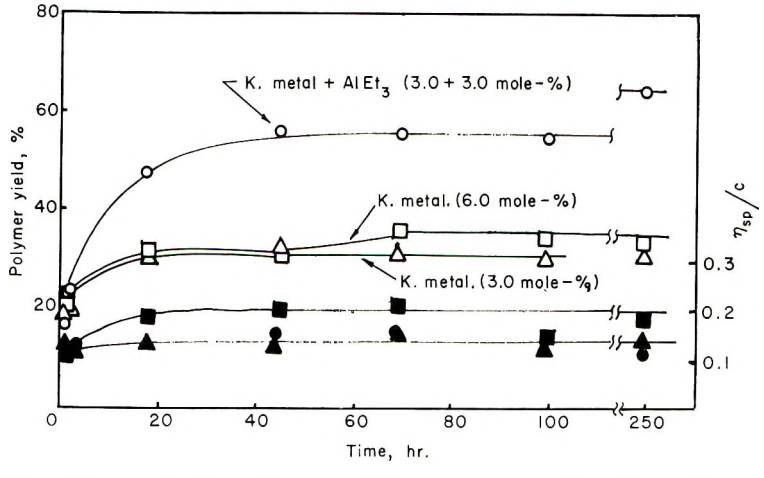

Fig. 9. Influence of added $AlEt_3$ on yield (○, △, □) and on the degree of polymerization of polymer (●, ▲, ■) in the polymerization of α-piperidone by using metallic sodium as catalyst: (○, ●) K metal (3.0 mole-%) + $AlEt_3$ (3.0 mole-%); (△, ▲) K metal (3.0 mole-%); (□, ■) K metal (6.0 mole-%). Polymerization temperature, 45°C.; α-piperidone (monomer), 0.022 mole; *N*-benzoyl-α-piperidone (initiator), 8.0 mole-%.

results may be qualitatively explained by considering the two different roles that the added $AlEt_3$ plays. First, the added $AlEt_3$ protects the *N*,*N*-diacyl imide group from side reactions by stabilizing the potassium salt through the formation of a certain type of complex, which is analogous to one derived from $MAlEt_4$.

Secondly, the added $AlEt_3$ increases the solubility of the potassium salt in the polymerization medium.

The polymerization systems containing α-piperidone and catalyst were subjected to heat treatment at various temperatures in their initiation stages. The effects of these heat treatments on the polymer yield and the polymer viscosity were examined (Fig. 11). The catalytic activity of the aluminum salt decreased remarkably at temperatures above 140°C., but that of the potassium salt was not so sensitive to the treatment temperature.

These heat-treated catalysts were not able to give satisfactory results, however.

Compared to the other above-mentioned catalysts, $KAlEt_4$ treated at a temperature below 80°C. has a more powerful polymerizing activity, and that treated at the temperature above 110°C. has about the same degree of activity as the K–$AlEt_3$ system. The decrease in the activities of $KAlEt_4$

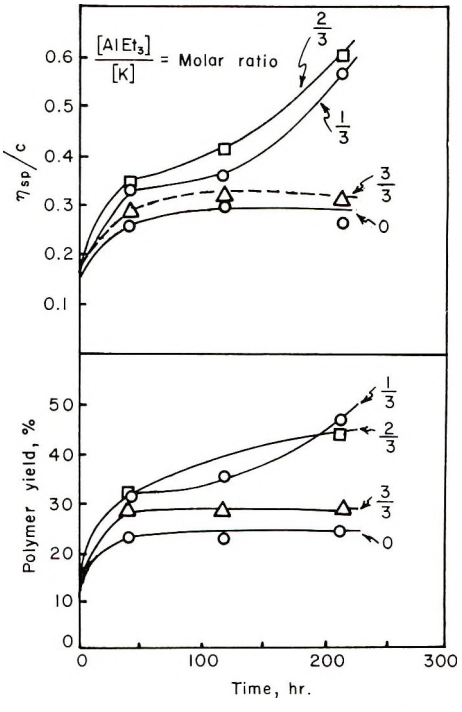

Fig. 10. Influence of added $AlEt_3$ on the yield and on the degree of polymerization of polymer in the polymerization of α-piperidone by using metallic potassium as catalyst. Polymerization temperature, 40°C.; α-piperidone (monomer), 0.022 mole; *N*-benzoyl-α-piperidone, 2.0 mole-%; metallic potassium (catalyst), 2.58 mole-%.

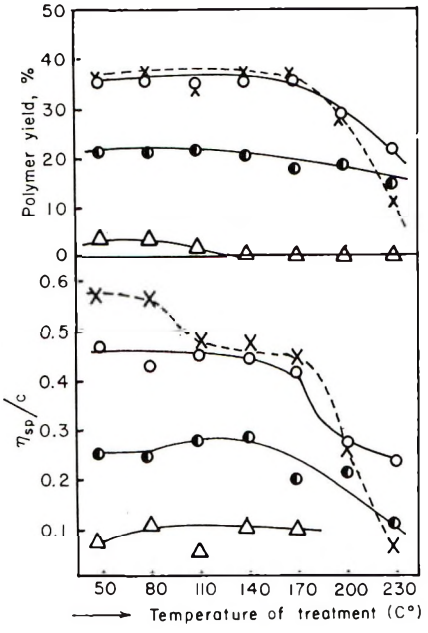

Fig. 11. Influence of heat treatment on the yield and on the degree of polymerization of polymer obtained with various catalysts: (×) $KAlEt_4$; (○) K metal + $AlEt_3$; (◑) K metal; (△) $AlEt_3$. The procedure for heat treatment: after the reaction of catalyst with lactam had been completed, the polymerization systems were allowed to stand at the specified temperature for 40 min. α-piperidone (monomer), 0.022 mole; $KAlEt_4$, 2.58 mole-%; metallic potassium, 2.58 mole-%; $AlEt_3$, 2.58 mole-%; *N*-benzoyl-α-piperidone, (initiator), 2.0 mole-%.

and of K–$AlEt_3$ systems at a temperature above 150°C. or so may be attributable to the transformation of the complex formed at room temperature into another complex; details are not yet known.

From the experimental results on the gasometry, the reaction of $MAlEt_4$ with a ring lactam may be considered to form a complex of the type I:

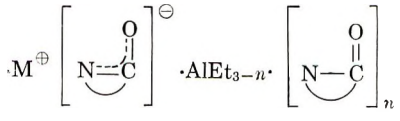

where $n = 0$, 1, or 2. The number of ethyl groups able to react with lactam in a $MAlEt_4$ molecule depends solely on the nature of the alkali metal and not on the lactam.

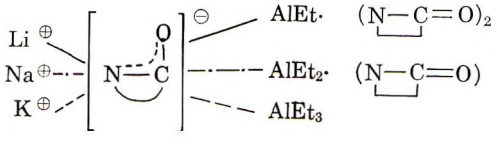

In conclusion, there are two advantages in the use of the $MAlEt_4$ and alkali metal–$AlEt_3$ catalyst systems. One is the increased solubility of catalyst, and the other is the protection of the endgroups of polymer from any side reaction by stabilization of the alkali metal salt as a complex. These two effects may be the reason why the very high molecular weight polymer was obtained in our reaction system.

The authors wish to express their appreciation to Miss. S. Sakurai for help in parts of the experiment.

References

1. Hanford, W. E., and R. M. Joyce, *J. Polymer Sci.*, **3,** 967 (1948).
2. Griehl, W., *Faserforsch. Textiltech.*, **7,** 207 (1956).
3. Wichterle, O., *Makromol. Chem.*, **35,** 174 (1960).
4. Cefelin, P., M. Chenelir, and O. Wichterle, *Coll. Czechoslov. Chem. Commun.*, **25,** 1267 (1960).
5. Wichterle, O., J. Kraliček, and J. Šebenda, *Coll. Czechoslov. Chem. Commun.*, **24,** 755 (1959).
6. Wichterle, O., E. Sittler, and P. Cefelin, *Coll. Czechoslov. Chem. Commun.*, **26,** 2897 (1961).
7. Saunders, J., *J. Polymer Sci.*, **30,** 479 (1958).
8. Kralicek, J., and J. Šebenda, *J. Polymer Sci.*, **39,** 493 (1958).
9. Šebenda, J., and J. Kraliček, *Coll. Czechoslov. Chem. Commun.*, **23,** 766 (1958).
10. Ney, W. O., Jr., W. R. Nummy, and C. E. Barnes, U. S. Pat. 2,638,463 (1953); W. O. Ney, Jr., and M. Crowther, U. S. Pat. 2,739,959 (1956).
11. Murahashi, S., H. Yuki, and H. Sekiguchi, *Ann. Rept. Inst. Fiber Res. (Osaka)*, **10,** 88, 93 (1957).
12. Murahashi, S., H. Yuki, and T. Suzuki, *Ann. Rept. Inst. Fiber Res. (Osaka)*, **11,** 50 (1958).
13. Champetier, G., and H. Sekiguchi, *Compt. Rend.*, **249,** 108 (1959).
14. Hall, H. K., *J. Am. Chem. Soc.*, **80,** 6404 (1958).
15. Yoda, N., and A. Miyake, *J. Polymer Sci.*, **43,** 117 (1960).
16. Chrzczonowicz, S., M. Wlodarczyk, and B. Ostaszewski, *Makromol. Chem.*, **38** 159 (1960).
17. Kobayashi, H., and K. Matuya, *J. Polymer Sci. A*, **1,** 111 (1963).
18. *Organic Synthesis, Coll. Vol.* E. C. Horning, Ed., Wiley, New York, 1955, p. 356.
19. Tani, H., N. Oguni, and T. Araki, *Bull. Chem. Soc. Japan*, **37,** 1245 (1964).
20. Wichterle, O., and U. Gregor, *J. Polymer Sci.*, **34,** 309 (1956).

Résumé

On a polymérisé des lactames à cinq, six, et sept membres à des températures inférieures à 80°C. en utilisant comme catalyseur le potassium métallique ou le $MAlEt_4$ (où M est Li, Na, ou K) et comme initiateur la *N*-acyl-lactame ou le diphénylcétène. En employant comme catalyseur le $MAlEt_4$, au lieu du potassium métallique, dans la polymérisation de l'α-pipéridone, la propagation a été poursuivie jusqu'à ce que la viscosité réduite du polymère atteigne une valeur de 0,9. Le polymère obtenu forme aisément des films. Les résultats expérimentaux obtenus dans les expériences gasométriques suggèrent que $MAlEt_4$ réagit avec la lactame pour former un complexe du type

$$\underbrace{M\cdot N\text{———}C{=}O}_{(CH_2)_n}\cdot AlX_3$$

(où M est Li, Na, ou K et X est un groupement éthyle ou 2 oxoalkylène-imine). On considère que les complexes formés augmentent la solubilité du catalyseur et protègent les groupes terminaux du polymère d'une réaction secondaire par la stabilisation du métal alcalin au sein du complexe. En plus le rôle du phénylcétène dans l'initiation a été révélée par le fait que la *N*-diphénylacétyl-lactame correspondante est obtenue par réaction du diphénylcétène avec la lactame et par le fait que la *N*-diphénylacétyl-lactame elle même peut être utilisée pour la polymérisation de l'α-pipéridone.

Zusammenfassung

Die Polymerisation von fünf-, sechs- und seibengliedrigen Lactamen mit metallischem Kalium oder $MalEt_4$ (wo M Li, Na oder K ist) als Katalysator und *N*-Acyllactam oder Diphenylketen als Starter wurde bei Temperaturen unterhalb 80°C ausgeführt. Mit $MAlEt_4$ anstelle von metallischen Kalium als Katalysator wurde das Wochstum bei der Polymerisation von α-Piperidon so lange fortgesetzt, bis die reduzierte Viskosität des Polymeren einen Wert von 0,9 erreichte. Das gebildete Polymere besitzt filmbildende Eigenschaften. Die gasometrischen Ergebnisse zeigen, dass $MAlEt_4$ mit dem Lactam unter Bildung eines Komplexes vom Typ

$$M \cdot N\text{———}C{=}O \cdot AlX_3$$
$$\quad\ \ \llcorner(CH_2)_{\overline{n}}\lrcorner$$

(wo M Li, Na oder K und X eine Athyl- oder 2-Oxo-alkylen-iminggruppe ist) reagiert. Es wird angenommen, dass die entsprechenden Komplexe die Löslichkeit des Katalysators erhöhen und die Endgruppen des Polymeren durch Stabilisierung des Alkalimetalls im Komplex gegen Nebenreaktionen schützen. Ausserdem konnte die Wirkungsweise des Diphenylketen als Starter an der Tatsache gezeigt werden, dass das entsprechende *N*-Diphenylacetyllactam aus der Reaktion von Diphenylketen mit Lactam erhalten wurde und dass *N*-Diphenylacetyllactam seinerseits für die Polymerisation von α-Piperidon brauchbar war.

Received May 11, 1965
Revised July 15, 1965
Prod. No. 4804A

JOURNAL OF POLYMER SCIENCE: PART A-1 VOL. 4, 319–336 (1966)

The Role of Diffusion in Propylene Polymerization

J. W. BEGLEY, *Phillips Petroleum Company, Research Division, Bartlesville, Oklahoma*

Synopsis

The role of monomer diffusion in the polymerization of propylene by organometallic catalysis was examined by use of mathematical models which couple the rate of diffusion through the polymer film surrounding the catalyst with the rate of surface reaction. An approximate form of a second-order, integrated rate equation was used to describe the disappearance of active sites on the surface. For the most conservative model conceivable, it was estimated that the particle size would have to be 10–100 times the size for the catalysts presently in use before diffusion time would be significant. The size of the catalyst was determined by photomicrographs and nitrogen adsorption surface areas. The surface areas for three different catalysts were 7, 20–21 and 35 $m.^2/g.$, respectively. The kinetic model without the diffusion term was used satisfactorily to correlate productivity data. The characteristic decline in reaction rate was examined in terms of the decay of active sites on the surface of the catalyst. The rate of decay was determined to be second order with respect to the site concentration. The kinetic model indicates that the total polymerization time for a specified productivity is the sum of the monomer diffusion time and the surface reaction time. The model derived by use of an approximate second-order decay function is unique because of the additivity of diffusion and reaction times, which is not the case when the second-order function is used rigorously.

Introduction

The question of monomer diffusion to the catalyst surface appears in the interpretation of kinetic data from many slurry polymerization systems.[1–3] Each of these systems displays a characteristic decline in rate with increasing time, suggesting a diffusion-controlled reaction. However, the decline in the number of active sites on the catalyst surface is another possible cause for the rate decline. Of course, a combination of these factors is also possible.

In the present work, a mathematical model is developed which takes into consideration simultaneously the two factors, decline in diffusion rate and active sites. The model is then used to show that diffusion is not a consideration in a propylene polymerization system using an organometallic catalyst. Productivity data are satisfactorily correlated by the model without the diffusion term included, which further substantiates the conclusion that diffusion is not a consideration. The rate decline was attributed to a decay in the active site concentration on the surface. The rate of site decay was found to be second-order in site concentration on the surface.

Literature Summary

Analytical treatment of the problem of diffusion in slurry polymerization has not been reported in the literature. However, in an indirect way, the role of diffusion has been discounted in several studies. Smith and Zelmer[1] ruled out diffusion on the basis of the polymer production rate being directly proportional to the catalyst concentration for several alkyl-metal promoted catalysts in ethylene polymerization. Lipman and Norrish[2] argue that for the gas-phase polymerization of ethylene the overall reaction kinetics are simple and would not be if diffusion were a factor. Secondly, the overall energy of activation of the reaction is about 3 kcal./mole, which is much lower than the activation energy for permeation. The activation energy for diffusion was estimated to be 11.6 kcal./mole by the method of Michaels and Bixler.[4] The activation energy for permeation is 14.6 kcal./mole, which is greater than the activation energy for diffusion by the heat of solution of ethylene in polyethylene.

Lipman and Norrish further comment that "if diffusional control is not a rate-determining factor, a model in which a continuous layer of polymer builds up around a catalyst particle is untenable, for such a model would predict diffusional control." They therefore suggest that the polymer is deposited on the catalyst sites in the form of "towers" to form a highly porous structure.

In commenting on the possible causes for the decline in catalyst activity, Wilson and Hurley[3] suggest that the polymer coating around the catalyst particles could interfere with the diffusion of the ethylene, catalyst components, or solvent to the catalyst surfaces. However, they state that diffusion can be calculated to be a possible rate limiting process only if the catalyst particles are larger than 1–10 μ in diameter. The sedimentation and filtration behavior of the catalyst used by Wilson and Hurley suggested that the particle agglomerates were larger than 10 μ. Therefore, diffusion was suspected as a limiting factor in the rate of polymerization.

In the studies by Smith and Zelmer and by Lipman and Norrish, the possibility of diffusion being a factor was discounted and the decline in rate was attributed to the decay of the number of active sites on the catalyst surface. The fraction of sites remaining at time t was determined by the ratio of the polymerization rate at t and the initial rate, i.e.,

$$\frac{n_s(t)}{n_s(0)} = f_t = \frac{(dP/dt)_t}{(dP/dt)_0} \tag{1}$$

where $n_s(0)$, $n_s(t)$ are respectively, the total number of reaction sites on the catalyst surface initially and at time t. By use of these data, the decay of active sites was subsequently found to be a second-order rate function, where the rate of disappearance of sites is second-order with respect to the site concentration.

$$d[n_s(t)]/dt = -k_D[n_s(t)]^2/4\pi r_c^2 \tag{2}$$

Here k_D is the reaction velocity constant for site decay in particles/site-cc. and r_c is the catalyst particle radius in centimeters. The integration of eq. (2) gives a relationship which can be used to test the second-order decay of sites.

$$\frac{1 - [n_s(t)/n_s(0)]}{[n_s(t)/n_s(0)]} = \frac{1 - f_t}{f_t} = \frac{k_D n_s(0) t}{4\pi r_c} \tag{3}$$

Rate data for several different catalysts were found to fit the relationship suggested by eq. (3). The catalyst systems included $TiCl_4$ plus trimethylaluminum in the study by Lipman and Norrish. In the studies by Smith and Zelmer, the catalysts were $CrO_3 \cdot SiO_2$ and $V_2O_5 \cdot SiO_2$ promoted by $(i\text{-}C_4H_9)_3Al$; $VOCl_3$ promoted by $(C_2H_5)_2AlCl$; $TiCl_4$ promoted by $(C_3H_5)_3Al$ or $(i\text{-}C_4H_9)_3Al$; and $(C_3H_5)_2TiCl_2$ promoted by $(CH_3)_2AlCl$. In spite of the chemical differences in the catalysts, all of the systems exhibited a second-order deactivation of active sites.

Smith and Zelmer speculate as to the mechanism of the site decay. For the second-order decay to be obeyed, two active sites must interact to form species of negligible activity. One possible molecular reaction suggested is,

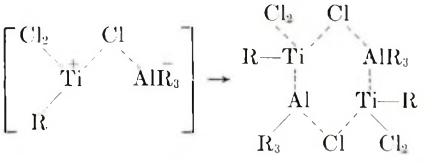

The six-membered ring compound is a nonstable intermediate state that disproportionates to give

which is the metal alkyl complexed with the transition metal. The titanium metal, however, is reduced to a lower valence state. The Ti^{+3} complex is not as active as the Ti^{+4} complex for ethylene polymerization.

Not all of the literature is in complete accord with the second-order mechanism of site decay. Friedlander,[5] in an unpublished study, discounts the second-order decay mechanism on the basis of the difficulty in devising a good physical description of the interaction of catalyst sites in complex or heterogeneous systems. A model based upon a mixed order (a combination of first- and a second-order deactivation) was used by Friedlander to analyze some of the data from the literature.

Kohn et al.[6] used a first-order deactivation of catalyst in a model to describe the kinetic data for the polymerization of propylene by titanium trichloride and diethylaluminum chloride. However, no direct test of the first-order mechanism was indicated. Instead, the kinetic model was used to satisfactorily predict molecular weights. This is not believed to be a

critical test of the order of site decay mechanism. Bier et al.[7] have also more or less assumed a first-order decay of active sites.

The activation energies E for the overall rate constants in the polymerization of propylene have been reported by several of the investigators. The values are summarized in Table I.

TABLE I
Activation Energies for Propylene Polymerization

Investigator	Catalyst	E, kcal./mole
Natta et al.[8]	$TiCl_3 + Al(C_2H_5)_3$	14
Kohn et al.[6]	$TiCl_3 + Al(C_2H_5)_2Cl$	10
Firsov et al.[9]	$TiCl_3 + Al(R)_3$	13.5

The activation energies for the overall rate are very close to the value for diffusion which adds further support to a diffusion-controlled reaction. The following analysis will, however, indicate the fallacy of using activation energy to say whether or not diffusion is a controlling factor in the overall rate.

Development of the Kinetic Model

The following development is based upon a spherical geometry for the original catalyst particles and the particles during the course of the polymerization. The catalyst particles are not spherical, but due to polymer growth on the edges, a shape nearly spherical probably results, and the assumption is probably good a large percentage of the polymerization time. However, in order to indicate the most unfavorable situation from the standpoint of diffusion, an analogous model is derived by using a rectangular geometry. The differential equation describing the diffusion of monomer through a constantly changing thickness of polymer coupled with reaction at the surface is very complex. In order to reduce the complexity, it was assumed that the diffusion rate can be described on the basis of the steady-state gradient across a spherical shell, i.e.,

$$\text{Rate} = [4\pi D_p(C_s - C_c)r]/[(r/r_c) - 1] \tag{4}$$

Here, D_p is diffusivity of propylene in polypropylene, C_s is the equilibrium solubility of propylene in polypropylene, C_c is propylene concentration in the polymer phase at the polymer–catalyst particle interface, r is polymer particle radius. The actual gradient across the shell will always be greater than or equal to the steady-state gradient. Consequently, our estimate of particle size for which diffusion rate becomes significant will be on the low side. The estimate will be made further conservative by use of a diffusion coefficient for nonsolvated polymer.

The rate of diffusion is also equal to the rate of surface reaction,

$$\text{Rate} = k_1 n_s(t) C_c \tag{5}$$

where k_1 is the reaction velocity constant for the surface reaction. By combining eqs. (4) and (5) the following expression is obtained for the monomer concentration in the polymer at the interface.

$$C_c = \frac{4\pi D_p C_s r}{4\pi D_p r + k_1 n_s(t)(r/r_c - 1)} \tag{6}$$

If eq. (6) is combined with eq. (7) for the site concentration as a function of productivity P, where K is an arbitrary constant,

$$n_s(t) = n_s(0)/(1 + KP) \tag{7}$$

the rate expression becomes

$$\text{Rate} = \frac{4\pi D_p k_1 C_s r}{[4\pi r D_p/n_s(0)](1 + KP) + k_1(r/r_c - 1)} \tag{8}$$

An interpretation of the expression for the site decay, eq. (7), will be examined thoroughly by use of experimental data after the role of diffusion has been clarified.

The definition for productivity in terms of particle radius is

$$P = (\rho_p/\rho_c)\,[(r/r_c)^3 - 1] \tag{9}$$

where ρ_c, ρ_p are density of catalyst and polymer, respectively (2.6 and 0.9 g./cc., respectively). The final differential equation is obtained by substituting eq. (9) into eq. (8) and equating the result to $4\pi r^2(dr/dt)\rho_p$, which is the weight rate of growth for the particle.

$$r\frac{dr}{dt}\rho_p = \frac{D_p k_1 C_s}{[4\pi r D_p/n_s(0)]\,\{1 + K(\rho_p/\rho_c)[(r/r_c)^3 - 1]\} + k_1(r/r_c - 1)} \tag{10}$$

Integration of eq. (10) between the limits, $t = 0$, $t = t$, and $r = r_c$, $r = r$, plus the use of eq. (9) for the definition of productivity gives the final kinetic model:

$$\frac{4}{3}\frac{\pi r_c^3 \rho_c}{k_1 n_s(0)\, C_s}\left\{P + \frac{K}{2}P^2\right\} + \frac{\rho_p r_c^2}{3D_p C_s}\left\{P\frac{\rho_c}{\rho_p} - \frac{3}{2}\left[\left(P\frac{\rho_c}{\rho_p} + 1\right)^{2/3} - 1\right]\right\} = t \tag{11}$$

where the first term is reaction time, the second term is diffusion time, and t is process time. Equation (11) can be interpreted as follows. For a specified catalyst productivity, the total process (polymerization) time is equal to the sum of the time of monomer diffusion to the surface plus the reaction time at the surface

In the integration of eq. (10), C_s, the solubility of propylene in polypropylene, was assumed to be independent of time. It should also be noted that in the derivation the question of how the polymer film grows from the inside was ignored. Instead, the assumption was made that the

catalyst particle is at any instant uniformly covered by the polymer and that the rate of polymer formation is equal to the rate of increase in radius of the polymer particle multiplied by the surface area and the polymer density.

The rate of propylene transferred from the bulk of the liquid phase to the surface of the polymer may be significant. The rate of mass transfer to the particle surface can be expressed in terms of a mass transfer coefficient k_L and the concentration difference between the liquid and the surface, C_s' being the concentration of propylene in the liquid phase at the interface between the liquid and the polymer–catalyst particle.

$$\text{Rate} = 4\pi r^2 k_L(C - C_s') \tag{12}$$

In the case when the particles are small and the slip velocity between the particle and the fluid is small, the mass transfer coefficient can be expressed in terms of the liquid diffusion coefficient for the monomer by use of the limiting value for the Sherwood Number equal to 2.0.

$$k_L = D_L/r \tag{13}$$

The rate equation in terms of the mass transfer relationship is

$$\text{Rate} = 4\pi r D_L(C - C_s') \tag{14}$$

The rate is also equal to the rate of diffusion across the polymer film.

$$4\pi r D_L(C - C_s') = 4\pi D_p(C_s' - C_c)r/(r/r_c - 1) \tag{15}$$

If we assume that phase equilibrium exists at the interface then,

$$C_s' = K_s C_s \tag{16}$$

where K_s is the equilibrium constant relating liquid phase propylene concentration and solubility of propylene in polypropylene, and eq. (15) can be solved for C_s.

$$C_s = \frac{D_L r C + [D_p C_c r/(r/r_c - 1)]}{D_L K_s r + [D_p r/(r/r_c - 1)]} \tag{17}$$

C is the propylene concentration in the liquid phase surrounding the polymer–catalyst particle. The solubility (C_s) of the monomer in the polymer at the edge of the polymer particle can be eliminated in the final differential equation by combining eq. (17) with the following:

$$k_1 n_s(t) C_c = [4\pi D_p(C_s - C_c)r/(r/r_c - 1)] \tag{18}$$

The following expression for C_c is obtained.

$$C_c = \frac{C}{\dfrac{k_1 n_s(t) K_s(r/r_c - 1)}{4\pi D_p r} + K_s + \dfrac{k_1 n_s(t)}{D_L 4\pi r}} \tag{19}$$

The final differential rate equation is

$$4\pi r^2 \frac{dr}{dt}\rho_p = \frac{C}{\dfrac{K_s(r/r_c - 1)}{4\pi D_p r} + \dfrac{K_s}{k_1 n_s(t)} + \dfrac{1}{4\pi r D_L}} \tag{20}$$

By use of the site decay function to replace $n_s(t)$ [eq. (7)] and the definition for productivity [eq. (9)], eq. (20) can be integrated to give the following kinetic model, where the first term represents reaction time, the second term, polymer–film diffusion time, and the third is liquid-film diffusion time.

$$\frac{4}{3}\frac{K_s r_c^3 \rho_c}{k_1 n_s(0) C_{\text{avg}}}\left\{P + \frac{K}{2}P^2\right\} + \frac{K_s r_c^2 \rho_p}{3 D_p C_{\text{avg}}}\left\{\frac{P\rho_c}{\rho_p} - \frac{3}{2}\left[\left(P\frac{\rho_c}{\rho_p} + 1\right)^{2/3} - 1\right]\right\}$$
$$+ \frac{\rho_p r_c^2}{D_p C_{\text{avg}}}\left\{\left(P\frac{\rho_c}{\rho_p} + 1\right)^{1/3} - 1\right\} = t \tag{21}$$

Here

$$C_{\text{avg}} = \int_0^t C dt/t$$

Equation (21) can be interpreted in much the same way as eq. (11). The total process (polymerization) time for a specified productivity is a sum of the time for the monomer to diffuse to the surface of the polymer particle, the diffusion time for the monomer in the polymer shell, and the reaction time on the surface of the catalyst.

The model based upon the use of a rectangular geometry is somewhat different from the one where a spherical geometry was assumed. With the rectangular geometry, the polymer surface is assumed to be parallel to the catalyst surface at all times, and the diffusion rate is expressed as follows:

$$\text{Rate} = D_p(C_s - C_c)(\text{S.A.})/L \tag{22}$$

where L is thickness of polymer or the catalyst surface and S.A. is particle surface area per unit weight of catalyst. When eq. (22) is combined with the expression for the rate of reaction at the surface,

$$\text{Rate} = k_1 n_s(t) C_c \tag{5}$$

the following equation for the monomer concentration at the catalyst surface is obtained:

$$C_c = \frac{D_p C_s(\text{S.A.})}{D_p(\text{S.A.})/n_s(t) + k_1 L} \tag{23}$$

The rate of polymer deposition is equal to the rate of reaction, i.e.,

$$\frac{dL}{dt}\rho_p = \frac{k_1 D_p C_s}{[D_p(\text{S.A.})/n_s(t)] + k_1 L} \tag{24}$$

If eq. (7) is again used for the decay function and the productivity is defined by the following expression,

$$P = (\text{S.A.})L\rho_p \tag{25}$$

the following differential equation is obtained.

$$\rho_p \frac{dL}{dt} = \frac{k_1 D_p C_s}{\dfrac{D_p(\text{S.A.})}{n_s(0)} + \dfrac{D_p(\text{S.A.})^2 \rho_p K L}{n_s(0)} + k_1 L} \tag{26}$$

Integration of eq. (26) between the limits, $L = 0$ and $L = L$, $t = 0$ and $t = t$, plus the use of eq. (25) for the definition of productivity gives the final kinetic equation for productivity:

$$\frac{1}{k_1 n_s(0) C_s}\left(P + \frac{K}{2}P^2\right) + \frac{p^2}{2(\text{S.A.})^2 \rho_p D C_s} = t \tag{27}$$

Here again, the total polymerization time t for a specified productivity is a sum of the reaction time on the surface plus the time of monomer diffusion to the surface. However, the diffusion time in the case of the rectangular geometry varies as the square of the productivity while the variation in the case of spherical geometry is nearly linear. As a consequence, the rectangular model will indicate a higher diffusion time than for the spherical model and is believed to be the most conservative estimate of the diffusion time for any model conceivable.

Estimation of the Diffusion Time

The relative importance of diffusion time compared to total polymerization time can be estimated by use of the diffusion terms in eqs. (11), (21), and (27). For the polymer-film diffusion time, the time coefficient contains the variables, r_c, the catalysts particle radius [surface area, S.A., in eq. (27)], and D_pC_s, the permeability factor for propylene through polypropylene.

The catalyst particle size was estimated by two different methods. First, nitrogen adsorption measurements were used to determine the surface area. Approximate checks on the surface area measurements were made by the use of photomicrographs of the catalysts. The surface areas for the three selected catalysts were found to be as given in Table II.

Unfortunately, the particle size is in the range where the field of view for the electron microscope cannot be large enough to permit a particle-size

TABLE II

Catalyst	Surface area, m.²/g.
1	7 ± 1
2	20–21
3	34

Fig. 1. Photomicrograph of catalyst 1. 1775×.

count. Figure 1 is an electron micrograph of catalyst 1.* The smallest particle is about 0.6 μ across while the largest particle is about 7 μ across. It is difficult to determine whether or not the large particles are agglomerates or very large particles. The nitrogen surface area for this catalyst is 7 ± 1 m.^{2}/g. If we assume a spherical shape, the average particle size is calculated to be near 0.3 μ. Although this value is within the range of dimensions observed in Figure 1 and would appear to indicate very little porosity in the particles, a particle size distribution would be necessary to obtain an average particle size. Figure 2 is a photomicrograph of catalyst 3. The field of view is large in this case but the magnification is not high enough for a particle-size count.

The permeability factor for propylene in polypropylene at 120°F. is 17,780 g.-mil/24 hr.-100 in.^{2} or 2.29×10^{-3} g.-cm./hr.-cm.^{2} according to the prediction method of Salame.[10] By use of this value in the diffusion-

* See Appendix I for a description of the procedures used in determining the surface areas and making the photomicrographs.

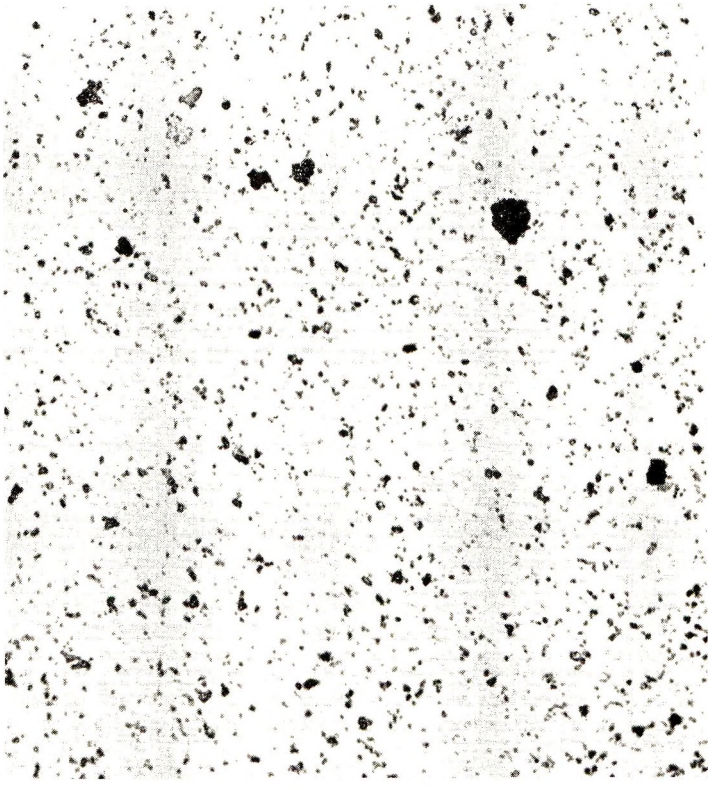

Fig. 2. Photomicrograph of catalyst 3. 150×.

time coefficient and various assumed particle sizes, the polymer–film diffusion times for productivities of 500 and 1000 are presented in Table III for the case of spherical geometry.

TABLE III
Estimate of Polymer–Film Diffusion Time: Spherical Geometry

Catalyst radius $r_c \times 10^4$, cm.	Diffusion time, hr. Productivity 500	Productivity 1000
0.16	0.000036	0.000074
1.6	0.0036	0.0074
16	0.36	0.74

The results indicate that the particle size would have to be in the range of 10 μ before the diffusion time is significant compared to the total polymerization time of several hours.

The diffusion model based upon a rectangular geometry should give the most conservative estimate of diffusion time.

TABLE IV
Estimate of Polymer–Film Diffusion Time: Rectangular Geometry

Catalyst surface area S.A., m.²/g.	Diffusion time, hr.	
	Productivity 500	Productivity 1000
7	0.00095	0.0038
0.7	0.095	0.38
0.07	9.5	38.0

As shown in Table IV, the diffusion time is not significant unless the surface area is less than 1 m.²/g. It is therefore demonstrated rather conclusively that diffusion cannot be a controlling factor in the rate of polymerization where the surface areas are 7 m.²/g. or greater and particle sizes are less than 1 μ on the average.

The liquid–film diffusion time can be estimated by use of the appropriate term in eq. (21). The diffusivity of propylene in a solvent is known to be of the order of 10^{-5} cm.²/sec. or 3.6×10^{-2} cm.²/hr. The diffusion times for various size particles are presented in Table V for a case where the concentration of propylene in the solvent is about 0.6 lb./gal. or 0.07 g./cc.

TABLE V
Estimate of Liquid–Film Diffusion Time

Catalyst radius $r_c \times 10^4$, cm.	Diffusion time, hr.	
	Productivity 500	Productivity 1000
0.16	1.05×10^{-6}	1.33×10^{-6}
1.6	1.05×10^{-4}	1.33×10^{-4}
16	1.05×10^{-2}	1.33×10^{-2}
160	1.05×10	1.33

According to these results, the liquid–film diffusion time would not be significant unless the catalyst particles are greater than 100 μ in diameter.

Kinetics of Site Decay

By the elimination of monomer diffusion as a possible controlling step in the rate of polymerization, the decline in the rate can be attributed solely to a decay of site concentration on the catalyst surface. The fraction of sites remaining on the surface can be determined by eq. (1) as suggested by Smith and Zelmer[1] and Lipman and Norrish.[2] The order of the rate of site decay has been tested for the results from polymerization experiments.

The productivity data were differentiated with respect to time and plotted versus time in Figure 3. Table VI is a tabulation of the data

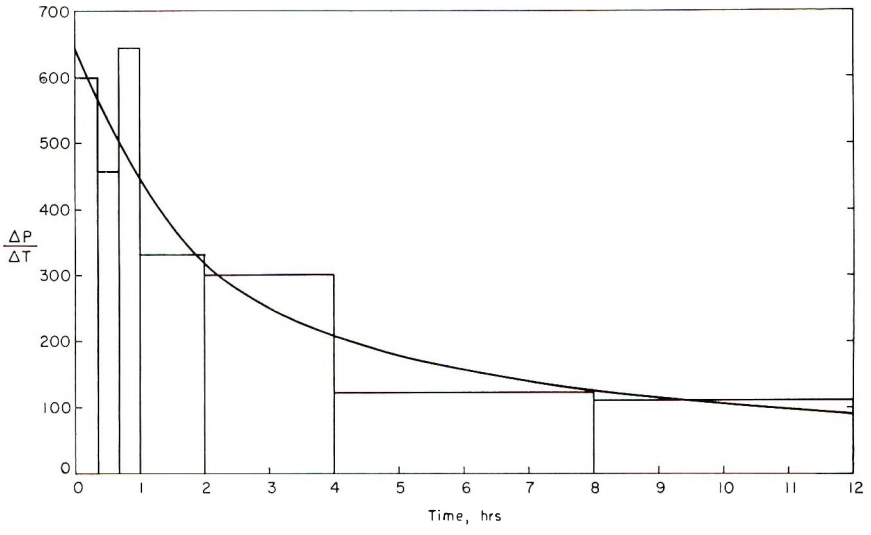

Fig. 3. Curve fit of rate data.

used in the analyses. The rate data were smoothed by use of the equal area principle, i.e.,

$$\int_0^t (\Delta P/\Delta t)dt = P_t$$

The fraction of sites remaining on the surface at any time was determined by use of the smoothed rate data.

TABLE VI
Data Used in the Analysis of Rate of Active Site Decay

Run no.	Time, hr.	P, lb./lb.	ΔP, lb./lb.	$\Delta P/\Delta t$, lb./lb.-hr.
1	0.333	52	52	156
2	0.667	109	57	171
3	1.0	166	57	171
4	2.0	296	130	130
5	4.0	510	214	107
6	8.0	703	207	51.8
7	12.0	911	208	52.0

If the site decay mechanism is first order, the log of the fraction of sites remaining on the surface should be a linear function of time as dictated by the integrated rate expression for first-order decay.

$$\ln f_t = k_D t \tag{28}$$

On the other hand, if the mechanism is second-order, the integrated rate expression, eq. (3), should be obeyed.

$$(1 - f_t)/f_t = [k_D n_s(0)/4\pi r_c^2]t \tag{3}$$

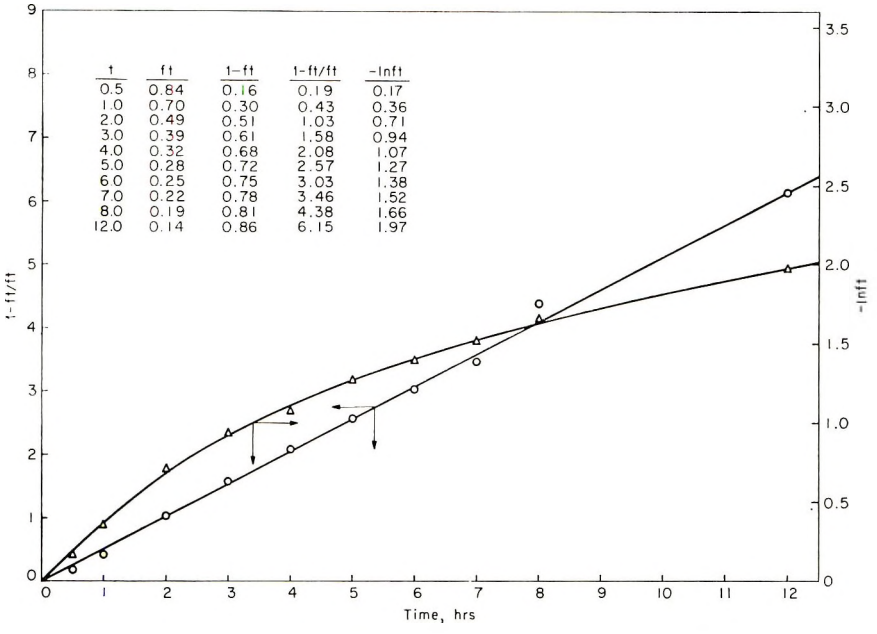

Fig. 4. Test of first- and second-order decay of active sites.

In Figure 4 the test for first and second order are presented. The second-order relationship fits the data adequately. The first-order relationship is definitely not acceptable. It is of interest to note that the following relationship for site decay which was used to develop eqs. (11), (21), and (27) is of the same form as the integrated second-order rate equation.

$$f_t = 1/1 + KP \tag{7}$$

The integrated rate equation is

$$f_t = \frac{1}{1 + [k_D n_s(0)t/4\pi r_c^2]} \tag{29}$$

Therefore, an approximate form of the second-order rate equation was used where the term, $k_D n_s(0)t/4\pi r_c^2$, was approximated by KP. This term can be estimated to any degree of accuracy desired by using higher order terms, e.g., $t = kP + K''P^2$. However, the number of terms in the final kinetic expression is increased by one term for each term added to the approximate relation. For example, if $t = KP$, the productivity equation is

$$A[P + (K/2)P^2] = t \tag{30}$$

If $t = KP + K''P^2$, then another term is added to eq. (30), i.e.,

$$A[P + (K/2)P^2 + (K''/3)P^3] = t \tag{31}$$

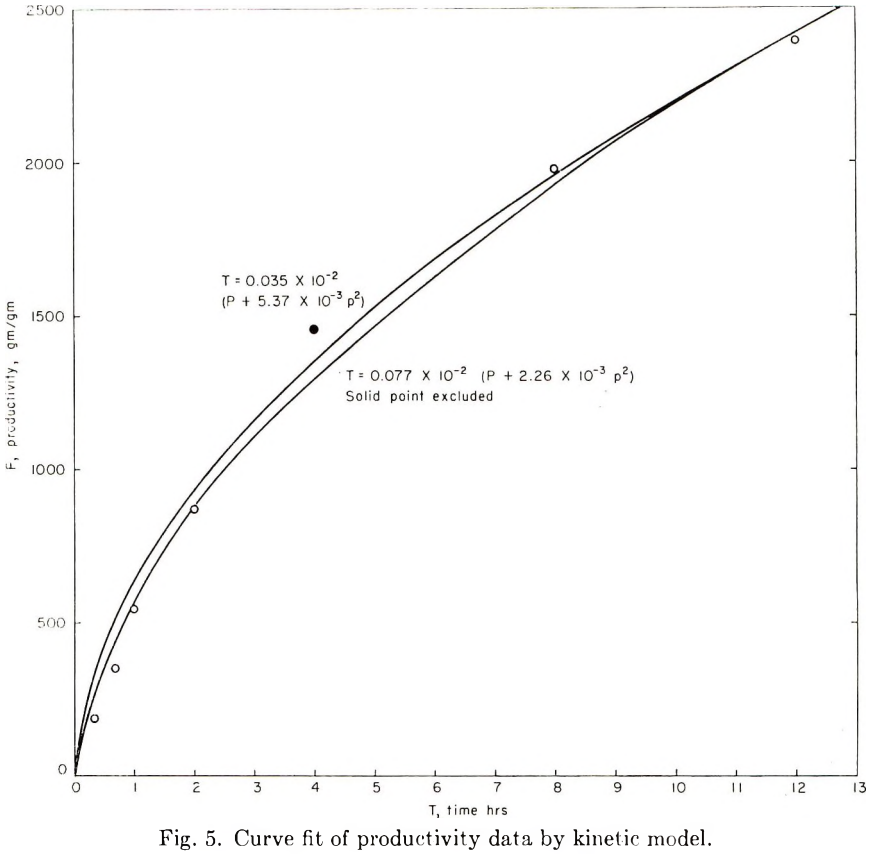

Fig. 5. Curve fit of productivity data by kinetic model.

In Figure 5, it is demonstrated that eq. (30) satisfactorily fits the experimental data so that apparently the function, $t = KP$, is a satisfactory approximation to use in the second-order kinetic function.

The approximate form of the relationship between productivity and time can be derived directly by the use of the second-order rate of site decay. The rate of reaction at the surface is

$$\text{Rate} = k_1 n_s(t) C \tag{32}$$

In terms of the polymer deposition on the particle, the rate is

$$\text{Rate} = 4\pi r^2 (dr/dt) \rho_p \tag{33}$$

When monomer diffusion is not a factor, eqs. (32) and (33) are equal.

$$4\pi r^2 (dr/dt) \rho_p = k_1 n_s(t) C \tag{34}$$

If eq. (29), the integrated second-order decay function, is used to replace $n_s(t)$, eq. (34) can be integrated between the limits $r = r_c$ and $r = r$, $t = 0$ and $t = t$ to obtain (35):

$$t = \frac{\exp\left\{{}^1/_3 r_c \rho_c k_D P / k_1 C\right\} - 1}{k_D n_s(0) / 4\pi r_c^2} \tag{35}$$

Equation (9), the definition of productivity, was used to eliminate r in eq. (35).

By expanding the right side of eq. (35) a functional form identical to eqs.(30) and (31) can be obtained.

$$t = \frac{{}^4/_3 r_c 3\rho_c}{k_1 n_s(0) C} \left\{ P + \frac{{}^1/_3 r_c \rho_c k_D}{2k_1 C} P^2 + \frac{1}{6}\left(\frac{{}^1/_3 r_c \rho_c k_D}{k_1 C} \right)^2 P^3 \right\} \tag{36}$$

On neglecting terms higher than second order, eq. (36) reduces to eq. (30), the equation which adequately fits the productivity data. The conditions which permit dropping higher terms are examined in Appendix II. Consequently, the use of the second-order rate of site decay leads directly to an equation which can be reduced to the form obtained by the use of an approximate second-order site decay function, i.e., $f_t = 1/(1 + KP)$.

Equation (36) gives a functional interpretation of the site decay constant. By equating the coefficients on the squared term in eqs. (30) and (36), the expression for the decay constant becomes,

$$K = {}^1/_3 r_c \rho_c k_D / k_1 C \tag{36a}$$

Therefore, the constant which has been referred to previously as a decay constant contains in addition to the rate constant for site decay, k_D, the polymerization rate constant, k_1.

Although eqs. (11), (21), and (27) are approximate because of the approximate form of the second-order decay used, they represent the data adequately and they are unique in the sense that the diffusion time and reaction time are separable and can be estimated independently. This is a significant advantage which is not obtained if the second-order decay function is not modified.

Conclusions

(*1*) An approximate form of the integrated rate equation for a second-order site decay mechanism was used to develop a kinetic model for propylene polymerization. In the model, the rate of monomer diffusion through the polymer film around the catalyst is coupled to the rate of surface reaction which decreases with a decay in site concentration with time. The approximate model indicates that the total polymerization time is a sum of two independent times, the surface reaction time and the monomer diffusion time.

(*2*) Photomicrographs and nitrogen adsorption surface area indicate that the catalyst size is very small. For three different catalysts, the respective surface areas are 7, 20–21, and 34 m.^{2}/g. The equivalent particle sizes for a spherical shape are 0.32, 0.1, and 0.06 μ. By use of the most conservative model conceivable, the diffusion time is estimated to be insignificant with particle sizes in the foregoing range. Particle size would have to be 10–100 times as large before diffusion could be significant. However, it is possible that diffusion would in no case be a consideration if the polymer

is deposited on the surface in towers to form a very porous structure as suggested by Lipman and Norrish.[2]

(3) The kinetic model without the diffusion term fit productivity data adequately, which is additional evidence for the lack of diffusional effects.

(4) By eliminating monomer diffusion as a possible cause for the characteristic decline in polymerization rate, characteristic data were analyzed on the basis of a catalyst site decay mechanism. The rate of site decay was found to be second-order in site concentration, which agrees with the studies by Lipman and Norrish[2] and Smith and Zelmer[1] for ethylene polymerization. First-order site decay was definitely not acceptable.

(5) When the second-order site decay equation is used in the derivation of the model describing the process of diffusion coupled with surface reaction, the final kinetic expression is quite complex, and the diffusion time and reaction time are not separable as in the case where an approximate form of the second-order decay function is used. The kinetic model developed by use of the approximate site decay equation is believed to be unique and convenient to use plus adequate for representing the productivity data.

APPENDIX I

Procedure For Determining Surface Areas And Making the Photomicrographs

The nitrogen surface areas were determined by the standard BET method. The catalyst samples were transferred to the BET sample bulbs in a nitrogen dry box. After connecting the sample bulbs to the apparatus, the samples were heated to 200°F. and evacuated to 0.1 μ.

In making the photomicrographs, the samples were also prepared in a nitrogen dry box. A nitrogen atmosphere in the electron microscope was used to avoid contact with the air during transfer of the sample. The slides for the light microscope were prepared in the dry box by first mixing the catalyst in a light mineral oil and then placing one drop of the mixture on the slide. A cover slide was placed on top of the drop. The sample was then transferred to the microscope in the normal room atmosphere.

APPENDIX II

Expansion of Equation (35)

Equation (35) can be expanded in terms of productivity to give eq. (36). If terms higher than second order are not included in the expansion, the kinetic expression is identical in form to that used to correlate the productivity data. It is of interest to determine the value of the coefficient in the expansion for which the terms higher than second order become practically insignificant. This can be accomplished by equating the right-hand side of eq. (35) to the sum of the first- and second-order terms in eq.

(36) multiplied by the term, $1/E$. The variable, E, represents the fractional approach to the real value of the series before truncation.

$$e^{KP} - 1 = (1/E)[P + (K/2)P^2]$$

This transcendental equation can be solved for K by trial and error for various assumed values of E and productivity.

In Table VII, values of K are presented for the case of 500 productivity and three different values of E. The results indicate that eq. (35) can be approximated very accurately by two terms in the expansion if K is less than 1.0×10^{-3}. The values of K were found to be less than 1.0×10^{-3} for the more active catalyst.

TABLE VII

E	$K \times 10^3$
0.99	0.4
0.95	1.2
0.90	1.7

References

1. Smith, W. E., and R. G. Zelmer, *J. Polymer Sci. A*, **1**, 2587 (1963).
2. Lipman, R. D. A., and R. G. W. Norrish, *Proc. Roy. Soc. (London)*, **A275**, 310 (1963).
3. Wilson, T. P., and G. F. Hurley, *J. Polymer Sci. C*, **1**, 281 (1963).
4. Michaels, A. S., and H. J. Bixler, *J. Polymer Sci.*, **50**, 413 (1961).
5. Friedlander, H. N., private communication during Gordon Conference, June 1963.
6. Kohn, E., H. J. L. Schuurmans, J. V. Cavender, and R. A. Mendelson, *J. Polymer Sci.*, **58**, 681 (1962).
7. Bier, von G., W. Hoffman, G. Lehmann, and G. Seydel, *Makromol. Chem.*, **58**, 1 (1962).
8. Natta, G., I. Pasquon, E. Giachetti, *Angew. Chem.*, **69**, 213 (1957).
9. Firsov, A. P., et al., *Vysokomol. Soedin.*, **3**, 1161 (1961).
10. Salame, M., *SPE Trans.*, **1**, 153 (October 1961).

Résumé

On a étudié le rôle de la diffusion du monomère dans la polymérisation du propylène par les organométalliques. Cette étude est basée sur l'emploi de modéles mathématiques qui couplent la vitesse de diffusion à travers du film du polymère environnant le catalyseur avec la vitesse de réaction à la surface de celui-ci. On a utilisé une équation de vitesse intégrée d'un ordre approximativement égal à deux, pour décrire la disparition des sites actifs sur la surface du catalyseur. En utilisant le modèle le plus convenable, on a estimé que la dimension des particules devrait être 10 à 100 fois celle du catalyseur employé avant que le taux de diffusion ne soit significatif. La dimension du catalyseur a été déterminée par photomicrographie et adsorption d'azote sur la surface libre; les surfaces libres pour trois catalyseures différents sont respectivement de 7, 20–21 et 35 m²/grm. Un modèle cinétique, ne tenant pas compte du terme de diffusion a été utilisé pour accorder les résultats de façon satisfaisante. On a étudié la diminution caractéristique de la vitesse de réaction en fonction de la disparition des sites actifs sur la surface du catalyseur. On a déterminé que la vitesse de disparition est de second ordre

par rapport à la concentration en ites actifs sur ce catalyseur. L'équation cinétique montre que le temps de polymérisation total pour un rendement donné est la somme du temps de diffusion du monomère et du temps de réaction sur la surface du catalyseur. Le modèle obtenu lorsqu'on utilise pour la disparition une équation du second ordre simplifiée, est unique, parce qu'on y additionne les temps de diffusion et de réaction, ce qui n'est pas le cas lorsqu'on utilise la fonction du second ordre rigoureusement.

Zusammenfassung

Die Rolle der Monomerdiffusion bei der Polymerisation von Propylen mit organometallischen Katalysatoren wurde durch Anwendung mathematischer Modelle, welche die Diffusionsgeschwindigkeit durch den den Katalysator umgebenden Polymerfilm mit der Geschwindigkeit der Oberflächenreaktion koppeln, untersucht. Eine Näherungsform einer integrierten Geschwindigkeitsgleichung zweiter Ordnung wurde zur Beschreibung des Verschwindens der aktiven Stellen in der Oberfläche verwendet. Bei Anwendung des denkbar konservativsten Modells kam man zu der Abschätzung, dass die Teilchengrösse die 10- bis 100fache Grösse des gegenwärtig verwendeten Katalysators haben müsste, bevor die Diffusionsdauer Bedeutung erlangen würde. Die Grösse des Katalysators wurde durch Mikroaufnahmen und aus der Oberflächengrösse für Stickstoffadsorption bestimmt. Die Oberflachengrösse für drei verschiedene Katalysatoren betrug 7 bzw. 20–21 bzw. 35 m^2/g. Das kinetische Modell ohne Diffusionsterme konnte die Polymerbildungsdaten befriedigend korrelieren. Das charakteristische Abklingen der Reaktionsgeschwindigkeit wurde zur Abnahme der aktiven Stellen an der Katalysatoroberfläche in Beziehung gesetzt. Die Abnahmegeschwindigkeit erwies sich als von zweiter Ordnung in bezug auf die Konzentration der aktiven Stellen. Das kinetische Modell zeigt, dass die Gesamtpolymerisationsdauer bei einer bestimmten Polymerbildung die Summe aus der Diffusionsdauer des Monomeren und der Dauer des Oberflächenreaktion ist. Die Besonderheit des durch Verwendung einer Abnahmefunktion von angenähert zweiter Ordnung abgekeiteten Modells ist die Additivität der Diffusions- und Reaktionsdauer; bei strenger Anwendung der Funktion zweiter Ordnung ist dies nicht der Fall.

Received May 14, 1965
Revised August 2, 1965
Prod. No. 4821A

JOURNAL OF POLYMER SCIENCE: PART A-1 VOL. 4, 337–347 (1966)

Relationship between Viscosity and Direct Current Conductivity in PVC

JUERG-HEINRICH KALLWEIT,* *Physikalisches Institut, Technische Hochschule, Braunschweig, Germany*†

Synopsis

In general, the d.c. conductivity σ has been considered to be inversely proportional to the viscosity η, but the relation $\sigma\eta$ = const. has not been proven in the case of the system poly(vinyl chloride)-dioctyl phthalate. The experimental results can be described by $\sigma\eta^{m-1/m}$ = constant if the plasticizer content is not too high. The ion mobility seems to depend on a local effective viscosity, which differs from that viscosity which is derived from retardation experiments.

Because both the viscosity and conductivity show a similar strong temperature dependence, it is a common assumption that the d.c. conductivity σ in high polymers depends mainly on the sample viscosity η. Walden's rule is often used as an approximation to describe the relationship

$$\sigma \sim 1/\eta \tag{1}$$

To check this relation, the same samples of poly(vinyl chloride) (PVC) with various plasticizer contents (Palatinol AH = dioctyl phthalate) were used to measure the viscosity and d.c. conductivity as functions of time and temperature.

Experimental

Samples with a thickness of 0.06 cm. were cut from materials having the compositions described in Table I.

TABLE I

Sample designation	PVC Vinolflex 332, % by weight	Plasticizer (Palatinol AH) + 0.5% stabilizer, % by weight
A	100	0
B	92	8
C	84	16
D	74	26
E	63	37
F	50	50

* Present address Feldmuele A. G., Viersen, Germany.

† Work completed at Research Institute, University of Alabama, Huntsville, Alabama.

The viscosity η was obtained from the results of creep studies carried out as described by Becker.[1] A rod-shaped sample was fixed at the upper end in perpendicular position and charged with a load at time $t = 0$. For small deformations, a tensile stress s_0 results, which is constant with respect to time. The relative change in the sample length $\epsilon(t)$ was measured as function of time with the help of a transformer system. The primary coil was fixed on the sample and introduced into the secondary one due to the elongation. The resulting electrical signal was an indication of the change in the sample length. The differentiation of the compliance J

$$J(t) = \epsilon(t)/s_0 \tag{2}$$

with respect to time,

$$dJ/dt = (d\epsilon/dt)(1/s_0) = 1/\eta \tag{3}$$

gives formally the equation for Newton's flow

$$s_0 = \eta(t)d\epsilon/dt \tag{4}$$

where $\eta(t)$ can be considered to be identical with the Trouton viscosity of the sample.[2] Equation (3) can be written

$$\frac{1}{\eta} = -\frac{J\, d[\log (1/J)]}{t\, d\, (\log t)} \tag{5}$$

The differentiation was obtained by graphical methods. It follows from eq. (3) that η must be a function of time. The viscosity of high polymers can be considered to be a criterion for the "friction force" between the position-changing segments of the molecular chains during stress. The decreasing possibility for position changes in the stress direction leads to an increase in the viscosity as a function of the load period. To eliminate this time dependence to the best extent possible, only the η values obtained 3 sec. after load charging were used for comparison with the values of the specific d.c. conductivity. Figure 1 shows the temperature dependence of the viscosity obtained after 3 sec. with the plasticizer content as parameter.

The experimental device for the determination of the specific d.c. conductivity has been described elsewhere.[3] The samples were again placed in a vacuum of about 10^{-4} Torr during the measurement. The applied voltage of 1000 v. introduced an electrical field strength of 16.7 kv./cm. Before each change of the sample temperature, all samples were heat-treated for 1 hr. at a temperature 30°C. above the glass transition temperatures T_g. Afterwards they were cooled slowly (or heated slowly) until the desired sample temperature was reached. This procedure was necessary to eliminate all polarization effects in the sample due to previous charging. Polarization effects are the reason for the strong time dependence of the conductivity in high polymers. Unfortunately, due to the time constant of the experimental device, it is not possible to measure very high resistances after approximately 3 sec. For this reason, the measured values for σ as a function of time were graphically extrapolated to 3

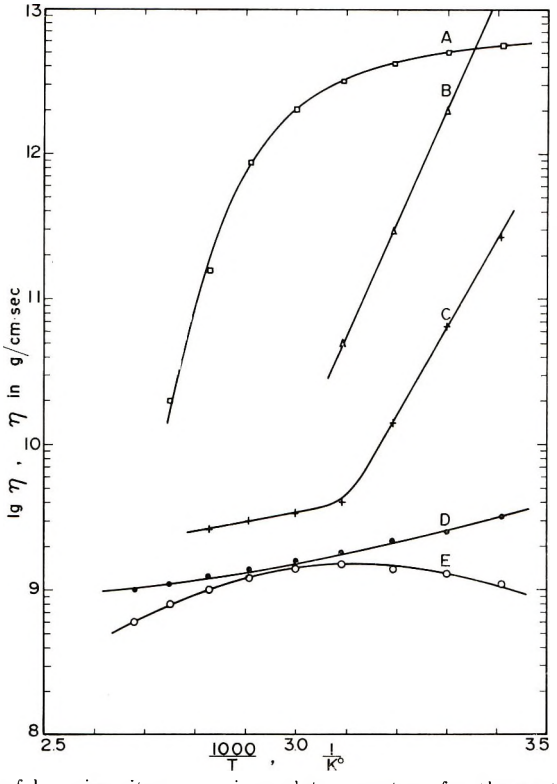

Fig. 1. Plots of log viscosity vs. reciprocal temperature for the system PVC/DOP with varying plasticizer content. The viscosity was measured after 3 sec. Samples A–E are explained in Table I.

sec. The error in σ due to the extrapolation is in all cases smaller than the error which would be obtained by using the σ values after a time exceeding the time constant of the device. Figure 2 shows the polarization voltage V_p as a function of temperature with the plasticizer content as parameter. The charging period was 600 sec.[4] The increase of V_p at higher temperatures and plasticizer contents is due to electrophoresis as proved by Wuerstlin.[5] Figure 3 shows the logarithm of the d.c. conductivity σ (σ extrapolated to 3 sec.) as a function of the reciprocal temperature $1/T$ with the plasticizer content as parameter. To facilitate comparison between the viscosity and conductivity, the dimensions in the remaining equations and figures are converted to CGS units.*

The assumed relationship $\sigma \sim 1/\eta$ follows from a simple model for the conduction process. An ion with the unit charge Q moves through the sample under the force of an electrical field $\mathbf{E}$ with constant velocity $\mathbf{u}$. In the equilibrium state, the electrical force $Q\mathbf{E}$ is equal to the friction force $\mathbf{F}$; $\mathbf{F}$ is considered to be proportional to the ion velocity $\mathbf{u}$

$$Q\mathbf{E} = \mathbf{F} = f\mathbf{u} \tag{6}$$

* σ in sec.$^{-1}$ times 1.113×10^{-12} is equal to σ in ohm^{-1}-cm.$^{-1}$

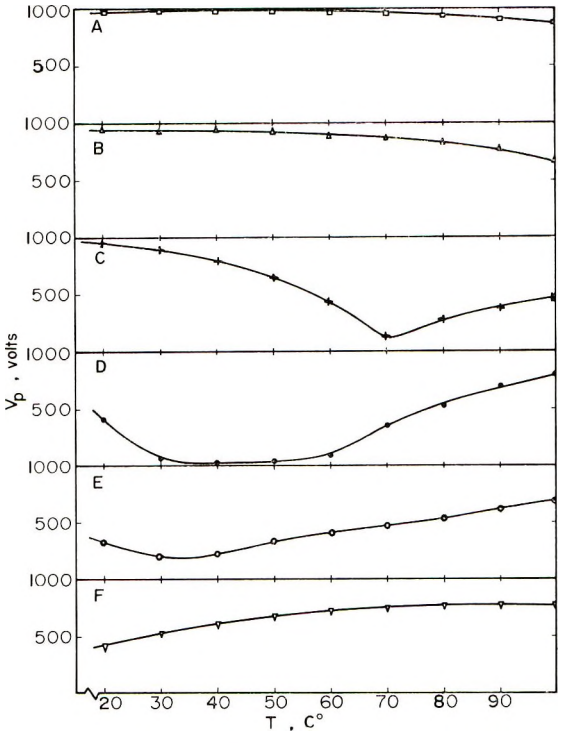

Fig. 2. Polarization voltage as function of temperature with varying plasticizer content. Charging time is 600 sec.; the applied voltage was 1 kv.

In the one-dimensional case, the velocity **u** can be considered to be identical with the mean drift velocity $\bar{u}$ in the direction of the field having an absolute value E. A first approximation for the factor f is given by Stoke's law

$$f = 6r_s\pi\eta \tag{7}$$

where r_s is the effective radius (Stoke's radius) of the ion with assumed spherical shape. The conductivity σ (in sec.$^{-1}$) can be written as

$$\sigma = zQc\bar{u}/E \tag{8}$$

where c is concentration in units of cm.$^{-3}$, Q is the charge unit (in cm.$^{3/2}$-g.$^{1/2}$ sec.$^{-1}$), z is the valence (z is taken to be 1 in this paper), and $\bar{u}$ and E have the units cm./sec. and cm.$^{-1/2}$-g.$^{1/2}$ sec.$^{-1}$, respectively. It then follows that

$$\sigma(T)\eta(T) = (Q^2/6\pi r_s)c(T) \tag{9}$$
$$= \text{const}\cdot c(T)$$

Since σ also contains the temperature-dependent concentration $c(T)$, the product $\sigma\eta$ should be almost temperature-independent, under the assumption that a variation of the temperature would influence the concentra-

tion $c(T)$ much less than the ion-velocity $\bar{u}(T)$ and the viscosity $\eta(T)$. Figure 4 shows that the expected relationship was not observed at all. There are two possible explanations: (*1*) Stoke's law is too crude of an approximation in the case of the high polymers tested; (*2*) the viscosity in Stoke's law is not identical with the viscosity η obtained by retardation experiments, which may be called "macroviscosity." But an effective local viscosity η' (microviscosity) must be used in connection with Stoke's law. Only in the case of fluids η is a good approximation for η'.

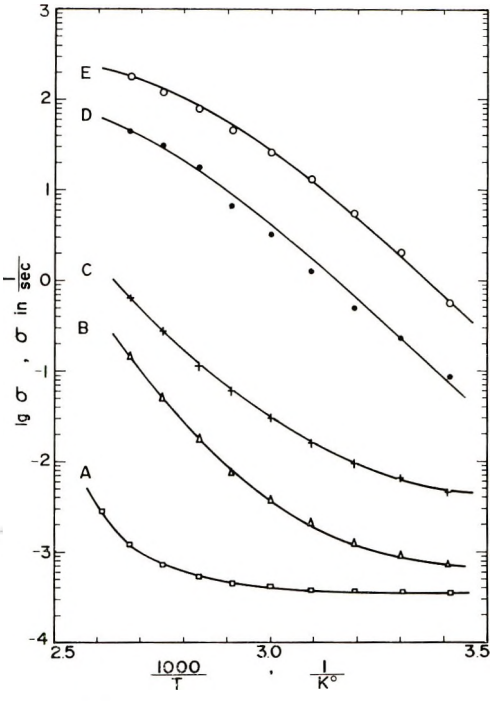

Fig. 3. Plots of log specific conductivity vs. reciprocal temperature for the system PVC/DOP with varying plasticizer content. The values for the conductivity were extrapolated to 3 sec. after voltage application and converted to CGS units by the relation: $\sigma\ (\text{sec.}^{-1}) = 9 \times 10^{11}\sigma\ (\text{ohm}^{-1}\text{-cm.}^{-1})$.

At first it was necessary to check whether or not any relationship between σ and η could be found. It is known from dielectric measurements on PVC[6] that the maximum value of the loss tangent depends on the magnitude of the sample viscosity η, regardless of whether a given viscosity was produced by a change in temperature or plasticizer content. Therefore, it was checked to determine which of the relationships between σ and η would apply for the lines of constant σ as shown in Figure 3. A correlation between σ and η was observed. The shape of the plot of log σ versus log η seemed to indicate a hyperbola. Afterwards, log η was plotted as a function of the product log $(\sigma\eta)$. The graphic representation (Fig. 5)

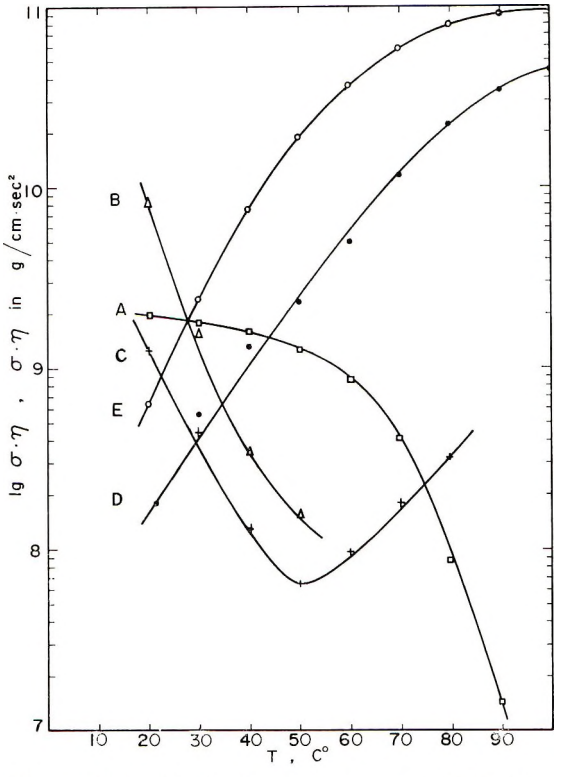

Fig. 4. Plots of log ($\sigma\eta$) vs. temperature; CGS units.

gives the desired possibility for the derivation of the relationship between σ and η.

$$\log \eta = m \log (\sigma\eta) + \text{const} \tag{10}$$

$$\sigma\eta^{m-1/m} = \text{const} \tag{11}$$

for samples A, B, and C. The tangent of the slope angle m may be derived with the help of the above plot.

Discussion

The experimental results seemed to show that it is problematic to use the viscosity values obtained by retardation experiments in connection with Stoke's formula, eq. (7). Suppose the question is raised of what results would be formally obtained when the numerical value $|\eta^{m-1/m}|$, disregarding dimensions, is identified with the numerical value of the effective local viscosity η'; hence

$$|\eta^{m-1/m}| = |\eta'|$$

Equation (1) can then be written

$$\sigma\eta' = \text{constant} \tag{12}$$

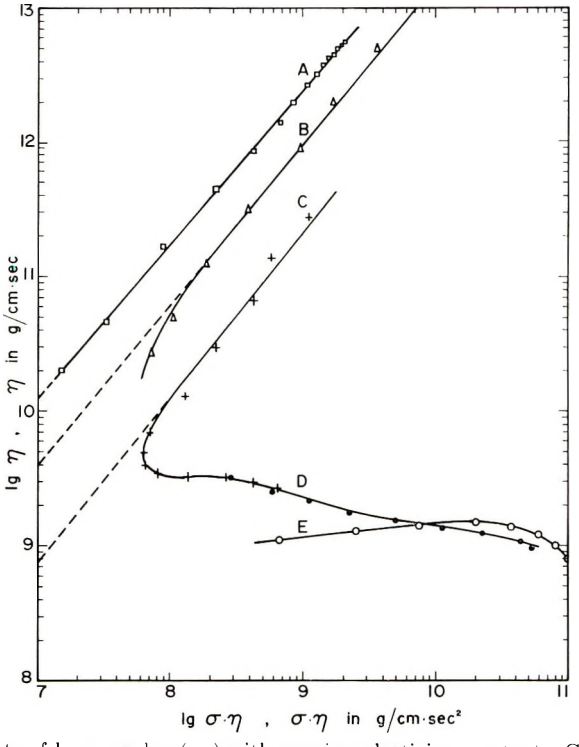

Fig. 5. Plots of log η vs. log ($\sigma\eta$) with varying plasticizer content; CGS units.

and eq. (12) is now of the form of eq. (9). Table II gives some typical values. Because m is nearly one, the magnitude of η' is unexpectedly low. It has been shown by Ferry,[7] however, that the order of the effective local viscosity for small foreign molecules may be of the calculated order.

TABLE II
Creep Viscosity η and Microviscosity η' vs. T

Sample	T, °K.	η, g./cm.-sec.	m	$\lvert\eta'\rvert = \lvert\eta^{(m-1)/m}\rvert$
A	293	5.5×10^{12}	1.15	4.5×10^{1}
	323	3.2×10^{12}		4.2×10^{1}
	343	9.0×10^{11}		3.5×10^{1}
B	293	1.3×10^{13}	1.17	7.9×10^{1}
	323	5.0×10^{10}		3.5×10^{1}
	343	?		?
C	293	2.7×10^{11}	1.22	1.1×10^{2}
	323	4.8×10^{9}		4.6×10^{1}
	343	2.8×10^{9}		4.3×10^{1}

It is, furthermore, interesting to note that a linear relationship between the logarithm of the resistivity at 25°C. and the activation energy E^* for the conduction process was observed for the system PVC–plasticizer[8] (see Fig. 6). Such a relationship may indicate that conduction is a rate-

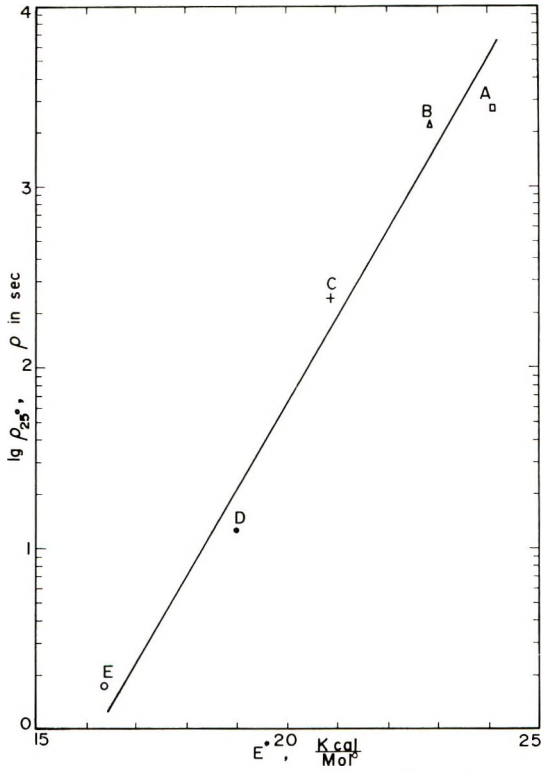

Fig. 6. Plots of log resistivity vs. activation energy. The resistivity is given in CGS units.

determined process which depends on the local effective viscosity (micro-viscosity) within the sample.

Equation (7), written now as

$$f = 6\pi r_s \eta' \tag{7a}$$

would give for the relation in eq. (9)

$$\sigma(T)\ \eta'(T) = (Q^2/6\pi r_s)c(T) \tag{9a}$$

Figure 7 shows that now the expected relationship is obtained. This result indicates continuation of the formal test by writing for the median drift velocity $\bar{u}$

$$\bar{u} = Q(E/6)\pi r_s \eta' \tag{13}$$

and for the conductivity

$$\sigma = c(Q^2/6)\pi r_s \eta' \tag{14}$$

where the mobility of the ions is given by

$$\mu_e = (Q/6)\pi r_s \eta' \tag{15}$$

The equation for the diffusion coefficient would be

$$D = (KT/6)\pi r_s \eta'$$

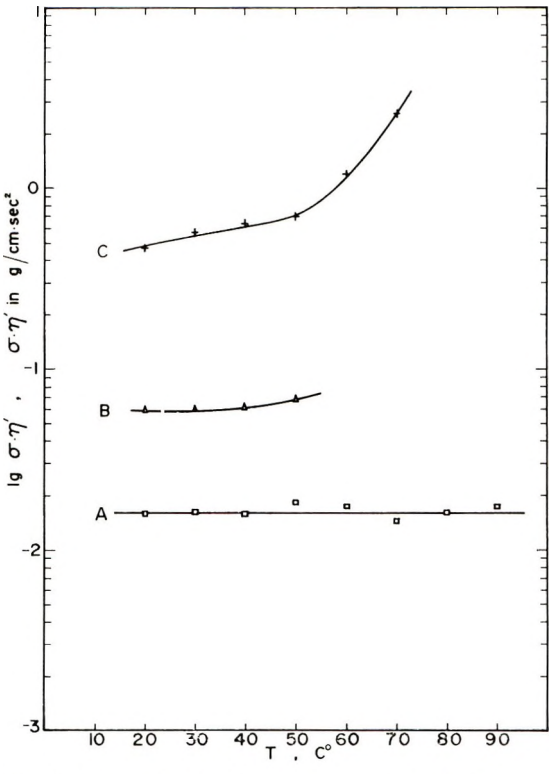

Fig. 7. Plots of log ($\sigma\eta'$) vs. temperature; CGS units.

because the definition of the mechanical mobility μ_m and of the electrical mobility yields the relationship $\mu_e = Q\mu_m$. Table III gives the numerical results for samples A, B, C and some values for sample D. The calculation could not be done without another assumption for the effective radius r_s of the ions. The kind of ions is not known, but most probably they will be molecular. Under this assumption, $r_s = 1 \times 10^{-7}$ cm. was chosen for the unknown radius r_s. The values for sample D were added to Table III to show that the nonlinear plots in Figure 5 do not give sensible values.

The crude approximations do not allow detailed discussion of the results summarized in Table III; these results seem to indicate, however, that the values for the ion velocity, concentration, and the diffusion coefficient are of a range which could be a fair approximation of the actual values. The values for the diffusion coefficient do not differ markedly from the values of Luther and Meyer,[10] who measured the diffusion coefficient of plasticizer in PVC. For sample C at 343°K., D was found to be 1.2×10^{-10} cm.²/sec in the present work and by Meyer $D = 1.4 \times 10^{-11}$ cm.²/sec. Those values for D are smaller than values for the diffusion of small molecules like N_2 or H_2 through high polymer membranes. Although it cannot be said that plasticizer molecules are responsible for the charge transport, the low order of the diffusion coefficient may indicate

TABLE III
Charge Carrier Speed, Mobility, Diffusion Coefficient, and Concentration Assuming r_s = 10A.

T, °K.	Sample	$\bar{u}$, cm./sec.	μ_c, cm.$^{3/2}$/g.$^{1/2}$	D, cm.^{2}/sec.	c, cm.$^{-3}$
293	A	$3.6_9 \times 10^{-4}$	$6.6_2 \times 10^{-6}$	4.7×10^{-10}	9.2×10^{10}
303		$3.7_2 \times 10^{-4}$	$6.6_5 \times 10^{-6}$	4.9×10^{-10}	9.4×10^{10}
313		$3.8_1 \times 10^{-4}$	$6.8_4 \times 10^{-6}$	5.0×10^{-10}	9.6×10^{10}
323		$3.9_7 \times 10^{-4}$	$7.1_2 \times 10^{-6}$	5.5×10^{-10}	9.6×10^{10}
333		$4.1_5 \times 10^{-4}$	$7.4_4 \times 10^{-6}$	6.0×10^{-10}	1.0×10^{11}
343		$4.7_1 \times 10^{-4}$	$8.9_4 \times 10^{-6}$	7.0×10^{-10}	1.0×10^{11}
353		$5.8_0 \times 10^{-4}$	$1.0_4 \times 10^{-5}$	9.0×10^{-10}	9.2×10^{10}
363		$7.5_2 \times 10^{-4}$	$1.3_5 \times 10^{-5}$	1.2×10^{-9}	1.0×10^{11}
293	B	$2.1_4 \times 10^{-4}$	$3.8_3 \times 10^{-6}$	2.7×10^{-10}	3.2×10^{11}
303		$2.7_4 \times 10^{-4}$	$4.9_2 \times 10^{-6}$	3.6×10^{-10}	3.4×10^{11}
313		$3.6_4 \times 10^{-4}$	$6.5_2 \times 10^{-6}$	5.0×10^{-10}	3.6×10^{11}
323		$4.7_1 \times 10^{-4}$	$8.4_7 \times 10^{-6}$	6.5×10^{-10}	3.8×10^{11}
293	C	$3.6_3 \times 10^{-4}$	$2.7_0 \times 10^{-6}$	1.9×10^{-10}	2.8×10^{12}
303		$1.8_4 \times 10^{-4}$	$3.3_2 \times 10^{-6}$	2.4×10^{-10}	3.4×10^{12}
313		$2.5_1 \times 10^{-4}$	$4.5_0 \times 10^{-6}$	3.4×10^{-10}	3.6×10^{12}
323		$3.7_2 \times 10^{-4}$	$6.6_5 \times 10^{-6}$	5.0×10^{-10}	4.4×10^{12}
333		$3.8_0 \times 10^{-4}$	$6.8_0 \times 10^{-6}$	5.5×10^{-10}	7.0×10^{12}
343		$3.9_1 \times 10^{-4}$	$7.0_4 \times 10^{-6}$	6.0×10^{-10}	1.4×10^{13}
293	D	3.1×10^{-14}	$5.5_6 \times 10^{-16}$	3.9×10^{-20}	2.2×10^{23}
313		6.2×10^{-14}	$1.1_2 \times 10^{-15}$	8.5×10^{-20}	8.8×10^{23}
333		8.3×10^{-14}	$1.5_0 \times 10^{-15}$	1.1×10^{-19}	4.2×10^{24}

that not very small molecules as charge carriers or ions with a not too small Stoke's radius are migrating under the force of the applied electrical field. The expected temperature dependence of the mobility of the single samples was obtained. However, it is difficult to understand that the mobility did not increase with increasing plasticizer content. The common assumption is that the increase of the conductivity with higher plasticizer content is chiefly due to the greater ion mobility. Here it would turn out that the ion concentration is the dominating factor. There are too few experimental results to understand how the defined microviscosity can be related to the free volume within the sample.[7,8]

The values for D and $\bar{u}$ can be used to estimate the order of the jump distance l of the charge carrier; $D = \bar{u}l/3$ is found according to the approximation used in this paper, to be independent of any specific sample. It seems better to measure the conductivity as function of the applied electric field and to use the reaction rate theory to evaluate the jump distance.[11,12] It may be noted however, that, under the assumption that the activation energy for the conductance process is of the same magnitude as the activation energy for diffusion, a jump distance can be estimated which is as unexpectedly high as the jump distance given by Foss and Dannhauser[11] for ions in polypropylene.

Other types of high polymer material must be tested before general conclusions can be made. The free volume should be determined in addition

to the viscosity, and the d.c. conductivity should be measured as a function of temperature and electric field strength.[12] Samples with varied plasticizer content and crystallinity should be studied. The understanding of the d.c. conductivity in high polymers depends on an exact knowledge of the mobility of the charge carriers.

The author would like to thank Dr. G. W. Becker, Physikalisch-Technische Bundesanstalt, Braundschweig, Germany, for the measurement of the viscosity and for many valuable discussions.

The samples are courtesy of Dr. Wuerstlin, Badische Anilin und Sodafabrik, Ludwigshafen, Germany.

The experiments were done in the Physikalisches Institut, Technische Hochschule, Braunschweig, Germany, for which thanks, are also due to the director Professor Dr. Cario.

This paper was partially supported by the National Aeronautics and Space Administration under grant NSG-381.

References

1. Becker, G. W., *Kolloid-Z.*, **166,** 4 (1959).
2. Mueller, F. H., und C. Engelter, *Kolloid-Z.*, **186,** 36 (1962).
3. Kallweit, J. H., *Kunststoffe*, **47,** 651 (1957).
4. Kallweit, J. H., *Kolloid-Z.*, **188,** 97 (1963).
5. Wuerstlin, F., *Kunststoff-Tech.*, **11,** 269 (1941).
6. Davies, J. M., R. F. Miller, and W. Busse, *J. Am. Chem. Soc.*, **63,** 361 (1941).
7. Ferry, J. D., *Viscoelastic Properties of Polymers*, Wiley, New York, 1961.
8. Warfield, R. W., and M. C. Petree, *Makromol. Chem.*, **58,** 139 (1962).
9. Ruetschi, P., *Z. Physk. Chem. (Frankfurt)*, **14,** 277 (1958).
10. Meyer, H., Dissertation, Braunschweig, 1958.
11. Foss, R. A., and W. Dannhauser, *J. Appl. Polymer Sci.*, **7,** 1015 (1963).
12. Amborski, L., *J. Polymer Sci.*, **62,** 331 (1962).
13. Glasstone, S., K. J. Laidler, and H. Eyring, *The Theory of Rate Processes*, McGraw-Hill, New York, 1941.

Résumé

Il est admis en général que la conductivité en courant continu, σ, est inversément proportionnelle a la viscosité η. La relation $\sigma \cdot \eta$ = constante n'a cependant pas été prouvée dans le cas du systéme PVC/DOP. Les résultats expérimentaux s'accordent avec la relation $\sigma \cdot \eta^{m-1/m}$ = constante pour autant que la teneur en plastifiant ne soit pas trop élevée. La mobilité ionique semble dépendre de la viscosité locale réelle qui diffère de la viscosité déterminées au départ d'expériences de retardement.

Zusammenfassung

Nach allgemeiner Auffassung soll die Gleichstromleitfaehigkeit σ umgekehrt proportional zur Viskositaet η sein. Die Beziehung $\sigma\eta$ = const. konnte jedoch fuer das System PVC–DOP nicht nachgewiesen werden. Die experimentellen Ergebnisse Koennen durch $\sigma\eta^{m-1/m}$ = const. beschrieben werden, wenn der Weichmachergehalt nicht zu hoch ist. Die Ionen-Beweglichkeit scheint von einer lokalen effektiven Viskositaet abzuhaengen, die nicht mit der Viskositaet identisch ist, die aus Retardations-Experimenten gewonnen werden kann.

Received March 17, 1965
Revised August 2, 1965
Prod. No. 4822A

JOURNAL OF POLYMER SCIENCE: PART A-1 VOL. 4, 349–365 (1966)

Pyrolysis of Vinyl and Vinylidene Fluoride Polymers: Influence of Prior γ-Irradiation

L. A. WALL, S. STRAUS, and R. E. FLORIN,
National Bureau of Standards, Washington, D. C.

Synopsis

Quantitative comparisons were made between the rates of thermal volatilization of several fluoropolymers before and after exposure to γ-radiation. The effects of γ-irradiation on poly(vinyl fluoride) and poly(vinylidene fluoride) were also investigated by swelling and sol–gel ratios. With both polymers as well as with polytrifluoroethylene, crosslinks occur predominantly, though there is an appreciable number of scissions. The rates of volatilization and char formation were enhanced by γ-radiation, whereas the previously studied polytrifluoroethylene did not produce more char upon irradiation, although radiation did accelerate its volatilization. It is believed that in polytrifluoroethylene the enhanced rates of volatilization occur by a different mechanism than in the case of the vinyl and vinylidene fluoride polymers.

INTRODUCTION

Although it might be expected that the rates of thermal volatilization of polymers would be decreased and greater amounts of nonvolatile residue formed in polymers that previously had been crosslinked by γ-irradiation, we found in earlier work on polytrifluoroethylene[1] that such crosslinking caused increased rates of volatilization and altered the kinetic character of the volatilization curves. The curves changed from those with maxima typical of pure random decomposition to ones without maxima, typically seen in the degradation of branched polyethylene.

Studies of the thermal volatilization of polytetrafluoroethylene, after prior irradiation, have not yet been reported, although such studies are now in progress. Polytetrafluoroethylene, according to recent work,[2–4] does have some tendency to crosslink on irradiation, though it is normally considered to be a polymer which degrades upon irradiation.[5] In this and prior work,[1] it was found that the presence of hydrogen in the units of a fluoropolymer facilitates crosslinking by high energy radiation. More quantitative aspects of the irradiation of fluoropolymers are presented elsewhere.[6]

The current work with poly(vinyl fluoride) and poly(vinylidene fluoride) was undertaken to round out the picture on the thermal volatilization of a series of fluoropolymers. The irradiation technique and the subsequent thermal decomposition were conducted in the absence of air to eliminate

complications arising from oxidation processes. The current polymers are of additional interest, in that they have different tendencies to produce stable residues up to approximately 500°C. Without prior exposure to γ-rays, poly(vinylidene fluoride)[7] yields a 30–35% char and poly(vinyl fluoride), about a 5% char, indicating a crosslinking process on heating.

MATERIALS

Both polymer samples were commercial preparations. The poly(vinyl fluoride) polymer was supplied as a 4-mil colorless film Teslar by E. I. du Pont de Nemours and Co. Its molecular weight is not known and there is apparently no known adequate solvent. The poly(vinylidene fluoride) polymer (Kynar), obtained from Pennsalt Chemicals, came as milky-white pellets. The molecular weight of this material was stated by the manufacturer to be approximately 600,000.

EXPERIMENTAL PROCEDURE

The poly(vinylidene fluoride) pellets were formed into a smooth milky-white sheet, approximately 10–12 mils thick, by application of a pressure of 2000 psi for 30 sec. at 242°C. The poly(vinyl fluoride) film was used as received. An attempt to bond it into a thicker film under heat and pressure was not successful. Both polymer films were cut into strips, placed into Pyrex tubes, and the tubes evacuated to approximately 10^{-5} mm. of Hg and sealed off. The films were irradiated by a Co^{60} source to doses of from 1 to 203 Mr; both fluoride polymers absorb approximately 0.51×10^{20} e.v./g. when given a dose of 1 Mr. In both cases, the polymer sample lost less than 2% of its original weight at the maximum radiation dose of 103×10^{20} e.v./g. The poly(vinylfluoride) samples discolored to a greenish hue at a dose of 19.4×10^{20} e.v./g., whereas the poly(vinylidene fluoride) samples showed a perceptible yellowing when given a dose of 43.9×10^{20} e.v./g. Continued irradiation for longer periods gave darker discolorations for both polymers. Besides pyrolysis, the sol content, gel swelling, and gel elasticity were determined, and dimensional changes of poly(vinyl fluoride) were observed. The extracting or swelling agent for poly(vinyl fluoride) was hot hexamethylphosphoramide, $[(CH_3)_2N]_3PO$, which does not actually dissolve the initial polymer but forms a highly swollen gel. The irradiated samples and original polymer film were immersed in the liquid at approximately 150–160°C. for 20 min., removed, weighed, and dried in a vacuum oven at the same temperature. Weight losses were recorded and the extraction repeated twice again, until further losses of weight were less than 1%. Swelling of the unirradiated and of the 0.51×10^{20} e.v./g. samples were too great for measurement of sol fraction. Rubber elasticity of the swollen strips was also determined at 25°C. in air and at 120°C. in solvent vapor.[6] Dimensions of the initial, swollen, and subsequently dried strips were measured by vernier calipers.

Similar extraction and swelling studies were made on poly(vinylidene fluoride), using dimethylformamide at 75°C. for approximately 10 min. The initial and the 0.51×10^{20} e.v./g. irradiated samples were disintegrated by excessive swelling. Extraction and drying were repeated twice until the last weight loss was less than 1%. The swelling and rubber elasticity measurements are described elsewhere.[6]

The techniques employed for thermal decomposition have been fully described previously.[7,8] A 15–20 mg. sample was placed into a small platinum tube, which was inserted into a larger platinum tube projecting horizontally from the vacuum apparatus. The furnace was heated to the required temperature and then moved quickly into position to heat the sample. It took approximately 5 min. for the temperature of the sample in the small platinum tube to reach equilibrium temperature. In all cases four fractions were obtained: (*1*) a residue, which remained in the small platinum tube; (*2*) a waxlike fraction, which condensed in the large platinum tube outside the heater; (*3*) a condensed fraction, volatile at room temperature; and (*4*) a gas fraction, volatile at liquid nitrogen temperature. Mass spectra were obtained in some cases for fractions 3 and 4. The distribution of the volatile products into the first three fractions helped to determine the effect of the radiation dose and the possible mechanism of breakdown. The volatiles obtained in fraction 4, in all cases, were extremely small in amount.

Precise measurement of the weight loss of the polymer as a function of time, on heating in a vacuum, was carried out with the use of the tungsten-spring balance. Samples were limited to 5–6 mg. and were heated in a platinum crucible by means of an electronically controlled heater. Loss in weight of sample was determined periodically by observing deflections of the crossline on the tungsten-spring with a cathetometer. Rates of volatilization at specific temperatures were calculated from these observations and plotted as rate, in per cent per minute, versus extent of volatilization, in per cent.

PROPERTIES OF IRRADIATED POLYMERS

Figure 1 shows logarithmic plots of sol fraction versus dose in 10^{-20} e.v./g. for both polymers. The curves correspond to the theoretical curves for a "most probable" initial molecular weight distribution, and for a constant ratio of scissions to crosslinked units per 100 e.v., β/α, as indicated by the numbers. The sol fractions may be systematically somewhat low at low doses, because of the larger thickness of swollen gel through which soluble material must diffuse during extraction and also because of the generally higher molecular weight and lower diffusivity of sol at low doses. A systematic error can also arise if HF, lost during crosslink formation or in other processes, is not removed until the extraction. The sol fraction would be raised by $3.3 \times 10^{-25} G(\text{-HF})r$, where G is in molecules per 100 e.v. and r is the dose in electron volts. This error can approach

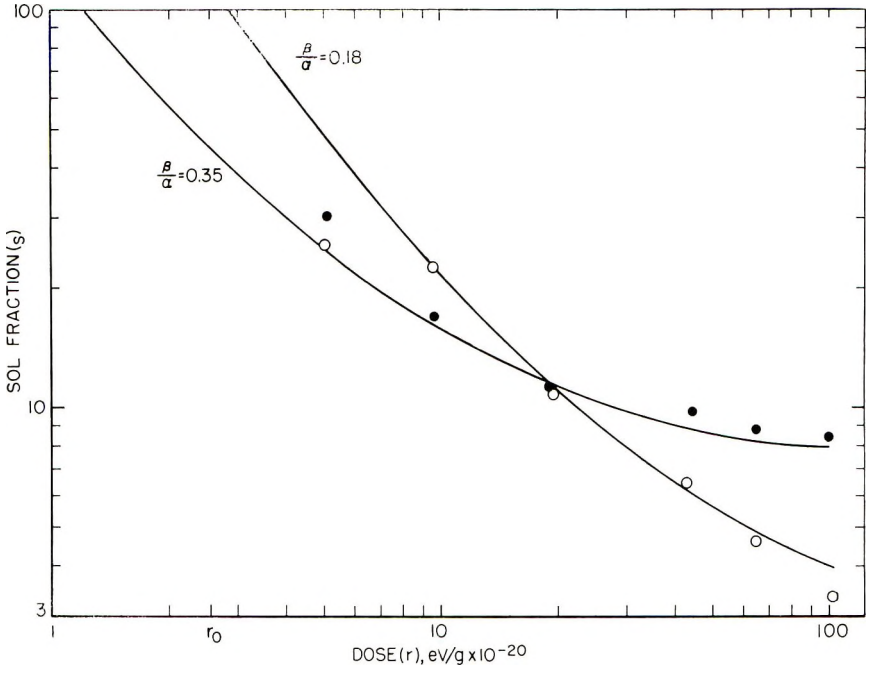

Fig. 1. Sol fractions as function of γ-ray dose for (O) poly(vinylidene fluoride); (●) poly(vinyl fluoride). Dose rate 5 × 10^{20} e.v./g.-hr.; curves theoretical for indicated β/α (scissions per 100 e.v.)/(crosslinked units per 100 e.v.).

1% at the highest doses employed here. Except for one point involving poly(vinylidene fluoride), the points appear to fit the curves within 1%, despite the uncertainty in the fulfillment of theoretical conditions. The associated uncertainty in β/α is about ±0.05, and because of systematic sources of error discussed, the given values are more likely to be too high than too low. The values of β/α from Figure 1, in conjunction with gel swelling and gel elasticity results reported elsewhere,[6] lead to the G values summarized in Table I. Values of the solvent–polymer interaction parameter χ are based on swelling and elasticity. Values for polytrifluoroethylene are given for comparison.

TABLE I
Radiation Yields and Values of the Solvent–Polymer Interaction Parameter χ

Polymer	Solvent	G_d/G_c	$G_c - 2G_d$	G_c[a]	G_a[b]	χ
CF_2CFH	Acetone	0.16–0.21	1.4	2.1–2.4	0.3–0.5	0.62
CF_2CFH	DMF	—	—	—	—	0.38
CF_2CH_2	DMF	0.18–0.21[c]	1.2	1.9–2.1	0.2–0.4	0.33
CH_2CHF	HMP	0.28–0.35[c]	3–7	6–16	1.8–4.0	−1.2

[a] Crosslinked units per 100 e.v.; twice the number of crosslinks.
[b] Scissions per 100 e.v.
[c] Identical to β/α, Fig. 1.

The values listed of G_c, G_d, and χ for poly(vinyl fluoride) are uncertain by a large factor because of the anisotropic character of the initial material, and will be discussed more fully in the Appendix.

RESULTS OF PYROLYSIS

Poly(vinyl Fluoride)

The original film was pyrolyzed in the tungsten-spring balance at three temperatures, as shown in Figure 2. The experimental observations for the polymer fell on straight lines up to about 85% volatilization except for initial low points at 365 and 373°C. Extrapolation of the straight lines to the rate axis for the three temperatures yielded apparent initial rates that gave an activation energy of 55 kcal./mole using the Arrhenius equation. Rate studies were then made in the spring-balance at 365°C. of the seven irradiated samples (radiation doses of 0.51, 5.0, 9.44, 19.38, 43.86, 63.24 and 103.53 ev./g. $\times 10^{-20}$ and also of the original unirradiated polymer. The results can be seen in Figure 3. The γ-irradiation treatment produces a tremendous change in the rates of volatilization as compared to the untreated polymer. Approximately 3% of the untreated polymer volatilized quickly in bringing the sample up to the temperature of pyrolysis. After the preheated furnace is placed in position around the tube containing the suspended sample, it takes approximately 15 min. for the sample to reach the temperature of pyrolysis. In our work, we consider the initial reading time to be at the end of the 15-min. period. In the case of the irradiated samples at low doses, over 30% of the polymer

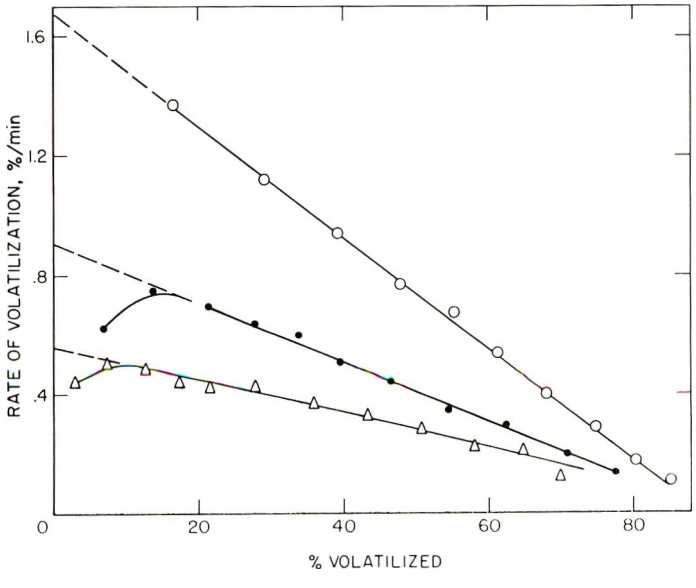

Fig. 2. Rate of volatilization of poly(vinyl fluoride): (○) 382°C.; (●) 373°C.; (△) 365°C.

has volatilized before the temperature is reached, and at the higher doses, this amount is over 40%. In other words, the irradiation treatment has weakened the polymer to the extent that fragments are eliminated at lower temperatures than previously. These rate curves also indicate that the greater the radiation dose, the greater the corresponding initial loss and

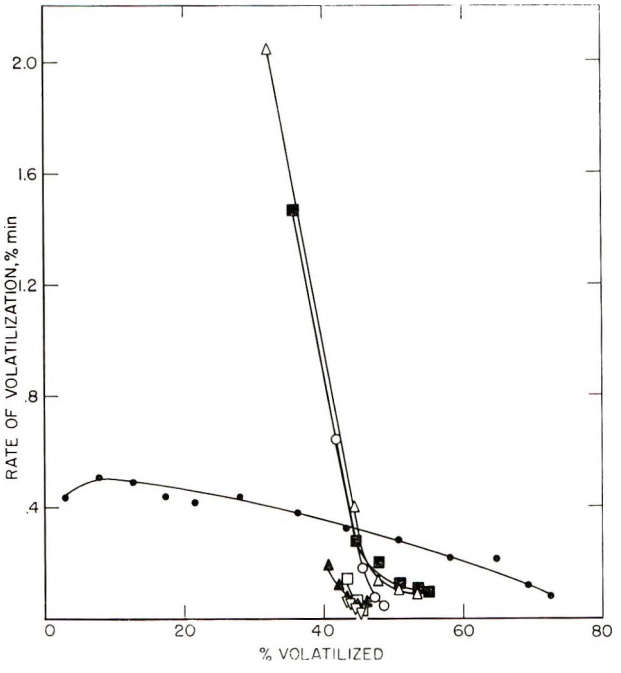

Fig. 3. Effect of prior γ-irradiation on the rate of volatilization at 365°C. of poly(vinyl fluoride) at various radiation doses (in e.v./g. $\times 10^{-20}$): (●) 0.00; (△) 0.51; (■) 5.0; (○) 9.44; (□) 43.9; (▲) 63.2; (▽) 104.

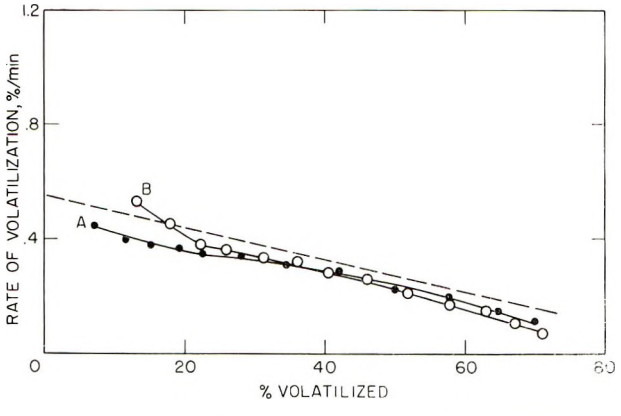

Fig. 4. Rate of volatilization at 365°C. of γ-irradiated poly(vinyl fluoride) after extraction with hexamethylphosphoramide with various radiation doses (in e.v./g. $\times 10^{-20}$): (– –) 0.00; (●) 9.44; (○) 104.

also the larger the yield of black char residue. Thus, the overall effects of radiation on the polymer are complex. Although the ordinary polymer properties indicate crosslinking (Table I), the progressive changes in the rate curves of Figure 3 are more characteristic of degradation. To study this complexity further, some pyrolyses were performed upon samples which had been extracted with hexamethylphosphoramide after irradiation. Rate studies were made at 365°C. in the tungsten-spring balance on two such samples: one at a low dose, 9.44×10^{20} e.v./g., and the other at high dose, 103.53×10^{20} e.v./g. The results are shown in Figure 4. The broken-line rate curve is the straight line slope shown in Figure 2 for the unirradiated polymer. The curves for both the extracted samples in Figure 4 are now quite similar to the untreated polymer except for initial differences. In addition, the irradiated rate curves in Figure 3 indicate residue formation after approximately 60–45% volatilization; the greater the dose the greater the residue. Extraction with the hot hexamethylphosphoramide nullifies the effect of the irradiation treatment on the rate curves.

Pyrolysis studies were made also on some of the polymer samples in the tube apparatus at 375°C. for 60 min. in all cases. The experimental results for poly(vinyl fluoride) are shown in Table II. The volatilization per cent column, for the samples before or after extraction with the hot hexamethylphosphoramide, clearly indicates a greater accumulation of char with increase of radiation dose. However, the extracted samples show less overall residue formation. This was also previously observed in Figure 4. The condensed volatiles (lines 1–4) indicate an increase in the

TABLE II
Pyrolysis of Poly(vinyl Fluoride) and Poly(vinylidene Fluoride) in a Vacuum

Polymer	Dose absorbed in sample, e.v./g. $\times 10^{-20}$	Volatilization, %	Volatiles, %[a]
Poly(vinyl fluoride)	Untreated	87.2	52.1
	9.44[b]	76.5	62.1
	43.86[b]	74.5	62.9
	103.53[b]	65.5	72.2
	9.44[c]	95.6	45.2
	43.86[c]	88.0	51.5
	103.53[c]	85.8	46.5
Poly(vinylidene fluoride)	Untreated	74.3	49.1
	9.44[b]	72.9	63.1
	43.86[b]	56.3	96.2
	103.53[b]	54.5	97.7
	9.44[c]	66.6	69.2
	43.86[c]	58.4	92.5
	103.53[c]	50.9	97.9

[a] Volatile at room temperature, mainly HF, per cent of column 2.
[b] Prior to extraction with solvent.
[c] After extraction with solvent.

amount of light volatiles collected from 52% at zero dose to 72% at the highest dose. When extracted samples are pyrolyzed (lines 5–7) condensed volatiles show very little difference from those characteristic of unirradiated material.

Mass spectrometric analyses of the condensed volatiles for the seven samples reveal the presence of a considerable amount of hydrogen fluoride gas and also of peaks extending to mass 167. The HF volatiles appear in the mass spectra as a large 85 peak corresponding to silicon tetrafluoride.[1] The evolved HF gas is probably converted to the SiF_4 by a reaction with the glass apparatus in the presence of traces of moisture.

The untreated polymer also shows a 78 peak (C_6H_6) that is almost half the 85 peak. After irradiation, the benzene peak becomes less pronounced and is then approximately only 10% of the 85 peak. After extraction, however, the 78 peak has become more significant again and is now approximately 40% of the 85 peak.

Table II clearly indicates that the greater the radiation dose introduced into the polymer, the greater the formation of small volatiles, which are readily eliminated at the elevated pyrolysis temperature. The residue, in all the experiments discussed, appeared as a black char that is easily pulverized. The waxlike fraction, on the other hand, appears greenish in color when from irradiated samples, and decidedly brown when from extracted samples.

Poly(vinylidene Fluoride)

Rate studies were made in the spring-balance on the seven irradiated samples and the untreated polymer at 410°C., a much higher temperature than for poly(vinyl fluoride). Previous rate experiments on another poly(vinylidene fluoride) polymer, prepared at the National Bureau of Standards by γ-initiation, gave typical maximum curves with an activation energy of 48 kcal./mole calculated on the basis of the maxima obtained.[7] The results of the rate studies on the current series, using the commercial polymer, are shown in Figures 5 and 6. The dashed rate curve is that of the previously studied polymer. The commercial sample, however, exhibits quite unusual rate curves (Fig. 6, curve *A*). The initial loss for the commercial polymer is greater, then is followed by a dip in the curve, and continues to a maximum peak, narrower in range than the dashed curve. The untreated commercial polymer shows a maximum at approximately 0.61%/min. and stabilized at a degree of volatilization of approximately 60%. The low-dosed samples, up to 19.76×10^{20} e.v./g., indicate either lower maxima or a similar maximum height, and there has been a shift in the position of the maxima to some extent. The samples, irradiated to a greater degree, all show definite increases in the volatilization rates, as compared to the untreated polymer. The sample irradiated by 103.53×10^{20} e.v./g., the highest radiation dose, shows a lower maximum than at the 63.24×10^{20} e.v./g. radiation dose. An explanation could be that with increase of radiation dose, the samples show greater initial losses and

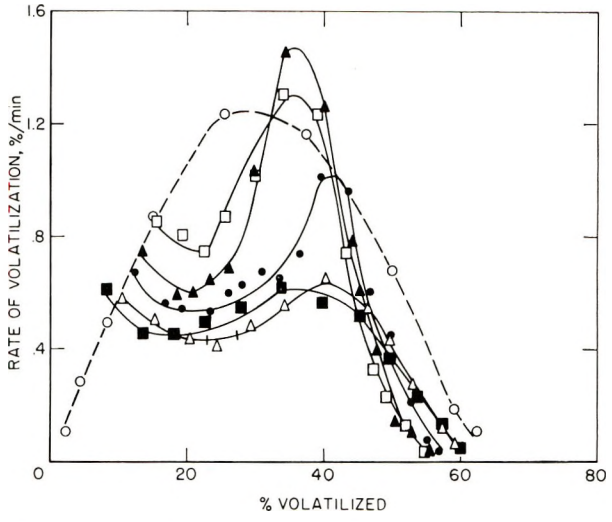

Fig. 5. Effect of prior γ-irradiation on the rate of volatilization at 410°C. of poly(vinylidene fluoride) with various radiation doses (in e.v./g. $\times 10^{-20}$): (○) polymer prepared by γ-initiation; (■) 0.00; (△) 19.4; (●) 43.9; (▲) 63.2; (□) 104.

also stabilize to a char at a lower degree of conversion. Apparently, the 103.53 $\times 10^{20}$ e.v./g. sample has exhausted enough of it volatiles, on initial heating, so that its maximum lies actually below that of the next lower irradiated sample. The total stabilization of the rate curve of the maximum treated sample as compared to the untreated polymer is approximately 5–6°C., as shown in Figure 5.

An attempt was made to determine the reason for the peculiar rate curve observed with the commercial polymer. Films of the two poly(vinylidene fluoride) samples, the commercial and the NBS polymer, were cast, with the use of hot dimethylformamide [$HCON(CH_3)_2$] as the solvent, and compared by infrared analysis. The only noticeable difference was observed at 6μ, where the presence of unsaturated double bonds in the commercial polymer is suggested. Another possible explanation is the possibility of residual catalyst left in the commercial polymer. A later poly(vinylidene fluoride) polymer, submitted by the company under the same trade name, gave a typical maximum rate curve (Fig. 6, curve *B*) which would have been more nearly ideal for the irradiation experiments.

From the rate curves in Figure 5, one might conclude that the thermal stability of the polymer varies inversely with the radiation dose. Any stabilization conferred by the crosslinking produced as a result of the γ-radiation treatment (see Table I) is not apparent from the rates of volatilization.

As with poly(vinyl fluoride), extracted samples (dimethylformamide solvent) behaved differently from unextracted.

Rate studies were made on four of the extracted and dried samples in the tungsten-spring balance at 410°C. Figure 7 indicates the experimental

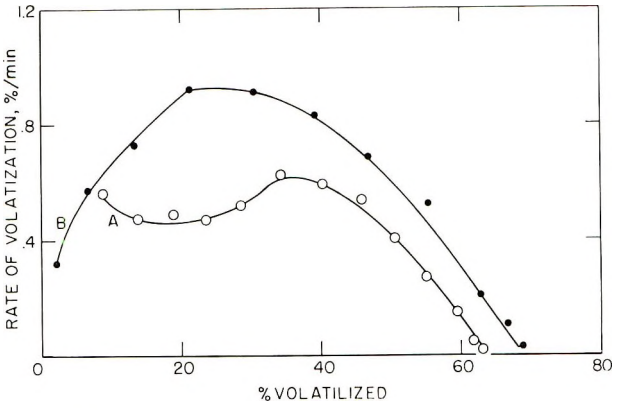

Fig. 6. Rate of volatilization of poly(vinylidene fluoride) at 410°C. for sample from various sources (○) sample A; (●) sample B.

points and curves. A definite increase in the rates of volatilization with radiation dose is clearly indicated. The sample irradiated by the lowest dose, 5.0×10^{20} e.v./g., still shows a maximum, whereas the highest dose of 103.53×10^{20} e.v./g., the rate curve is practically a straight line. In addition, the samples irradiated to a greater extent also stabilized earlier to yield a larger residue. The peculiar initial hump in the irradiated curves, observed in Figure 5, has been completely eliminated after the extraction process.

Pyrolysis studies in the tube apparatus were made at 450°C. for 1 hr. on some of the polymer samples. Lines 8–14 in Table II indicate the results obtained. The volatilization per cent column shows the extent of stabilization of the polymer samples with radiation dose. The phenomena exist before and after extraction to approximately the same degree. The condensed volatiles, in the last column, indicate an increase in the yield of small fragments to almost 100% collection at the higher radiation doses. As in the case of poly(vinyl fluoride), the HF volatiles are by far the most prominent; the hydrogen fluoride volatiles appear in the mass spectra as silicon tetrafluoride. Mass spectra of the untreated polymer, line 8, indicate very little benzene as a volatile product. The irradiated samples, lines 9–11, however, indicate more benzene in the decomposition products; approximately 10–15% of the hydrogen fluoride volatiles. After extraction with the dimethylformamide solvent, the benzene yield again becomes small.

The highest peak in the mass spectra is mass 167. All peak heights, except for the 78 peak in the irradiated samples, are quite insignificant, by contrast, when compared to the 85 peak. Most of the smaller masses are indicative of fluorine-containing compounds. This is also true in the case of the volatiles for poly(vinyl fluoride). Determination of constituents is quite difficult, since there are not many fluorine identification patterns available.

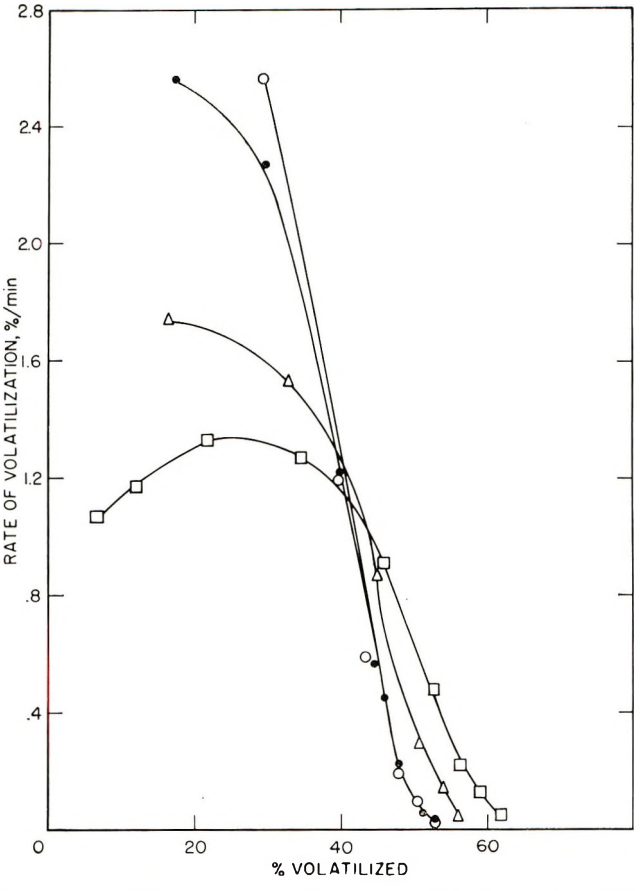

Fig. 7. Rate of volatilization at 410°C. of γ-irradiated poly(vinylidene fluoride) after extraction with dimethylformamide with various radiation doses (in e.v./g. $\times 10^{-20}$): (□) 5.0; (△) 19.4; (●) 43.9; (○) 104.

The residues of all the poly(vinylidene fluoride) samples retained their original shape as a black char; however, they could easily be crushed into a powder. The small amount of heavier waxlike volatiles appeared brownish in color.

DISCUSSION

It is evident that the γ-irradiation of the two polymers, poly(vinyl fluoride) and poly(vinylidene fluoride), exerts a considerable influence on their chemical structure[11,12] and hence on their thermal decomposition behavior. In that the initial rates of volatilization are increased by prior γ-radiation, the results are similar to those found previously[1] with polytrifluoroethylene. The present results are dissimilar in at least one way from the earlier ones since, upon irradiation, poly(vinyl fluoride) and poly(vinylidene fluoride) have a greater tendency for the thermal formation of residues.

In the pyrolysis of the three fluorohydropolymers, hydrogen fluoride formation[11] is accelerated by prior irradiation. During γ-irradiation it was found that in all three fluorohydropolymers crosslinking was the predominant process over scission (see Table I). However, scissions do occur to an appreciable extent.

The thermal decomposition mechanisms of these polymers are quite complicated, but they can be discussed in terms of two competing net processes: (*1*) decomposition by rupture of the chain-carbon bonds and (*2*) decomposition by the splitting off of the adjacent pendant atoms of hydrogen and fluorine as hydrogen fluoride. Schematically one would write:

$$\sim\!\!\sim CF_2CH_2(CF_2CH_2)_iCF_2CH_2\sim\!\!\sim$$

$$\swarrow^{k_c} \qquad \searrow^{k_F}$$

$$xCF_2CH_2 + yCF_2X(CH_2CF_2)_jCH_2X \qquad iHF + \sim\!\!\sim CF_2CH_2(CF{=}CH)_iCF_2CH_2$$

where X = H, F, or —CX=CX_2.

If the polymer decomposed entirely by process k_c, then no residue would be formed, and the fractional conversion or fractional weight loss would be written thus:

$$C(t) = 1 - \frac{\sum_{L}^{\infty} iQ_i(t)}{\sum_{1}^{\infty} iQ_i(0)}$$

where $Q_i(0)$ is the number of molecules of having i units at zero time, i.e., at the beginning of the decomposition process, $Q_i(t)$ the number of molecules at time t, and L the smallest molecule which must degrade in order to evaporate.

On the other hand, if the polymer decomposed by process k_F, there would be a finite residue and at complete conversion for the k_F reaction, as written above, the fractional weight loss would be 0.3125. For poly(vinyl fluoride), the fractional weight loss after the removal of one hydrogen fluoride unit per monomer would be 0.244 and for polytrifluoroethylene 0.435. For reasons of clarity, we label our abscissas in the figures as per cent volatilized instead of fractional weight loss.

The fluorohydropolymers studied here decompose normally by both mechanisms. Poly(vinylidene fluoride) produces more hydrogen fluoride than poly(vinyl fluoride), and a large amount of residue. At 400°C. the reaction stops at very near to 62.5% volatilized, which is stoichiometric for the production of two molecules of hydrogen fluoride for each monomer unit in the polymer. Thus, the decomposition of poly(vinylidene fluoride) is to a large extent by the k_F process, though the production[7] of some volatile hydrofluorocarbon and some hydrofluorocarbon wax, equal to about two-thirds by weight of the hydrogen fluoride produced, indicates that the k_c process is not negligible.

The thermal volatilization of unirradiated poly(vinyl fluoride) is found to be nearly 100% even though hydrogen fluoride production is also nearly stoichiometric.[13] Like the pyrolysis of poly(vinyl chloride),[14] where benzene and some other aromatic compounds are found, the pyrolysis of poly(vinyl fluoride) produces some benzene.

Upon irradiation, as had been anticipated, the now crosslinked poly(vinyl fluoride) forms a residue in about the expected stoichiometric amounts, a result not found previously with polytrifluoroethylene[1] (Fig. 3). There was also a greatly enhanced rate of initial volatilization in which hydrogen fluoride was being produced.

With unirradiated poly(vinylidene fluoride), nearly the maximum residue for the volatilization of two hydrogen fluoride molecules is produced; however an increased residue formation does occur with the irradiated polymer (Figs. 5 and 7). The rate of hydrogen fluoride evolution, or conversely, the rate of char or residue formation, is again greatly increased.

Extraction of the irradiated polymers, which was done in order to demonstrate that the observed effects were not due to the rapid evaporation of low molecular weight fragments produced by scission during the radiolysis of the polymer, completely changed the result with poly(vinyl fluoride) but not with poly(vinylidene fluoride) and polytrifluoroethylene[1] (Fig. 4). The k_F process is probably autocatalytic, that is, the production of a few unsaturated sites in the polymer tends to accelerate the further release of hydrogen fluoride.[15] For such an autocatalytic process, the type of plot shown in Figures 2–7 would go through a maximum. On the other hand, if process k_c were a random one, a maximum in the rate would also occur.[16]

The effects of extraction with hexamethylphosphoramide on the pyrolysis of irradiated poly(vinyl fluoride) suggest that the treatment removed the unsaturated sites. This is not unlikely in view of the chemical nature of the solvent and of the polymer. The pyrolysis of polytrifluoroethylene is altered by prior irradiation[1] in a very different fashion from that found for the systems investigated in this work. The changes produced in volatilization of the polytrifluoroethylene do not suggest an enhanced rate of hydrogen fluoride evolution but a change from a linear chain to a branched chain structure, as the rate curves for volatilization before irradiation are similar to those for linear polyethylene, while upon irradiation the curves become similar to those found for branched polyethylene.[17]

APPENDIX

Crosslinks and Scissions in Poly(vinyl Fluoride)

The estimation of crosslinking in poly(vinyl fluoride) was complicated by the presence of a highly deformed initial network. When the unirradiated sheet material was cautiously heated at 150–200°C., the thickness increased by a factor of 8–10 and the length and width decreased by a factor of 3, with excellent retention of rectangular form, little discoloration, and negligible weight loss. The same results were obtained by swelling

and drying, with greater discoloration and weight loss. Swelling of irradiated material occurred principally in the direction of thickness. This indicates that the sheet material contained a crosslinked network at an extension ratio $\alpha = 0.10$–0.125 in the direction of thickness as well as a network formed by radiation at $\alpha = 1$. Under these circumstances and taking the first $\alpha = {}^1/_9$, the ideal rubber equation leads to the relations (1), (2), and (3) for lengthwise extension of swollen gel, compression of swollen gel in direction of thickness and gel swelling, respectively.

$$\frac{9\nu_1 + \nu_2}{V_0} = \frac{F}{A'RTW[x - (1/x^2)]} \tag{1}$$

$$\frac{9\nu_1 + \nu_2}{V_0} = \frac{F\theta^2}{A'RTq[Z - (1/Z^2)]} \tag{2}$$

$$-[\ln(1 - v_2) + v_2 + \chi_1 v_2^2] = \frac{\bar{v}_1\nu_2}{V_0}\left[\left(\frac{\nu_1}{81\nu_2} + 1\right)^{1/3}\left(9\,\frac{\nu_1}{\nu_2}\right)^{2/3} - \left(\frac{\nu_1}{\nu_2} + 1\right)\frac{\nu_2}{2}\right] \tag{3}$$

Here ν_1 = moles of effective crosslinked chains remaining from original network; ν_2 = moles of effective crosslinked chains formed by radiation; V_0 = original volume, in cubic centimeters; $q = 1/v_2$ = swollen volume/original volume; F = force of compression or extension, in dynes; A' = cross-sectional area of original sheet normal to direction of extension, in square centimeters; W = width of swollen gel/width of original sheet; θ = thickness of swollen gel/thickness of original sheet; x = length, stretched, swollen/length, unstretched, swollen; Z = thickness, compressed, swollen/thickness, unstressed, swollen; $R = 8.31 \times 10^7$ ergs/deg.-mole; T = absolute temperature; $\bar{v}_1$ = molar volume of solvent. Since one of the two networks is usually strained beyond the limits of ideal rubber theory, the relations are at best semiquantitative here. The results in Table III are discordant by a factor of 2 and also imply an increase in the crosslink density of the original network ν_1/V_0, which is difficult to imagine.

The ratio of original to radiation-produced crosslinked chains, ν_1/ν_2, can also be computed from the dimensional changes of irradiated pieces, after relaxation by heat or by swelling and drying, by applying the theory of permanent set.[9] The relation can be stated in the form:

$$n_M L_x^2/n_x L_u^2 = (L_x^3 - L_s^3)/(L_s^3 - L_u^3) \tag{4}$$

In the present application, n_M and n_x are the effective crosslinked chain densities, ν_1/V and ν_2/V, of the original and radiation-generated crosslinked networks. L_u, L_x, and L_s are, respectively, the thicknesses of the relaxed unirradiated sheet, of the sheet during irradiation, and of the sheet relaxed after irradiation. Table IV shows the ratios of the two networks, computed from relaxation by heat. The ratios L_u/L_x and L_s/L_x have been

TABLE III
Crosslinked Chain Concentration in Irradiated Poly(vinyl Fluoride)

Dose, e.v./g. $\times 10^{-20}$	Temp., °K.	Volume swelling ratio q[a]	Width swelling ratio W[a]	$\frac{F}{A'[x-(1/x^2)]}$ g./cm.^{2}	$\frac{9\nu_1+\nu_2}{V_0}$, moles/cm.^{3} $\times 10^4$
0	300	37.4	1.16[b]	766[c]	4.6
0	300	37.4	1.16[b]	449[c]	2.6
0.51	300	21.7	1.18[d]	525[c]	1.48
5.0	300	18.1	0.70	1,490	0.84
	300	<18.0	0.65	1,860	1.13
9.44	300	15.2	1.24	10,300	3.3
	300	<15.0	1.04	14,400	5.5
	393	<15.0	0.83	6,030	2.1
19.83	300	<7.0	1.03	19,200	7.3
	300	7.1	1.17	30,400	10.3
	300	<7.0	0.96	38,000	15.6
	393	<7.0	0.92	22,000	7.0
	393	<7.0	0.92	27,000	8.5
63.24	300	<4.1	1.05	64,000	24.0
	300	2.3	0.94	78,000	32.6
	393	3.8	1.21	78,000	19.3

[a] Ratio prevailing during measurement, not necessarily equilibrium value.
[b] Thickness ratio 27.6.
[c] $F/A'(Z - 1/Z^2)$ in compression.
[d] Thickness ratio 12.4.

taken as (length $\times$ width)$^{-1}$ because of the poor experimental precision, $\pm 10\%$, of direct thickness measurements. Although these computations probably exaggerate the contribution of the most strained network (ν_2 at low doses, ν_1 at high doses), they indicate that some of the original network survives even after a dose of 124 Mr, which seems to imply a low yield of scissions. The process actually observed is, of course, the composite of radiation and swelling or heating. If a part of the crosslinks initiated by radiation are not completed until the swelling or heating is at an advanced

TABLE IV
Dimensional Changes of Heated Irradiated Poly(vinyl Fluoride) Sheet

Dose, e.v./g. $\times 10^{-20}$	Relaxed thickness ratio[a]	Computed ν_1/ν_2[b]
0	10	∞
0.51	6.72	43.3
5.0	4.18	7.7
9.44	3.37	3.9
19.38	2.44	1.38
63.24	1.4–1.77	0.46–0.2

[a] Heat-relaxed thickness divided by thickness as received; estimated from length and width changes.
[b] From permanent set theory.[9]

stage, the effect on the computation could be an apparent increase in ν_1 as well as ν_2 with radiation. The basic source of the error is the assumption of only two networks, neglecting intermediate networks formed during the relaxation.

Assuming that ν_1/V_0 does not increase with dose, and using the 120°C. values of gel elasticity, the resultant $G_c - 2G_d$ is 15 to 25. Combined with the $G_d/G_c = 0.28$, the lowest estimated from sol content, this yields absurdly high values, $G_d = 7$, $G_c = 30$. If ν_1 is allowed to increase and represents a mixture of crosslinked chains originally present and others formed during relaxation or swelling, then the total crosslinked chain density at 124 Mr is only about 2 to 3 $\times$ 10^{-4} mole/cm.^{3}, $G_c - 2G_d$ = 1.5–2.5, G_c = 3.4–5.7, and G_d = 0.95–1.6. Another aspect of the experimental crosslinked chain densities suggests that all the values in Table III may be too high by a large factor. The values determined at 393°K. are appreciably lower than those at 300°K. It has been argued theoretically that when there is a decided energy preference for extended zigzag or close helical configurations, the rubber elasticity should deviate from the ideal[10] in such a way that

$$-\partial \ln (F/T)/\partial(1/T) \cong \epsilon/R \tag{5}$$

where F is the force, T is the absolute temperature, and ϵ is an energy difference parameter. Experimental results suggest that ϵ is zero for most polymers, but is +540 cal, for polyethylene. The present temperature difference interpreted in this way would indicate a negative ϵ of several hundred calories, corresponding to a preference for *gauche* configurations and coiled chains in poly(vinyl fluoride). Since the theoretical treatment implies

$$F/F_{\text{ideal}} = 2/(2/3 + 4/3 \exp\{\epsilon/RT\})$$

the observed force can lead to an overestimate of ν/V up to threefold for large negative ϵ. The G values would be correspondingly reduced.

Application of the swelling equation to the unirradiated poly(vinyl fluoride) in hexamethylphosphoramide leads to χ values of -1.5 to -3 for the system at 130°C.; these could likewise be reduced to one-third if ϵ is large and negative. The crosslink yield G_c is thus highly indeterminate, ranging from G_c = 1.2 to G_c = 30. A high value is not unreasonable, if it includes the postirradiation effects of solvents or heat. High values of G_c and G_d, if real, correlate well with the observed rapid loss of HF during pyrolysis.

References

1. Straus, S., and L. A. Wall, *SPE Trans*, **4**, 61 (1964).
2. Florin, R. E., and L. A. Wall, *J. Res. Natl. Bur. Std.*, **65A**, 375 (1961).
3. Wall, L. A., and R. E. Florin, *J. Appl. Polymer Sci.*, **2**, 251 (1959).
4. Bowers, G. H., and E. R. Lovejoy, *Ind. Eng. Chem. Prod. Res. Develop.*, **1**, 89 (1962).

* Based on research supported by the National Aeronautics and Space Administration.

5. Lawton, R. J., A. M. Bueche, and J. S. Balwit, *Nature*, **172**, 76 (1953).
6. Yoshida, T., R. E. Florin, and L. A. Wall, unpublished data.
7. Madorsky, S. L., and S. Straus, *J. Res. Natl. Bur. Std.*, **63A**, 261 (1959).
8. Madorsky, S. L., *J. Polymer Sci.*, **9**, 133 (1952).
9. Tobolsky, A. V., *Properties and Structure of Polymers*, Wiley, New York, 1960, p. 242.
10. Flory, P. J., C. A. J. Hoeve, and A. Ciferri, *J. Polymer Sci.*, **34**, 337 (1959); for discussion see ref. 9, p. 311.
11. Bresee, J. C., J. R. Flanary, J. H. Goode, C. D. Watson, and J. S. Watson, *Nucleonics*, **14**, No. 9, 74 (1956).
12. Byrne, J., T. W. Costikyan, C. B. Hanford, D. L. Johnson, and W. L. Mann, *Ind. Eng. Chem.*, **45**, 2549 (1953).
13. Madorsky, S. L., V. E. Hart, S. Straus, and V. A. Sedlak, *J. Res. Natl. Bur. Std.*, **51**, 327 (1953).
14. Stromberg, R. R., S. Straus, and B. G. Achhammer, *J. Polymer Sci.*, **35**, 355 (1959).
15. Boyer, R. F., *J. Phys. Colloid Chem.*, **51**, 80 (1947).
16. Simha, R., and L. A. Wall, *J. Phys. Chem.*, **56**, 707 (1952).
17. Wall, L. A., *Effect of Branching on the Thermal Decomposition of Polymers*, Soc. Chem. Ind. Monograph No. 13, London, 1961, p. 146.

Résumé

On a comparé quantitativement la vitesse de volatilisation thermique de divers polymères fluorés, avant et après irradiation γ. Les effets de l'irradiation γ sur le Fluorure de polyvinyle, et le fluorure de polyvinylidène ont aussi été étudiés par gonflement et on a déterminé des rapports sol-gel. On observe chez ces deux polymères, ainsi que chez le polytrifluoroéthylène, une prédominance du pontage, bien qu'il y ait bon nombre de ruptures. Les vitesses de volatilisation et de dégradation du polymère augmentent par irradiation γ, alors que les études antérieures sur le polytrifluoroéthylène ne relataient pas d'augmentation de dégradation après irradiation, mais bien une accélération de leur volatilisation. On croit cependant que l'augmentation des vitesses de volatilisation chez le polytrifluoroéthylène se passe par un mécanisme différent de celui déterminé dans le cas des polymères vinyliquee et vinylidèniques fluorés.

Zusammenfassung

Ein quantitativer Vergleich zwischen der thermischen Verflüchtigungsgeschwindigkeit einiger Fluorpolymerer vor und nach Einwirkung von γ-Strahlung wurde durchgeführt. Der Einfluss der γ-Bestrahlung auf Polyvinylfluorid und Polyvinylidenfluorid wurd auch durch Bestimmung des Quellungsgrades und des Sol-Gelverhältnisses untersucht. Bei beiden Polymeren und auch bei Polytrifluoräthylen tritt vorwiegend Vernetzung ein, obgleich auch eine beträchtliche Anzahl von Kettenspaltungen auftritt. Die Geschwindigkeit der Verflüchtigung und der Bildung von Verkohlungsrückständen wurden durch γ-Bestrahlung erhöht, während das früher untersuchte Polytrifluoräthylen nach Bestrahlung keinen grösseren Verkohlungsrückstand erzeugte, obgleich die Bestrahlung seine Verflüchtigung beschleunigte. Es wird angenommen, dass bei Polytrifluoräthylen die gesteigerte Verflüchtigungsgeschwindigkeit durch einen Mechanismus erzeugt wird, der von denjenigen bei den Vinyl- und Vinylidenfluoridpolymeren verschieden ist.

Received November 4, 1964
Prod. No. 4824A

JOURNAL OF POLYMER SCIENCE: PART A-1 VOL. 4, 367–375 (1966)

Donor–Acceptor Interaction in Cationic Polymerization. VI. Influence on the Molecular Weight of Polyisobutylene of Some Anions Derived from the Complexes of Aluminum Trichloride with Some Electron Donors

Z. ZLÁMAL, A. KAZDA, and L. AMBROŽ, *Research Institute of Macromolecular Chemistry, Brno, Czechoslovakia*

Synopsis

The concentration dependence of the specific conductivity of complexes of aluminum trichloride with ethanol, diethyl ether, and phenetole in a molar ratio of 1 : 1 and in 2EtOH·$AlCl_3$ and EtOH·$2AlCl_3$ complexes has been measured. Conductivity measurements were carried out in ethyl chloride at −78.5°C. Molar conductivity and the degree of dissociation of the complexes studied are concentration-independent which proves an extensive association of ions. Polymerizations of isobutylene carried out in the presence of these complexes and under the same conditions as the conductivity measurements have shown that the molecular weight of polyisobutylene formed is inversely proportional to the concentration of the complex over the whole range of concentrations studied. It can be deduced from the relation between the specific conductivity and the molecular weight that only the ionized part of the complex asserts itself in the chain-breaking processes. The chain-breaking efficiencies of various anions are given and allow one to draw conclusions about the mode of ionization of donor molecules after the interaction with the acceptor, viz. aluminum trichloride.

INTRODUCTION

In previous work[1–3] we have studied the specific electrical conductivity of systems consisting of aluminum trichloride and basic components with continuously changing stoichiometric ratios. We have shown that the specific conductivity of the systems changes very abruptly with changing molar ratios of both components. The molecular weight of polyisobutylene formed by polymerization in these solutions also varies in a similar way.

In the present investigation we report results of measurements of changes in specific conductivity and molecular weight of polyisobutylene which are caused only by varying the concentrations of both compounds, the stoichiometric ratio of donor and acceptor being the same.

As in other papers of this series, we will attempt to show that the length of macromolecule, as formed in the given system, is defined in the first place by bimolecular reactions between the growing ends and the free

anions. As the rates of polymerizations have not been measured, we cannot draw any conclusions whether there is termination or chain transfer. Neither can we draw definite conclusions about the catalytic efficiency of the studied complexes.

EXPERIMENTAL

Materials Used

The quality of ethyl chloride, isobutylene, and aluminum trichloride and methods of purification were the same as described earlier.[3] Complete removal of moisture was aimed at in the case of other chemicals. After washing with water and subsequent distillation, the ethers were freed from residual moisture by refluxing them with metallic sodium and by distillation. Alcohols were dehydrated with calcined CaO or BaO.

Nitrogen used in all manipulations as a protection against atmospheric moisture was dried in a P_2O_5 tower. Residual moisture was removed by bubbling the nitrogen through ethyl chloride cooled to −78.5°C.; nitrogen was at the same time saturated with ethyl chloride vapors at the temperature of measurement so that it did not carry away vapors of solvent from the measured solutions. Nitrogen dried in this way contained less than 15 ppm of water.

Experimental Technique

Polymerization,[1] conductivity measurements,[2] and molecular weight determination[4] were carried out as described earlier. All polymerizations were run at one monomer concentration, [M] = 3.68 mole/l.

The studied complexes were prepared by reacting $AlCl_3$ and the donor in ethyl chloride solution. A desired quantity of $AlCl_3$ was weighed out into a glass tube containing ethyl chloride; most of the $AlCl_3$ dissolved at 0°C. under stirring. The solution of $AlCl_3$ in ethyl chloride was exposed to the relatively high temperature (0°C.) for 10 min. at the most so that changes caused by a decomposition of the labile complexes (evolution of HCl etc.) were insignificant and could not influence subsequent measurements. In another tube the donor was added; its quantity was carefully determined with respect to $AlCl_3$ so as to form the complex of the desired composition. After addition of the donor the remaining $AlCl_3$ dissolved—usually very quickly—and the solution turned pale yellow. After that ethyl chloride was added to the desired weight and the solution of the complex (its concentration was about 60 mmole/l.) was quickly connected to a measuring buret and cooled to −85°C. by a mixture of methyl chloride and solid CO_2. At this temperature it was allowed to stand for 60 min. before use, so as to eliminate any possible influence of aging.

This solution was then measured out into ground test tubes from jacketed burets kept at 0°C. and was diluted to the desired concentration with pure ethyl chloride. After closing the top of the test tube by the conduc-

tivity cell with a ground joint, the solution was cooled to −78.5°C. and its conductivity was measured. All manipulation was done in the atmosphere of dry nitrogen.

In the range of low concentrations of the complex the natural basic impurities in ethyl chloride were already perceptible; these impurities shifted the original stoichiometric ratio in favor of the basic component. It was necessary to neutralize them by a solution of aluminum trichloride in ethyl chloride (its concentration was about 6 mmole/l.). The size of the correction was determined tentatively by adding a correcting solution to 10 ml. of the stock complex solution. The mixture was made up to 20 ml. with pure ethyl chloride and the specific conductivity was measured. It was found out in this way, how much of the correcting solution must be added to obtain the minimum conductivity characterizing the precise 1:1 composition of the complex. The amount of the correcting solution varied from 1 to 3 ml.

The conductivity caused by neutralized impurities $\varkappa_0$ could then be subtracted from the measured values $\varkappa$ so that values of conductivity and molecular weights of polymer obtained in solvents of varying purity could be compared. The quantity of correcting $AlCl_3$ solution calculated for total volume of solvent to be used in polymerization or in conductivity measurement was added before the complex was measured. In the polymerization experiments the value $1/M_0$ was analogously subtracted; this value corresponded to the molecular weight of polyisobutylene formed by means of the correcting quantity of $AlCl_3$ after neutralization by natural basic impurities present in ethyl chloride.

The complexes of donors with aluminum trichloride, having the molar ratio 2:1 and 1:2, were prepared in the same way as 1:1 complexes, an excess of about 10 mole-% of basic or acid compound being added, so that the concentration of these complexes in all measurements was one order lower than the concentration of the 1:1 complex. The conductivity or the value of $1/\bar{M}$ corresponding to the excess of the simultaneously present 1:1 complex was subtracted from the results. In all probability such results are subject to a larger error than data relating to the 1:1 complex.

RESULTS AND DISCUSSION

Figure 1 shows the dependence of the specific conductivity $\varkappa$ on the concentration of complexes of some donors with aluminum chloride in the 1:1 molar ratio. All dependences are strictly linear,[5] as also is the case in Figure 2, where the same dependences are shown for the $2EtOH \cdot AlCl_3$ and $EtOH \cdot 2\ AlCl_3$ complexes.

A linear dependence of the specific conductivity $\varkappa$ on the concentration indicates that the molar conductivity Λ and the degree of dissociation γ are concentration-independent. As the measured range is still too far from infinite dilution where such behavior of studied electrolytes would be easy to understand, the observed facts can best be explained on the grounds of the association of ions.

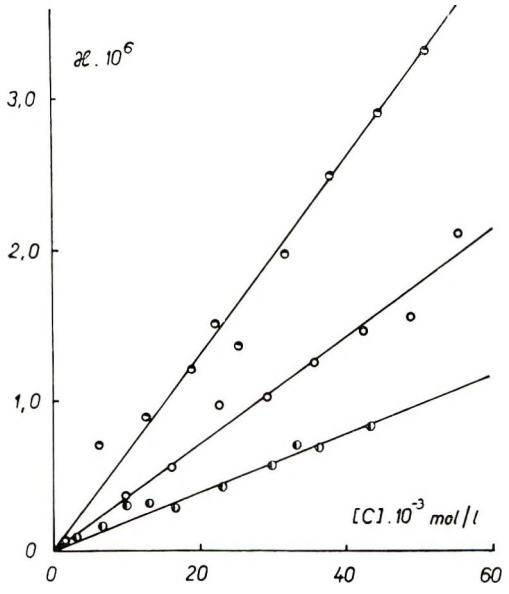

Fig. 1. Dependence of the specific conductivity on the concentration of $AlCl_3$ complexes in ethyl chloride at −78.5°C.: (◓) $EtOEt \cdot AlCl_3$ complex; (○) $EtOH \cdot AlCl_3$ complex; (◐) $C_6H_5OEt \cdot AlCl_3$ complex.

The independence of γ or Λ of concentration means that the number of osmotically effective particles is not changed by ionization of the solution. The following two dissociation schemes are the simplest of those satisfying the above condition:

$$2\ AB \rightleftharpoons A^{\oplus} + (BAB)^{\ominus} \tag{1}$$

or

$$2\ AB \rightleftharpoons (ABA)^{\oplus} + B^{\ominus} \tag{2}$$

It is impossible to tell from our experiments whether eq. (1) or eq. (2) is valid, but the existence of a free proton is unlikely and therefore we assume eq. (2) to be more correct. The equilibrium constant is then given by the relation:

$$K = [ABA^{\oplus}][B^{\ominus}]/[AB]^2 = [B^{\ominus}]^2/[AB]^2 \tag{3}$$

If the equilibrium constant is expressed in terms of the overall concentration $[c]$ of the monomeric complex and the degree of dissociation γ, we obtain the following expressions:

$$AB \rightleftharpoons 1/2\ ABA^{\oplus} + {}^1/_2\ B^{\ominus}$$

and therefore

$$[AB] = [c](1 - \gamma)$$

$$[ABA^{\oplus}] = [B^{\ominus}] = {}^1/_2\ [c]\gamma$$

then

$$K = \frac{[c]^2\gamma^2}{4[c]^2(1-\gamma)^2} = \frac{\gamma^2}{4(1-\gamma)^2} \tag{4}$$

and K is concentration-independent.

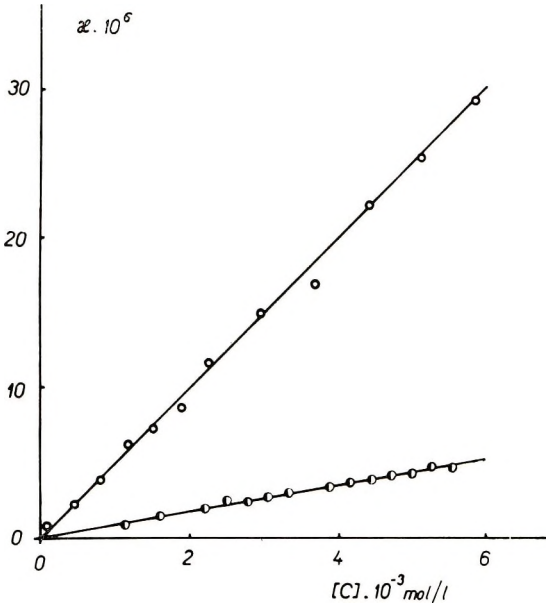

Fig. 2. Dependence of the specific conductivity on the concentration of (O) 2EtOH·–$AlCl_3$ complexes and (◐) EtOH·2$AlCl_3$ complexes in ethyl chloride at −78.5°C.

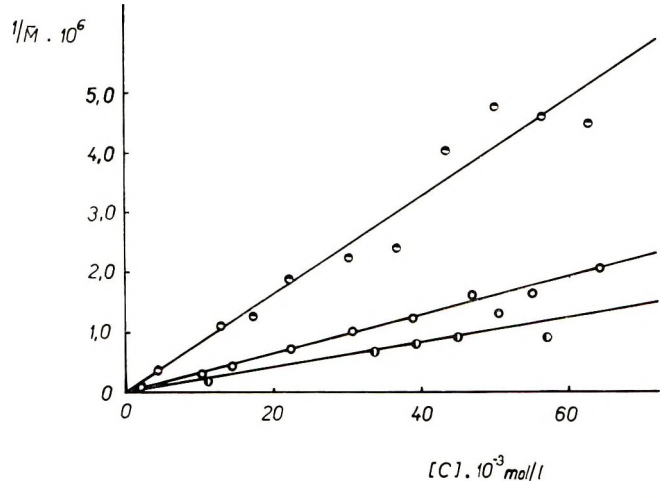

Fig. 3. Dependence of the reciprocal of the molecular weight of polyisobutylene on the concentration of $AlCl_3$ complexes in ethyl chloride at −78.5°C.: (◓) EtOEt·$AlCl_3$; (O) C_6H_5OEt·$AlCl_3$; (◐) EtOH·$AlCl_3$.

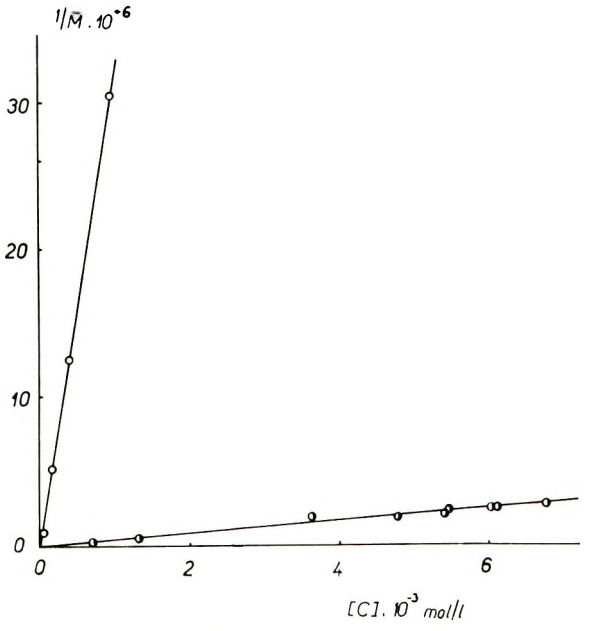

Fig. 4. Dependence of the reciprocal of the molecular weight of polyisobutylene on the concentration of (○) $EtOH \cdot 2AlCl_3$ complexes and (◑) $2EtOH \cdot AlCl_3$ complexes in ethyl chloride at −78.5°C.

The straight lines of Figures 1 and 2 pass through the origin, fulfilling the simple equation

$$\varkappa = k[c] \tag{5}$$

From the definition of molar conductivity

$$\Lambda = 10^3 \varkappa/[c] \tag{6}$$

it follows that the slope of the lines and therefore the constant in eq. (5) is equal to $\Lambda \times 10^{-3}$. The value of Λ of the 1:1 complexes is governed only by the degree of dissociation and by ion mobility:

$$\Lambda = F \gamma(v_A + v_K) \tag{7}$$

where $F = 96{,}500$ coulombs, and v_A, v_K are anion and cation mobility, respectively. The values of Λ are given in Table I for the dimer complexes studied.

In the presence of these complexes the polymerization of isobutylene was carried out by the usual methods and the reciprocal of the molecular weight (measured viscometrically) was plotted against complex concentration after the correction was subtracted. The results are given in Figures 3 and 4.

The linearity of all reported relationships indicates that the Mayo equation holds so that we can write:

$$1/M = k_1[c]/k_2[M] \tag{8}$$

where $\bar{M}$ is the molecular weight of polyisobutylene, [M] is monomer concentration, [c] is complex concentration, k_2 and k_4 are constants of propagation and transfer with complex, respectively.

However, plots of conductivity vs. composition for the majority of studied donor–aluminum trichloride pairs[1–3] show that the undissociated and therefore nonconductive types of complexes are very poor terminators or chain transfer agents. Practically only the ionized part of the complex asserts itself in the process of chain breaking, so that eq. (8) is written more exactly as

$$1/\bar{M} = k_4\gamma[c]/k_2[M] \tag{9}$$

We cannot determine the degree of dissociation γ from these measurements as we do not know the mobilities of the ions. In Table I the values of the product $\gamma\ k_4/k_2$ are given instead, which characterizes the chain-breaking efficiency of the complexes studied and which is read from the slopes of lines in Figures 3 and 4.

It is necessary to consider whether the degree of dissociation of the complexes does not differ excessively in conductivity experiments and in polymerization runs. Decreased dielectric constant caused by the addition of monomer could lead to decreased γ and so to increased molecular weight and to decreased conductivity. In one of the previous papers[6] it was shown that this does not happen in the presence of $AlCl_3$ complexes with donors which are more basic than ethyl chloride. The excess of as much as 30% of hexane or benzene causes only a small decrease in conductivity of the complex solution and its influence on molecular weight of polyisobutylene was negligible. Therefore we can divide eq. (5) by eq. (9) and so eliminate γ. We get an expression for $1/\bar{M}$ as a function of $\varkappa$:

$$1/\bar{M} = k_4\ \varkappa \times 10^3/k_2[M]F(v_A + v_K) \tag{10}$$

From eq. (10) we can calculate the values of the product $(k_2/k_4)\ (v_A + v_K)$. These are given in Table I together with the molecular weights of the dimer complexes. We suppose this product to be more descriptive for following considerations than $\gamma\ k_4/k_2$. Even if the mobilities of the cor-

TABLE I

Complex	Anion assumed	Λ	$\gamma(k_4/k_2)$	$(v_A + v_K)$ (k_2/k_4)	Molecular weight of the complex
$EtOH \cdot AlCl_3$	$AlCl_3OEt^{\ominus}$	0.0350	7.4×10^{-5}	5.0×10^{-3}	359
$EtOEt \cdot AlCl_3$	$AlCl_3OEt^{\ominus}$	0.0655	3.0×10^{-4}	2.3×10^{-3}	415
$C_6H_5OEt \cdot AlCl_3$	$AlCl_3OEt^{\ominus}$	0.0194	1.2×10^{-4}	1.7×10^{-3}	511
$2ETOH \cdot AlCl_3$	$AlCl_3OEt^{\ominus}$	5.015	1.6×10^{-3}	32.2×10^{-3}	451
$EtOH \cdot 2AlCl_3$	$Al_2Cl_6OEt^{\ominus}$	0.886	1.2×10^{-1}	7.9×10^{-5}	626

responding ions are unknown and influenced by the polymer formed, it is still unlikely that the approximately equally large molecules of complexes with similar chemical properties in the same solvent should display mobilities differing in their order of magnitude. The relationship for γ appears less illustrative.

Now let us compare data from Table I with our assumptions regarding the role of the anions. In the first four cases we assume the same anions and therefore the same chain-breaking efficiency expressed by the k_4/k_2 ratios. The different molar conductivities of these complexes point, however, to the different number of ions existing per mole of the complex. When the influence of the degree of dissociation is eliminated by means of eq. (10), very similar quantities are obtained in the first three lines of column 5. These numbers now depend only on mobilities, and their relative agreement shows that the mobilities of ions are similar also. The values of the product decrease moderately with increasing molecular weight of the complex, as could be expected.

There is one exception in the case of the $2EtOH \cdot AlCl_3$ complex, which shows a molar conductivity probably a hundred times higher than the other complexes with the same anion. However, this complex decreases the molecular weight not by a hundred times but only about twenty times; this proves that the increased molar conductivity is due not only to the increasing number of ions, i.e., to the degree of dissociation γ, but probably also to the increase of their mobility. It is also possible that the role of the cation in the complexes of the 2:1 type during polymerization differs somewhat from the complexes of the 1:1 type. This leads us to the conclusion that the nearly tenfold difference in the value of the product $(v_A + v_K)(k_2/k_4)$ is as yet no proof of a change in the composition of the anion from the assumed structure.

In the last case, in the $EtOH \cdot 2AlCl_3$ complex, we assume another anion than in the remaining complexes of Table I, i.e., a more effective chain breaker than $[AlCl_3OEt]^{\ominus}$. The molecule of this complex is not sufficiently more bulky than the others to permit us to explain the decrease of the value of $(v_A + v_K)(k_2/k_4)$ two orders below the $EtOH \cdot AlCl_3$ complex by decreased ion mobility. Neither is Λ so high that we might explain the increase of the value of $\gamma\, k_4/k_2$ more than three orders over the $EtOH \cdot AlCl_3$ complex by an increase of γ. We must therefore suppose that the value of the transfer constant k_4 has increased.

The above data show that the method of comparing conductivity measurements with molecular weights of polyisobutylene formed by polymerization in these solutions can give information about the terminating effectivity of various donors—or, more exactly, of the anions of their complexes with aluminum trichloride—as well as about the mode of their ionization. It is shown in the same way that the electrochemical processes taking place in solutions of Friedel-Crafts catalysts influence the mechanism and the kinetics of cationic polymerization more than has hitherto been admitted.

References

1. Ambrož, L., and Z. Zlámal, *J. Polymer Sci.*, **30**, 381 (1958).
2. Zlámal, Z., and L. Ambrož, *J. Polymer Sci.*, **29**, 595 (1958).
3. Zlámal, Z., and A. Kazda, *J. Polymer Sci. A*, **1**, 3199 (1963).
4. Zlámal, Z., J. Ambrož, and L. Ambrož, *Chem. Listy*, **49**, 1606 (1955).
5. Zlámal, Z., paper presented at Symposium on Macromolecules, Wiesbaden, Germany, 1959, Section III, A14.
6. Zlámal, Z., and A. Kazda, *J. Polymer Sci.*, **53**, 203 (1961).

Résumé

La dépendance vis à vis de la concentration de la conductivité spécifique de complexes de trichlorure d'aluminium avec l'éthanol, l'éther diéthylique et le phénétol en rapport molaire 1:1 et de complexes 2 EtOH. $AlCl_3$ et $EtOH{\cdot}2AlCl_3$, a été mesurée. Les mesures de conductivité ont été faites dans le chlorure d'éthyle à $-78,5°C$. La conductivité molaire et le degré de dissociation des complexes étudiés sont indépendants de la concentration, ce qui prouve une forte association des ions. Les polymérisations de l'isobutylène, exécutées en présence de ces complexes et dans les mêmes conditions que les mesures de conductivité, ont montré que le poids moléculaire du polyisobutylène formé est inversément proportionnel à la concentration du complexe dans tout le domaine de concentration étudié. On peut conclure de la relation entre la conductivité spécifique et le poids moléculaire que, seulement, la partie ionisée du complexe intervient das le processus de rupture de chaînes. Les efficacités de rupture de chaînes de plusieurs anions sont données et permettent de tirer des conclusions sur le mode d'ionisation des molécules du donneur après l'interaction avec l'accepteur tel que le trichlorure d'aluminium.

Zusammenfassung

Die Konzentrationsabhängigkeit der spezifischen Leitfähigkeit von Komplexen aus Aluminiumtrichlorid mit Äthanol, Diäthyläther und Phenetol im molaren Verhältnis 1:1 und in den Komplexen 2 $EtOH{\cdot}AlCl_3$ und $EtOH{\cdot}\ 2AlCl_3$ wurde gemessen. Leitfähigkeitsmessungen wurden in Äthylchlorid bei $-78,5°C$ ausgeführt. Die molare Leitfähigkeit sowie der Dissoziationsgrad der untersuchten Komplexe sind konzentrationsunabhängig, was eine weitgehende Ionenassoziation beweist. In Gegenwart dieser Komplexe und unter den Bedingungen der Leitfähigkeitsmessungen ausgeführte Polymerisationsversuche an Isobutylen zeigten, dass das Molekulargewicht des gebildeten Polyisobutylens im ganzen untersuchten Konzentrationsbereich umgekehrt proportional der Konzentration des Komplexes ist. Aus der Beziehung zwischen spezifischer Leitfähigkeit und Molekulargewicht kann man ableiten, dass nur der ionisierte Anteil des Komplexes in "Kettenabbruchs-" prozessen wirksam ist. Die "Kettenabbruchswirksamkeit" verschiedener Anionen wird angebegen; man kann daraus Schlüsse auf die Art der Ionisierung von Donormolekülen nach Wechselwirkung mit dem Akzeptor, nämlich Aluminiumtrichlorid ziehen.

Received November 13, 1964
Revised June 15, 1965
Prod. No. 4829A

JOURNAL OF POLYMER SCIENCE: PART A-1 VOL. 4, 377–391 (1966)

Vinyl Polymerization by Cobaltic Ions in Aqueous Solution: Part I. Polymerization of Methyl Methacrylate

K. JIJIE, M. SANTAPPA, and V. MAHADEVAN, *University Department of Physical Chemistry, Alagappa Chettiar College, Madras, India*

Synopsis

Polymerization of methyl methacrylate initiated by cobaltic ions in perchloric, nitric and sulfuric acids was studied in the temperature range 15–25°C. In all three acids, water oxidation occurred as a side reaction. In $HClO_4$ and HNO_3 media monomer oxidation was shown to be an additional complicating feature. Rates of cobaltic ion disappearance, monomer disappearance, and chain lengths of polymers were measured with variations in [M], [Co^{3+}], [H^+], initially added [Co^{2+}], and temperature. In $HClO_4$ and HNO_3 experimental results favored simultaneous initiation by Co^{3+} and $CoOH^{2+}$ species, while in H_2SO_4, Co^{3+} ions alone were the active entities. An appropriate kinetic scheme to fit all the experimental observations is proposed. The various rate constants were evaluated.

INTRODUCTION

The powerful oxidizing capacity of trivalent cobalt has been shown in the recent investigations reported by Waters and his associates,[1–5] Bawn,[6–11] Sutcliffe and co-workers,[12–16] Higginson and co-workers[17,18] and others. A wide variety of organic compounds—aromatic as well as aliphatic aldehydes, alcohols, ketones, olefins, and hydrocarbons—have been found to be susceptible to oxidation by cobaltic ions, and kinetics of these reactions have been reported in detail. Oxidation of inorganic substrates, especially of Ce^{3+}, by Co^{3+} has been studied by Sutcliffe and Weber.[12–14] These authors have also made a spectrophotometric study of the existence of various ion pair species of Co^{3+} present in perchloric[19] and sulfuric acid[14] media. Water oxidation by cobaltic ions has been reported in detail by Bawn and White[6] and by Baxendale and Wells.[20] Apart from a brief mention by Baxendale and Wells that Co^{3+} initiates vinyl polymerization, no detailed studies on kinetics of such polymerization reactions have been attempted so far. We present in the following sections the results of a systematic study of the polymerization of methyl methacrylic (MMA) by aqueous Co^{3+} in perchloric, nitric, or sulfuric acid in the temperature range 15–25°C. From the experimental results conclusions with regard to the nature of the initiating and terminating species have been drawn and certain rate parameters evaluated.

EXPERIMENTAL

Reagents

All the materials used in the preparation of reagents were B.D.H. or E. Merck analytical reagent grade products. Doubly-distilled, deionized (by passage through a mixed bed of Bioderminrolit) water was used for preparation of various reagents.

Preparations

Cobaltic perchlorate was prepared by anodic oxidation[15] for over 12 hr. of ca. 0.1*M* cobaltous perchlorate solution in 4–6*M* perchloric acid, in a divided cell at 0°C. with the use of platinum electrodes.

Cobaltous perchlorate was obtained by repeated fuming of cobaltous nitrate with $HClO_4$ followed by recrystallization from an acidic solution. Stock solutions of Co^{3+} were found to be 99% pure and were stored at −10°C.

Cobaltic nitrate was prepared by a procedure essentially identical to that for cobaltous perchlorate, the reagents, however, being nitric acid and cobaltous nitrate. Stock solutions of cobaltic nitrate were more stable than those of the perchlorate.

Cobaltic sulfate was prepared[6,21] as a solid by anodic oxidation of a saturated solution of cobaltic sulfate (T. T. English pure; recrystallized) in 10*N* sulfuric acid; the solid was thoroughly washed with ice-cold 10*N* H_2SO_4 and dissolved in precooled (−10°C.) 4–6*N* H_2SO_4 as a stock solution. Stock solutions of cobaltic sulfate free from any peracid were used. All the cobaltic salts were always freshly prepared and used immediately.

Sodium perchlorate (used for adjustment of ionic strength in $HClO_4$ medium) was prepared by neutralization of Na_2CO_3 with $HClO_4$.

Other reagent solutions, like sodium nitrate, potassium or sodium bisulfate, etc., were prepared from A. R. products.

Methyl methacrylate (Rohm & Haas) was freed from inhibitor by means of alkali, washed, dried over anhydrous sodium sulfate, distilled under reduced pressure, and stored at 5°C.

Estimations

Stock solutions of cobaltic ion in the three acid media were analyzed for the total $[Co^{2+}] + [Co^{3+}]$ content by the method of Latinen and Burdett.[22]

The cobaltic ion concentration was estimated by running aliquot portions into excess standard Fe^{2+}, the unreacted latter being back-titrated with Ce^{4+} either potentiometrically or by titrimetry with ferroin as indicator.

Rates of cobaltic ion disappearance ($-R_{Co}$) were evaulated by titrimetry from the filtrate after filtration of the polymer.

Free acid concentration in the Co^{3+} solution was estimated by gentle warming to decompose Co^{3+} to Co^{2+}, followed by titration with standard alkali with bromocresol green as indicator.

Chain length (n) measurements of the PMMA samples were carried out by viscometry in benzene solutions by use of the equation of Baxendale et al.:[23]

$$n = 2.81 \times 10^3 [\eta]^{1.32}$$

where $[\eta]$ is intrinsic viscosity and n is chain length of the polymer.

The rate of polymerization R_p was determined by the usual gravimetry, while the rate of total monomer disappearance, $-R_M$, was estimated by bromometric estimation of the residual monomer in the filtrate after the polymer was filtered off.

Kinetic Measurements

The thermostat was a large Dewar vessel (4-l. capacity, height 15 in., diameter 6 in.) equipped with a stirrer and thermometer. Temperature was maintained with an accuracy of ± 0.1°C. The reaction vessel consisted of a long Pyrex test tube ($8 \times 1^1/_2$ in.) fitted with a B-24 socket. A B-24 cone, to which were fused an inlet tube ($7^1/_2$ in. long) and an outlet tube, fitted this socket. A thermostatted reaction mixture consisting of monomer, acid, and corresponding sodium salt was deaerated by bubbling oxygen-free nitrogen through the inlet tube for about 20–30 min. Co^{3+} stock solution was then added through the outlet tube which was then closed with a rubber gasket. An all-glass wash bottle containing monomer at the same concentration as the reaction mixture was interposed in the nitrogen train to minimize loss of monomer due to deaeration. After the required time of the experiment (ca. 25–30 min.) the course of polymerization was arrested by addition of Fe^{2+}. The polymer was filtered off. R_p, $-R_{Co}$, $-R_M$, etc. were evaluated as described above.

Degassing of the system was also effected by the usual high vacuum technique after freezing the system with liquid air. No difference was observed in the R_p values, but a disparity in the $-R_{Co}$ values was observed between the two techniques of degassing, the higher $-R_{Co}$ values in the high vacuum technique arising as a result of oxidation of water, monomer, etc. during degassing; in degassing by N_2, addition of Co^{3+} towards the end might obviously minimize consumption of Co^{3+} in side reactions during the process of deaeration. In this work the nitrogen flushing procedure was adopted for all experiments.

RESULTS AND DISCUSSION

Polymerization of MMA initiated by Co^{3+} ($[Co^{3+}] = 5 \times 10^{-4}$–$1.5 \times 10^{-2} M$) was found to be very fast in the range 15–25°C., $[H^+] = 0.4$–$2M$; $[H^+] = 1.0M$ was used in most of the experiments.

The free-radical nature of the reaction was inferred from the short induction periods observed in the undeaerated systems, whereas in the degassed system the induction period was absent. Polymerization commenced within a few seconds, as indicated by the appearance of turbidity. Use of conventional inhibitors was not possible because of the powerful oxidizing nature of Co^{3+} ions. Steady-state rates were obtained within 15 min. but with an unavoidable conversion of monomer exceeding 50%. Another important feature of the system was that even under conditions of high acidity and low temperature, oxidations of water, monomer, etc., in side reactions other than consumption of the monomer in polymerization reaction, invariably occurred, and were complicating features which could not be eliminated completely.

Variation of $-R_{Co}$

A linear variation of $-R_{Co}$ with [M] (Fig. 1) with considerable intercepts on the y-axis in the three acid media at constant $[H^+]$ was observed.

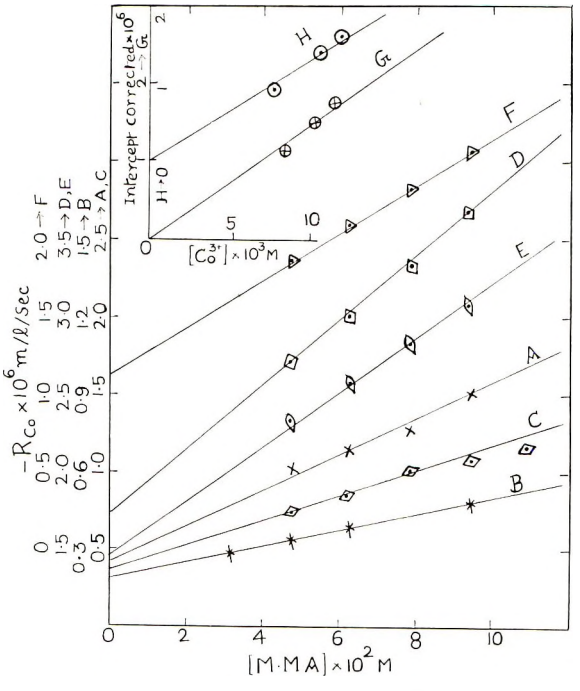

Fig. 1. Variation of $-R_{Co}$ with [MMA] at constant $[H^+]$. (*A*) in H_2SO_4, $[Co^{3+}] = 8.083 \times 10^{-3}M$, $[H^+] = 1.0M$; $\mu = 1.5M$, 20°C.; (*B*) in H_2SO_4, $[Co^{3+}] = 6.489 \times 10^{-3}M$, $[H^+] = 1.0M$, $\mu = 1.5M$, 15°C.; (*C*) in HNO_3, $[Co^{3+}] = 9.554 \times 10^{-3}M$, $[H^+] = 1.0M$, $\mu = 1.2M$, 15°C.; (*D*) in $HClO_4$, $[Co^{3+}] = 12.04 \times 10^{-3}M$, $[H^+] = 1.0M$, $\mu = 1.7M$, 20°C. (*E*) in $HClO_4$, $[Co^{3+}] = 10.68 \times 10^{-3}M$, $[H^+] = 1.0M$, $\mu = 1.7M$, 20°C.; (*F*) in $HClO_4$, $[Co^{3+}] = 8.831 \times 10^{-3}M$, $[H^+] = 1.0M$, $\mu = 1.7M$, 20°C.; (*G*) intercept corrected vs. $[Co^{3+}]$, $HClO_4$ medium, 20°C.; (*H*) intercept corrected vs. $[CO^{+3}]$, HNO_3 medium, 20°C.

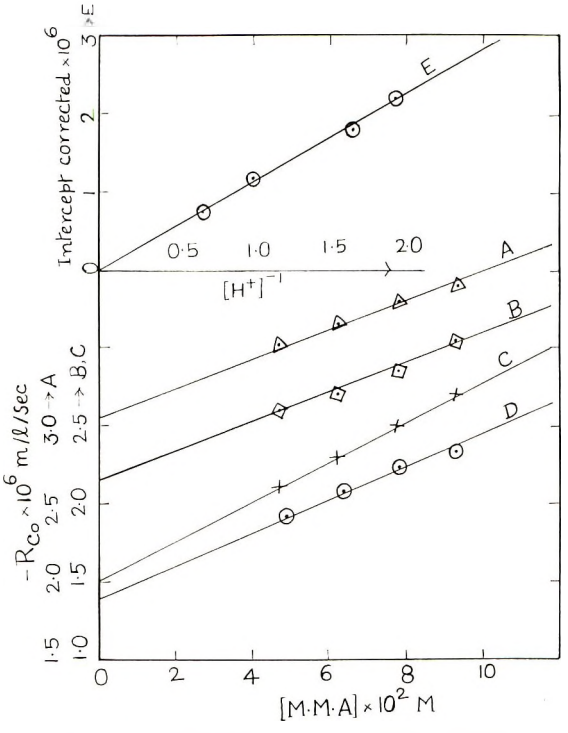

Fig. 2. Variation of $-R_{Co}$ with [MMA] at various [H^+] in $HClO_4$ medium, [Co^{3+}] = $8.5 \times 10^{-3}M$, $\mu = 1.7M$, 20°C.: (*A*) [H^+] = $0.5147M$; (*B*) [H^+] = $0.60M$; (*C*) [H^+] = $1.0M$; (*D*) [H^+] = $1.5M$; (*E*) intercept corrected vs. [H^+]$^{-1}$.

The magnitudes of these intercepts in $HClO_4$ and HNO_3 media were much greater than blank rates, i.e., water oxidation rates under identical conditions in the absence of monomer; in H_2SO_4 medium, however, the intercept corresponded roughly to the blank rate. The blank rate in $HClO_4$ or HNO_3 was 10–15% and in H_2SO_4 it was 30–40% of the total rate. It is evident that in the Co^{3+}–monomer–$HClO_4$ or HNO_3 system, apart from water oxidation reaction, consumption of monomer as an oxidative side reaction also occurs. The nature of this side reaction was found to depend on [Co^{3+}] and $1/[H^+]$ and to be independent of [M]. From plots of $-R_{Co}$ versus [M] at different initial [Co^{3+}], but constant [H^+], the corresponding intercepts were corrected for water oxidation under identical conditions. Similarly corrected intercept values were obtained from plots of $-R_{Co}$ versus [M] at constant [Co^{3+}] but different [H^+] (Fig. 2). Plots of corrected intercept versus [Co^{3+}] at constant [H^+] (Fig. 1*G*, 1*H*) or versus $1/[H^+]$ at constant [Co^{3+}] (Fig. 2*E*) were linear, passing through the origin. Obviously this reaction is independent of [M] and was found to be so experimentally, as found by the constant difference between R_p and $-R_M$ for various concentrations of monomer.

Figure 3 shows the first-order dependence of $-R_{Co}$ on [Co^{3+}]. Deviations from linearity were observed at [Co^{3+}] $\geq 2 \times 10^{-2}M$ in $HClO_4$ and

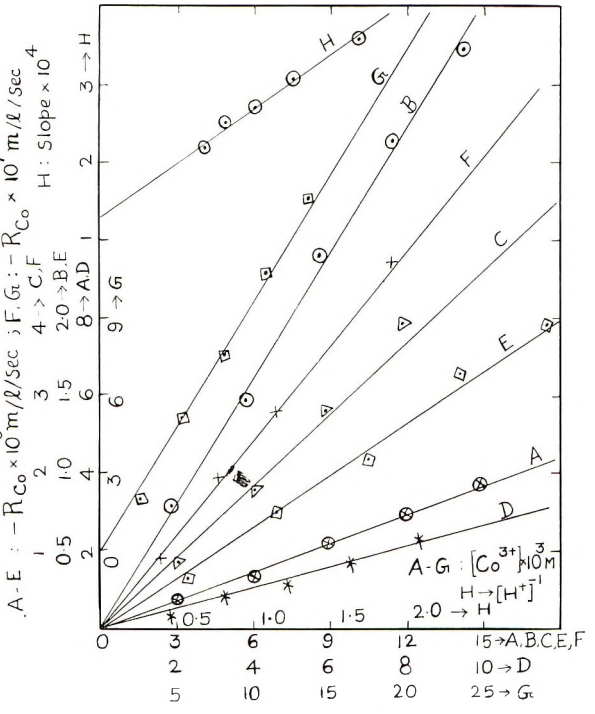

Fig. 3. Variation of $-R_{Co}$ with $[Co^{3+}]$: (*A*) in $HClO_4$, $[H^+] = 1.25M$, $\mu = 1.7M$, $[MMA] = 7.793 \times 10^{-2}M$; 20°C.; (*B*) in $HClO_4$, $[H^+] = 1.0M$, $\mu = 1.7M$, $[MMA] = 7.793 \times 10^{-2}M$, 20°C.; (*C*) in $HClO_4$, $[H^+] = 0.8M$, $\mu = 1.7M$, $[MMA] = 7.793 \times 10^{-2}M$ 20°C.; (*D*) in HNO_3, $[H^+] = 1.0M$; $\mu = 1.2M$, $[MMA] = 9.353 \times 10^{-2}M$, 20°C.; (*E*) in HNO_3, $[H^+] = 1.0M$; $\mu = 1.2M$, $[MMA] = 7.793 \times 10^{-2}M$, 15°C.; (*F*) in H_2SO_4, $[H^+] = 1.0M$, $\mu = 1.5M$; $[MMA] = 7.793 \times 10^{-2}M$, 15°C.; (*G*) in H_2SO_4, $[H^+] = 1.0M$, $\mu = 1.5M$, $[MMA] = 6.234 \times 10^{-2}$ *M*, 20°C.; (*H*) k_{obs} vs. $[H^+]^{-1}$ in $HClO_4$, 20°C.

HNO_3 media. For $[Co^{3+}] < 2 \times 10^{-2}M$, water oxidation was negligible. Our experiments on water oxidation for $[Co^{3+}] = 5 \times 10^{-4}$ to $3 \times 10^{-2}M$ have shown that the rate law for water oxidation is of the form $-R_{Co} = k_w[Co^{3+}]^{1.5}/[H^+]$ in $HClO_4$ and HNO_3 media. The deviation from linearity at higher $[Co^{3+}]$ is therefore due to water oxidation becoming quite significant. In sulfuric acid medium, however, the water oxidation rate, which was significant even at low $[Co^{3+}]$, was subtracted from total $-R_{Co}$ to give corrected $-R_{Co}$, which when plotted against $[Co^{3+}]$ gave a linear plot (Fig. 3*F*, 3*G*).

The influence of $[H^+]$ on $-R_{Co}$ is very interesting. In $HClO_4$ and HNO_3 media, plots of $-R_{Co}$ versus $1/[H^+]$ were linear with substantial intercepts on the y-axis (Fig. 4), indicating the importance of an acid-independent reaction, i.e., Co^{3+} (aq.) was the initiating species. The inverse dependence on $[H^+]$ evidently indicates that the hydrolysis product $CoOH^{2+}$ is involved in the radical production step. The inverse dependence on $[H^+]$ arising from the participation of $CoOH^{2+}$ in reac-

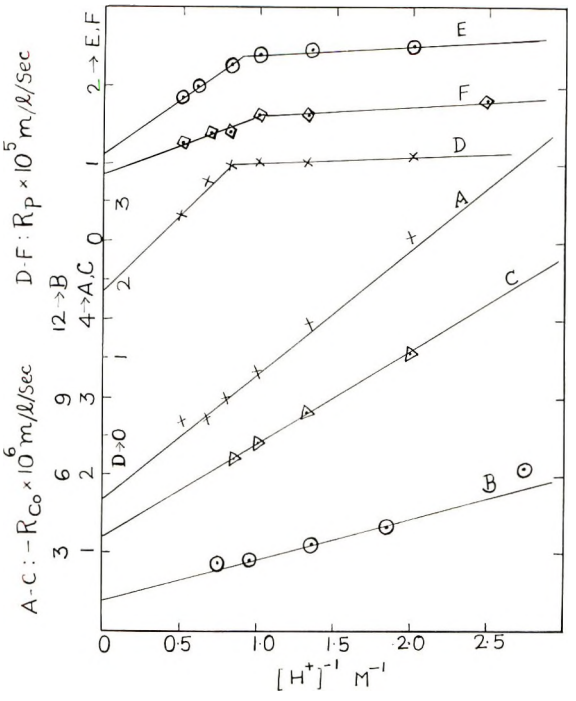

Fig. 4. Variation of $-R_{Co}$ and R_p with $[H^+]$: (*A*) $-R_{Co}$ vs. $[H^+]^{-1}$ in $HClO_4$, $[Co^{3+}] = 9.605 \times 10^{-3}M$, $\mu = 2.1M$, [MMA] = $9.353 \times 10^{-2}M$, 20°C.; (*B*) $-R_{Co}$ vs. $[H^+]^{-1}$ in $HClO_4$, $[Co^{3+}] = 9.824 \times 10^{-3}M$; $\mu = 1.7M$, [MMA] = $9.353 \times 10^{-2}M$, 20°C.; (*C*) $-R_{Co}$ vs. $[H^+]^{-1}$ in HNO_3, $[Co^{3+}] = 9.824 \times 10^{-3}M$, $\mu = 2.1M$, [MMA] = $7.793 \times 10^{-2}M$, 20°C.; (*D*) R_p vs. $[H^+]^{-1}$ in $HClO_4$, conditions same as (*A*); (*E*) R_p vs. $[H^+]^{-1}$ in HNO_3, conditions same as (*C*); (*F*) R_p vs. $[H^+]^{-1}$ in HNO_3, $[Co^{+3}] = 9.824 \times 10^{-3}M$, $\mu = 2.1M$, [MMA] = $7.015 \times 10^{-2}M$, 20°C.

tion sequences has been observed in many oxidation reactions involving cobaltic ions. On the other hand, $-R_{Co}$ values were sensibly constant to changes in $[H^+]$ in sulfuric acid medium which again emphasized the importance of Co^{3+} (aq.) as an initiating species and the inert nature of species such as $CoSO_4^+$, which is preponderant in this medium. Similar conclusions have been drawn by Hoare and Waters[2] in their studies on oxidation of diethyl ketone. Bawn and Sharp's studies[10] on oxidation of olefins also point out to bare Co^{3+} (aq.) ions as the reactive entities in H_2SO_4 medium. The strict inverse dependence on the first power of $[H^+]$ also emphasizes the fact that dimeric species of Co^{3+} are inactive. Further, our experimental conditions were not favorable for the existence of such polynuclear species. The effect of $[H^+]$ on $-R_{Co}$ was also studied by another method. From slopes of a series of plots of $-R_{Co}$ versus $[Co^{3+}]$ at constant [M] but different $[H^+]$ a series of k_{obs} values at different $[H^+]$ were obtained. k_{obs} was found to vary linearly with $1/[H^+]$ (Fig. 3).

Addition of salts such as $NaClO_4$ in $HClO_4$, $NaNO_3$ in HNO_3, and sodium or potassium bisulfate in H_2SO_4 did not have considerable influence on

$-R_{Co}$; the rates increased only 5–10% for a fivefold increase in ionic strength μ. The possibility of any nitrate ion pairs of Co^{3+} being the active species in HNO_3 and the species $CoSO_4^+$ and other sulfate complexes in H_2SO_4 is therefore to be excluded.

Initially added cobaltous ions did not affect the reaction rates, thus indicating the absence of any Co^{3+}/Co^{2+} equilibrium in the radical production steps.

Variation of R_p

R_p values were strictly proportional to $[M]^2$ (Fig. 5) in all three acid media. This emphasizes the importance of linear termination in preference to the normal mode of mutual combination of the macroradicals. The

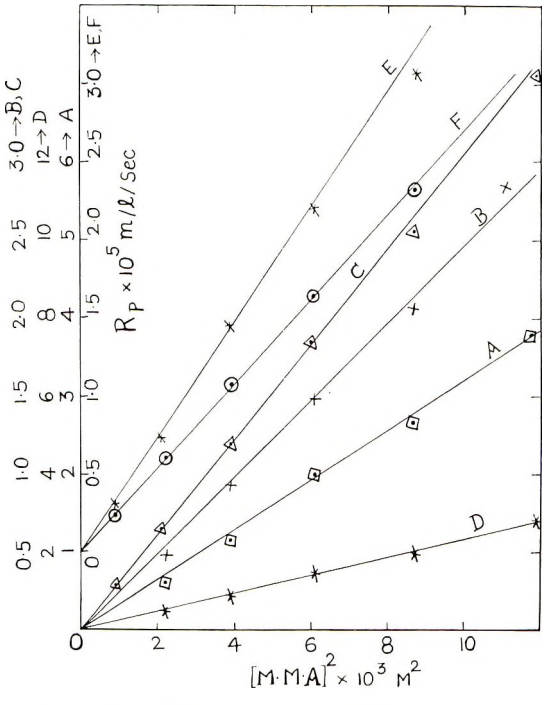

Fig. 5. Variation of R_p with $[MMA]^2$ at μ = 1.5–1.7M; $[Co^{3+}] \approx 1 \times 10^{-4}M$, $[H^+]$ = 1.0M: (A) in $HClO_4$, 20°C.; (B) in $HClO_4$, 15°C.; (C) in HNO_3, 20°C.; (D) in HNO_3, 15°C.; (E) in H_2SO_4, 20°C.; (F) in H_2SO_4, 15°C.

discrepancies observed between the water oxidation rates and the intercepts in $-R_{Co}$ versus [M] plots in $HClO_4$ and HNO_3 media, leading to the conclusion of monomer oxidation, necessitated the evaluation of $-R_M$ and R_p. It was found that $-R_M > R_p$ and that $-R_M - R_p$ was practically constant and independent of [M] which proved the correctness of the earlier assumptions with regard to existence of side monomer oxidation

and the rate of the latter being independent of [M]. It is however to be emphasized that the rate of monomer oxidation is significant for $-R_{Co}$ values but insignificant for R_p values. In sulfuric acid medium, $R_p \approx -R_M$ indicating the absence of any such monomer oxidation reaction, which supports the earlier conclusion drawn from $-R_{Co}$ versus [M] plots in which the intercepts were equivalent to the blank rates. Bawn and Sharp[10] in their studies on oxidation of olefins by cobaltic ions in H_2SO_4 have also established the fact that the rates of oxidations of olefins are independent of [olefin] but directly proportional to $[Co^{3+}]$.

R_p values were independent of $[Co^{3+}]$, which again indicates preferential linear termination. Termination by metal ions in the case of other monomers, i.e., acrylonitrile,[24-31] acrylamide,[32-36] styrene,[30,31] has been very well established, both in aqueous and nonaqueous media. MMA has been found to be susceptible to oxidative linear termination by Ce^{+4} [29] and Cu^{+}, [37] and it is quite likely that in this system also Co^{3+} ions terminate the polymer chains.

The effect of $[H^+]$ on R_p in the three acid media offered contrasting results. In H_2SO_4 medium, the rates were independent of $[H^+]$. If initiation and termination involved like species such as Co^{3+} (aq.) or $CoSO_4^+$ or $CoOH^{2+}$, R_p would be independent of $[H^+]$ in all cases; on the other hand, $-R_{Co}$ would be independent of $[H^+]$ for Co^{3+} (aq.) and inversely proportional to $[H^+]$ for $CoSO_4^+$ or $CoOH^{2+}$ species. Our experimental results conform to Co^{3+} (aq.) being initiator and terminator in H_2SO_4 medium. In $HClO_4$ and HNO_3 media, R_p versus $1/[H^+]$ plots are flat at lower acidities and linear at higher acidities with intercepts on the y-axis (Fig. 4). The flat nature of the plots is explicable on the basis of either Co^{3+} or $CoOH^{2+}$ acting as initiators as well as terminators. The possibility of Co^{3+} (aq.) may be excluded, since in this region of $[H^+]$, $-R_{Co}$ still varied as $1/[H^+]$, suggesting the ion pair $CoOH^{2+}$ as the active species at lower acidities. This is understandable since the effective concentration of $[CoOH^{2+}]$ will be greater at lower acidities. The linear portion of the plot at higher acidity may arise if initiation is by $CoOH^{2+}$ and termination is by Co^{3+}. The intercept of R_p versus $1/[H^+]$ plot evidently corresponds to an acid-independent reaction path involving Co^{3+} (aq.) ions both as initiators and terminators. Therefore in $HClO_4$ and HNO_3 medium, Co^{3+} (aq.) and $CoOH^{2+}$ appear to initiate and terminate the chains.

R_p values were found to be slightly increased ($\sim 10\%$) with a fivefold increase in the ionic strength of the medium.

Initially added Co^{2+} ions had no effect on R_p values.

Chain Lengths n

Figure 6 shows the direct dependence of n on [M] and inverse dependence on $[Co^{3+}]$ in all the three acid media. n values were found to be unaffected by acidity and ionic strength in all cases.

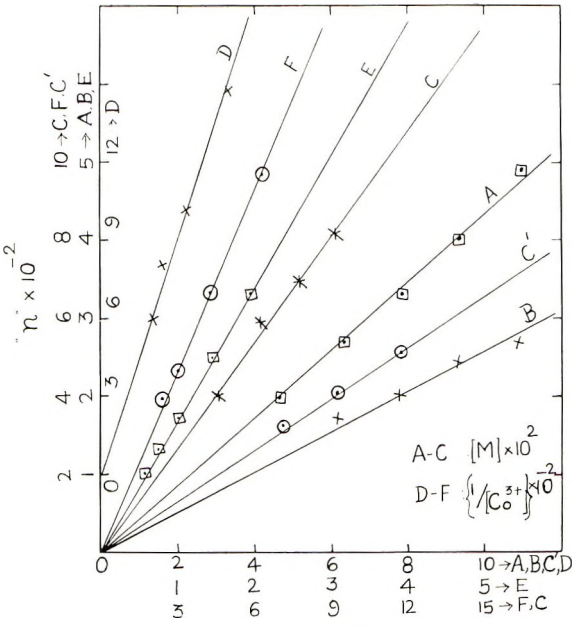

Fig. 6. Variation of chain length n with [MMA] and $[Co^{3+}]$: (*A*) n vs. [MMA] in $HClO_4$, $[Co^{3+}] = 9.4 \times 10^{-3}M$, $[H^+] = 1.0M$, $\mu = 1.5M$, 15°C.; (*B*) n vs. [MMA] in HNO_3, $[Co^{3+}]$: $12.28 \times 10^{-3}M$, $[H^+] = 1.0M$, $\mu = 1.2M$, 20°C.; (*C*) n vs. [MMA] in H_2SO_4, $[Co^{3+}] = 4.7 \times 10^{-3}M$, $[H^+] = 1.0M$, $\mu = 1.5M$, 15°C.; (*C'*) n vs. [MMA] in H_2SO_4, $[Co^{3+}] = 3.2 \times 10^{-3}M$, $[H^+] = 1.0M$, $\mu = 1.5M$, 20°C.; (*D*) n vs. $[Co^{+3}]^{-1}$ in $HClO_4$, [MMA] = $9.35 \times 10^{-2}M$, $[H^+] = 1.0M$, $\mu = 1.2M$, 15°C.; (*E*) n vs. $[Co^{+3}]^{-1}$ in HNO_3, [MMA] = $7.793 \times 10^{-2}M$, $[H^+] = 1.0M$, $\mu = 1.2M$, 20°C.; (*F*) n vs. $(Co^{+3}]^{-1}$ in H_2SO_4, [MMA] = $6.234 \times 10^{-2}M$, $[H^+]$: $1.0M$, $\mu = 1.5M$, 15°C.

Kinetic Scheme

The foregoing experimental results may be explained on the basis of the following sequence of reactions.

Radical production steps:

$$Co^{3+} + M \xrightarrow{k_{r1}} Co^{2+} + R\cdot$$

$$CoOH^{2+} + M \xrightarrow{k_{r2}} Co^{2+} + OH^- + R\cdot$$

Initiation step:

$$R\cdot + M \xrightarrow{k_i} R - M\cdot$$

Propagation step:

$$R - M\cdot + M \xrightarrow{k_p} R - M - M\cdot$$

$$R - M - M\cdot + M \xrightarrow{k_p} R - M - M - M\cdot$$

Termination step (linear):

$$R - M_n\cdot + Co^{3} \xrightarrow{k_{t1}} Co^{2+} + H^+ + P$$

$$R - M_n\cdot + CoOH^{2+} \xrightarrow{k_{t2}} Co^{2+} + OH^- + H^+ + P$$ (at lower acidities)

Assuming the stationary-state kinetics for R· and R $-$ M_n· and that k_p, k_t, etc. are independent of chain length, the following rate laws for R_p and $-R_{Co}$ may be arrived at.

In $HClO_4$ and HNO_3 media

$$-R_{Co} = 2\left(k_{r1} + \frac{K_1 k_{r2}}{[H^+]}\right)[Co^{3+}][M] + \frac{k_m[Co^{3+}]}{[H^+]} + \frac{k_w[Co^{3+}]^{1.5}}{[H^+]} \quad (1)$$

if

$$Co^{3+} + H_2O \overset{K_1}{\rightleftharpoons} CoOH^{2+} + H^+$$

The first term on the right-hand side of eq. (1) represents cobaltic ion consumption in radical production; the second and the third terms represent monomer and water oxidation rates, respectively.

$$R_p = k_p/k_{t1}(k_{r1} + K_1 k_{r2}/[H^+])[M]^2 \quad (2)$$

$$n = k_p[M]/k_{t1}[Co^{3+}] \quad (3)$$

At lower acidities, initiation and termination involves $CoOH^{2+}$, and under these circumstances

$$R_p = (k_p/k_{t2})k_{t2}[M]^2 \quad (4)$$

In H_2SO_4 medium where Co^{3+} (aq.) ions initiate as well as terminate, the rate laws are

$$-R_{Co} = 2k_{r1}[Co^{3+}][M] + k_w[Co^{3+}]^{1.5 \text{ or } 2}/[H^+] \quad (5)$$

The second term on the right-hand side of eq. (5) represents water oxidation rate; $[Co^{3+}]^{1.5}$ at $[Co^{3+}]$: $\leq 4 \times 10^{-3}M$ and $[Co^{3+}]^2$ at $[Co^{3+}] > 4 \times 10^{-3}M$·

$$R_p = (k_{r1}k_p/k_{t1})[M]^2 \quad (6)$$

and the expression for n is given by eq. (3).

Water oxidation parts of rate laws in eqs. (1) and (5) were arrived at by systematic studies on water oxidation carried out under identical conditions.

The conclusions drawn regarding the nature of active species in HNO_3 and H_2SO_4 media were further supported by a study of the effect of addition of NO_3^-, HSO_4^-, and $SO_4^=$ on the reaction rates in $HClO_4$ medium at constant ionic strength, sodium perchlorate being used for the latter purpose. Nitrate ions did not affect $-R_{Co}$ as well as R_p. The rates with regard to various variables were similar to those in the absence of nitrate ions, and therefore the active species are the same as in $HClO_4$ and $Co^{3+}.NO_3^-$ complex, if formed, does not seem to be effective. On the other hand, $-R_{Co}$ values decreased with addition of HSO_4^- or $SO_4^=$ to the system, while R_p values were unaffected. This may be understood if it is remembered that in $HClO_4$, R_p values are independent of the initiator concentration while $-R_{Co}$ values depend on the latter. The decrease of the initiator concentration by complexing with HSO_4^- or $SO_4^=$ therefore

does not affect R_p. On the other hand, addition of HSO_4^- or $SO_4^=$ decreases the effective $[Co^{3+}]$ and $[CoOH^{2+}]$ (by complexing) and therefore would decrease the $-R_{Co}$ values. This clearly proves that sulfate complexes are not involved in radical production steps. Another interesting aspect was that $-R_{Co}$ and R_p were independent of $[H^+]$ in the presence of HSO_4^- and $SO_4^=$. This is to be understood again in terms of depletion of $[CoOH^{2+}]$ due to the formation of sulfate complexes resulting in Co^{3+} becoming the active entities as observed in H_2SO_4 medium.

Evaluation of Rate Constants

From slopes of plots of $-R_{Co}$ versus $[M]$, values of $(k_{r1} + K_1k_{r2}/[H^+])$ in $HClO_4$ and HNO_3 media and k_{r1} in H_2SO_4 medium were evaluated.

Slopes of plots of intercept (corrected) versus $[Co^{3+}]$ at constant $[H^+]$ or versus $1/[H^+]$ at constant $[Co^{3+}]$ in $HClO_4$ and HNO_3 media yield $k_m/[H^+]$ or $k_m[Co^{3+}]$, and hence k_m was evaluated.

k_{r1} in $HClO_4$ and HNO_3 media was evaluated from intercepts of plots of $-R_{Co}$ versus $1/[H^+]$ or k_{obs} versus $1/[H^+]$.

From R_p versus $[M]^2$ plots, the terms $(k_p/k_{t1})(k_{r1} + K_1k_{r2}/[H^+])$ in $HClO_4$ or HNO_3 or $k_{r1}k_p/k_{t1}$ in H_2SO_4 were evaluated, and hence k_p/k_{t1} values in the three acid media evaluated with known values of k_{r1}, k_{r2}, K_1, etc.[12]

From experiments conducted at 15 and 20°C., $E\,k_{r1} = 20.18$ kcal./mole in $HClO_4$ and 33.66 kcal./mole in H_2SO_4; $E\,k_p/k_{t1} = -16.8$ kcal./mole in HNO_3 and -22.5 kcal./mole in H_2SO_4 were evaluated. ($E\,k_{r1}$ = energy of activation for the radical propagation step and $E\,k_p/k_{r1}$ = difference in activation energies of the propagation and termination reactions.)

From slopes of plots of $-R_{Co}$ versus $[Co^{3+}]$ in H_2SO_4 medium, k_{r1} can be evaluated, while in $HClO_4$ and HNO_3 medium the slope will be a composite term comprising of the rate constants k_{r1}, k_{r2}, and k_m. The very good agreement between k_{r1} values evaluated from $-R_{Co}$ versus $[M]$ as well as $-R_{Co}$ versus $[Co^{3+}]$ plots in H_2SO_4 medium strongly supported the absence of oxidation of monomer in this medium.

From the values of k_{r1} and $k_{r1} + (K_1k_{r2}/[H^+])$ in $HClO_4$ and HNO_3 media it was evident that they were of the same order. This is possible only if $k_{r1} \approx k_{r2}$, in which case, since K_1 is of the order 10^{-2},[12] the term K_1k_{r2} becomes insignificant in comparison with k_{r1}. Therefore k_{r2} cannot be evaluated accurately from $(k_{r1} + (K_1k_{r2}/[H^+]))$. For similar reasons, k_{r2} could not be evaluated from $(K_1k_{r2}[M] + k_m)[Co^{3+}]$, if $k_m \approx k_{r2}$. The validity of the reaction mechanism involving two initiators in $HClO_4$ and HNO_3 media was substantiated by the agreement of the experimental slopes of $-R_{Co}$ versus $[Co^{3+}]$ plots with the calculated values, the latter having been obtained from $k_{r1} + K_1k_{r2}/[H^+]$ and k_m. All the rate parameters are listed in Table I.

k_p/k_{t1} values evaluated from plots of n versus $[M]$ or $1/[Co^{3+}]$ were invariably greater than those from R_p versus $[M]^2$ plots. n values were in the range 50–900 only, and such short chain lengths introduce errors in

TABLE I

Medium	Temp., °C.	$k_{r1} \times 10^4$ l./mole-sec.[a]	$k_m \times 10^{4a}$	$(2k_{r2}K_1[M] + k_m) \times 10^4$	$\left(k_{r1} + \frac{K_1k_{r2}}{[H^+]}\right) \times 10^4$	k_p/k_{t1}	$2\left(k_{r1} + \frac{K_1k_{r2}}{[H^+]}\right)[M] + \frac{k_m}{[H^+]} \times 10^4$ Exptl.	Calc.
H_2SO_4	15	2.63				10.43		
	20	7.35				5.34		
$HClO_4$	15				5.93	4.22	2.93	2.94
	20	8.39	1.342	1.4	8.53	3.79		
	25				10.64	4.34		
HNO_3	15				4.22	5.57	2.66[b]	2.535
	20	7.91	1.285	1.187	8.03	3.83		
							2.69[c]	2.78

[a] Average value from both methods mentioned in text.
[b] At $[H^+] = 1.5M$ at 20°C.
[c] At $[H^+] = 1.0M$ at 20°C.

the viscometric methods of computing the same. The observed discrepancy in $k_p/k_{t^{\frac{1}{2}}}$ values is most probably due to this factor as well as the heterogeneous nature of the polymer.

Baxendale and Wells[20] have remarked that probably OH radicals formed during water oxidation are responsible for polymerization. Experimental results reported in this paper do not fit in with such a scheme, however. Under conditions of initiation by OH, deviations from strict proportionality of R_p versus $[M]^2$, $-R_{Co}$ versus $[M]$, etc. should have been envisaged. Further, infrared spectra of polymers prepared by Co^{3+} initiation revealed the absence of a peak corresponding to an OH· group. Norrish and Edgecombe[38] reported the interesting observation of the presence of Ce in their polymer [poly(methyl acrylate) and polyacrylonitrile] samples obtained from Ce^{4+} initiation. In the case of cobaltic-initiated polymers, ignition of PMMA was devoid of any residue. Further, acidic extract after ignition showed no green coloration on addition of excess HCO_3^- and H_2O_2, indicating the absence of Co in the polymer.

One of us (K. J.) is thankful to the Ministry of Education, Government of India and to the University Grants commission for the award of Research Scholarship and Junior Research Fellowship, respectively, during the tenure of which this work was completed.

References

1. Hoare, D. G., and W. A. Waters, *J. Chem. Soc.*, **1962**, 965.
2. Hoare, D. G., and W. A. Waters, *J. Chem. Soc.*, **1962**, 971.
3. Cooper, T. A., and W. A. Waters, *J. Chem. Soc.*, **1964**, 1538.
4. Hoare, D. G., and W. A. Waters, *J. Chem. Soc.*, **1964**, 2552, 2560.
5. Waters, W. A., and J. Kemp, *Proc. Roy. Soc. (London)*, **A274**, 480 (1963).
6. Bawn, C. E. H., and A. G. White, *J. Chem. Soc.*, **1951**, 331.
7. Bawn, C. E. H., and A. G. White, *J. Chem. Soc.*, **1951**, 339.
8. Bawn, C. E. H., and A. G. White, *J. Chem. Soc.*, **1951**, 343.
9. Bawn, C. E. H., *Discussions Faraday Soc.*, **No. 14**, 181 (1953).
10. Bawn, C. E. H., and J. A. Sharp, *J. Chem. Soc.*, **1957**, 1856, 1866.
11. Bawn, C. E. H., and J. E. Jolley, *Proc. Roy. Soc. (London)*, **A237**, 297 (1957).
12. Sutcliffe, L. H., and J. R. Weber, *Trans. Faraday Soc.*, **52**, 1225 (1956).
13. Sutcliffe, L. H., and J. R. Weber, *Trans. Faraday Soc.*, **55**, 1892 (1959).
14. Sutcliffe, L. H., and J. R. Weber, *Trans. Faraday Soc.*, **57**, 91 (1961).
15. Hargreaves, G., and L. H. Sutcliffe, *Trans. Faraday Soc.*, **51**, 786 (1955).
16. Kirwin, J. B., F. D. Peat, P. J. Proll, and L. H. Sutcliffe, *J. Phys. Chem.*, **67**, 2288 (1963).
17. Ashurst, K. G., and W. C. E. Higginson, *J. Chem. Soc.*, **1956**, 343.
18. Rosseinsky, D. R., and W. C. E. Higginson, *J. Chem. Soc.*, **1960**, 31.
19. Sutcliffe, L. H., and J. R. Weber, *J. Inorg. Nuclear Chem.*, **12**, 281 (1960).
20. Baxendale, J. H., and C. F. Wells, *Trans. Faraday Soc.*, **53**, 800 (1957).
21. Swann, S., and T. Xanthakos, *J. Am. Chem. Soc.*, **53**, 400 (1931).
22. Latinen, H. A., and L. W. Burdett, *Anal. Chem.*, **23A**, 1268 (1951).
23. Baxendale, J. H., S. Bywater, and M. G. Evans, *J. Polymer Sci.*, **1**, 237 (1946).
24. Dainton, F. S., and P. H. Seaman, *J. Polymer Sci.*, **39**, 279 (1959).
25. Watanabe, M., and H. Kiuchi, *J. Polymer Sci.*, **58**, 103 (1962).
26. Bengough, W. I., S. A. Macintosh, and I. C. Ross, *Nature*, **200**, 567 (1963).
27. Katai, A. A., V. K. Kulshreshtha, and R. H. Marchessault, *J. Polymer Sci. C*, **2**, 403 (1963).

28. Bamford, C. H., A. D. Jenkins, and R. Johnston, *Trans. Faraday Soc.*, **58,** 1212 (1962).
29. Ananthanarayanan, V. S., and M. Santappa, *Indian J. Chem.*, **2,** 330 (1964).
30. Bamford, C. H., A. D. Jenkins, and R. Johnston, *Nature*, **177,** 992 (1956).
31. Bamford, C. H., A. D. Jenkins, and R. Johnston, *Proc. Roy. Soc. (London)*, **A239,** 214 (1957).
32. Mino, G., S. Kaizerman, and E. Rasmussen, *J. Polymer Sci.*, **38,** 393 (1959).
33. Collinson, E., F. S. Dainton, and G. S. McNaughton, *Trans. Faraday Soc.*, **53,** 489 (1957).
34. Collinson, E., and F. S. Dainton, *Nature*, **177,** 1224 (1956).
35. Collinson, E., F. S. Dainton, D. R. Smith, G. J. Trudel, and (in part) S. Tazuke, *Discussions Faraday Soc.*, **No. 29,** 188 (1960).
36. Collinson, E., F. S. Dainton, B. Mile, S. Tazuke, and D. R. Smith, *Nature*, **198,** 26 (1963).
37. Menon, C. C., and S. L. Kapur, *J. Polymer Sci.*, **54,** 45 (1961).
38. Norrish, R. G. W., and F. H. C. Edgecombe, *Nature*, **197,** 282 (1963).

Résumé

On a étudié la polymérisation du méthacrylate de méthyle, initiée par les ions cobaltiques, dans les acides perchloriques, nitriques et sulfuriques, dans un domaine de température compris entre 15 et 25°C. Dans ces trois acides, il existe une réaction secondaire d'oxydation de l'eau. De plus une complication supplémentaire due á l'oxydation du monomère se produit dans les acides perchloriques et nitriques. On a mesuré la variation de la vitesse de disparition des ions cobaltiques et du monomère ainsi que la variation de la longueur des chaînes polymériques en fonction de la concentration en monomère, en ion cobaltique Co^{3+}, en ion H^+, en ion cobalteux Co^{+2} ajoutés initialement et en fonction de la température etc . . . Dans les acides perchloriques et nitriques, les résultats expérimentaux font supposer une initiation simultaneé par les ions Co^{+3} et $CoOH^{+2}$ tandis qu'en milieu sulfurique la seule espèce active serait Co^{+3}. Un schéma cinétique permettant de rendre compte des résultats expérimentaux a été proposé et les différentes constantes de vitesses ont été calculées.

Zusammenfassung

Die Polymerisation von Methylmethacrylat wurde bei Anregung mit Co^{3+} Ionen in Perchlor-, Salpeter- und Schwefelsäure im Temperaturbereich von 15–25°C untersucht. In allen drei Säuren trat als Nebenreaktion die Oxydation des Wassers auf. In $HClO_4$ und HNO_3 trat eine zusätzliche Komplikation durch die Monomeroxydation auf. Die Geschwindigkeit des Verbrauchs des Co^{3+}-Ions und des Monomeren, sowie die Kettenlänge der Polymeren wurde bei Variation von [M], $[Co^{3+}]$, $[H^+]$, anfänglich zugesetztem $[Co^{2+}]$, Temperatur etc. gemessen. In $HClO_4$ und HNO_3 sprechen die Versuchsergebnisse für einen gleichzeitigen Start durch Co^{3+} und $CoOH^{2+}$, während in H_2SO_4 nur die Co^{3+}-Ionen wirksam sind. Ein zur Erklärung aller Versuchsergebnisse geeignetes kinetisches Schema wurde aufgestellt und die verschiedenen Geschwindigkeitskonstanten ermittelt.

Received June 14, 1965
Prod. No. 4830A

JOURNAL OF POLYMER SCIENCE: PART A-1 VOL. 4, 393–406 (1966)

Vinyl Polymerization by Cobaltic Ions in Aqueous Solution. Part II. Polymerization of Acrylonitrile and Methyl Acrylate

K. JIJIE, M. SANTAPPA, and V. MAHADEVAN, *University Department of Physical Chemistry, Alagappa Chettiar College, Madras, India*

Synopsis

Polymerization of methyl acrylate in $HClO_4$ and HNO_3 was studied in the temperature range 10–15°C. The kinetics of the polymerization were found to be very simple, involving initiation and termination by cobaltic ions. Kinetic studies on polymerization of acrylonitrile in $HClO_4$ and HNO_3 revealed that water oxidation, and monomer oxidation were side reactions as in the case of methyl methacrylate. Experimental evidence favored the simultaneous initiation by Co^{3+} and $CoOH^{2+}$ species. In H_2SO_4, certain unusual features were encountered. At low $[Co^{3+}]$, linear termination as well as termination by mutual combination occurred. Another interesting aspect was that $CoSO_4^+$ initiated at low $[Co^{3+}]$. This was unlike the case of other monomers in H_2SO_4. The rates of polymerization and rates of cobaltic ion disappearance were measured with respect to changes in [M], $[Co^{3+}]$, $[H^+]$, temperature, etc. The various rate constants were evaluated.

In the preceding paper[1] we reported the results of a study on kinetics of polymerization of methyl methacrylate by cobaltic ions in aqueous perchloric, throughout nitric, and sulfuric acid media. Results on polymerization of acrylonitrile (AN) and methyl acrylate (MA) monomers with the same initiator system are now presented. The behavior of AN in $HClO_4$ and HNO_3 is similar to that of methyl methacrylate (MMA) in the same media, but in H_2SO_4 contrasting results are obtained. Kinetics of MA polymerization in $HClO_4$ and HNO_3 closely resemble that of MMA polymerization in H_2SO_4.

EXPERIMENTAL

Acrylonitrile (American Cyanamid or Eastman Kodak product) was freed from inhibitor by washing with 5% alkali followed by 10% orthophosphoric acid, washed well with water, dried over anhydrous calcium chloride, and distilled under reduced pressure. The middle fraction was stored at 5°C. and used for the experiments.

Methyl acrylate (Light & Co.) was freed from inhibitor by repeated washing with alkali, washed with water, dried over anhydrous sodium sulfate, and distilled under vacuum.

Reagents, estimations and kinetic measurements were as described in Part I.[1] Chain lengths of poly(methyl acrylate) were obtained from the equations of Sen et al.[2] and Fuhrman and Mesrobian:[3]

In benzene at 35°C.:

$$[\eta] = 1.282 \times 10^{-4}[M]^{0.7143}$$

In acetone at 20°C.:

$$n = 11.2[\eta \times 100]^{1.22}$$

RESULTS AND DISCUSSION

Polymerization of MA was rapid even at 10°C. with very high conversions in about 15 minutes. Consequently experiments were carried out in the temperature range 10–15°C. and reaction times were restricted to 7–10 min. Steady-state rates were found to be attained within 2 min. Acrylonitrile appeared to be an ideal monomer in the sense that steady state was attained in about 5 min., the conversion not exceeding 20% even after 30–40 minutes. In contrast to MA, polymerization of AN

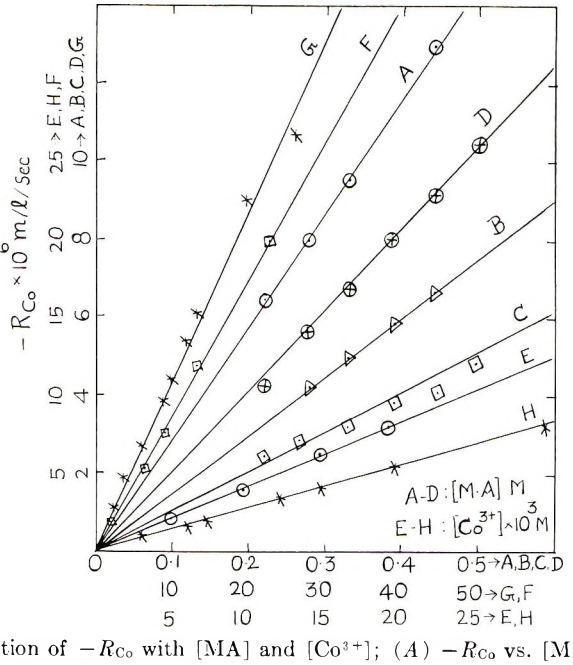

Fig. 1. Variation of $-R_{Co}$ with [MA] and $[Co^{3+}]$; (*A*) $-R_{Co}$ vs. [MA], in $HClO_4$, $[Co^{3+}] = 9.961 \times 10^{-3}M$, $\mu = 1.2M$, $[H^+] = 1.0M$, 15°C.; (*B*) $-R_{Co}$ vs. [MA], in $HClO_4$, $[Co^{3+}] = 10.13 \times 10^{-3}M$, $\mu = 1.2M$, $[H^+] = 1.0M$, 10°C.; (*C*) $-R_{Co}$ vs. [MA], in HNO_3, $[Co^{3+}] = 11.33 \times 10^{-3}M$, $\mu = 1.2M$, $[H^+] = 1.0M$, 10°C.; (*D*) $-R_{Co}$ vs. [MA], in HNO_3, $[Co^{3+}] = 10.58 \times 10^{-3}M$, $\mu = 1.2M$ $[H^+] = 1.0M$, 15°C.; (*E*) $-R_{Co}$ vs. $[Co^{+3}]$, in $HClO_4$, [MA] = 0.276*M*, $[H^+] = 1.5M$, $\mu = 2.0M$, 10°C.; (*F*) $-R_{Co}$ vs. $[Co^{+3}]$, in $HClO_4$, [MA] = 0.276*M*, $[H^+] = 1.5M$, H^+; $\mu = 2.0M$, 15°C.; (*G*) $-R_{Co}$ vs. $[Co^{+3}]$, in HNO_3, [MA] = 0.2214*M*; $[H^+] = 1.2M$, $\mu = 1.5M$, 15°C.; (*H*) $-R_{Co}$ vs. $[Co^{+3}]$, in HNO_3, [MA] = 0.2214*M*; $[H^+] = 1.2M$; $\mu = 1.5M$, 10°C.

proceeded at a much lesser rate. A disparity in $-R_{Co}$ values between degassing by nitrogen and deaeration under high vacuum (using liquid air) was observed, the latter method yielding larger rates due to reasons discussed in Part I for MMA. However R_p values were the same by both methods of degassing. Deaeration by nitrogen only was adopted in all experiments.

Rates of Cobaltic Ion Disappearance $-R_{Co}$

A linear variation of $-R_{Co}$ with [M] (Figs. 1 and 2) was observed with MA as well as AN. In the case of MA., the plots do not have any intercepts (Fig. 1) on the y-axis, thus emphasizing the absence of monomer oxidation reaction. The behavior of AN in $HClO_4$ and HNO_3 media, on the other hand, was similar to that of MMA discussed in Part I. The disparity in the magnitudes of intercepts on the y-axis and water oxidation rates under the same conditions suggested the oxidation of monomer as a side reaction. In sulfuric acid medium at low $[Co^{3+}]$, ($\leq 5 \times 10^{-3}M$), the intercepts corresponded to blank rates; at high $[Co^{3+}]$, ($> 5 \times 10^{-3}M$),

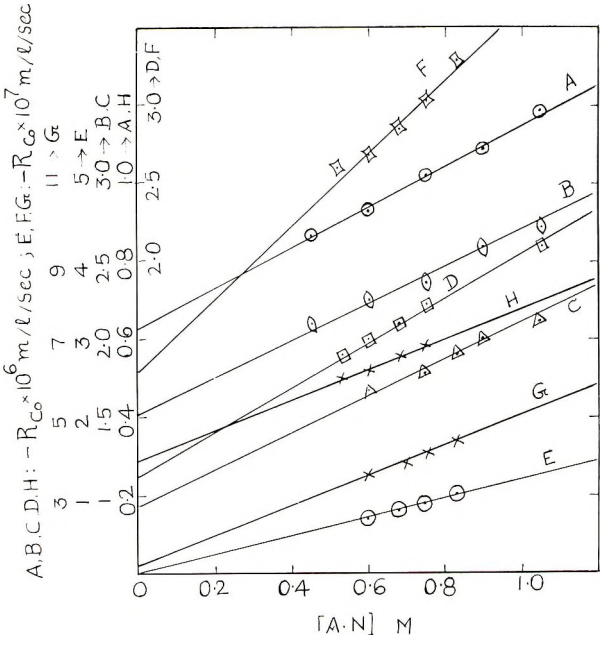

Fig. 2. Variation of $-R_{Co}$ with [AN] = (A) in $HClO_4$, $[Co^{+3}] = 9.465 \times 10^{-3}M$, $[H^+] = 1.0M$, $\mu = 1.08M$, 15°C.; (B) in $HClO_4$, $[Co^{+3}] = 9.738 \times 10^{-3}M$, $[H^+] = 1.0M$, $\mu = 1.08M$, 20°C.; (C) in HNO_3, $[Co^{+3}] = 15.41 \times 10^{-3}M$, $[H^+] = 1.0M$, $\mu = 1.2M$, 15°C.; (D) in HNO_3, $[Co^{+3}] = 10.19 \times 10^{-3}M$, $[H^+] = 1.0M$, $\mu = 1.2M$, 20°C.; (E) in H_2SO_4, $[Co^{+3}] = 1.654 \times 10^{-3}M$, $[H^+] = 1.0M$, $\mu = 1.5M$, 20°C.; (F) in H_2SO_4, $[Co^{+3}] = 3.721 \times 10^{-3}M$, $[H^+] = 1.0M$; $\mu = 1.5M$; 20°C.; (G) in H_2SO_4, $[Co^{3+}] = 7.3 \times 10^{-3}M$; $[H^+] = 1.0M$, $\mu = 1.5M$, 20°C.; (H) in H_2SO_4, $[Co^{3+}] = 8.923 \times 10^{-3}M$, $[H^+] = 1.0M$, $\mu = 1.5M$, 20°C.

discrepancies were observed, probably due to monomer being consumed in side reactions as in perchloric and nitric acid media.

Variation of $-R_{Co}$ with $[Co^{3+}]$ offered conflicting results. A first-order dependence of $-R_{Co}$ on $[Co^{3+}]$ was observed for AN as well as MA in perchloric and nitric acid media (Figs. 1, 3, and 4). In the case of AN, at higher concentrations of $[Co^{3+}]$ ($> 2 \times 10^{-2}M$) in $HClO_4$ and HNO_3, deviations from linearity occurred, probably due to water oxidation becoming significant. In H_2SO_4 with AN, the order with respect to $[Co^{3+}]$

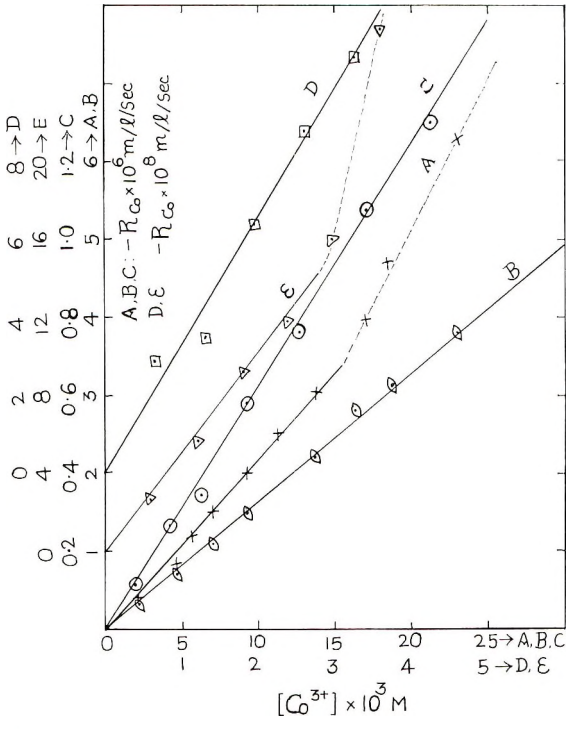

Fig. 3. Variation of $-R_{Co}$ with $[Co^{3+}]$: (A) in $HClO_4$, [AN] = 0.7539M, $[H^+]$ = 1.5M, μ = 2.0M, 20°C.; (B) in HNO_3, [AN] = 0.7539M, $[H^+]$ = 1.5M; μ = 2.0M, 20°C.; (C) in HNO_3, [AN] = 0.7539M, $[H^+]$ = 1.5M; μ = 2.0M, 15°C.; (D) in H_2SO_4, [AN] = 0.4523M, $[H^+]$ = 1.0M, μ = 1.5M, 20°C.; (E) in H_2SO_4, [AN] = 0.7539M, $[H^+]$ = 1.0M, μ = 1.5M, 20°C.

seemed to depend very much on $[Co^{3+}]$. For concentrations of $[Co^{3+}]$ of approximately 5×10^{-4}–$4 \times 10^{-3}M$, a linear variation of $-R_{Co}$ with $[Co^{3+}]$ was observed (Fig. 3); for higher concentrations an order of 1.4–1.6 was obtained. This variable order may arise from the following possibilities. At higher concentrations monomer oxidation rate may have an order with respect to $[Co^{3+}]$ greater than unity. It is also possible that dimers of Co^{3+} which lead to higher orders for the latter may participate in radical production step. The high solubility of AN in water compared to other monomers may facilitate both these possibilities.

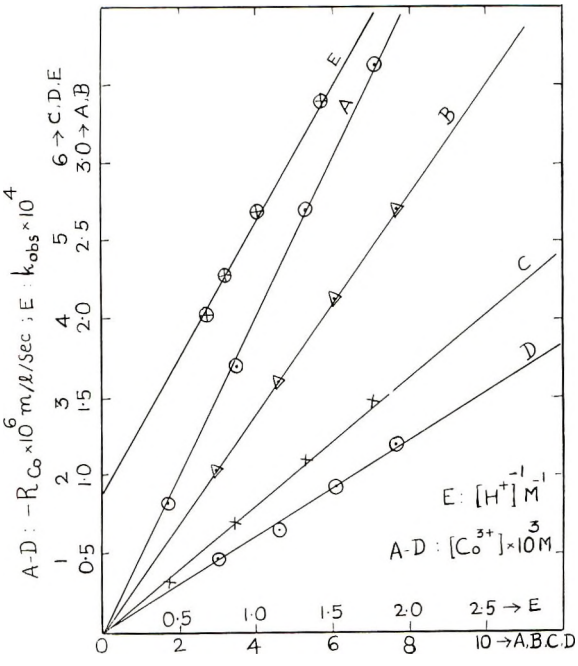

Fig. 4. Variation of $-R_{Co}$ vs. $[Co^{3+}]$ at various $[H^+]$ and K_{obs} vs. $[H^+]^{-1}$ in $HClO_4$, [AN] = 0.7539*M*, μ = 1.7*M*, 25°C.: (*A*) $[H^+]$ = 0.7*M*; (*B*) $[H^+]$ = 1.25*M*; (*C*) $[H^+]$ = 1.0*M*; (*D*) $[H^+]$ = 1.5*M*; (*E*) = K_{obs} vs. $[H^+]^{-1}$.

The influence of $[H^+]$ on $-R_{Co}$ was again interesting. In the case of MA the rates were practically constant with changes in acidity, indicating Co^{3+} (aq.) as the active species. With AN, an inverse dependence of $-R_{Co}$ on $[H^+]$ was observed in all the three acid media (Fig. 5). Also, plots of $-R_{Co}$ versus $1/[H^+]$ or k_{obs} versus $1/H^+$ (cf. Part I)[1] (Fig. 4*E*) have considerable intercepts on the *y*-axis, indicating the importance of an acid-independent reaction i.e., Co^{3+} (aq.) ions being involved in the radical production step. The acid-dependent reaction may be due to oxidation of AN with no polymerization and/or to interaction of $CoOH^{2+}$ or $CoSO_4^+$ with AN leading to polymerization. The strict inverse first-power dependence on $[H^+]$ excluded the possibility of dimers of Co^{3+} taking part in the reaction in perchloric and nitric acid media. In sulfuric acid, deviations from linearity of the plots of $-R_{Co}$ versus $1/[H^+]$ suggested the possibility of dimers taking part in the reaction, which is in accordance with the orders greater than unity observed for $[Co^{3+}]$ in the plots of $-R_{Co}$ versus $[Co^{3+}]$ in sulfuric acid medium.

$-R_{Co}$ values were constant with changes in ionic strengths μ (by addition of NO_3^- in HNO_3 and ClO_4^- in $HClO_4$) in the case of MA, which excluded the possibility of participation of $CoNO_3^{2+}$, if present in HNO_3 medium, in the reaction sequence. The effect of ionic strength in the case of AN was interesting. In perchloric and nitric acid, $-R_{Co}$ values were

only slightly increased (5–10%) for a fivefold increase in μ. In H_2SO_4, $-R_{Co}$ values were found to be directly proportional to $[HSO_4^-]$ (Fig. 5A) for $[Co^{3+}] \approx 5 \times 10^{-4}$–$3 \times 10^{-3}M$ while inversely proportional to

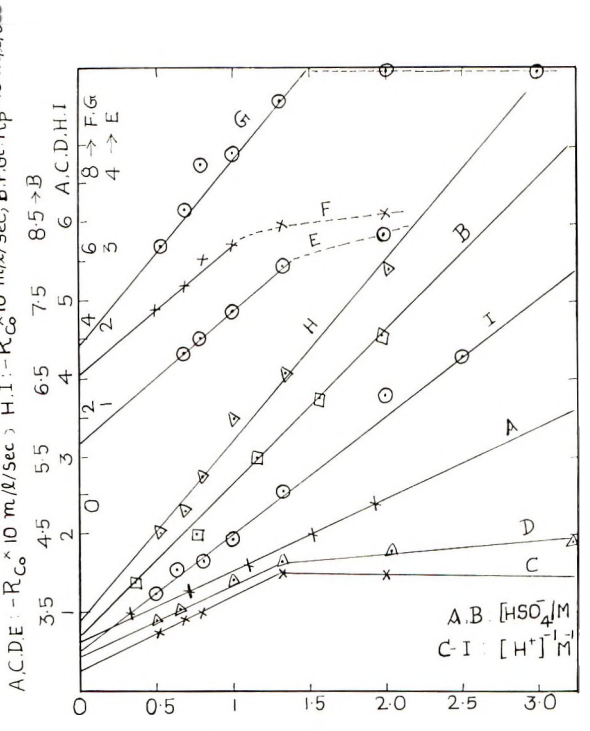

Fig. 5. Variation of $-R_{Co}$ and R_p with $[HSO_4]$ and with $[H^+]$ of (*A*) $-R_{Co}$ vs. $[HSO_4]$, in H_2SO_4, $[Co^{3+}] = 9.8 \times 10^{-4}M$, [AN] = 0.4523*M*, $[H^+] = 0.3M$, $\mu = 2.0M$, 20°C.; (*B*) R_p vs. $[HSO_4]$, in H_2SO_4, $[Co^{3+}]$: $3.7 \times 10^{-3}M$, [AN] = 0.5277*M*, $[H^+] = 0.3M$, $\mu = 2.0M$, 20°C., (*C*) $-R_{Co}$ vs. $[H^+]^{-1}$, in H_2SO_4, in H_2SO_4, $[CO^{3+}] = 1.995 \times 10^{-3}M$, [AN] = 0.7539*M*, $\mu = 2.1M$, 20°C.; (*D*) $-R_{Co}$ vs. $[H^+]^{-1}$, in H_2SO_4, $[Co^{3+}] = 4.692 \times 10^{-3}M$, [AN] = 0.4523*M*, $\mu = 2.1M$, 20°C.; (*E*) $-R_{Co}$ vs. $[H^+]^{-1}$, in H_2SO_4, $[Co^{3+}] = 6.658 \times 10^{-3}M$, [AN] = 0.5277*M*, $\mu = 2.1M$, 20°C.; (*F*) R_p vs. $[H^+]^{-1}$, in H_2SO_4, conditions same as (*E*); (*G*) R_p vs. $[H^+]^{-1}$, in H_2SO_4, conditions same as C; (*H*) $-R_{Co}$ vs. $[H^+]^{-1}$, in $HClO_4$, $[Co^{3+}] = 11.15 \times 10^{-3}M$, [AN] = 0.7539*M*, $\mu = 2.0M$, 20°C.; (*I*) R_{Co} vs. $[H^+]^{-1}$, in $HClO_4$, $[Co^{+3}] = 9.8 \times 10^{-3}M$, [AN] = 0.7539*M*, $\mu = 2.1M$, 20°C.

$[Co^{3+}] > 3 \times 10^{-3}M$. It can be easily shown on the basis of $CoSO_4^+$ being the active species at lower $[Co^{3+}]$, that

$$\frac{1}{k_{obs}} = \frac{1}{k_a} + \frac{[H^+]}{k_a K_2 [HSO_4^-]}$$

where k_{obs} is the observed rate constant and k_a the theoretical rate constant and therefore there is direct proportionality between rate and $[HSO_4^-]$. K_2 is the equilibrium constant for $Co^{3+} + HSO_4^- \rightleftharpoons CoSO_4^+ + H^+$. If $CoOH^{2+}$

(present in very small concentrations) is the active species under conditions of high $[Co^{3+}]$:

$$\frac{1}{k_{obs}} = \frac{1}{k'_a} + \frac{[H^+]}{k'_a K_1} + \frac{K_2[HSO_4^-]}{k'_a K_1}$$

and therefore there is inverse proportionality between rate and $[HSO_4^-] \cdot K_1$ is the hydrolytic equilibrium constant for Co^{3+} and k'_a is the theoretical rate constant. From the above considerations it is therefore concluded that in the polymerization of AN in H_2SO_4 at low $[Co^{3+}]$ the active species are Co^{3+} and $CoSO_4^+$, while at high $[Co^{3+}]$, the active entities are Co^{3+} and $CoOH^{2+}$.

Initially added Co^{2+} ($[Co^{3+}]/[Co^{2+}] = 1/20$) had no effect on $-R_{Co}$.

Rates of Polymerization: R_p

Rates of monomer disappearance, $-R_M$, were followed by bromometry in the case of MA in $HClO_4$. It was found that $-R_M$ and R_p were comparable within the limits of experimental error. This indicated nonexistence of monomer oxidation as a side reaction. The bromometric method for confirmation of monomer oxidation reaction was not applicable to AN.

A strict proportionality of R_p with $[M]^2$ was shown by both monomers in $HClO_4$, HNO_3, and H_2SO_4 (Figs. 6 and 7), thus indicating linear termina-

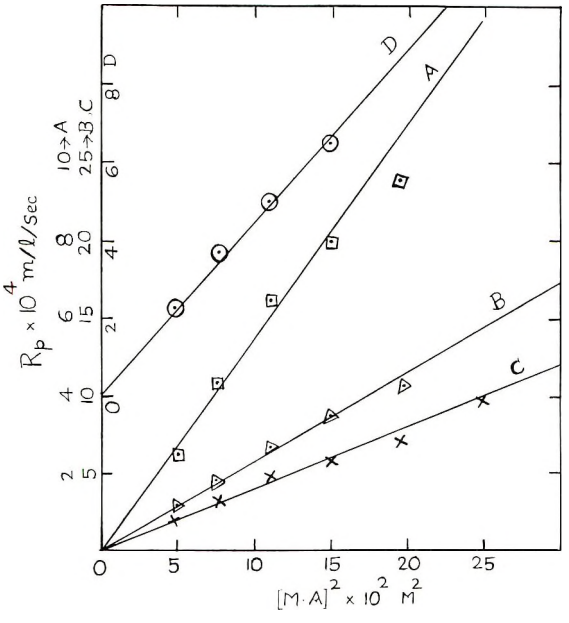

Fig. 6. Variation of R_p with [MA]: (*A*) in $HClO_4$, $[Co^{3+}] \sim 1 \times 10^{-2}M$, $[H^+] = 1.0M$, $\mu = 1.2M$, 15°C.; (*B*) in $HClO_4$, $[Co^{3+}] = \sim 1 \times 10^{-2}M$, $[H^+] = 1.0M$, $\mu = 1.2M$, 10°C.; (C)in HNO_3, $[Co^{3+}] = \sim 1 \times 10^{-2}M$, $[H^+] = 1.0M$, $\mu = 1.2M$, 10°C.; (*D*) in HNO_3, $[Co^{3+}] = \sim 1 \times 10^{-2}M$, $[H^+] = 1.0M$, $\mu = 1.2M$ 15°C.

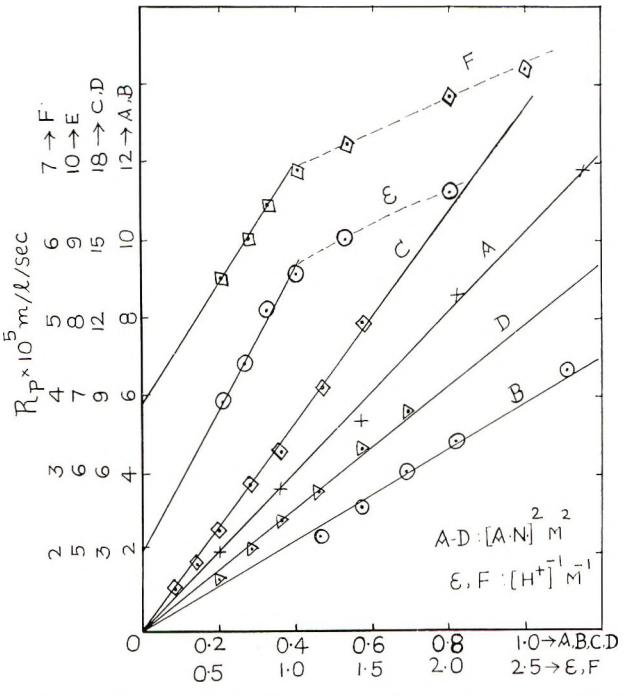

Fig. 7. Variation of R_p with [AN] and with $[H^+]^{-1}$: (*A*) R_p vs. $[AN]^2$, in $HClO_4$, $[Co^{+3}] = 1 \times 10^{-3}$–$1 \times 10^{-2}M$, $[H^+] = 1.0M$, $\mu = 1.2M$, 20°C.; (*B*) R_p vs. $[AN]^2$, in HNO_3, $[Co^{+3}] = 1 \times 10^{-3}$–$1 \times 10^{-2}M$, $[H^+] = 1.0M$, μ $1.2M$, 15°C.; (*C*) R_p vs. $[AN]^2$, in H_2SO_4, $[Co^{+3}] = >5 \times 10^{-3}M$, $[H^+] = 1.0M$, $\mu = 1.5M$, 20°C.; (*D*) R_p vs. $[AN]^2$, in H_2SO_4, $[Co^{+3}] = >5 \times 10^{-3}M$, $[H^+] = 1.0M$, $\mu = 1.5M$, 15°C.; (*E*), R_p vs. $[H^+]^{-1}$ in $HClO_4$, $[Co^{3+}] = 11.15 \times 10^{-3}M$, $[AN] = 0.7539M$, $\mu = 2.0M$, 20°C.; (*F*) R_p vs. $[H^+]^{-1}$ in HNO_3, $[Co^{3+}] = 13.06 \times 10^{-3}M$, $[AN] = 0.7539M$, $\mu = 2.1M$, 20°C.

tion of chains by Co^{3+}. In H_2SO_4 with AN, it was found that at low $[Co^{3+}]$(viz. $\lesssim 4 \times 10^{-3}M$), R_p still varied as $[M]^2$, but slopes of plots of R_p versus $[M]^2$ decreased with decreasing $[Co^{3+}]$. Log slopes (of R_p versus $[AN]^2$ plots) when plotted against log $[Co^{3+}]$ yielded a slope of 0.5. $R_p \propto [Co^{3+}]^{0.5}$ pointed to the possibility of mutual termination in this region of low $[Co^{3+}]$. It is possible that mixed termination takes place, linear and mutual, the latter increasing with decreasing $[Co^{3+}]$. An exact dependence of 3/2 powers of [AN] on R_p required for mutual termination may be realized at very low $[Co^{3+}]$ of the order $10^{-4}M$, but under the latter conditions induction periods of long duration set in.

The fact that R_p was independent of $[Co^{3+}]$ at all concentrations of the latter in the case of AN and MA in $HClO_4$ and HNO_3 and with AN in H_2SO_4 at $[Co^{3+}] \gtrsim 4 \times 10^{-3}M$ suggested exclusive linear termination by Co^{3+}. Termination of polyacrylonitrile by Fe^{3+} has been established.[6–7] Other metal ions, such as chromous,[8] Cu^{2+},[4,9] and ceric[10–12] ions have also been found to be efficient terminators of polyacrylonitrile radicals.

In the case of MA, R_p values were unaffected by changes in $[H^+]$, which showed that Co^{3+} ions were the initiators and terminators. Initiation

and termination by the same species such as $CoOH^{2+}$ or even $CoNO_3^{2+}$ would also lead to such constancy of rates with $[H^+]$, but if such were the case, an inverse dependence of $-R_{Co}$ on $[H^+]$ should have been observed which of course was not the case. With AN, in all three acid media (Figs. 5 and 7), plots of R_p versus $1/[H^+]$ were linear at higher acidities and flat at lower acidities, with appreciable intercepts on the ordinate. Intercepts were indicative of Co^{3+} being the active species. The flat nature of the plots suggested participation of $CoOH^{2+}$ species in initiation and termination processes in $HClO_4$ and HNO_3. In H_2SO_4, in addition to $CoOH^{2+}$, there is a possibility of $CoSO_4^+$ species initiating and terminating the polymer chains. R_p would be independent of $[H^+]$ and $[HSO_4^-]$ if $CoSO_4^+$ initiated and terminated. This was in fact observed when $[HSO_4^-]$ was varied at constant μ at high $[Co^{3+}]$. That Co^{3+} initiated and terminated for the flat region in $HClO_4$ or HNO_3 was discounted because of the variation of $-R_{Co}$ versus $1/[H^+]$ in this region in the two acids. In this respect AN closely resembled MMA (Part I).[1] The linear variation of $-R_{Co}$ with $1/[H^+]$ was to be ascribed to initiation by $CoOH^{2+}$ and termination by Co^{3+} in $HClO_4$ or HNO_3. In H_2SO_4, initiation might be by $CoOH^{2+}$ as well as $CoSO_4^+$ and termination by Co^{3+}. R_p varied with $1/[H^+]$ and $[HSO_4^-]$ when the latter was varied at constant μ at low $[Co^{3+}]$. Probably at low $[Co^{3+}]$, $CoSO_4^+$ initiated and at high $[Co^{3+}]$, $CoOH^{2+}$ initiated, termination in H_2SO_4 being effected by Co^{3+} ions in both cases.

Initially added Co^{2+} ions did not have any influence on R_p both for MA as well as AN in all the acid media.

The effect of added salts ($NaClO_4$ in $HClO_4$, $NaNO_3$ in HNO_3, and HSO_4^- in H_2SO_4) was not significant in the case of MA (cf. Part I), but the case of AN presented interesting features. For a fivefold increase in the ionic strength μ, the rates R_p were almost doubled irrespective of the acid medium. This might be more due to the polar nature of the monomer. Bamford et al.[13] have shown that the acrylonitrile radical $CH_2\dot{C}HCN$ is capable of forming complexes with added salts like LiCl, $LiNO_3$, etc. and have further stated that the increase in the R_p values is due to the propagation step being subjected to a salt effect. The order of catalyzing effectiveness $Cl^- > NO_3^- > ClO_4^-$ has been indicated. Hence the possibility of the complex $CoNO_3^{2+}$ in HNO_3 being the initiator and therefore contributing towards enhancement in R_p with increasing μ had to be discounted. If $CoNO_3^{2+}$ initiates, $-R_{Co}$ should increase with $[NO_3^-]$. Confirmation for $CoNO_3^{2+}$ not being the active species was obtained by addition of $[NO_3^-]$ at constant μ (adjusted with $NaClO_4$) in $HClO_4$ medium, when no changes in either R_p or $-R_{Co}$ were observed. In H_2SO_4 the effect of μ as well as $[HSO_4^-]$ at constant μ on R_p was studied in detail to distinguish between a genuine salt effect and the effect of $CoSO_4^+$ being the active species. Increase of μ with HSO_4^- enhanced R_p. Increase of $[HSO_4^-]$ at constant μ increased R_p (Fig. 5*B*) at $[Co^{3+}] \lesssim 3 \times 10^{-3}M$ but R_p remained practically constant for $[Co^{3+}] > 3 \times 10^{-3}M$. Under

the latter conditions a fivefold increase in $[HSO_4^-]$ brought hardly 5% increase in R_p. This behavior was in conformity with the conclusions already drawn that Co^{3+} and $CoSO_4^+$ were the active species at low $[Co^{3+}]$ and Co^{3+} and $CoOH^{2+}$ were initiators at high $[Co^{3+}]$, Co^{3+} ions being the terminators under both conditions.

Chain Lengths *N*

In the case of MA, n values were found to decrease with increasing $[Co^{3+}]$. Results on the effect of [M] on n were not reliable, though an increasing trend of n with increasing [M] was observed. This anomaly was probably due to the narrow range of [M] that had to be used. With AN, the polymer samples from all the three acid media were insoluble in dimethylformamide, probably due to crosslinking. Intermolecular azomethine crosslinking as well as ring structure involving propagation crosslinks has been proposed to account for the insolubility of polyacrylonitrile.[14-17]

The unavoidable occurrence of water oxidation, especially in H_2SO_4, along with the polymerization suggested the possibility of initiation by OH· produced during water reaction. Infrared spectra of poly(methyl acrylate), however, showed negative evidence for the presence of OH. However polyacrylonitrile samples from both $HClO_4$ and H_2SO_4 media showed a broad absorption band at 2.8–2.9 μ due to either bonded OH or NH group. Absence of OH group in other polymers prepared under the same conditions argued strongly in favor of the NH group rather than an OH group in polyacrylonitrile. Further, kinetic results did not favor initiation by OH radicals.

Kinetic Scheme and the Rate Laws

The experimental results discussed in the preceding sections can be adequately explained on the basis of the following reaction scheme.

Radical production steps:

$$Co^{3+} + M \xrightarrow{k_{r1}} R\cdot + Co^{2+}$$

$$CoOH^{2+} + M \xrightarrow{k_{r2}} R\cdot + Co^{2+} + OH$$

$$CoSO_4^+ + M \xrightarrow{k_{r3}} R\cdot + Co^{2+} + SO_4^-$$

Initiation:

$$R\cdot + M \xrightarrow{k_i} R{-}M\cdot$$

Propagation:

$$R{-}M + M \xrightarrow{k_p} R{-}M{-}M\cdot$$

$$R{-}M{-}M\cdot + M \xrightarrow{k_p} R{-}M{-}M{-}M\cdot$$

Termination

$$R{-}M_n\cdot + Co^{3+} \xrightarrow{k_{t1}} P + Co^{2} + H^+$$

Assuming the usual stationary-state kinetics for initiation and termination by Co^{3+} in case of MA

$$-R_{Co} = 2k_{r1}[M][Co^{3+}] \quad (1)$$

$$R_p = (k_p/k_{t1})[M]^2 \quad (2)$$

$$n = (k_p/k_{t1})[M]/[Co^{3+}] \quad (3)$$

All the experimental results favor the conclusion that Co^{3+} (aq.) initiates as well as terminates.

For AN in $HClO_4$ and HNO_3, initiation by Co^{3+} and $CoOH^{2+}$ appeared to be favored. The rate laws are:

$$-R_{Co} = 2\left(k_{r1} + \frac{K_1k_{r2}}{[H^+]}\right)[Co^{3+}][M] + \frac{k_m[Co^{3+}]}{[H^+]} + \frac{k_w[Co^{3+}]^{1.5}}{[H^+]} \quad (4)$$

$$R_p = (k_p/k_{t1})\left\{k_{r1} + (K_1k_{r2}/[H^+])\right\}[M]^2 \quad (5)$$

K_1 is the hydrolytic equilibrium constant. The second and third terms on the right-hand side of eq. (4) represent rates for monomer oxidation and water oxidation, respectively. For AN in H_2SO_4, Co^{3+}, and $CoSO_4^+$ initiate at low $[Co^{3+}]$, and the rate laws are:

$$-R_{Co} = 2\left(k_{r1} + \frac{K_2k_{r3}[HSO_4^-]}{[H^+]}\right)[Co^{3+}][M] + \frac{k_w[Co^{3+}]^{1.5}}{[H^+]} \quad (6)$$

$$R_p = (k_p/k_{t1})\left\{k_{r1} + (K_2k_{r3}[HSO_4^-]/[H^+])\right\}[M]^2 \quad (7)$$

The second term on the right-hand side of eq. (6) represents water oxidation (cf. part I). At high $[Co^{3+}]$, in H_2SO_4 medium, the rate laws (4) and (5) are applicable.

Evaluation of Rate Constants

From plots of $-R_{Co}$ versus [M] or $[Co^{3+}]$, for MA, values of k_{r1} were evaluated. The good correspondence between the two sets of values proved the correctness of the conclusions regarding the absence of monomer oxidation in this system (cf. MMA system in H_2SO_4).[1]

From plots of R_p versus $[M]^2$, k_pk_{r1}/k_{t1} and hence k_p/k_{t1} was evaluated for MA polymerization. From experiments conducted at 10 and 15°C., the activation energy values for k_{r1} and k_p/k_{t1} were computed.

TABLE I

Medium	Temperature, °C.	$k_{r1} + (K_1k_{r2}/[H^+])$ $\times 10^5$
$HClO_4$	15	5.540
	20	12.83
	25	19.32
HNO_3	15	3.380
	20	7.736
H_2SO_4	15	2.39
	20	3.23

TABLE II
Rate Parameters in the Polymerization of MA and AN

Monomer	Medium	Temp., °C.	$k_{r1} \times 10^4$, l./mole-sec.[a]	$k_{r2} \times 10^3$, l./mole-sec.	$k_m \times 10^5$	k_p/k_{t1}	Ek_{r1}, kcal./mole	Ek_p/k_{t1}, kcal./mole	10^5 slope of $-R_{Co}$ vs. $[Co^{3+}]$ plots[b]	
									Exptl.	Calc.
MA	$HClO_4$	10	7.61			8.02	19.6	−23.63	—	—
		15	13.98			3.9				
	HNO_3	10	5.22			7.523	18.89	−16.73	—	—
		15	9.84			4.493				
AN	$HClO_4$	15				1.17	17.46	—		
		20	0.536	6.29	9.66	0.80			14.61	14.59
		25	0.885	6.71	10.07	1.16				
	HNO_3	15				1.51	—	−6.73		
		20	0.346	3.59	8.79				10.74	10.20
	H_2SO_4	15				4.96		+6.99		
		20	0.093	2.00	4.19	6.19			3.50	3.52

[a] Average values from $-R_{Co}$ vs. $1/[H^+]$ or k_{obs} vs. $1/[H^+]$ plots.

[b] In $HClO_4$ and HNO_3, slope of $-R_{Co}$ vs. $[Co^{3+}]$ plot: $k_{r1} + (K_1k_{r2}/[H^+]) + (k_m/2[M])$, assuming water oxidation negligible. In H_2SO_4, at low $[Co^{3+}]$, monomer oxidation is negligible and therefore slope $= k_{r1} + (K_2k_{r2}[HSO_4^-]/[H^+])$.

The value of $\{k_{r1} + (K_1k_{r2}/[H^+])\}$ for AN was evaluated from pots of $-R_{Co}$ versus [M]; the values obtained are shown in Table I. The value of $\{k_{r1} + (K_2k_{r3}[HSO_4^-]/[H^+])\}$ at low cobaltic ion concentrations was computed (3.33×10^{-5} at 20°C.) from $-R_{Co}$ versus [M] plots.

k_{r1} values from intercepts of $-R_{Co}$ versus $1/[H^+]$ or k_{obs} versus $1/[H^+]$ plots and k_{r2} values in $HClO_4$ and HNO_3, as well as K_2k_{r3} in H_2SO_4, from known values of k_{r1} were evaluated for AN. An average value (from $-R_{Co}$ versus [M] plots at low $[Co^{3+}]$ and $-R_{Co}$ versus $1/[H^+]$ at low $[Co^{3+}]$) of 1.75×10^{-5} at 20°C. was obtained for K_2K_{r3} in H_2SO_4. From experiments conducted at 15, 20, and 25°C., Ek_{r1} values and Ek_p/k_{t1} were evaluated.

From slopes of $-R_{Co}$ versus $1/[H^+]$ plots and k_{r2} and K_1, k_m was computed for AN in $HClO_4$ and HNO_3 and at high $[Co^{3+}]$ in H_2SO_4.

$k_p/k_{t1}\{k_{r1} + (K_1k_{r2}/[H^+])\}$ and hence k_p/k_{t1} was evaluated for AN from plots of R_p versus $[M]^2$.

The proposed reaction mechanism appeared to be fairly substantiated by close agreement between the experimental slope of plot of $-R_{Co}$ versus $[Co^{3+}]$ and that calculated from various rate constants. All the rate parameters are given in Table II.

From the foregoing results it is evident that polymerization of AN in $HClO_4$ and HNO_3 media shows strong resemblance to that of MMA in the same media.[1] However, the behavior of AN in H_2SO_4 is of a complex nature, and it is surprising to note that with this monomer alone experimental evidence indicated $CoSO_4^+$ as one of the active species. Probably this was facilitated by the high solubility of the monomer in water. Another interesting aspect was that polymerization of MA is similar to that of MMA in H_2SO_4. Our results with acrylamide (AAm) in $HClO_4$ indicated that the $CoOH^{2+}$ species initiated polymerization, while termination proceeded by mutual combination. A striking feature of these polymerization studies was that invariably with MMA, AN, and AAm, monomer oxidation occurred as a side reaction in $HClO_4$ and HNO_3. The exceptional behavior of MA in this respect is understandable from its extremely high reactivity. In general, it may be concluded that though many similarities are exhibited in kinetics of vinyl polymerization by cobaltic ions, the actual mechanism of polymerization varies and depends on the nature and reactivity of the monomers as well as the reaction medium.

One of us (K. J.) is thankful to the Ministry of Education, Government of India, and to the University Grants Commission for the award of Research Scholarship and Junior Research Fellowship, respectively, during the tenure of which this work was completed.

References

1. Jijie, K., M. Santappa, and V. Mahadevan, *J. Polymer Sci. A*, **4**, 377 (1966)
2. Sen, J., S. R. Banerjee, and S. R. Palit, *J. Sci. Ind. Res. (India)*, **11B**, 90 (1952).
3. Fuhrman, N., and R. B. Mesrobian, *J. Am. Chem. Soc.*, **76**, 3281 (1954).
4. Dainton, F. S., and P. H. Seaman, *J. Polymer Sci.*, **39**, 279 (1959).
5. Dainton, F. S., and D. G. L. James, *J. Polymer Sci.*, **39**, 299 (1959).

6. Colebourne, N., E. Collinson, D. J. Currie, and F. S. Dainton, *Trans. Faraday Soc.*, **59,** 1357 (1963).
7. Dainton, F. S., and D. G. L. James, *Trans. Faraday Soc.*, **54,** 649 (1958).
8. Collinson, E., F. S. Dainton, D. R. Smith, G. J. Trudel and (in part) S. Tazuke, *Discussions Faraday Soc., No.* **29,** 188 (1960).
9. Watanabe, M., and H. Kiuchi, *J. Polymer Sci.*, **58,** 103 (1962).
10. Katai, A. A., V. K. Kulshreshtha, and R. H. Marchessault, *J. Polymer Sci. C*, **2,** 403 (1963).
11. Ananthanarayanan, V. S., and M. Santappa, *Indian J. Chem.*, **2,** 330 (1964).
12. Ananthanarayanan, V. S., Thesis, Madras Univ., Oct. 1964.
13. Bamford, C. H., A. D. Jenkins, and R. Johnston, *J. Polymer Sci.*, **29,** 355 (1958).
14. Schurz, J., *J. Polymer Sci.*, **28,** 438 (1958).
15. Grassie, N., and J. N. Hay, *J. Polymer Sci.*, **56,** 189 (1962).
16. Takata, T., I. Hiroi, and M. Taniyama, *J. Polymer Sci. A*, **2,** 1567 (1964).
17. Funt, B. L., and F. D. Williams, *J. Polymer Sci. A*, **2,** 865 (1964).

Résumé

On a étudié la polymérisation de l'acrylate de méthyle dans l'acide perchlorique et l'acide nitrique dans un domaine de température allant de 10 à 15°C. Les cinétiques de polymérisation très simples impliquent une initiation et une terminaison par les ions cobaltiques. L'étude cinétique relative à la polymérisation de l'acrylonitrile dans les acides perchloriques et nitriques révèle l'existence de réactions secondaires d'oxydation de l'eau et du monomère comme dans le cas du méthacrylate de méthyle. Les résultats expérimentaux sont en faveur d'une initiation simultanée par les espèces Co^{+3} et $CoOH^{+2}$. Dans l'acide sulfurique, on rencontre certains faits inhabituels: à basse concentration en ion Co^{3+}, se produisent aussi bien une terminaison linéaire qu'une terminaison par recombinaison mutuelle. Un autre aspect intéressant est le fait que l'espèce $CoSO_4^+$ initie à basse concentration en Co^{+3}, ce qui ne se produit pas avec les autres monomères dans le même milieu. Les vitesses de polymérisation et de dispartition des ions cobaltiques ont été mesurées en fonction des concentrations en monomère, en ions Co^{+3}, en ions H^+ et en fonction de la température. On a calculé les différentes constantes de vitesse.

Zusammenfassung

Die Polymerisation von Methylacrylat wurde im Temperaturbereich von 10–15°C. in $HClO_4$- und HNO_3-hältigen Systemen untersucht. Die Polymerisationskinetik erwies sich als sehr einfach; Start und Abbruch erfolgte durch Kobalt-3-ionen. Kinetische Untersuchungen der Acrylonitrilpolymerisation in $HClO_4$- und HNO_3-Systemen zeigte, dass als Nebenreaktionen Wasseroxydation und Monomeroxydation wie im Fall des Methylmethacrylats auftraten. Die Versuchsergebnisse sprechen für eine gleichzeitige Anregung durch Co^{3+} und $CoOH^{2+}$. Im H_2SO_4-System wurde ein ungewöhnliches Verhalten beobachtet. Bei niedriger Co^{3+}-Konzentration trat sowohl linearer Abbruch als auch Abbruch durch wechselseitige Kombination auf. Ein weiterer interessanter Aspekt war der Start durch $CoSO_4^+$ bei niedrigem $[Co^{3+}]$. Das steht im Gegensatz zum Verhalten anderer Monomerer im H_2SO_4-Medium. Die Polymerisationsgeschwindigkeit und die Geschwindigkeit des Umsatzes der Co^{3+}-Ionen wurde in Abhängigkeit von [M], $[Co^{3+}]$, $[H^+]$, Temperatur etc. gemessen. Die verschiedenen Geschwindigkeitskonstanten wurden ermittelt.

Received June 14, 1965
Prod. No. 4831A

JOURNAL OF POLYMER SCIENCE: PART A-1 VOL. 4, 407–418 (1966)

Solution Properties of Cellulose Triacetate. I. Fractional Precipitation

P. HOWARD and R. S. PARIKH, *Battersea College of Technology, London, England*

Synopsis

Using petroleum ether as a precipitant and chloroform–acetone mixture as solvent, six fractions of cellulose triacetate were obtained by fractional precipitation. The molecular weight of each fraction was obtained from osmotic pressure measurements carried out on chloroform solutions. It was shown that virtual nonfractionability of cellulose triacetate with regard to molecular weight occurred in this system. This behavior was also observed in attempts to fractionate it from tetrachloroethane or acetic acid solutions. These results are explained by the hypothesis that specific polymer–solvent interaction takes place due to hydrogen bonding.

INTRODUCTION

The attempted fractionation of cellulose triacetate from solution, although reported by a number of workers, has generally given anomalous results which are not clearly understood. In some cases limited fractionation has been reported, while in others nonfractionation or reverse-order fractionation takes place. An additional factor likely to affect fractionability is the degree of acetylation, since the solubility of cellulose acetate in acetone, for example, decreased markedly in the region of 59% acetic acid content[1] and the term "triacetate" has not always been confined to the fully acetylated cellulose (62.50% acetic acid content). Only slight fractionation of cellulose triacetate with some reverse-order precipitation was found by Lachs et al.[2] for acetic acid–acetone solutions with water as precipitant. Levi and Giera[3] showed that cellulose diacetate could be successfully fractionated by using an adsorption column, but no fractionation occurred in the case of the triacetate although it was adsorbed to the same extent. Since their diacetate was prepared by hydrolysis of the triacetate, they suggested that the original cellulose was virtually homogeneous with respect to chain length and a broader distribution resulted on hydrolysis. Subsequent partial fractionation from acetic acid[4] by using benzene as precipitant was attributed to degradation of the triacetate during the precipitation and drying stages. However, more recent work[5] employing a column fractional-solution technique with methylene chloride–heptane mixtures has confirmed the virtual nonfractionability of the triacetate in these systems. Some fractionation of cellulose triacetate in

water–acetic acid systems has also been reported by Bezzi and Croatto,[6] the ratio of the highest to lowest value of the viscosity number being 1.8. Precipitation from chloroform–acetone solution with petroleum ether has given fractions differing little in degree of polymerization,[7] while the use of a ternary solvent and binary precipitant system appears to be successful.[8] Münster[9] has discussed fractionation from binary solutions using an extension of the thermodynamic approach of Schulz; reverse-order precipitation observed in the cellulose triacetate–tetrachloroethane–petroleum ether system was accounted for by the magnitude of the coefficients in the theoretical distribution equations. The thermodiffusion method of Langhammer[10] for fractionating cellulose triacetate appears to be promising but few results are available for comparison. So far the best method of obtaining a series of cellulose triacetate fractions of wide molecular weight range seems to be by reacetylating fractions of lower acetyl content.[11]

So far the fractionation efficiency in each case has been assessed from viscosity measurements. Assuming the limiting viscosity number to be related to the average molecular weight according to the Mark-Houwink equation, $[\eta] = K(\bar{M})^{\alpha}$, then the effectiveness of viscosity values for molecular weight comparison depends on the value of α. Thus for $\alpha < 1$, the viscosity number ratio for the first and last fractions would be smaller than the corresponding molecular weight ratio, while for $\alpha > 1$ little change in molecular weight may still give rise to a considerable change in viscosity. In the present work molecular weights are measured osmotically or obtained from viscosity measurements by use of a previously determined viscosity–molecular weight relationship.

EXPERIMENTAL

Materials

Cellulose triacetate was prepared by acetylating purified Texas cotton supplied by Dr. J. Honeyman of the Cotton, Silk and Man-Made Fibres Research Association. An acetylation mixture of carbon tetrachloride, acetic acid, and acetic anhydride with perchloric acid catalyst was used; the experimental conditions and method of analysis are described elsewhere.[12] Three samples were prepared and are designated here as CT/1 ($\bar{M}_n$ = 28,600; AcOH = 62.1%), CT/2 ($\bar{M}_n$ = 38,200; AcOH = 62.2%), and CT/3 ($\bar{M}_n$ = 34,800; AcOH = 62.0%). All solvents used were reagent grade unless otherwise stated.

Osmotic Pressure and Viscosity Measurements

Osmotic pressure measurements were made in AnalaR chloroform solutions at 25 ± 0.005°C. in a Pinner-Stabin osmometer[13] using Ultracella-filter feinst membranes (35 mm. diameter) which were conditioned in the solvent before use. The rapid dynamic method of Bruss and Stross[14] was employed for osmotic pressure measurements. Number-average molecular weights were evaluated from limiting reduced osmotic-head values

obtained by least squares treatment of the h/c versus c data. The method gave good linear plots for rate of flow versus pressure head in the range 0.3–3.0 $\times$ 10^{-4} ml./min. and the osmotic head h at zero flow rate was obtained by least-squares treatment. Applied asymmetry head corrections were less than 1%, and solutions were aged overnight before examination.

Viscosity–concentration runs were made in a dilution viscometer at 25 $\pm$ 0.01°C. for samples dissolved in AnalaR chloroform. Solutions were prefiltered (No. 3 sinter) and measurements were made within the concentration range 0.1–1.1 g./100 ml. The limiting viscosity number (L.V.N.) in each case was obtained by least-squares treatment of the linear viscosity number versus concentration plot. Kinetic energy and end-effect corrections were negligible and were not applied.

Choice of Solvent–Precipitant System

Preliminary experiments were carried out in order to find the best solvent–precipitant system giving easily separable precipitates and a low precipitation value consistent, as far as possible, with a gradual increase in the amount precipitated with increasing precipitant.

A 1% (w/v) stock solution of cellulose triacetate (CT/3) in chloroform or an azeotrope was first prepared; in the case of the azeotropes the triacetate was first dissolved in chloroform and then diluted with the second component. Different precipitants were gradually added to aliquots of the polymer solution at room temperature, with constant stirring, until the first appearance of turbidity when the volume added was taken as the precipitation value. A little more precipitant was added and the solutions warmed to 40–45°C. and then allowed to stand overnight (16 hr.) in order to reach phase equilibrium, when the nature of the precipitated phase was examined. Preliminary fractionation experiments with a solvent vaporization method showed it to offer no advantages over fractional precipitation by nonsolvent addition and was therefore not pursued. The results of the preliminary studies are shown in Table I.

With butyl acetate as precipitant and chloroform–acetone as solvent, the turbidity of the solution increased with time; thus an initially clear solution containing 3 ml. of butyl acetate gave a precipitate which separated out only after a week. These results (Table I) showed that the most promising system for the fractionation of cellulose triacetate was a chloroform–acetone solution with petroleum ether as precipitant. These systems had low precipitation values and gave easily visible and separable precipitates. The final choice of precipitant was made by comparison of the precipitates and shapes of the precipitation-composition curves for the three petroleum ether fractions.

Increasing amounts of each petroleum ether were added to aliquots of a 1% cellulose triacetate (CT/1) solution in chloroform–acetone mixture (1:1, v/v) at room temperature. The precipitation value was noted each time, and after addition of sufficient precipitant the mixture was stirred for 5 min., warmed to 40°C., and left to stand overnight. Precipitates

TABLE I
Precipitation Values and Nature of Precipitate for 1% Cellulose Triacetate (CT/3) in Various Solvents

Solvent	Precipitant	Precipitation value, ml./25 ml. soln.	Total vol. precipitant, ml./25 ml. soln.	Nature of ppt. after 16 hr.
Chloroform	Petroleum ether, 60/80 fraction	11.0	16.8	Very swollen, does not settle out
	Butyl acetate	13.3	16.0	Very swollen, does not settle out
	Ethanol	—	26.0	Does not settle out Same refractive index as solution
	Cyclohexanol	—	15.0	"
	Benzene	—	10.0	"
	Toluene	—	25.0	"
Chloroform–ethanol azeotrope (93:7, v/v)	Petroleum ether, 100/120 fraction	14.0	—	Swollen precipitate; does not settle out
	Butyl acetate	15.3	—	"
	Amyl acetate	14.2	—	"
	n-Heptane	15.5	—	"
Chloroform–acetone (1:1, v/v)	Petroleum ether, 100/120 fraction	3.5	4.6	Amorphous precipitate; settled out well
	Petroleum ether, 60/80 fraction	4.0	5.0	"
	Butyl acetate	—	6.5	"
	Benzene	—	12.0	Does not settle out Same refractive index as solution
	Chlorobenzene	—	16.3	"

were separated off by centrifuging, stirred up with fresh solvent–precipitant mixture of the same composition as the supernatant liquid, and finally centrifuged off and dried to constant weight at 110°C. The results are recorded in Table II and gave the precipitation–composition curves shown in Figure 1. The mean of each set of precipitation values (column 2 of Table II) is plotted in Figure 1.

It can be seen from the precipitation curves in Figure 1 that virtually all the polymer is precipitated out when 40% of the original volume of solution is added as precipitant. Little difference exists between the curves for the petroleum ether 60/80 and 80/100 fractions, although they are less steep than that for the 100/120 fraction. Since the 60/80 fraction gave a slightly more swollen precipitate than that for the 80/100 fraction, it was decided to use the latter for the fractionation of cellulose triacetate.

TABLE II
Cumulative Precipitation Data for 1% Cellulose Triacetate (CT/1) in Chloroform-Acetone Solution (1:1, v/v)

Petroleum ether fraction	Precipitation value, ml./25 ml. soln.	Total vol. precipitant, ml./25 ml. soln.	Wt. % precipitated
60/80	3.7	5.0	26.2
	3.8	7.5	86.9
	3.9	10.0	96.7
80/100	4.0	5.0	18.9
	3.8	6.1	44.9
	3.7	7.0	83.4
	3.7	8.0	90.1
100/120	2.8	5.0	59.0
	2.8	6.0	74.7
	2.8	7.0	96.9

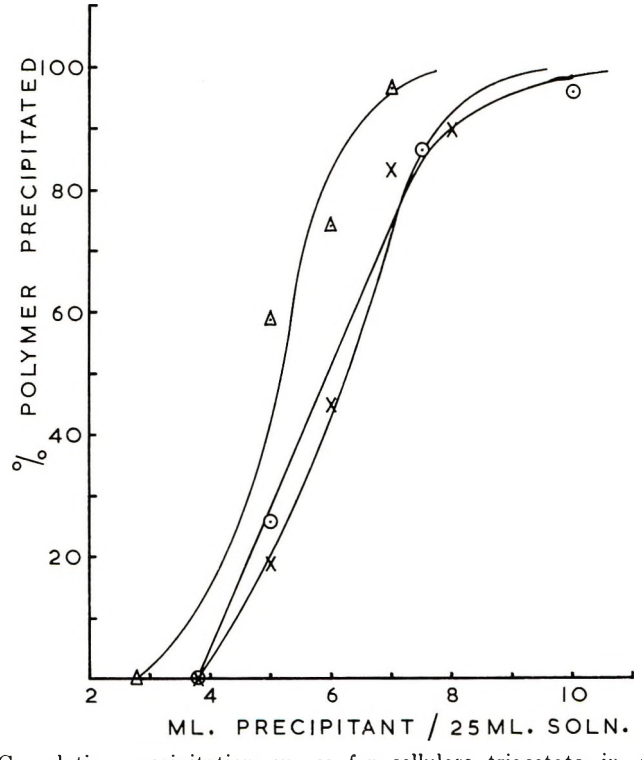

Fig. 1. Cumulative precipitation curves for cellulose triacetate in chloroform–acetone solution: (⊙) 60/80 petroleum ether; (×) 80/100 petroleum ether; (△) 100/120 petroleum ether.

Fractionation Procedure

The fractionation apparatus was that described by Hall[15] and consisted essentially of a thermostatted 5-liter vessel containing the stirred solution

to which the precipitant could be added. A 20-g. portion of cellulose triacetate (CT/1) was dissolved in 1 liter of chloroform and then diluted with 1 liter of acetone and the solution thermostatted at 25°C. in the fractionation vessel overnight. A 400-ml. portion of petroleum ether (80/100) was then slowly added from a buret over a period of 3 hr., the solution being continuously stirred. This volume was chosen so as to precipitate about 15% of the polymer in the first fraction. Since this first fraction appeared to be rather large, a further 200 ml. of solvent mixture was added at this stage. To ensure the attainment of equilibrium between the two phases, the bath temperature was raised to 40°C. so as to dissolve the precipitate and allow it to reform again on cooling to 25°C. However, even after 2 hr. at the higher temperature the precipitate showed no signs of redissolving and, if anything, a slight increase in turbidity appeared to take place. The temperature was consequently lowered to 25°C. and the precipitated phase allowed to settle out overnight. In all cases the precipitate had settled out after 2 hr., no further change in its volume being noticed after a further 12 hr. The fractionation vessel was then removed from the bath and the precipitated polymer separated by centrifuging, while the clear supernatant solution was transferred to a second (identical) fractionation vessel thermostatted at 25°C. This first fraction was successively washed with acetone and precipitant and centrifuged off, in order to eliminate low molecular weight material, and dried to constant weight at 110°C. (fraction 1A). Addition of a little precipitant to a portion of the acetone washings from the 1A fraction gave a further precipitate; consequently excess 80/100 petroleum ether was added to the washings to precipitate out all the triacetate. This portion, regarded as a diluted chloroform–acetone extract, was dried at 110°C. as before and was called fraction 1B.

After thermostatting the remaining solution for a few hours a second fraction was precipitated as before, including warming to 40°C.; this and subsequent fractions were washed with a solvent–precipitant mixture of the same composition as the supernatant liquid, following by the precipitant, and then dried at 110°C. In all, six fractions were obtained, and the last one was recovered by evaporation of the solution. This sample (fraction 6) when dried was partly soluble in acetone and since it probably contained a considerable amount of very low molecular weight material it was not investigated further. Molecular weights of each of the other fractions were obtained osmometrically except for fraction 5, where a viscometric method was used, employing the relationship, $[\eta] = 2.83 \times 10^{-7} \bar{M}_n^{1.40}$ previously found.[16]

Precipitation from Acetic Acid and Tetrachloroethane Solutions

Exploratory experiments were made to see whether any improvement in fractionation took place from acetic acid and tetrachlorethane solutions, by comparing the molecular weight of the first fraction with that of the totally precipitated cellulose triacetate.

From a 1% solution of cellulose triacetate (CT/2) in acetic acid and in tetrachlorethane at room temperature a proportion was precipitated out

by dropwise addition of petroleum ether (100/120) to the stirred solutions. The mixture was warmed to 30°C. in each case and then left to stand for 16 hr. when the two phases were separated by centrifugation. The precipitated polymer was redissolved in its respective solvent and reprecipitated to minimize low molecular weight contamination; in the case of acetic acid the temperature was raised to 100°C. to hasten dissolution. These first fractions were then centrifuged off, washed with precipitant, and dried at 110°C. Their number-average molecular weights were evaluated from L.V.N. values in chloroform at 25°C. by using the above relationship and compared with the molecular weight of the polymer completely precipitated from chloroform.

RESULTS

The fractionation results for the various solvents are shown in Table III. Values of the polymer–solvent interaction parameter χ were obtained from the slopes of the reduced osmotic head in centimeters per gram per 100 ml. solution (h/c) versus concentration plots from

$$\pi/c = (RT/\bar{M}_n) + (RTd_0/100M_0d^2)(0.5 - \chi) \quad (1)$$

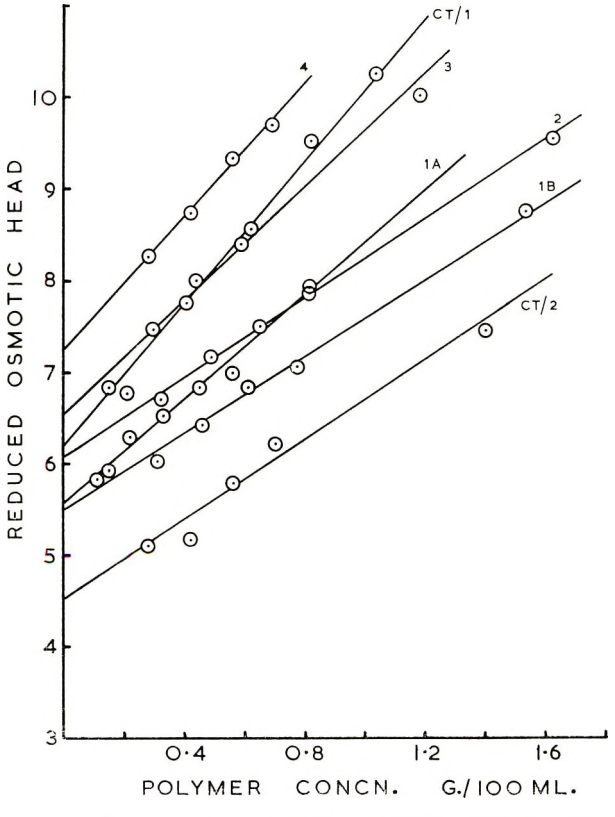

Fig. 2. Reduced osmotic head vs. concentration plots for cellulose triacetate samples.

TABLE III
Fractional Precipitation of Cellulose Triacetate from Various Solvents

Solvent	Fraction	Wt.-% precipitated	h/c ($c \to 0$), cm./g.-ml.	L.V.N., dl./g.	$\bar{M}_n$	χ
Chloroform-acetone (1:1, v/v)	1A	8.8	5.56	—	30,900	0.34
	1B	5.3	5.49	—	31,300	0.38
	2	12.6	6.07	—	28,300	0.38
	3	28.9	6.54	—	26,250	0.34
	4	25.3	7.24	—	23,600	0.30
	5	3.4	—	0.210	15,600	—
Unfractionated	CT/1	—	6.20	—	28,600	0.27
Tetrachlorethane	First	35	—	0.720	37,700	—
Acetic acid	First	25	—	1.05	49,200	—
Chloroform	—	99	—	0.720	37,700	—
Unfractionated	CT/2	—	4.49	—	38,200	0.38

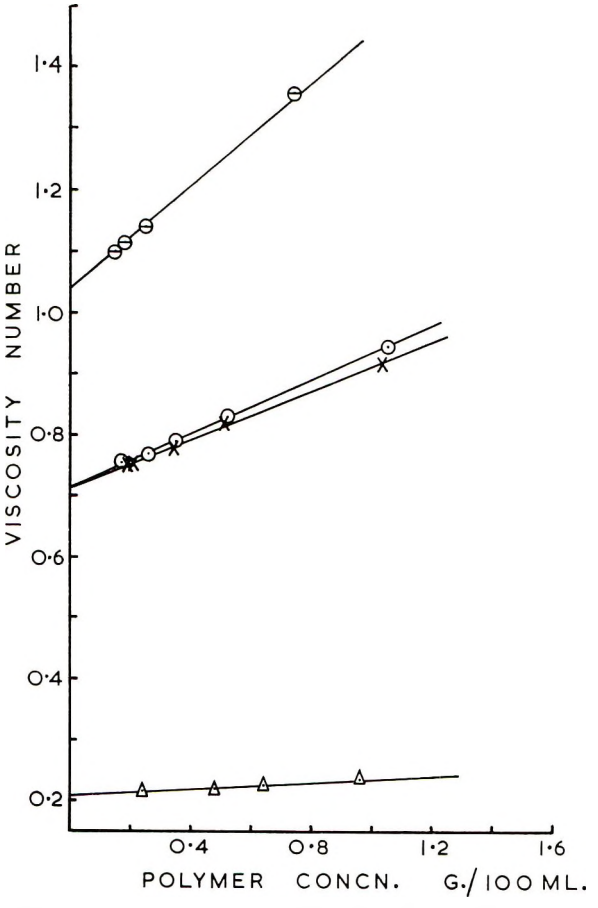

Fig. 3. Viscosity number vs. concentration plots for cellulose triacetate samples: (⊖) 25% precipitated from acetic acid; (⊙) 99% precipitated CT/2 from chloroform; (×) 35% precipitated from tetrachloroethane; (△) fraction 5.

Limiting h/c values were converted to π/c values by multiplying by the solvent density (d_0). Here M_0 is the molecular weight of the solvent, and a density (d) of 1.29 g./ml. for cellulose triacetate was taken from the literature.[17] Owing to the small amount of fraction 5 obtained (0.7 g.) its molecular weight was determined viscometrically. The reduced osmotic head (h/c) versus concentration plots are shown in Figure 2 and the viscosity number versus concentration plots shown in Figure 3.

DISCUSSION

It is evident from the results obtained (Table III) that, in spite of careful control of the fractionation conditions and choice of solvent and precipitant, only slight fractionation with respect to molecular weight takes place. This is confirmed in the case of tetrachlorethane as solvent (later discussion shows that it must also be expected for chloroform) but not for acetic acid, where substantially better molecular weight separation is noted and supports the findings of previous workers.[4,6] The possibility of poor fractionation being due to occlusion of low molecular weight material seems unlikely, in view of the washing of fractions with solvent–precipitant mixture and their complete reprecipitation in the case of tetrachlorethane and acetic acid. The molecular weight of the first fraction from acetic acid may, if anything, be low since some degradation may have occurred while heating the solution. The fractionation behavior of cellulose triacetate can only be attributed to some type of polymer–solvent interaction which adversely affects the relative distribution ratios, between swollen polymer phase and solution, for each of the molecular weight species present.

The thermodynamic requirement for equilibrium between the precipitated and solution phases, that the respective chemical potentials for the solvent and each polymeric species are the same in each phase, leads to the relationships[18]

$$\ln (v'_x/v_x) = \sigma x \tag{2}$$

and

$$\sigma = v(1 - 1/\bar{x}_n) - v'(1 - 1/\bar{x}'_n) + \chi[(1 - v)^2 - (1 - v')^2] \tag{3}$$

Thus the volume fraction v'_x of polymeric species of chain length x, in the swollen precipitated phase, must always be greater than its corresponding value, v_x, in the dilute solution phase, provided σx is greater than unity. The exponential increase in the proportion of higher molecular weight species in the precipitated phase as x increases accounts for the successful fractionation of polymers by precipitation from solution. The magnitude of σ is dependent on the volume fractions of polymer in the solution and precipitated phases, denoted by v and v', respectively, and on the number-average chain lengths $\bar{x}_n$ and $\bar{x}'_n$ of the polymer in the two phases. The interaction parameter χ includes both enthalpy and entropy terms for the

mixing of liquid polymer (noncrystalline with randomly oriented chains) with the solvent. Thus it can be expressed by

$$\chi = \chi_H + \chi_S \tag{4}$$

and in the absence of specific polymer–solvent interaction the enthalpy of mixing term χ_H has been estimated by using the cohesive energy density approach.[19] The χ_S term includes additional entropy contributions due to polymer–solvent interaction and chain flexibility and, together with the statistically derived configurational entropy of mixing, makes up the total entropy of mixing, ΔS_m, for the process. Scott[20] has shown that, for certain values of v, v', and $\bar{x}_n$, the value of σ decreases very rapidly when the value of χ is decreased below 0.5, thereby reducing the efficiency of fractionation [eq. (1)]. It is clear that for zero or slightly negative values of σ both nonfractionability or reverse-order precipitation are possible. Conversely, all other factors being equal, a better fractionation with respect to molecular weight would be obtained for higher values of χ. Thus, the factors believed to affect the magnitude of the polymer–solvent interaction parameter χ are heat of mixing of polymer and solvent, flexibility of the polymer chain, and its molecular weight, as already discussed by Huggins.[21]

Spurlin,[22] on the basis of the Lewis acid-base theory, has classified chemical groups in order of increasing solvating ability and suggested that molecules (or units of a polymer chain) containing acid groups could be solvated by those containing basic or electron donor groups. If in the present system cellulose triacetate behaves as a base, then its solvation by acidic compounds such as chloroform, tetrachlorethane, and acetic acid would be expected. It is of course well known that chloroform, for example, forms azeotropes with such basic solvents as acetone and methyl acetate, and such strong interaction is accounted for by hydrogen bonding between the two components. In the same way it is proposed that chloroform, tetrachlorethane, and acetic acid form hydrogen-bonded complexes with cellulose triacetate in solution represented in the case of chloroform by

$$\mathrm{R{-}O{-}\underset{\displaystyle \underset{\displaystyle CH_3}{|}}{C}{=}O} + \mathrm{H{-}CCl_3} \rightleftharpoons \mathrm{R{-}O{-}\underset{\displaystyle \underset{\displaystyle CH_3}{|}}{C}{=}O{\cdots}H{\cdots}CCl_3} \tag{5}$$

where R represents the rest of the structural unit forming part of the cellulose triacetate chain. A maximum of three chloroform molecules per glucopyranose unit could be taken up by this means. Confirmation of this is provided by the infrared data of Clément[23] for cellulose triacetate dissolved in chloroform, tetrachlorethane, or methylene chloride. Heats and entropies of dilution for cellulose triacetate in tetrachlorethane, from osmotic pressure studies, also provide evidence for considerable solvation in this system.[24] It is interesting to note that, unlike cellulose diacetate or nitrate, the triacetate dissolves rapidly with little swelling in the solvents studied. This is attributed to hydrogen bond formation between polymer and solvent molecules, the associated enthalpy change largely compensating for the dispersion energy required to separate the polymer chains.

Assuming that the value of χ_S [eq. (4)] is virtually independent of the type of solvent, as found for poly(methyl methacrylate),[25] then clearly the heat of mixing contribution, χ_H, will largely determine the magnitude of χ. Thus if the heat of mixing is either very small or becomes slightly negative in the case of cellulose triacetate solutions, then the consequent reduction in the χ value could result in a correspondingly much larger decrease in the value σ which would account for the very poor fractionability observed in these systems. The relatively low mean value of 0.34 for χ in chloroform (Table III) and the value of 0.29 reported[24] for tetrachlorethane are in agreement with the nature of the polymer–solvent interaction proposed.

The comparatively better molecular weight separation noted for cellulose triacetate in acetic acid solution (Table III) and noted earlier[4,6] can also be explained. Acetic acid exists mainly in the dimerized form due to intermolecular hydrogen bonding, so in the case of cellulose triacetate a restriction in the number of hydrogen bonds formed between polymer and solvent molecules would be expected. This means that the heat evolved due to hydrogen bond formation would be smaller for a given polymer molecule than in the case of chloroform and tetrachlorethane, so that the heat of mixing term χ_H should be larger (more positive) in the case of acetic acid. It follows, from what has been said earlier, that this should increase the value of χ [eq. (4)] for this system and hence improve the fractionability. As far as can be ascertained from the literature, the value of χ for cellulose triacetate in acetic acid has not been determined.

The theoretical relationship between osmotic pressure and molecular weight [eq. (1)] implies that the value of χ should remain constant over the molecular weight range investigated. In the present case it is seen to vary between 0.27 and 0.38 (Table III), and a similar variation in the π/c versus c slope has also been observed for cellulose acetate fractions in acetone.[26,27] There is some tendency for χ to increase with molecular weight in the case of cellulose triacetate (Table III), corresponding with the highest slope being observed for the lowest molecular weight as found by Moore and Tidswell;[26] this, however, is opposite to the trend reported by Philipp and Bjork.[27] Further conclusions seem unwise, since the present results refer only to a very narrow molecular weight range.

The comparable values of χ for cellulose triacetate in tetrachlorethane and chloroform are consistent with the same type of polymer–solvent interaction occurring in both cases. Similarly, both chloroform and tetrachlorethane are very good solvents for cellulose triacetate, the latter having a much higher solubility in these than in acetic acid.[28]

Assuming that specific polymer–solvent interaction in the form of hydrogen bonding leads to poor fractionation, then it might be expected that polymers such as poly(methyl methacrylate) and poly(vinyl acetate) would be difficult to fractionate from proton-donor solvents such as chloroform, tetrachlorethane, or methylene chloride. As far as can be ascertained from the literature,[29] fractional precipitation from these systems has not been reported, although a chloroform–benzene solvent mixture (1:3) has been successfully used for poly(methyl methacrylate).

References

1. Choudhury, P. K., *J. Indian Chem. Soc.*, **24**, 271 (1947).
2. Lachs, H., J. Kronman, and J. Wajs, *Kolloid-Z.*, **79**, 91 (1937).
3. Levi, G. R., and A. Giera, *Gazz. Chim. Ital.*, **67**, 719 (1937).
4. Levi, G. R., U. Villotta, and M. Monticelli, *Gazz. Chim. Ital.*, **68**, 589 (1938).
5. Okunev, P. A., and O. G. Tarakanov, *Khim. Volokna*, **6**, 44 (1963).
6. Bezzi, S., and U. Croatto, *Atti Ist. Veneto Sci.*, **99**, 905 (1939–40).
7. Thinius, K., and L. Dimter, *Plaste Kautschuk*, **6**, 547 (1959).
8. Kido, I., and K. Suzuki, *Sen-i Gakkaishi*, **16**, 83 (1960).
9. Münster, A., *J. Polymer Sci.*, **5**, 333 (1950).
10. Langhammer, G., *Makromol. Chem.*, **21**, 74 (1956).
11. Fort, R. J., R. J. Hutchinson, W. R. Moore, and M. Murphy, *Polymer*, **4**, 35 (1963).
12. Howard, P., and R. S. Parikh, *Indian J. of Chem.*, **3**, 191 (1965).
13. Pinner, S. H., and J. V. Stabin, *J. Polymer Sci.*, **9**, 575 (1952).
14. Bruss, D. B., and F. H. Stross, *J. Polymer Sci.*, **55**, 381 (1961).
15. Allen, P. W., Ed., *Techniques of Polymer Characterization*, Butterworths, London, 1959.
16. Howard, P., and R. S. Parikh, unpublished work.
17. Dulmage, W. J., *J. Polymer Sci.*, **26**, 277 (1955).
18. Flory, P. J., *Principles of Polymer Chemistry*, Cornell Univ. Press, Ithaca, 1953.
19. Small, P. A., *J. Appl. Chem.*, **3**, 71 (1953).
20. Scott, R. L., *J. Chem. Phys.*, **13**, 178 (1945).
21. Huggins, M. L., *Ann. N. Y. Acad. Sci.*, **44**, 431 (1942).
22. Spurlin, H. M., in *Cellulose and Cellulose Derivatives*, Part III, E. Ott, H. M. Spurlin and M. W. Grafflin, Eds., Interscience, New York, 1955.
23. Clément, P., *Ann. Chim. (Paris)* [12], **2**, 420 (1947).
24. Hagger, O., and A. J. A. van der Wyk, *Helv. Chim. Acta*, **23**, 484 (1940).
25. Tompa, H., *Polymer Solutions*, Butterworths, London, 1956.
26. Moore, W. R., and B. M. Tidswell, *J. Appl. Chem.*, **8**, 232 (1958).
27. Phillip, H. J., and C. F. Bjork, *J. Polymer Sci.*, **6**, 549 (1951).
28. Howard, P., and R. S. Parikh, unpublished work.
29. Guzmann, G. M., *Progress in High Polymers*, Vol. I., J. C. Robb and F. W. Peaker, Eds., Heywood, London, 1961.

Résumé

On a obtenu six fractions de triacétate de cellulose par précipitation fractionnée dans l'éther de pétrole à partir d'une solution dans un mélange chloroforme–acétone. Le poids moléculaire de chaque fraction a été déterminé par osmométrie en solution chloroformique. On a montré que la soi-disant non-fractionabilité du triacétate de cellulose en fonction de son poids moléculaire, a lieu dans ce système. Ce comportement est aussi observé dans le cas d'un fractionnement à partir d'une solution dans le tétrachloroéthane ou l'acide acétique. On explique ces résultats par l'hypothèse d'une interaction spécifique polymère–solvant, due à un lien hydrogène.

Zusammenfassung

Mit Petroläther als Fällungsmittel und Chloroform-Acetongemisch als Lösungsmittel wurden sechs Zellulosetriacetatfraktionen durch fraktionierte Fällung erhalten. Das Molekulargewicht jeder Fraktion wurde osmotisch in Chloroformlösung bestimmt. Es wurde gezeigt, dass praktisch eine Fraktionierung des Zellulosetriacetats nach dem Molekulargewicht in diesem System nicht möglich war. Dies Verhalten wurde auch bei Fraktionerungsversuchen aus Tetrachloräthan- oder Essigsäurelösungen beobachtet. Die Ergebnisse werden durch die Annahme erklärt, dass auf Grund der Wassertoffbindung eine spezifische Polymer-Lösungsmittelwechselwirkung stattfindet.

Received June 1, 1965
Prod. No. 4834A

JOURNAL OF POLYMER SCIENCE: PART A-1 VOL. 4, 419–430 (1966)

γ-Radiation-Induced Ionic Polymerization of Pure Liquid Styrene

R. C. POTTER, C. L. JOHNSON, and D. J. METZ, *Brookhaven National Laboratory, Upton, New York* and R. H. BRETTON, *Department of Engineering and Applied Science, Yale University, New Haven, Connecticut*

Synopsis

Pure liquid styrene, carefully purified and exhaustively dried, exhibits kinetic behavior under γ-irradiation that can best be described in terms of an ionic mechanism. This is based on the observed linear dependence of the rate of polymerization on the dose rate, the independence of molecular weight on the same parameter, and comparison with the thermal and ultraviolet initiated polymerization of monomer prepared under the same stringent conditions. The highest rate of conversion to polymer is 400%/hr. at a dose rate of 10^6 rads/hr., corresponding to a $G_{(-\text{monomer})} \approx 40{,}000$.

INTRODUCTION

Prior to the studies of Worrall[1–4] and Dainton[5] on the radiation polymerization of liquid isobutylene, it had been fairly well established and accepted that radiation-induced vinyl polymerization in liquid monomers proceeded via a free-radical mechanism. These conclusions had been based on the kinetic behavior exhibited by these systems by using criteria developed from years of experimental data amassed in studies of chemically and photochemically initiated reactions. The polymerization of isobutylene by high energy radiation and the kinetic behavior of the process with respect to various experimental parameters caused much speculation as to the universality of this behavior and initiated several investigations of other monomers.

Much of the published work spurred by this quest has centered on employing extremely low temperatures[1–5] (to favor ionic over free-radical propagation), solid additives[2,3] (to act as electron traps), or solvents of reasonably high dielectric constant[6,7] (to promote stabilization of ion-pairs and free ions).

On the other hand, several workers have concentrated on studying ultrapure and ultradry hydrocarbon monomers,[8–13] preferring to avoid the additional problems occasioned by the presence of either a second phase or a homogeneously distributed second component. These studies have all been plagued with a common problem—irreproducibility of absolute values of the data. However, in the case of α-methylstyrene, Williams[9,10] and Hirota[14,15] have been able to propose mechanisms which involve ionic inter-

mediates, but these workers do not yet agree as to the nature of the species present. We hope to be able to shed some additional light on this particular reaction in a subsequent publication.

The present communication involves studies which we have conducted with styrene. Despite the fact that the kinetics of the radiation-induced polymerization of liquid styrene monomer had been long ago established, on the basis of data collected from workers all over the world and using various types of ionizing radiation, we undertook a reinvestigation based on suspicion and blessed by a sprinkling of serendipity. Our suspicions have been rewarded in that we have unquestionably uncovered a heretofore unobserved kinetic behavior of styrene.

EXPERIMENTAL PROCEDURE

Monomer Purification

Styrene (Eastman Organic Chemical Co.) is purified by distillation through a 6-ft. Heli-grid packed column, under a helium atmosphere (42 mm. Hg). Purity of the distillate is established by vapor-phase chromatographic analysis with a 4-ft. column of 20% Ucon 50 HB 2000 on 60/80 Chromosorb P with flame ionization detection. Sample purity generally ranges between 99.90 and 99.95%.

Sample Preparation

A sample of approximately 15 ml. is collected in an ampule (see vessel A, Fig. 1) that is attached to the product take-off assembly of the still. When sample collection is completed, the contents of the ampule are frozen, after the ampule has been isolated from the distillation apparatus by freezing a U-tube filled with monomer that is interposed between the still and the ampule containing the monomer. The ampule is then removed from the still by flame sealing at 1 (Fig. 1).

Vessel A is then sealed to the high vacuum manifold through the side arm containing breakseal 2, and the monomer is kept frozen during the subsequent steps. Vessel B, containing silica gel, and vessel C (an ampule in early experiments, a dilatometer in later ones) are enclosed in an electrically heated oven (shown by broken lines) and are heated to desired temperature for bake-out. The remainder of the manifold and glass tubing connections which do not fit within the oven are wrapped in heater tape. The pressures achieved during bake-out are in the range 10^{-7}–10^{-8} torr.

After bake-out has been completed, the breakseal 2 is broken, and the monomer in vessel A is degassed by successive freezing–pumping–thawing cycles. The thoroughly degassed monomer is then distilled onto the silica gel by surrounding vessel B with an ice–water mixture. When approximately 10 ml. of monomer have been transferred, the contents of vessels A and B are frozen, and vessel A is removed from the manifold by flame sealing. Monomer is allowed to equilibrate with the silica gel in vessel B at room temperature, after which it is distilled into vessel C by surrounding

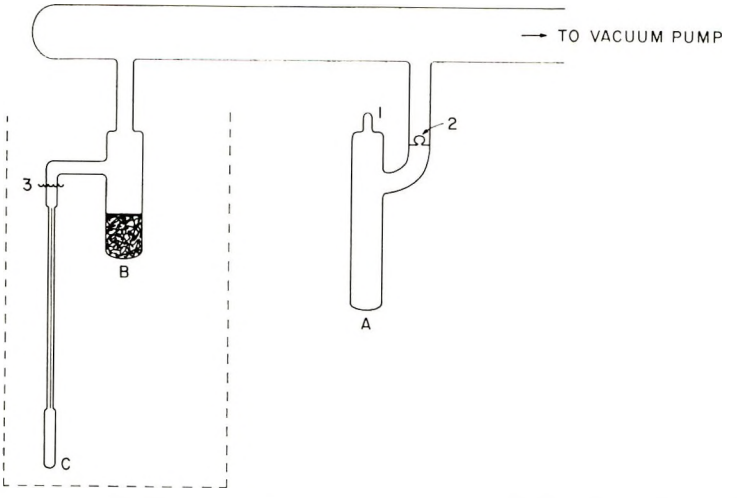

Fig. 1. Schematic diagram of sample preparation manifold. Broken line indicates approximate position of baking oven. Ampules baked according to schedule in Table I; dilatometers baked at 400°C. for 36 hr.

that vessel with an ice–water mixture. When sufficient monomer has been transferred to C, both B and C are frozen with methanol–Dry Ice baths and vessel C is sealed at point 3 and removed from the manifold. The sample thus prepared is then stored at Dry Ice temperature until it is ready for irradiation.

Irradiations and Dosimetry

Irradiation of samples is done in one of several Co^{60} γ-ray cells. Those irradiations involving dilatometric studies were performed in "dry" cells providing visual access to the sample by means of periscopes. Ampule experiments were conducted in an underwater irradiation facility. In either situation, temperature control was achieved by the use of ice–water baths for 0°C., and electrically heated constant temperature baths for higher temperatures.

Dosimetry was performed by either directly employing the Fricke dosimeter[16] ($G_{Fe^{+++}} = 15.5$) or an n-on-p solar cell[17] that was periodically recalibrated against a Fricke dosimeter.

Rate of Polymerization

In ampule experiments, after irradiation the ampules were opened, a measured aliquot of the sample therein was taken, diluted with benzene, and slowly added to a large excess of methanol. The precipitated polymer was separated by filtration, washed several times with methanol, dried, and weighed. The rate of polymerization of each sample was calculated from the weight of isolated polymer and the length of time of the irradiation.

The rate of polymerization in the dilatometric experiments was calculated from the rate of contraction of volume of the sample, assuming a linear

relationship between per cent volume contraction and per cent conversion to polymer to be a reasonably reliable measure over the conversion range of 0–20%. Repeated checks by isolation and weighing of polymer confirmed that this procedure was reliable to within 1%. To minimize the heat transfer problem occasioned by the very high rates of polymerization encountered, the dilatometers were constructed with a bulb surface-to-volume ratio of approximately 5:1. This was achieved by employing thin (ca. 5 mm. from front to rear) long, rectangular bulbs (ca. 2.5 × 8.5 cm.). This design also minimizes the problem of dose rate distribution from front to rear of the sample.

Molecular Weight

The viscosity-average molecular weights of several polymer samples were calculated from intrinsic viscosity values determined from dilute solution viscosity measurements in benzene at 30°C. by using the relationship:[18]

$$[\eta] = 1.54 \times 10^{-4} \overline{M}_v^{0.73}$$

EXPERIMENTAL RESULTS

Table I contains data that were obtained in ampule irradiations, under several combinations of bake-out temperatures and times. For purposes of comparison several entries of more classical values[19,20] have also been included. Although these data do not warrant a very searching quantitative analysis, several points are rather obvious. These are: (*1*) rates of polymerization that are considerably higher than previously reported values can be achieved; (*2*) the accepted dependence of the rate of polymerization on the square root of the dose rate may not hold; (*3*) the average molecular weight of the polymer does not depend on the dose rate or the rate of polymerization; (*4*) the rate of polymerization is strongly dependent on the conditions of sample preparation, and the molecular weight may be somewhat governed by the same experimental parameter; (*5*) irreproducibility of the rate of polymerization is a serious problem.

In view of the last cited observation, we decided to undertake a more detailed investigation of the rate of polymerization and its order dependence on the dose rate by means of dilatometry. By using dilatometers with sufficiently long stems and maintaining a large ratio of bulb volume to volume in the stem, we have been able to investigate rate of polymerization versus dose-rate for a given (and hence inherently reproducible) single system.

The results of such studies with several dilatometer samples are presented graphically in Figure 2. Included in this figure are the lower full curve calculated from the data compiled by Chapiro[21] (corrected to 0°C. assuming an activation energy of 7.15 kcal./mole)[21] and a superimposed broken line with a slope of one-half. These two entries show the accepted square-root dependence of rate of polymerization on dose rate from previously reported data.

TABLE I
Radiation-Induced Polymerization of Styrene

Sample	Baking temperature, °C.	Baking time, hr.	Irradiation temperature, °C.	Dose rate, Mrad/hr.	Total dose, Mrad	Conversion per unit dose, wt.-%/Mrad	$R_p \times 10^4$, mole/l./sec.	$\bar{M}_v \times 10^{-3}$
Ballantine[20]	—	—	22	0.190	9.12	2.5	0.12	42.0
Chapiro[21]	—	—	20	0.012	—	5.0	0.014	84
1	—	—	30	0.224	0.250	2.4	0.13	—
2	250	4	0	0.041	0.200	6.4	0.065	68.9
3	250	4	0	0.205	0.100	6.1	0.31	63.8
4	250	4	0	0.205	0.100	0	0	—
5	250	4	0	0.205	0.100	3.0	0.15	—
6	250	4	0	1.0	0.25	7.0	1.7	67.3
7	400	10	0	0.205	0.100	15.3	0.78	—
8	400	10	0	3.2	0.10	8.0	6.3	—
9	400	12	0	0.224	0.250	57.2	3.2	78.9
10	400	12	0	0.224	0.112	56.3	3.1	79.3
11	400	12	0	0.224	0.112	9.2	0.52	72.1
12	400	12	0	0.224	0.112	24.1	1.3	75.2
13	400	12	0	0.224	0.112	3.6	0.20	—
14	400	12	30	0.224	0.250	48.0	2.58	60.8

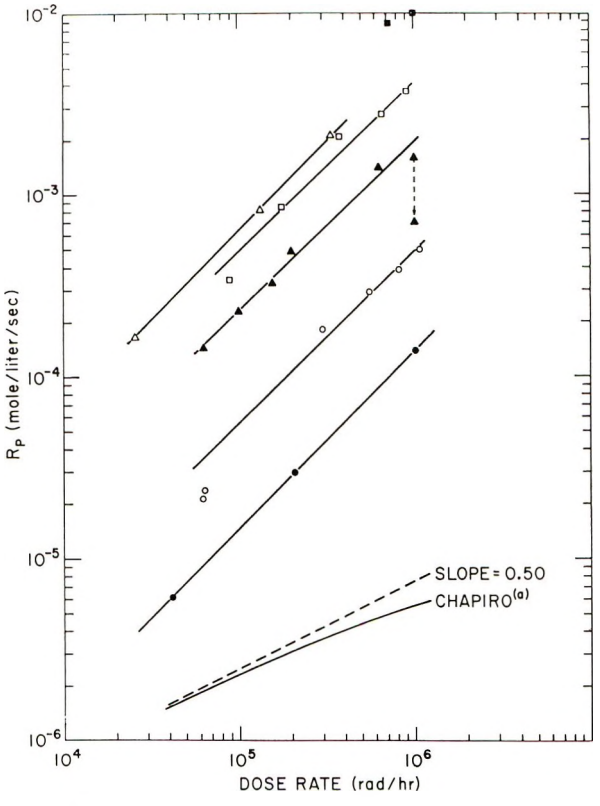

Fig. 2. Rate of polymerization of styrene at 0°C. vs. dose rate: (●) ampules; (○) S-5; (▲) S-6; (□) S-7; (■) S-8; (△) S-10 (at 40°C.). (a) See Chapiro.[21]

The lowest of our experimental curves shown in Figure 2 is composed of data obtained in three ampule experiments. These are identified in Table I as samples 2, 3, and 6 and correspond to the maximum rates observed under the stipulated conditions of sample preparation (see Table I). The remaining curves in Figure 2 refer to the data we have obtained dilatometrically. With the exception of the one sample (S-10) all of these data were obtained at 0°C. Two points are immediately obvious. First, our data show an order dependency of the rate of polymerization on the dose rate which differs widely from the square-root value, previously accepted,

TABLE II
Order Dependence of Rate of Polymerization on Dose Rate ($R_p \propto I^n$)

Sample	Order dependence (n)
Ampules	0.98
S-5	0.94
S-6	0.92
S-7	0.93
S-10	0.97

and hover about the value 1.0. The actual order dependencies, as calculated from the lines in Figure 2, are collected and given in Table II.

Secondly, our dilatometric rates clearly demonstrate that rates of polymerization, under comparable dose rates, can be as great as three orders of magnitude higher than previously reported values.

It is unfortunate that there are still variations in actual rates among the various dilatometer samples. However, despite these variations, the order dependence of the rates is, within the limits of experimental error, identical from one sample to another.

The two uppermost points in Figure 2 are not connected by a curve, since it is not recommended that much reliance be placed on "sympathetic" curves. As a basis for speculation below, however, let it be noted that the slope of a straight line connecting these two points would be 0.5. It should be stated that the reason that only two dose rates were obtained with this sample is that its rate of polymerization was so high, that there was not enough dilatometer stem left for any lower dose measurements.

In order to investigate the possibility that the extreme conditions of sample preparation (monomer purity, dryness of monomer and glassware) might have so affected the system that even the more conventional polymerization kinetics of styrene might have been correspondingly altered, we prepared a dilatometer on which the following sequence of experiments was performed at 40°C.: (*1*) thermal initiation, (*2*) ultraviolet initiation, and (*3*) γ-ray initiation.

The thermal rate of initiation which we observed was 5.4×10^{-7} mole/l./sec. as compared to a value of 5.0×10^{-7} mole/l./sec. quoted by Boundy and Boyer.[22]

We were not able to directly compare the rates of polymerization which we obtained under ultraviolet irradiation with published data as to absolute value. Instead, we have plotted the rate of polymerization versus intensity of illumination (as measured by a solar cell) in Figure 3. The order dependency of our measured rates on intensity is 0.45, establishing the square-root dependence on intensity for our sample for this mode of initiation.

Also plotted in Figure 3 are the results of our γ-radiation-initiated polymerization of the same sample, as a function of dose rate. For this mode of initiation we obtain, once again, a linear dependence (0.97) of rate of polymerization on dose rate.

The data of the γ-radiation-initiated reaction of this latter sample are also plotted in Figure 2, where it can be seen that these data fall within the spread of results previously obtained at 0°C.

One final point can be mentioned, involving sample S-6 in Figure 2. When the desired dose rate range had been covered, the top of the dilatometer was cut off and the bulb of the dilatometer was cooled to Dry Ice temperature. It is presumed that such treatment caused the introduction of small quantities of oxygen (air) and water into the sample by diffusion through the 50-cm. length of 1-mm. capillary. The dilatometer was thermally re-equilibrated at 0°C. and reirradiated. Compared to the

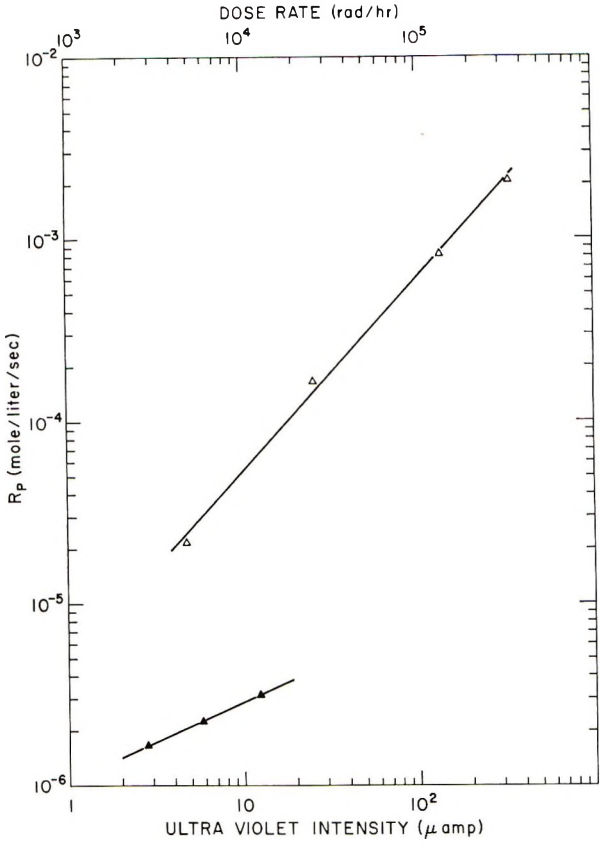

Fig. 3. Rate of polymerization of styrene at 40°C. vs. intensity of ultraviolet light and γ-ray dose rate.

initially measured rate of polymerization at a dose rate of 10^6 rads/hr., the rate decreased by a factor of two after exposure to the atmosphere.

CONCLUSIONS AND DISCUSSION

A linear dependence of the overall rate of polymerization on the dose rate (rate of initiation) and the apparent lack of dependence of the molecular weight on the dose rate appears to eliminate the bimolecular termination of growing chains as the primary mode of termination in the reactions studied in this work. Since it has been well established that the free-radical polymerization of styrene involves a bimolecular recombination of propagating radicals[23] and our results appear to rule out this type of termination, we are led to seek for an explanation in terms of either a novel free-radical kinetic scheme or some type of ionic mechanism.

It is simple to show that, if the rate of disappearance of monomer in the initiation step of the conventional free-radical mechanism cannot be neglected with respect to the rate of consumption of monomer in the

propagation step, then the rate of polymerization will involve two terms, one which is proportional to the square root of the initiator concentration and the other proportional to the first power of that concentration. The second (linear) term, however, becomes negligible under the condition that even a modestly long kinetic chain length is involved. Since the molecular weights of our polymers certainly indicate a chain length comparable to values obtained in the conventional free-radical polymerization of styrene, where the square-root dependence on catalyst concentration is known to hold, we must reject this as an explanation of our kinetic results.

Can an ionic mechanism be rationalized? We believe that it can, especially in view of several recent findings in the basic mechanisms of the radiolysis of hydrocarbons. An oft repeated and, admittedly, oversimplified scheme depicting the interaction of a high energy photon with a covalently bonded molecule can be given as follows:

$$AB + h\nu \rightarrow AB^+ + e^- + h\nu' \tag{1}$$

$$AB + h\nu \rightarrow AB^* + h\nu'' \tag{2}$$

$$AB^+ + e^-_{(\text{thermal})} \rightarrow AB^* \tag{3}$$

$$AB + e^-_{(\text{thermal})} \rightarrow AB^- \tag{4}$$

$$AB^* \begin{cases} \rightarrow A\cdot + B\cdot & (5a) \\ \rightarrow A^+ + B^- \text{ or } A^- + B^+ & (5b) \end{cases}$$

Process (1) depicts, in a chemical formulation, the classical Compton scattering process, in which a high energy electron is ejected from the molecule AB and the photon energy (and direction) are altered. Reaction (2) certainly occurs in the gaseous state, and corresponds to simple excitation of the substrate. Reaction (3) shows the recombination of an ion, produced in reaction (1), with an electron [also resulting from reaction (1)] after it has become thermalized, or nearly so. The product of this reaction is a molecule of the substrate which is in an excited state by virtue of the energy liberated in the charge neutralization process. Reaction (4) competes with reaction (3). The former corresponds to the "solvation" of a (nearly) thermal electron, and the extent to which it may occur will be a function of the electron affinity of the molecule AB. Reactions (5a) and (5b) show the decomposition of excited molecules, formed in either reaction (2) or (3) into normal (or excited) radicals or ions.

Strong theoretical arguments had indicated that the electron generated in reaction (1), even in a solvent of such high dielectric constant as water, did not, on the average escape the parent ion.[24] Thus, the lifetime of ions originally formed in reaction (1) were considered to be extremely short, and the net effect of the initial interactions were considered to be the formation of excited molecules, either directly as in reaction (2) or indirectly

by reaction (1) followed immediately by reaction (3). More recent studies on the role of the solvated electron in aqueous media[25] and studies on the induced direct current conductivity in organic media[26] lead to the strong suspicion that the Compton electrons generated in reaction (1), and also secondary electrons produced during the interaction of the Compton recoil electrons during their thermalization, are capable of being separated by rather large distances from their parent ions, even in media of low (macroscopic) dielectric constant.

Based on this type of evidence, it would not then be surprising to find styryl cations and/or styryl anions in irradiated liquid styrene. The presence of both of these species has been reported by Hamill,[27] based on spectrophotometric analysis of dilute solutions of styrene in frozen, amorphous 3-methylpentane irradiated at liquid nitrogen temperature. In addition, Hirota[28] has recently reported the detection of the anion of α-methylstyrene (formed by electron capture by the monomer) by flash spectrophotometry in irradiated liquid monomer.

We feel justified, then, in ascribing the kinetic results we have presented to an ionic propagation process. On the basis of the data available, we cannot offer an unequivocal choice as to whether the principal propagation species is the cation or the anion. That it is probably one and not both is indicated by the linear dependence of the rate of polymerization on the dose rate and the independence of the molecular weight on the dose rate. If both ionic species were propagating in approximately equivalent concentrations, one might expect the dose rate dependence of the rate to be to the one-half power, and the molecular weight to exhibit an inverse square root dependence on the dose rate.

Since the growing styryl anion would be extremely sensitive to and readily destroyed by any protonic impurity, such as traces of water, which tendency is probably greater than that leading to the deactivation of the growing styrene cation, we tend to believe that the propagating species in the kinetic data presented here are more probably cations.

If this argument has any validity, one would expect that more and more exhaustive drying of the monomer would lead to increasing overall rates of polymerization, since, in the total absence of water, the styryl anion should also propagate. Under these conditions, we would predict that ultimately the rate of polymerization, although increased in absolute magnitude by extremely exhaustive drying, would begin to exhibit a square-root dependence on the dose rate. Recalling our remarks in a previous section on "sentimental" curves, those dilatometric results which yielded the highest absolute rates of polymerization, yield a "sentimental" two-point straight line with a slope of one-half. Fortuitous? Probably! We are at present avidly experimentally pursuing this possibility.

Summarizing our results, and stripping away all vestiges of speculation, even that which is reasonably well-founded in other experimental findings, we have demonstrated that exhaustive purification and drying of styrene leads to kinetic results which are completely at variance with the accepted

behavior of this monomer under irradiation in the liquid state. Our method of preparation affects neither the normal thermal rate of polymerization nor the kinetics of the ultraviolet-initiated polymerization, both of which are generally accepted as being free-radical processes. The kinetic results we obtain with γ-radiation initiation are not inconsistent with an ionic mechanism, and we therefore postulate that such a mechanism is operating in our system.

We would like to take this opportunity to thank Dr. D. S. Ballantine for several helpful suggestions, especially regarding details of dilatometric measurements. One of us (R. C. P.) would also like to acknowledge his appreciation to the authorities of the Graduate School at Yale University, for allowing him to pursue his graduate research at Brookhaven National Laboratory.

This work was performed under the auspices of the U. S. Atomic Energy Commission.

This work is taken in part from the Doctoral dissertation of R. C. Potter to be written and submitted to the Graduate Faculty of Engineering and Applied Science, Yale University.

Note added in proof: The authors regret that, through an oversight, no reference was made to the fine work published by Okamura and co-workers [*J. Polymer Sci. B*, **3**, 363 (1965)] on their work with styrene. It is to be noted that both reports agree quite well in those areas that have been investigated in common.

References

1. Davison, W. H. T., S. H. Pinner, and R. Worrall, *Chem. Ind. (London)*, **1957**, 1274.
2. Worrall, R., and A. Charlesby, *Intern. J. Appl. Radiation Isotopes*, **4**, 84 (1958).
3. Worrall, R., and S. H. Pinner, *J. Polymer Sci.*, **34**, 229 (1959).
4. Davison, W. H. T., S. H. Pinner, and R. Worrall, *Proc. Roy. Soc. (London)*, **A252**, 187 (1959).
5. Collinson, E., F. S. Dainton, and H. A. Gillis, *J. Phys. Chem.*, **63**, 909 (1959); *J. Polymer Sci.*, **34**, 241 (1959).
6. Okamura, S., T. Higashimura, and S. Futami, *Doitai To Hoshasen*, **1**, 216 (1958).
7. Chapiro, A., and V. Stannett, *J. Chim. Phys.*, **56**, 830 (1959).
8. Hirota, K., K. Kuwata, and K. Makino, *Doitai To Hoshasen*, **1**, 104 (1958).
9. Bates, T. H., J. V. F. Best, and T. F. Williams, *Nature*, **188**, 469 (1960).
10. Best, J. V. F., T. H. Bates, and T. F. Williams, *Trans. Faraday Soc.*, **58**, 192 (1962).
11. Baumann, C. G., and D. J. Metz, *J. Polymer Sci.*, **62**, S141 (1962).
12. Johnson, C. L., and D. J. Metz, paper presented at 145th Meeting, American Chemical Society, New York, September 1963.
13. Metz, D. J., *Trans. Am. Nucl. Soc.*, **7**, 313 (1964).
14. Hirota, K., and F. Takemura, *Bull. Chem. Soc., Japan*, **35**, 1037 (1962).
15. Hirota, K., and M. Katayama, *Ann. Rept. JARRP*, **5**, 205 (1964).
16. *ASTM Standards*, Am. Soc. Testing Materials, Philadelphia, 1963, ASTM D 1671-63, Standard Method of Test for Absorbed Gamma Radiation Dose in the Fricke Dosimeter.
17. Muller, A. C., F. X. Rizzo, and L. Galanter, *Nucl. Sci. Eng.*, **19**, 400 (1964).
18. Mayo, F. R., R. A. Gregg, and M. S. Matheson, *J. Am. Chem. Soc.*, **73**, 1691 (1951).
19. Ballantine, D. S., P. Colombo, A. Glines, and B. Manowitz, *Chem. Eng. Progr.*, **50**, 267 (1954).
20. Chapiro, A., and P. Wahl, *Compt. Rend.*, **238**, 1803 (1954).

21. Chapiro, A., *Radiation Chemistry of Polymeric Systems*, Interscience, New York, 1962, p. 164.
22. Boundy, R. H., and R. F. Boyer, *Styrene, Its Polymers, Copolymers and Derivatives*, Reinhold, New York, 1952, p. 220.
23. Smith, W. V., *J. Am. Chem. Soc.*, **71**, 4077 (1949).
24. Samuel, A. H., and J. L. Magee, *J. Chem. Phys.*, **21**, 1080 (1953).
25. Hart, E. J., and J. W. Boag, *J. Am. Chem. Soc.*, **84**, 4090 (1962).
26. Hummel, A., and A. O. Allen, private communication.
27. Guarino, J. P., and W. H. Hamill, *J. Am. Chem. Soc.*, **86**, 777 (1964).
28. Katayama, M., M. Hatada, K. Hirota, H. Yamazaki, and Y. Ozawa, *Bull. Chem. Soc. Japan*, **38**, 851 (1965).

Résumé

Du styrène liquide pur, soigneusement purifié et complétement séché présente sous irradiation gamma un comportement cinétique qui peut être le mieux décrit en termes d'un mécanisme ionique. Ceci est basé sur la dépendance linéaire observée de la vitesse de polymérisation avec la vitesse de dose, l'indépendance du poids moléculaire vis-à-vis du même paramètre et la comparaison avec la polymérisation initiée thermiquement et par rayons ultra-violet dans les mêmes conditions rigoureuses. La plus grande vitesse de conversion en polymère est de 400%/h., à une vitesse de dose de 10^6 rad/h., correspondant à une G (−monomère) de ≈ 40.000.

Zusammenfassung

Sorgfältig gereinigtes und erschöpfend getrocknetes reines flüssiges Styrol zeigt bei Gammabestrahlung ein kinetisches Verhalten, welches am besten durch einen ionischen Mechanismus beschrieben werden kann. Diese Folgerung beruht auf der beobachteten linearen Abhängigkeit der Polymerisationsgeschwindigkeit von der Dosisleistung, von der Unabhängigkeit des Molekulargewichts vom gleichen Parameter und auf dem Vergleich mit der thermisch und UV-angeregten Polymerisation des unter den gleich strengen Bedingungen erhaltenen Monomeren. Die höchste Polymerisationsgeschwindigkeit ist 400% h^{-1} bei einer Dosisleistung von 10^6 rad· h^{-1}, entsprechend einem G (-Monomeren) ≈ 40.000.

Received August 27, 1965
Prod. No. 4843A

NOTES

On the Form III Transformation of Polybutene-1

Temperature-dependent phase transitions of polybutene-1 in the form III modification have recently been discussed in a number of publications.[1,2] The exact nature of the form III to form II transformation and the accompanying transition phenomena have remained in doubt, although a number of divergent theories have been proposed to explain the transformations observed by DTA, x-ray diffraction, and dilatometric techniques.

The divergence of opinions, which exists between various research laboratories, on the nature of the form III transformation, is believed to have arisen as a result of differences in heating rates, which were employed at various locations in the study of this temperature dependent phase transition. Although the three known polymorphs of polybutene-1 can be distinguished by their x-ray diffraction patterns as well as by other methods, an additional crystalline phase of polybutene-1, commonly labeled form I′ polybutene-1,

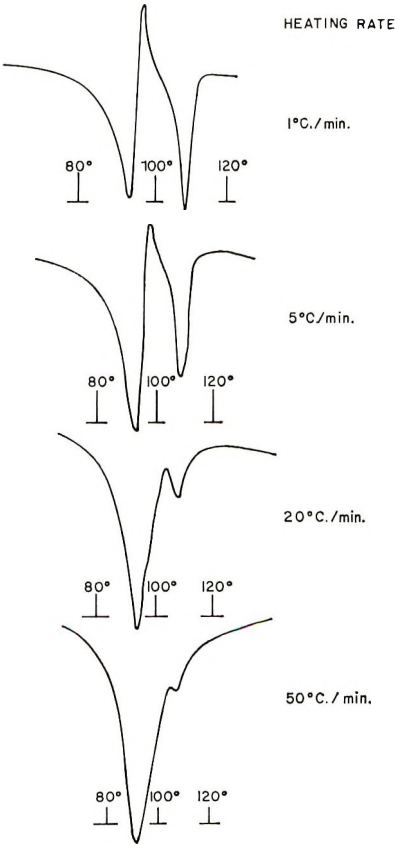

Fig. 1. DTA curves: unannealed form III.

cannot be differentiated from the high melting form I modification of polybutene-1 by common x-ray and infrared methods. This low melting form I′ modification of polybutene-1 was initially identified by Holland and Miller[3] on the basis of single crystal studies.

Our own observations of the form III to form II transformation at relatively slow heating rates (2–3°C. min.), have led to the conclusion that the form III to form II transition is accompanied by the formation, growth, and melting of the form I′ modification of polybutene-1.[4] The presence of the latter, under certain conditions, is believed to have

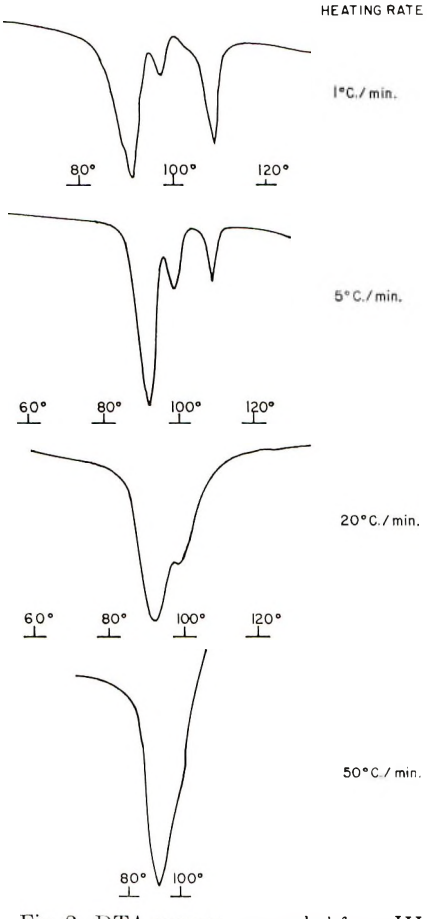

Fig. 2. DTA curves: annealed form III.

led to existing differences of opinion on the nature of the form III transformation of polybutene-1.

The realization that the form I′ modification can also occur during the form III to form II transition has allowed us to design our experiments in such a way as to permit positive identification of the nature of the form III to form II transition.

It is known from classical nucleation theory that the growth of crystals from a melt is governed by both a favorable energy balance, as well as the probability of molecules, or chain transitions across the energy barrier to stable nucleus formation. The latter condition allows the separation of purely time-dependent crystallization processes, from first-order solid–solid transition phenomena.

Differential thermograms of polybutene-1 in the form III modification at various heating rates are shown in Figure 1. It can be seen that the intensity of the form III endotherm remains unchanged at the various heating rates, although the size of the form II modification endotherm decreases proportionally with increasing heating rate. These results demonstrate that the form III phase undergoes a melting transition at 96°C., which fails to recrystallize to the form II phase at higher heating rates. The lack of a melting peak at 100°C. at the faster heating rates (20 and 50°C./min.) also indicates that the crystallization of form I′, presumably from the form III modification, is suppressed at the faster heating rates.

However, since the melting endotherm at 100°C. is somewhat masked by the recrystallization exotherm at 97–98°C., it was of interest to attempt to intensify the former by growing it in the presence of the form III modification. This was achieved by annealing a sample of polybutene-1 in the form III modification at 94°C. for a period of 8 days. DTA thermograms of his sample at various heating rates are shown in Figure 2. Here again, it can be clearly seen that the form II modification fails to recrystallize at the higher heating rates, although now, both the form III and form I′ melting peaks, are clearly discernible.

Conclusions

DTA analysis of the form III modification of polybutene-1 at various heating rates shows conclusive evidence that the form III modification undergoes a melting transition at 96°C., followed by immediate recrystallization, at sufficiently slow heating rates, to the form II modification. Crystallization of a low melting form I′ polymorph from amorphous regions, followed by melting of this crystalline phase at 100°C. and recrystallization to form II, accompanies the form III to form II transition. As in all crystallization processes, the formation and melting of the various phases is very rate sensitive.

We wish to thank Mr. D. Ditoro for the preparation of the DTA thermograms.

References

1. Geacintov, C., R. S. Schotland, and R. B. Miles, *J. Polymer Sci. C*, **6**, 197 (1964).
2. Danusso, F., G. Gianotti, and G. Polizzotti, *Makromol. Chem.*, **80**, 13 (1964).
3. Holland, V. F., and R. L. Miller, *J. Appl. Phys.*, **35**, 3241 (1964).
4. Geacintov, C., R. B. Miles, and H. J. L. Schuurmans, paper presented at 150th Meeting, American Chemical Society, Atlantic City, Sept. 12–17, 1965.

C. Geacintov
R. B. Miles
H. J. L. Schuurmans

Research and Technical Division
Edison Township Laboratory
Mobil Chemical Company
Metuchen, New Jersey

Received September 3, 1965

Furoylation of Cellulose

The industrial use of cellulose esters has been increasing continuously during recent years. With the progress of the utilization of esters, research on the mechanism of cellulose esterification reactions has also been intensified. Many workers have also studied the kinetics of the reactions in order to have a detailed picture of the transformation mechanism. A study of the kinetics requires a precise method of analysis of the product which should be little affected by the side products of the reaction. Most of the kinetics studies have, therefore, been carried out with acetylation, benzoylation, or nitration where the esters are less affected by the side products. In most of the above cases and in many others also, the reactions have been studied in a homogeneous solution. But industrially, the esterification is done by the heterogeneous process; therefore, more attention is needed on the study of heterogeneous kinetics. In order to obtain a complete picture of the mechanism, the reaction should be continued up to total substitution. It appears that in a majority of the cases at higher substitution, esters go into solution and this complicates the study. However, it was noted that the reaction of cellulose with furoyl chloride in the presence of pyridine leads to an insoluble trisubstituted cellulose. It was, therefore, thought that it would be worthwhile to review this reaction in order to explore the possibility of studying its kinetics.

The mechanism of the furoylation reaction has been assumed to be as follows:

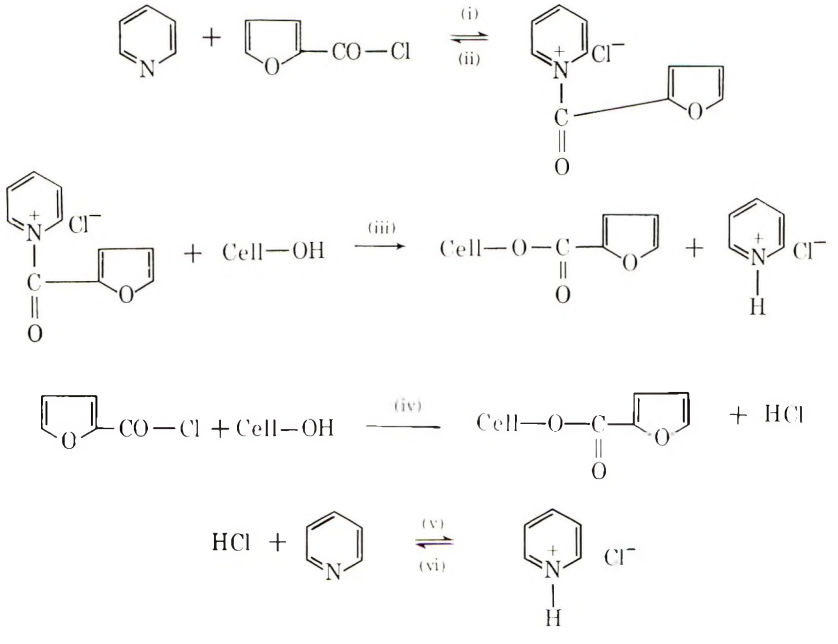

Kobe and Montonna[1] in 1931, the time when commercial development of furfural was progressing rapidly, attempted to make cellulose furoate. Due to the great similarity of furoic acid and benzoic acid, they thought that cellulose furoate would be similar to cellulose benzoate. But they concluded from their experimental results that a portion of the cellulose degraded during the reaction to give a highly substituted amorphous ester which was black or brown in color. They further concluded from saponification data that one of the substituted hydroxyl groups was hindered. However, this ester has not attracted much attention of the cellulose chemists. This was probably because of the unpromising future of a highly colored product.

Following the procedure of Kobe and Montonna furoylation was carried out at 51 and 99°C. with the reagent furoyl chloride–pyridine–tetrachloroethane, mixed in the proportion of 3:3:20. Furoyl chloride was mixed with pyridine in the cold, diluted with tetrachloroethane, and heated to dissolve the precipitate. One gram of the fiber in the form of cheesecloth was then added to the mixture and reacted for the required time. The product was then washed with pyridine, methanol, hot water, and finally dried at 105°C.

Saponification was carried out according to the method of Genung and Mallat[2] with 0.25*N* alcoholic-alkali solution.

It was observed that at 51°C. almost no substitution took place even after 5 hr. of reaction and at 99°C. only 0.27 D.S. (saponification value) is reached after reacting for 1.75 hr. Upon reacting with 3 ml. of furoyl chloride and 23 ml. of pyridine only, for the same time, the D.S. goes as high as 2.12, but the ester becomes brown in color. In the presence of tetrachloroethane substitution up to D.S. 2.2 could be reached only on refluxing for 2.5 hr, but again the product was brown. An unsuccessful attempt was made to wash out the color by using various solvents including binary mixtures. Hot extraction and cold extraction were attempted.

A kinetic run was made at 100°C., using furoyl chloride and pyridine in the proportion of 1:5 by volume and chloride and cellulose hydroxyl groups in the molar proportion of 2:1. The results (Table I) showed the interference of the colored products with the saponification value. On the other hand, it is noticed that the reaction is very rapid. Further experiment was conducted at the same temperature by reacting the fibers for only 2 and 6 min. and the D.S. was found to be 0.91 and 2.32, respectively. The samples were also slightly colored when reacted for 6 min., but remained white up to 2 min. of reaction. It was further observed that if the reaction with the fiber is started imme-

TABLE I
Rate of Furoylation at 100°C.

Reaction time, min.	Apparent D.S. (saponification value)
10	2.70
20	3.29
31	3.90
40	3.24
63	3.59
90	3.98
120	3.15
150	3.40
180	3.51
240	3.26
300	3.72

TABLE II
Effect on the Ester of Reacting the Fiber with Aged Reagent

Reagents	Color of ester	Apparent D.S. from	
		Wt. gain	Saponification
Pyridine + furoyl chloride (heated for 3.5 hr. before reacting with fibers)	Deep brown	2.44	2.50
Pyridine + furoyl chloride (freshly mixed)	White	1.79	1.80

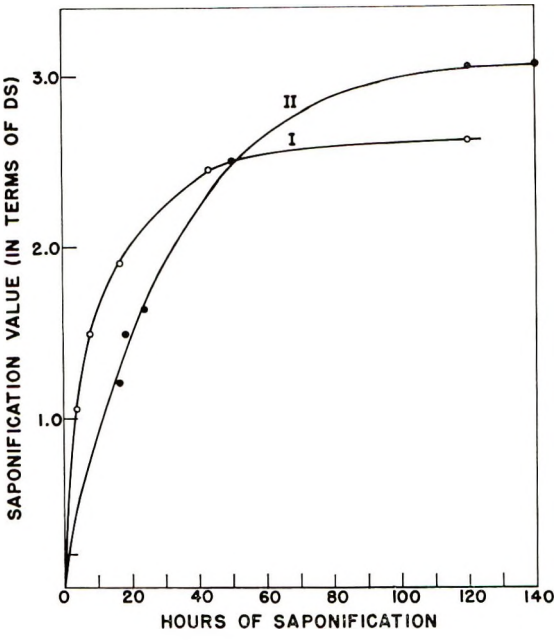

Fig. 1. Saponification value (in terms of D.S.) as a function of time saponification. (I) Partially substituted ester (D.S., 2.61); (II) trisubstituted ester.

diately after the mixing of the pyridine and furoyl chloride, the color intensity decreases for a short time of reaction. Table II shows the effect on the ester of reacting the fiber with aged reagent (chloride + pyridine).

It was therefore believed that the color of the sample was not due to the degradation of cellulose, as was mentioned by Kobe and Montonna, but to some other side product of the reagents.

Some preliminary studies on the interaction between pyridine and furoyl chloride reveal that furoyl chloride, immediately after addition to pyridine, forms a yellowish-white precipitate which gradually turns to brown and on heating dissolves to form a brown solution. When this solution was refrigerated, it deposited white globular crystals together with long brown crystals. On heating further for 10 min. and refrigerating again, these white crystals decreased. After 3 hr. of heating they disappeared completely. On refrigerating, only the brown crystals remained in the mixture. The temperature of the system was then raised to room temperature and the system was kept open to the atmosphere for 24 hr. A thick brown liquid formed which did not recrystallize on refrigeration.

In another experiment the yellow precipitate, which formed immediately after adding chloride to pyridine, was decanted and kept in a vacuum desiccator. The precipitate gradually turned to a brown liquid. On exposing the brown liquid to fresh fibers and partially substituted cellulose furoate (D.S., 1.79; color, white) at room temperature for 20 hr., it was observed that the ester but not the untreated fibers picked up the color and retained it even after washing and drying. Possibly, the colored compound forms a stable complex with the substituted group of the cellulose only.

It is concluded that furoyl chloride and pyridine initially form an unstable complex which decomposes to a brown colored compound and this, in turn, forms a stable complex with the ester groups.

Rate of the saponification was studied in order to determine whether or not any substituted group is hindered as suggested by Kobe and Montonna.[1] Two samples with

minimum color were taken, one trisubstituted and another partially substituted. These were saponified up to 190 hr. Figure 1 shows the rates of the saponification. It may be seen that a smooth curve could be fitted to the plot up to the saturation value. From the figure, the rate of saponification of the partially substituted ester is greater than the rate of saponification of the trisubstituted ester as is often observed. Neither plot shows any break in the curve. The present investigation, therefore, does not indicate that any substituted group is hindered.

Several other bases, such as *N*,*N*-dimethylcyclohexylamine, triethylamine, lutidine, and 2-picoline, have also been tried as reaction media instead of pyridine, but in all cases, except with picoline, the complex which formed with fuoryl chloride did not go into solution even at temperatures above 100°C. In the case of picoline, the color of the fibers did not improve. On the other hand, the reaction rate was decreased significantly.

In fact, the present investigation indicates only one possibility of obtaining a triester with minimum by-product, by reacting at a high temperature for a short time. The reaction should be carried out immediately after mixing pyridine and furoyl chloride. Contrary to the statement of Kobe and Montonna[1] that the browning is due to degradation of cellulose, it is now believed to be due to the side products of the furoylation reaction. Regarding saponification of ester, no substituted group has been found to be more resistant to alkali than the other.

The authors wish to thank Dr. C. M. Conrad for his valuable suggestions.

References

1. Kobe, K. A., and R. E. Montonna, *J. Am. Chem. Soc.*, **53**, 1889 (1931).
2. Genung, L. B., and R. C. Mallatt, *Ind. Eng. Chem., Anal. Ed.*, **13**, 369 (1941).

Pronoy K. Chatterjee*
David J. Stanonis

Plant Fibers Pioneering Research Laboratory
Southern Utilization Research and Development Division
United States Department of Agriculture
New Orleans, Louisiana

Received August 31, 1965

* Postdoctoral Resident Research Associate, 1963–1965.

Preparation and Properties of Poly($\alpha,\alpha,\alpha',\alpha'$-Tetrachloro-p-Xylylene) Films

As shown earlier,[1] $\alpha,\alpha,\alpha',\alpha'$-tetrachloro-*p*-xylylene can be prepared by passing $\alpha,\alpha,\alpha,\alpha',\alpha',\alpha'$-hexachloro-*p*-xylene vapors over copper at 500°C. at reduced pressures:

(I)

Pure, crystalline (I) can be isolated from the pyrolysis vapors in the form of yellow needles. These, either in the crystalline form or as solutions, polymerize rapidly at room temperature to form poly($\alpha,\alpha,\alpha',\alpha'$-tetrachloro-*p*-xylylene), a colorless polymer. During the solid state polymerization of (I) there appears to be no change in the shape of the crystals. The polymer does not melt below 350°C.; at higher temperatures it slowly turns dark without melting. This material cannot be fabricated by classical methods because it is also completely insoluble in all common solvents. Attempts to prepare films by deposition of tetrachloro-*p*-xylylene vapors on cold surfaces have failed. Only yellowish crystals are formed which turn white and rapidly form a polymer.

In order to prepare a coherent film of poly(tetrachloro-*p*-xylylene), (I) has to be deposited in an amorphous state, i.e., as a glass or a liquid and has to be polymerized in this state. The most common experiment seems to deposit (I) at temperatures higher than its melting point. The melting point of (I) cannot be determined by conventional methods because of its high reactivity.[1] Attempts were made to determine the melting point by rapid immersion of crystals[1] of (I) into preheated liquids. All samples polymerized at once without melting.

Vapors of (I) have been passed over surfaces which were heated to various temperatures (20–150°C.) Below 90°C. only crystals of (I) formed. At 100°C. crystals and a large amount of clear film were recovered; at 120°C. and at higher temperatures, only film was produced. This film was treated with an *N,N'*-tetramethylphenylene-diamine solution and gave a positive indication for (I).[1] Heating of the film at about 190°C. for 0.5 hr. completed the polymerization of (I). The presence of free radicals in the freshly prepared film was indicated by a strong ESR signal. When the film was heated to 200°C. in vacuum, the signal disappeared completely within a few minutes. Our investigations of the deposition at various temperatures did not show a small temperature range in which the transition from crystals to film occurred as one would expect if the melting point of (I) were an important variable. From 90 to 110°C. crystals, as well as film, were obtained.

The fact that (I) is deposited as a clear, amorphous film at elevated temperature and as crystals at low temperatures may be explained by another hypothesis. During the deposition of the monomer two competing reactions occur: (*a*) the crystallization of (I) and (*b*) direct polymerization of (I) as soon as it comes in contact with the surface. The higher the temperature, the faster the polymerization; at 120°C. the rate of polymerization is far in excess of the rate of crystal formation.

If this hypothesis were true, other sources of energy should affect the deposition in the same way. (I) shows strong absorptions in the ultraviolet region, therefore, the deposition was carried out with radiation at room temperature. However, only yellow crystals, which turned white rapidly forming polymers, were produced. These results force the conclusion that for film formation the deposition of the monomer in the liquid state is essential.

The mechanical properties of the original poly($\alpha,\alpha,\alpha',\alpha'$-tetrachloro-*p*-xylylene) film and of the film after heat aging at 190°C. for 60 hr., can be seen below. The electrical properties are summarized in Tables I and II.

	Tensile modulus, psi	Tensile strength, psi	Softening range, °C.
Original	480,000	8,000	280–290
After air aging at 195°C. for 60 hr.	400,000	4,400	—

TABLE I
Electrical Properties of Poly($\alpha,\alpha,\alpha',\alpha'$-Tetrachloro-*p*-Xylylene (at 20°C.)

Frequency	Dielectric constant	Dissipation factor
60 cycles	2.81	2.67×10^{-4}
1 kc	2.81	2.54×10^{-4}
10 kc	2.81	2.54×10^{-4}
100 kc	2.81	2.54×10^{-4}

Dielectric strength was run according to ASTM-D 149. All values were converted to $^1/_8$ in. Actual measured readings were about 4870 v./mil for a film of 2.09-μ thickness which was deposited on aluminum. The film was aged at 175°C. in air.

TABLE II
Properties of Heat-Aged Poly($\alpha,\alpha,\alpha',\alpha'$-Tetrachloro-*p*-Xylylene) Film on Aluminum Foil

Elapsed aging time, hr.	Dielectric strength, v./mil ($^1/_8$ in. thickness)	Dissipation factor $\times 10^{-4}$
0	620	5.5
1	620	11.0
17	670	4.0
70	575	2.3
186	525	6.0
500	575	4.5

Films which had been kept in 50% aqueous potassium hydroxide solution, and concentrated nitric and hydrochloric acids, as well as basic hydrogen peroxide solution for two months, were not noticeably attacked.

The author wishes to thank Dr. R. Shaw for ESR spectroscopic determinations.

Reference

1. Gilch, H. G., *Angew. Chem.*, **77**, 592 (1965); *Intern. Ed.*, **4**, 598 (1965).

H. G. Gilch*

Research and Development Laboratories
Plastics Division
Union Carbide Corporation
Bound Brook, New Jersey

Received June 2, 1965
Revised October 1, 1965

* Present address: Farbenfabriken Bayer AG., Werk Uerdingen, Wissenschaftliches Hauptlaboratorium, Krefeld, Germany.

Aromatic Polyesteramideimides

The recent communication by Unishi[1] concerning the polymerization of isophthalyl dihydrazide (I) with pyromellitic dianhydride prompts us to report work in our laboratory on the reaction of (I) with *p*-phenylene-bis(trimellitate) dianhydride[2] (II). The new thermally stable polymer is a linear polyesteramideimide which was prepared in a two step process as shown in the following scheme

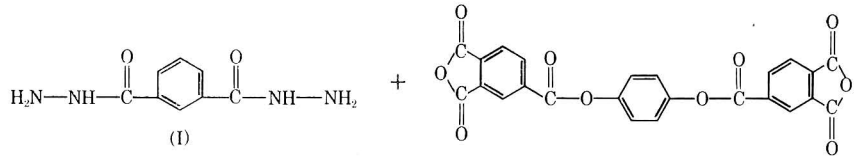

(I)

(II)

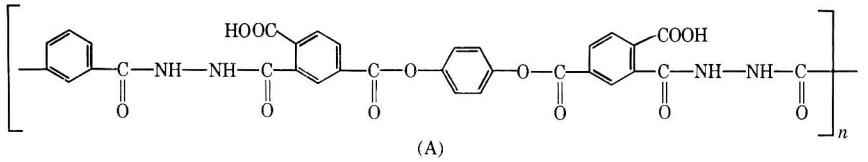

(A)

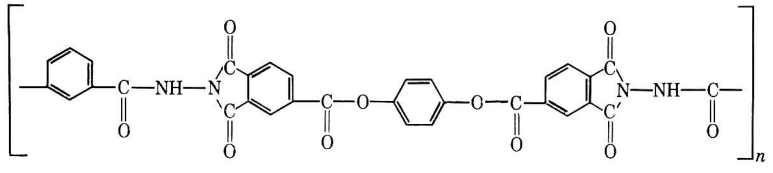

(B)

In the first step, the polyesterhydrazide (A) was prepared by the solution polycondensation reaction. To a mixture of isophthalyl dihydrazide (1.94 g.) and *p*-phenylene-bis(trimellitate) dianhydride (4.58 g.) was added dimethylformamide (60 ml.). The mixture was stirred for 1 hr. at room temperature to yield a viscous polyesterhydrazide solution. This solution was cast directly on glass plates and dried in an air circulating oven at 110°C. for 10 hr. to give tough clear films.

Solid fibrous polymer was precipitated by pouring the polymer solution into water. The polymer was washed with methyl alcohol in a Waring Blendor, filtered, and finally dried at 75°C. under vacuum. The yield was quantitive and the inherent viscosity was 1.18 in dimethylformamide (0.5% at 30°C.). The infrared spectrum of this polyesterhydrazide film is shown in Figure 1 (curve A).

ANAL. Calcd. for $(C_{32}H_{20}N_4O_{12})_n$: C, 58.89; H, 3.07; N, 8.59. Found: C, 58.05; H, 2.57; N, 8.79.

The polymer at this stage is soluble in dimethylformamide, dimethylacetamide, dimethylsulfoxide, *N*-methyl-2-pyrrolidone, and pyridine.

In the second step, the polymer film was heated in an air circulating oven for 1 hr. at 200°C. followed by an additional hour at 240°C., and finally for 30 min. at 300°C. During the heating cycle, the soluble polymer cyclized to form the imide ring along the polymer chain and a polyesteramideimide of high molecular weight was obtained.

The infrared spectrum of the cyclized product is shown in Figure 1 (curve *B*). The dehydration process was followed by the disappearance of the amide I band at 1650 cm.$^{-1}$ and by the appearance of new bands at 1793 and 718 cm.$^{-1}$ characteristic of the imide ring. The polymer at this point was insoluble in organic solvents. Intermediate stages in the cyclization are shown in Figure 2.

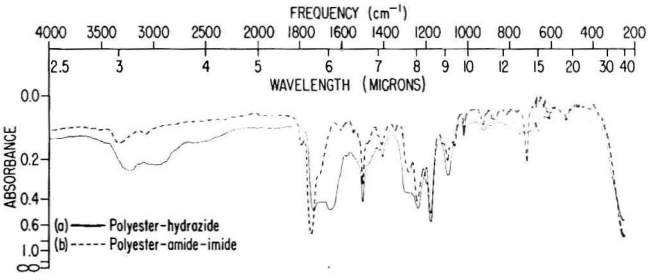

Fig. 1. Polymer before and after cyclization.

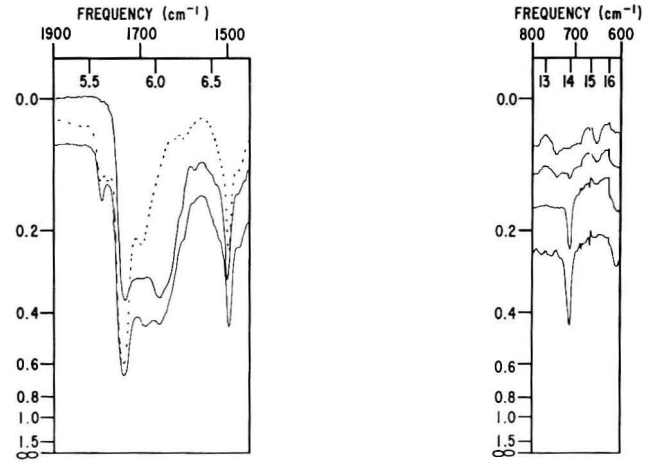

Fig. 2. Intermediate stages of cyclization.

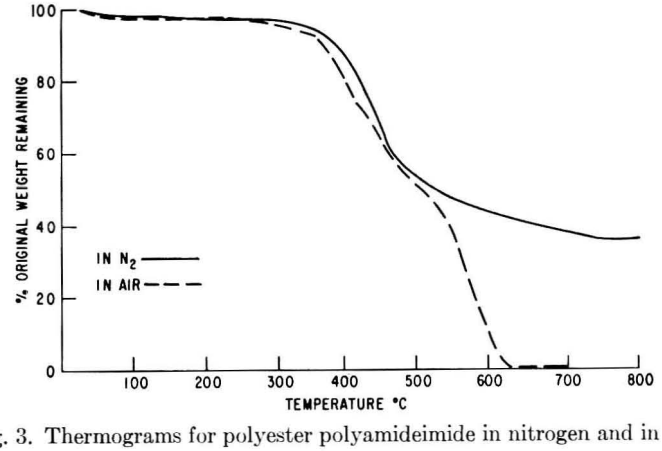

Fig. 3. Thermograms for polyester polyamideimide in nitrogen and in air.

ANAL. Calcd. for $(C_{32}H_{16}N_4O_{10})_n$: C, 62.33; H, 2.60; N, 9.09. Found: C, 62.37; H, 2.63; N, 8.97.

The thermal stability of the resulting cyclized polymer was measured in both nitrogen and air by thermogravimetric analysis as shown in Figure 3. Decomposition in air started around 350°C. In a nitrogen atmosphere, the weight loss was about 75% when heated to 800°C. over a 3 hr. period.

Although Unishi questioned the possible formation of an oxidiazole ring during cyclization of the hydrazide, he made no mention of the possible formation of a six-membered phthalazinedione. Actually a substantial body of literature[3] seems to justify the claim that nitrogen-substituted phthalimides normally rearrange to the more stable six-membered ring. For example, *N*-aminophthalimide (III) readily converts to phthalazine-1,4-dione (IV) at its melting point.

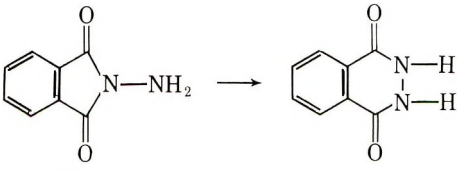

(III) (IV)

However, we have found that *N*-benzamidophthalimide (V), which was synthesized by two methods following the procedures described by Nishie and Kakimoto,[4] was recovered unchanged after 5 min. at 350°C.

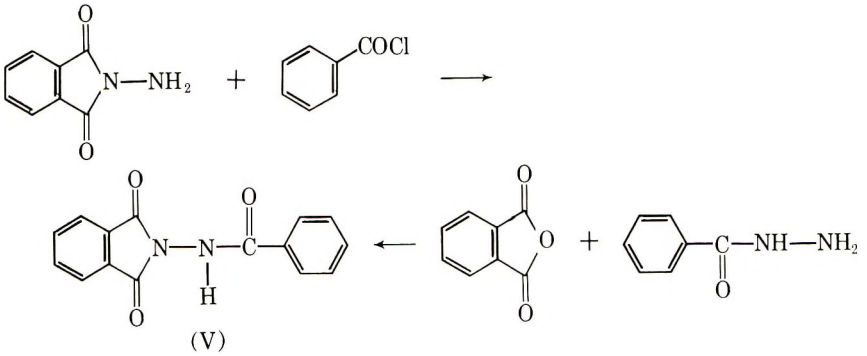

(V)

Infrared bands at 1775–1800 and 700–725 cm.$^{-1}$[5] are consistently observed in all of the imides we have examined. This includes numerous aromatic polymers and the model compounds: V, *N*-phthalimidophthalimide, III, and *N*-phenylphthalimide. Since the *N*-substituting group has varied among these model compounds with no apparent effect on the two "imide"* bands, it is assumed that the assignment holds for our compounds. The two infrared bands were found to be independent of solid state. That is, the bands were observed when the crystalline materials were examined as Nujol mulls and also when examined in solutions in dimethylsulfoxide. The phthalazinedione (IV) has no substantial absorption in the 700–725 cm.$^{-1}$ region. It does have a band at 1782 cm.$^{-1}$ in the crystal state but this band is crystal-structure dependent; it is not detected in dimethylsulfoxide solution.

Our chemical and spectral evidence indicates the *N*-amidoimide structure for our polymer is in agreement with Unishi's published structure.

* The assignment may well be limited to the phthalimides as opposed to succinimides. We have not examined the limitations of the assignment in relation to structures that may be attached at the 3,4-positions.

References

1. Unishi, T., *J. Polymer Sci. B*, **3,** 679 (1965).
2. Loncrini, D. F., U. S. Pat. 3,182,073 (1965).
3. Elderfield, R. C., *Heterocyclic Compounds*, Vol. 6, Wiley, New York, 1957, p. 219–233.
4. Nishie, J., and S. Kakimoto, *Nippon Kagaku Zasshi*, **79,** 1403 (1958); *Chem. Abstr.*, **54,** 5665 (1960).
5. Sroog, C. E., S. Abramo, C. Berr, W. Edwards, A. Endrey, and K. Oliver, *Polymer Preprints*, **5,** 132 (1964).

D. F. Loncrini
W. L. Walton
R. B. Hughes

Insulating Materials Department
General Electric Company
Schenectady, New York

Received September 27, 1965
Revised October 29, 1965

Catalytic Polymerization of 1,3-Disilacyclobutane Derivatives

In a recent publication, Weyenberg and Nelson[1] describe a method for the polymerization of 1,1,3,3-tetramethyl-1,3-disilacyclobutane using platinum on carbon or chloroplatinic acid as catalysts at 100°C. Additional results of a similar nature have been obtained in this laboratory.

It has been found that $PtCl_2$, $IrCl_6^{-2}$, $RuCl_6^{-2}$, $AuCl_4^-$, $PdCl_2$, and RuI_3, in addition to $PtCl_6^{-2}$ and Pt on carbon, will initiate polymerization of 1,3-disilacyclobutane derivatives[2] such as $[(CH_3)_2SiCH_2]_2$, $[C_6H_5(CH_3)SiCH_2]_2$, $[Cl(CH_3)SiCH_2]_2$, and $[C_2H_5O(CH_3)SiCH_2]_2$. The polymerizations were carried out in bulk or in benzene or toluene solutions, using catalyst concentrations of 10^{-5} to 10^{-2} mole-% added as solids or as water solutions when possible. The most active catalysts found were $PtCl_2$, K_2PtCl_6, and $H_2PtCl_6 \cdot 6H_2O$. High polymer conversions were generally obtained.

The character of the polymers varied from extremely viscous, tacky liquids to insoluble, glassy resins depending on the nature, concentration, and activity of both starting materials and catalysts, as well as the temperature. The polyisobutylene analog, polydimethylsilmethylene, could be prepared as a high molecular weight clear rubber, M_n (number-average molecular weight determined by osmometry) around 200,000 ± 1%, with very slight flow properties. This resulted from initiation in bulk with chloroplatinic acid solution at 25°C. At higher temperatures or in solution lower molecular weight (as low as M_n = 8500 ± 1%) products were obtained.

Polyphenylmethylsilmethylene, the poly-α-methylstyrene analog, varied in properties from a clear, tough rubber, soluble in benzene, to a clear, glassy resin which only swelled in common organic solvents. This variance is due to the degree of polymerization. The lower molecular weight species resulted from solution polymerization. The high molecular weight products could be fused at temperatures below 350°C. (above which degradation began). Copolymers from mixtures of $[C_6H_5(CH_3)SiCH_2]_2$ and $[(CH_3)_2SiCH_2]_2$ were generally more rubbery, and were usually insoluble even at ratios of 1:3.

The silicon functional cyclics, $[C_2H_5O(CH_3)SiCH_2]_2$ and $[Cl(CH_3)SiCH_2]_2$ gave low yield viscous liquid polymers. The former was initiated, with difficulty, by platinum

TABLE I
Summary of Polymerization Reactions

Compound	Catalyst, mole-%		Temp., °C.	Conversion, %
$[(CH_3)_2SiCH_2]_2$	$H_2PtCl_6.6H_2O$ (soln.)	10^{-2}	80	94.5[a]
"	"	"	25	84.1[b]
" 50% benzene	"	"	80	94.9
"	K_2PtCl_6 (solid)	10^{-3}	"	>90
"	$PtCl_2$ (solid)	"	"	94.5
"	K_2IrCl_6 (solid)	10^{-5}	"	7.8
"	"	10^{-4}	"	16.5
$[C_6H_5(CH_3)SiCH_2]_2$	"	10^{-2}	"	>90[c]
$[C_6H_5(CH_3)SiCH_2]_2$ (1 part) $[(CH_3)_2SiCH_2]_2$ (3 parts)	$H_2PtCl_6 \cdot 6H_2O$ (soln.)	"	"	>90
$[C_2H_5O(CH_3)SiCH_2]_2$ (1 part) $[(CH_3)_2SiCH_2]_2$ (9 parts)	"	"	"	>90
$[Cl(CH_3)SiCH_2]_2$ (1 part) $[(CH_3)_2SiCH_2]_2$ (99 parts)	$PtCl_2$ (solid)	10^{-3}	"	88.2

[a] ANAL. Calcd. for $(C_3H_8Si)_n$: C, 49.91; H, 11.17. Found: C, 49.81; H, 11.01, $M_n = 3.17 \times 10^4 \pm 1\%$.

[b] $M_n = 1.92 \times 10^5 \pm 1\%$.

[c] ANAL. Calcd. for $(C_8H_{10}Si)_n$: C, 71.57; H, 7.51. Found: C, 72.14; H, 7.48.

on carbon, $H_2PtCl_6 \cdot 6H_2O$ solid, or $PtCl_2$. They both hydrolized in air to insoluble, brittle rubbers. Each was successfully copolymerized in small amounts with $[(CH_3)_2SiCH_2]_2$. The resulting copolymers were crosslinked by hydrolysis to tough, rubbery products insoluble in common organic solvents.

A sampling of polymerization results is given in Table I.

Qualitative experiments using $[(CH_3)_2SiCH_2]_2$ showed that $AuCl_4^-$, $RuCl_6^{-2}$, RuI_3, and $PdCl_2$ gave positive results but the polymers were usually of low molecular weight.

The infrared spectra of all the polymers showed bands around 1050 and 1350 cm.$^{-1}$. The former is characteristic of linear Si—CH_2—Si[3] and the latter, a CH_2 deformation, is characteristic of compounds having a Si—CH_2—Si structure.[3] Many of the polymers showed weak evidence for the presence of ≡SiOH, especially those initiated by catalysts dissolved in water.

Discussion

In the polymerization reactions reported here, where the catalysts were metal salts, evidence for reduction to the metal was noted. (For instance, a gold mirror was produced when $AuCl_4^-$ was used.) The reduction of silver cations by 1,1,3,3-tetramethyl-1,3-disilacyclobutane has been reported[4] but the nature and products of the reaction have not been fully investigated.[5] It may therefore be postulated that the metal may be the ultimate initiator in these systems.

One might postulate that the metal may act as a radical initiator. Unpublished results of this laboratory have shown that typical radical initiators such as di-*t*-butyl-peroxide and azo-diisobutyronitrile do not initiate polymerization of disilacyclobutane derivatives. Also, no carbon–carbon or silicon–silicon bonds could be detected (by infrared or proton magnetic resonance spectra) in the polymer backbone although random radical recombination should result in the formation of these bonds.

An alternative reaction scheme may be postulated as follows:

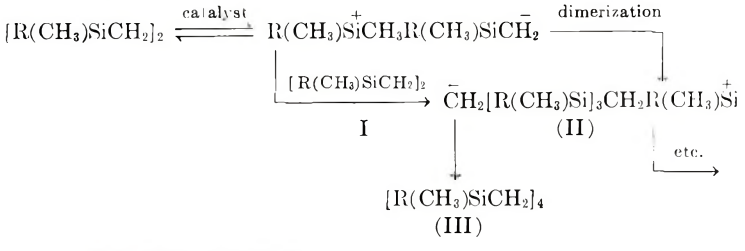

where R = CH_3, C_6H_5, C_2H_5O, Cl.

The ring opening occurs possibly by disruption of the electron arrangement in the ring by the electrophilic nature of the catalyst. The heterolytic fission product (I), can either reform the ring, dimerize with a like species, or interact with another ring by nucleophilic or electrophilic attack. The disilacyclobutane is subject to both types of mechanisms.[4,6] However, it is felt that the electrophilic interaction by the siliconium ion is more likely.

A similar ionic mechanism might also be proposed for the interaction of certain silicon hydrides with silacyclobutane and disilacyclobutane derivatives as reported by Weyenberg and Nelson[1] and by Nametkin, Vdovin, and Grinberg.[7]

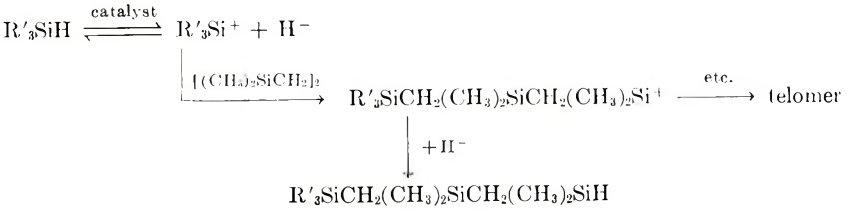

According to the proposed reaction scheme, polymer termination could occur by head–tail neutralization forming large cyclics. Neutralization could also occur by interaction with available anions and cations such as OH^- and H^+ which would be present if water were used. (The infrared spectra of several of the polymer systems showed the presence of ≡SiOH). This could occur during polymerization or on workup. The isolation of small quantities of 1,1,3,3,5,5,7,7-octamethyl-1,3,5,7-tetrasilacyclooctane (III) from the polymerization of $[(CH_3)_2SiCH_2]_2$ in this investigation supports the existence of the postulated intermediate (II), (R═CH_3). Ring closure becomes more difficult after the chain grows beyond eight members, therefore, chain lengthening would be more prevalent.

Considerable energy is released on polymerization. This is explained by the formation of a linear Si—C—Si structure from the less favorable ring structure and from an apparently low ring opening activation energy. Further investigation is being carried out to elucidate the nature of the bonding in these rings and the mode of reaction with a variety of reagents.

References

1. Weyenberg, D. R., and L. E. Nelson, *J. Org. Chem.*, **30,** 2618 (1965).
2. Kriner, W. A., *J. Org. Chem.*, **29,** 1601 (1964).
3. Kriegsman, H., *Z. Electrochem.*, **61,** 1088 (1957).
4. Knoth, Jr., W. H., and R. V. Lindsey, Jr., *J. Org. Chem.*, **23,** 1392 (1958).
5. It has been observed in this laboratory that certain oxidized metals, such as Mo^{+5}, Fe^{+3}, Mn^{+7} and Co^{+3}, were easily reduced to lower oxidation states by disilacyclobutane derivatives. A number of reactions of disilacyclobutanes will be reported more fully at a later date.
6. Kriner, W. A., unpublished experiments.
7. Nametkin, N. S., V. M. Vdovin, and P. L. Grinberg, *Izv. Akad. Nauk SSSR, Ser. Khim.* **1964,** 1133; *Chem. Abstr.*, 7039e.

William A. Kriner*

Department of Chemistry
University of Pennsylvania
Philadelphia, Pennsylvania

Received June 16, 1965
Revised October 26, 1965

* Present address: Saint Joseph's College, Philadelphia, Pennsylvania.

α,ω-Glycols from Polyisobutylene

Previous workers in this laboratory have obtained α,ω-glycols with isobutylene recurring units by ozonolysis of a butyl rubber of molecular weight 800,000 (containing 2 mole-% of isoprene almost exclusively in the 1,4-configuration), followed by reduction with lithium aluminum hydride. Number-average molecular weights close to the theoretical value of 2848 were obtained from measurements of the hydroxyl equivalents of the resulting glycol.[1]

Attempts at chain extension of these glycols with diisocyanates produced quantities of insoluble product suggesting the presence of tri- and polyfunctional glycols, probably due to small amounts of 1,2-structure in the isoprene segment of the original butyl rubber.

We have fractionated these glycols by column chromatography on acid-washed alumina and obtained a number of distinct products, one of which is present in only trace amounts. Determination of molecular weights using both vapor phase osmometry and endgroup analysis indicates that in general these glycols have a functionality slightly greater than two. The higher molecular weight polymers were eluted from the column first.

Prolonged ozonization of the original rubber does not appear to affect the quantities of the fractionated glycols.

Experimental and Results

The preparation of these glycols has been described previously.[1]

In a typical separation, 25 g. of glycol were dissolved in a minimum of benzene and chromatographed on acid-washed alumina. Elution with benzene gave a colorless gum (fraction FI) which comprised the majority of the original sample. Further elution with 5 vol.-% methanol in benzene gave a negligible quantity of a colorless gum followed by a second major sample (fraction FII) which at first was colorless but yellowed towards the end of the elution. Fractions FI and FII were redissolved in petroleum ether (30–60°C.), filtered, and evaporated to dryness.

All samples of fraction FII were mixed and subjected to a second fractionation eluting with 5 vol.-% methanol in benzene, when two poorly resolved fractions were obtained (fraction FIIA and fraction FIIB), the former was colorless and the latter, a golden yellow. The glycol eluted from the column last had the strongest absorptions, due to the hydroxyl group, at 2.98, 8.95, and 9.47 mμ. The viscosities, molecular weights, hydroxy equivalents, etc., are given in Table I (p. 448).

The financial support of the Textile Fibers Department of E. I. du Pont de Nemours & Company is gratefully acknowledged.

References

1. Marvel, C. S., and E. B. Jones, *J. Polymer Sci. A*, **2**, 5313 (1964).

2. Ogg, C. L., W. L. Porter, and C. O. Willis, *Ind. Eng. Chem., Anal. Ed.*, **17**, 394 (1945).

William H. Stubbs*
Christopher Robert Gore†
C. S. Marvel

Department of Chemistry
University of Arizona
Tucson, Arizona

* Postdoctoral Research Associate supported by Textile Fibers Department of E. I. du Pont de Nemours and Co., 1963–1964.

† Postdoctoral Research Associate supported by Textile Fibers Department of E. I. du Pont de Nemours and Co., 1964–1965.

TABLE I
Polyisobutylene Glycols

Glycol fraction	CRG/PIBG 2		PIBG 8		PIBG 12			
	FI	FII	FI	FII	FI	FII	FIIA	FIIB
Approx. % eluted	65	19	65	20	55	30	—	—
Viscosity[a]	0.097	0.060	0.118	0.074	0.104	0.060	0.076	0.044
Hydroxy equivalents[b]	2430	890	3050	—	3490	—	1225	465
Mol. wt. (from hydroxy equivalents)	4860	1780	6100	—	6980	—	2450	930
Mol. wt.[c] (by V.P.O.)	4540	—	6370	—	9640	—	2820	940
Analysis								
% C found	85.66	—	84.43	—	85.27	—	83.02	—
% C calculated	85.11	—	85.23	—	85.31	—	84.49	—
% H found	14.37	—	14.24	—	14.18	—	13.58	—
% H calculated	14.22	—	14.23	—	14.25	—	14.16	—

[a] Inherent viscosity in the range 0.5–1.0%; tetrahydrofuran as solvent and measured at 30°C.

[b] Hydroxy equivalents determined by acetic acid/pyridine method.[2]

[c] Molecular weights by vapor pressure osomometry were measured by Dr. A. J. Ultee and Mr. A. V. Price of the Textile Fibers Department (Benger Laboratory) of E. I. du Pont de Nemours & Company at Waynesboro, Virginia.